WDM and Galaxy Formation

N. Menci
Osservatorio Astronomico di Roma - INAF

Outline

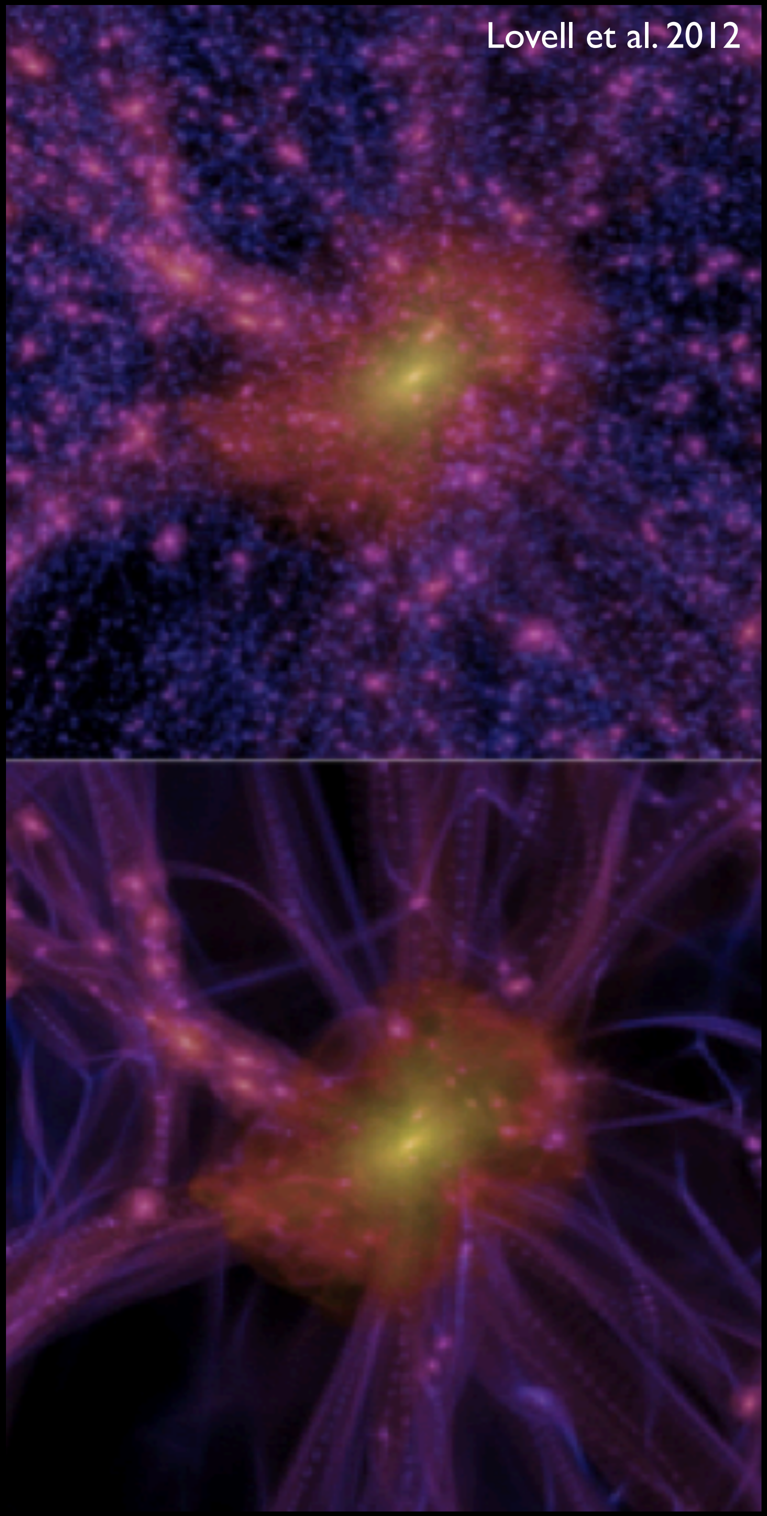

"Ab Initio" Galaxy Formation in DM dominated Universe
- Power Spectrum
- Free Streaming Scale
- Connecting baryon physics to DM haloes: semi-analytic models

Galaxy Formation in Cold Dark Matter:
- Basic properties
- The small-scale crisis: Galaxies and AGN
- Feedback scale
- Is baryon physics a solution ?

Galaxy Formation in Warm Dark Matter scenarios
- Galaxy and AGN luminosity functions
- The luminosity function of satellites
- Hints from abundance matching: the V_{max}-M_* relation
- The star formation properties of satellites

Limits to Warm Dark Matter candidate mass
- High-redhsift galaxy counts
- Luminosity function of ultra-faint galaxies at z=2
- Dwarf galaxies in clusters down to M_{UV}=-10

Galaxies are the tip of the iceberg (underlying DM distribution)

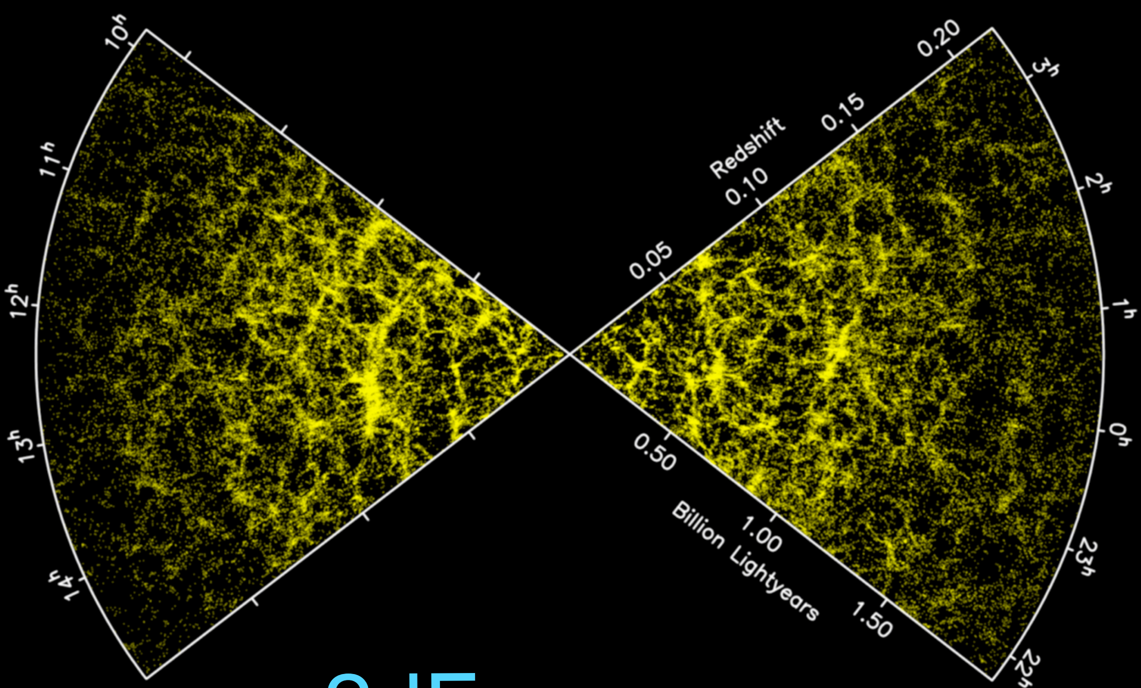

2dF survey

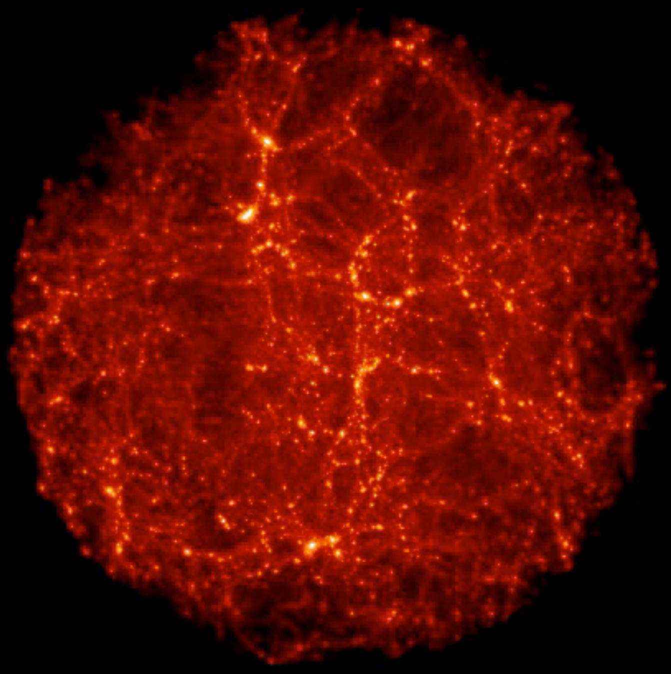

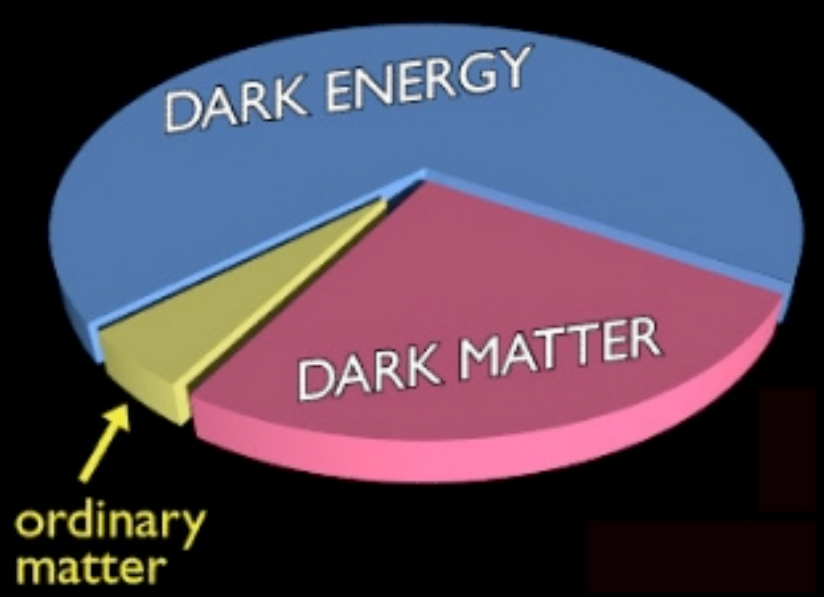

Galaxies are the tip of the iceberg (underlying DM distribution)

Galaxy Formation Theory

Describe the collapse and evolution of the DM clumps dominating the gravitational dynamics

Connect properties of ordinary matter (gas physics, star formation,astrophysical processes) to the potential wells of DM condensations

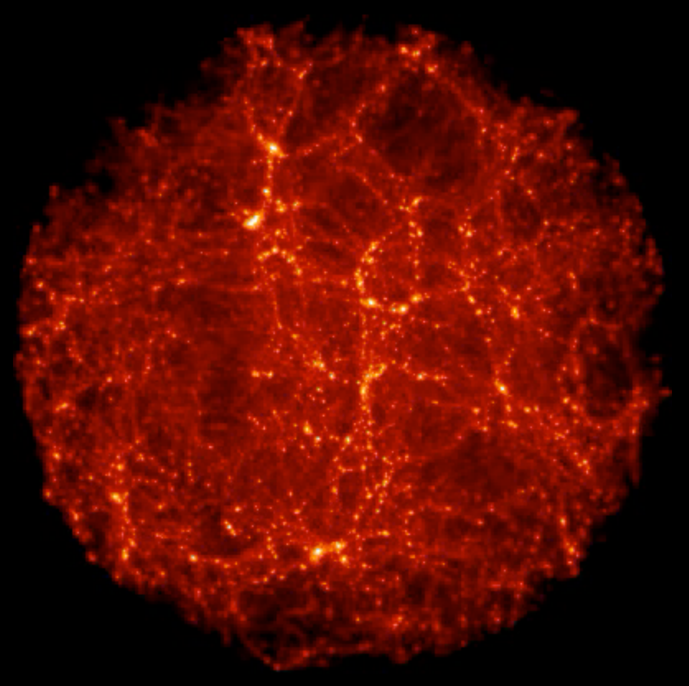

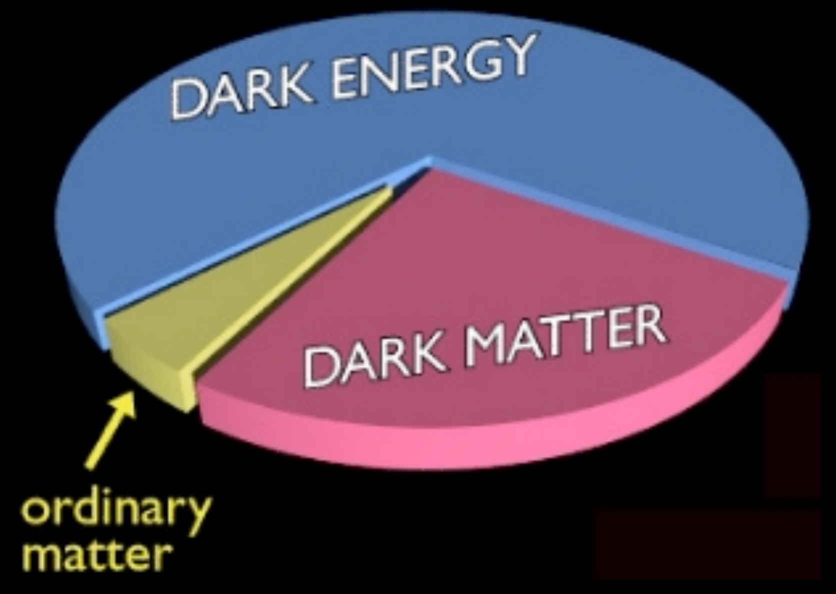

Galaxies are the tip of the iceberg (underlying DM distribution)

Galaxy Formation Theory

Describe the collapse and evolution of the DM clumps dominating the gravitational dynamics

Connect properties of ordinary matter (gas physics, star formation,astrophysical processes) to the potential wells of DM condensations

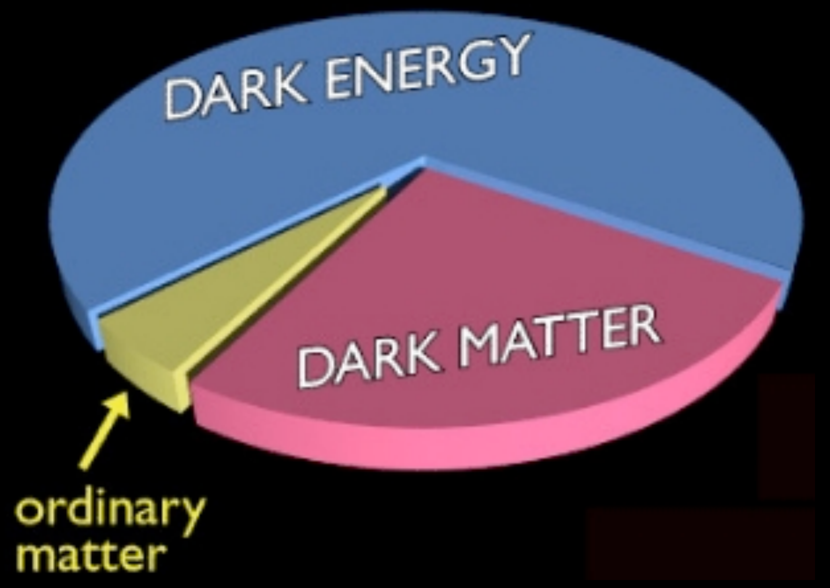

Galaxies are the tip of the iceberg (underlying DM distribution)

Diemand et al. 2008

Galaxy Formation Theory

Describe the collapse and evolution of the DM clumps dominating the gravitational dynamics

Connect properties of ordinary matter (gas physics, star formation,astrophysical processes) to the potential wells of DM condensations

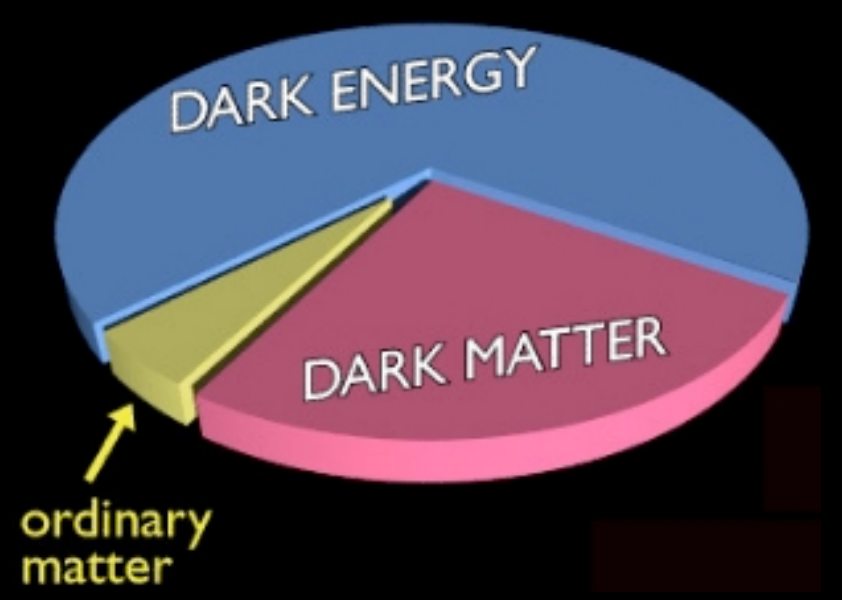

Cosmic Structures form from the collapse of overdense regions in the DM primordial density field, and grow by gravitational instability

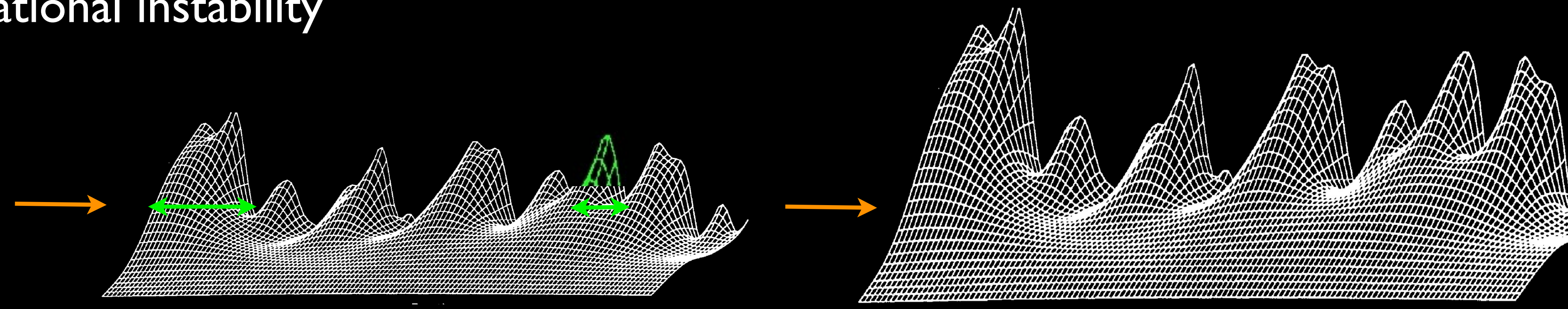

R=2π/k

$$M = \frac{4\,\pi}{3}\,\rho\,R^3$$

$$\langle \delta_M^2 \rangle = \sigma^2(M)\,g(t)$$

Gaussian Random field

$$\delta = \frac{\delta\rho}{\rho}$$

$$p(\delta_k) = \frac{1}{\sqrt{2\pi}\,\sigma_k}\,e^{\frac{\delta_k^2}{2\,\sigma_k^2}}$$

Mean (square) value of perturbations of size R(~1/k) enclosing a mass M

$$P(k) = \frac{1}{V}\,\langle |\delta_k|^2 \rangle$$

$$\sigma_M^2 = \frac{1}{(2\pi)^3\,V}\int^{M\leftrightarrow k} dk\,k^2\,P(k)$$

$$\sigma_M^2 \leftrightarrow P(k)$$

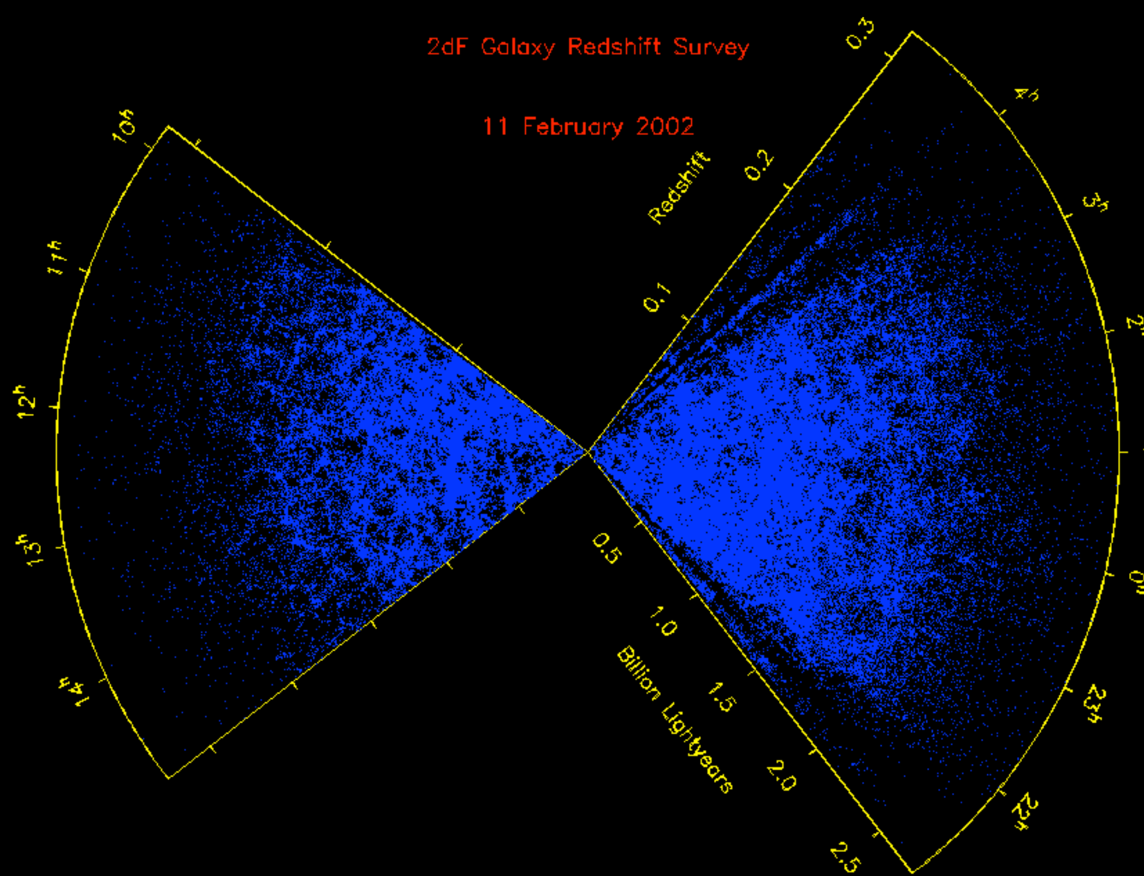

Cosmic Structures form from the collapse of overdense regions in the DM primordial density field, and grow by gravitational instability

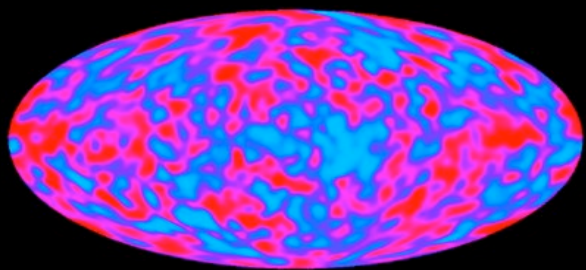

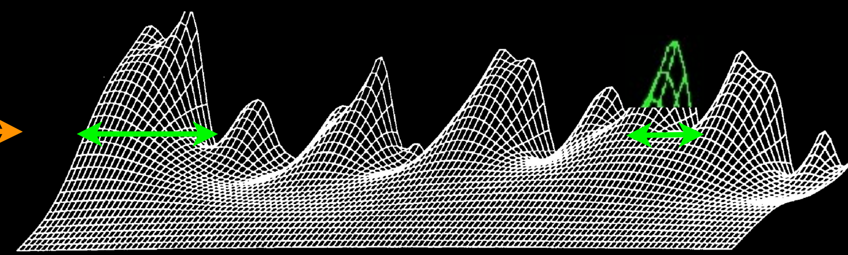

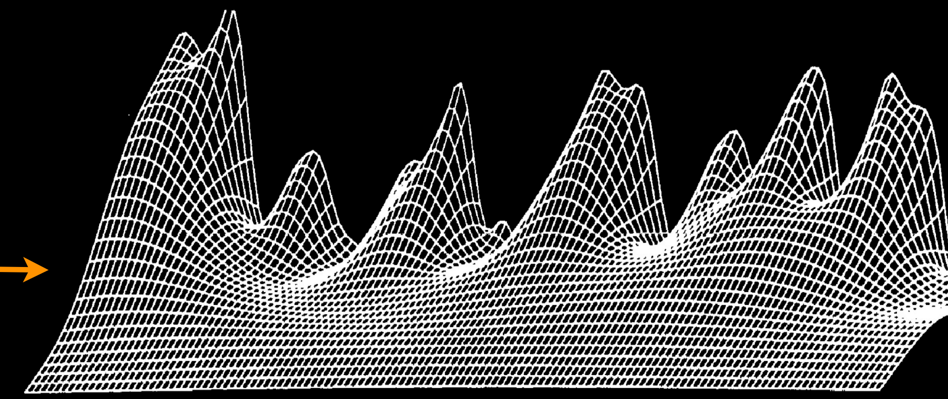

R=2π/k

$$M = \frac{4\,\pi}{3}\,\rho\,R^3$$

$$\langle \delta_M^2 \rangle = \sigma^2(M)\,g(t)$$

Gaussian Random field

$$\delta = \frac{\delta\rho}{\rho}$$

$$p(\delta_k) = \frac{1}{\sqrt{2\pi}\,\sigma_k}\,e^{\frac{\delta_k^2}{2\,\sigma_k^2}}$$

Mean (square) value of perturbations of size R(~1/k) enclosing a mass M

$$P(k) = \frac{1}{V}\,\langle|\delta_k|^2\rangle$$

$$\sigma_M^2 = \frac{1}{(2\pi)^3\,V}\int^{M\leftrightarrow k} dk\,k^2\,P(k)$$

$$\sigma_M^2 \leftrightarrow P(k)$$

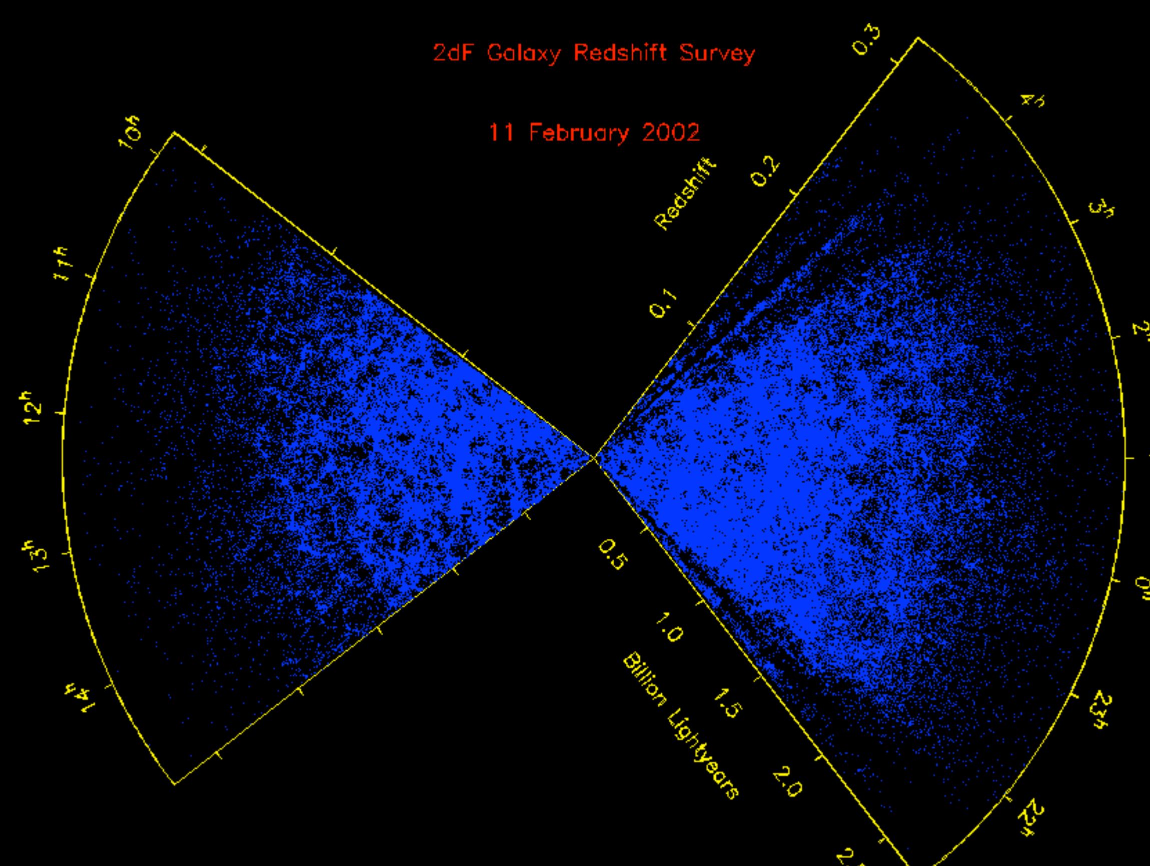

The Variance of the perturbation field

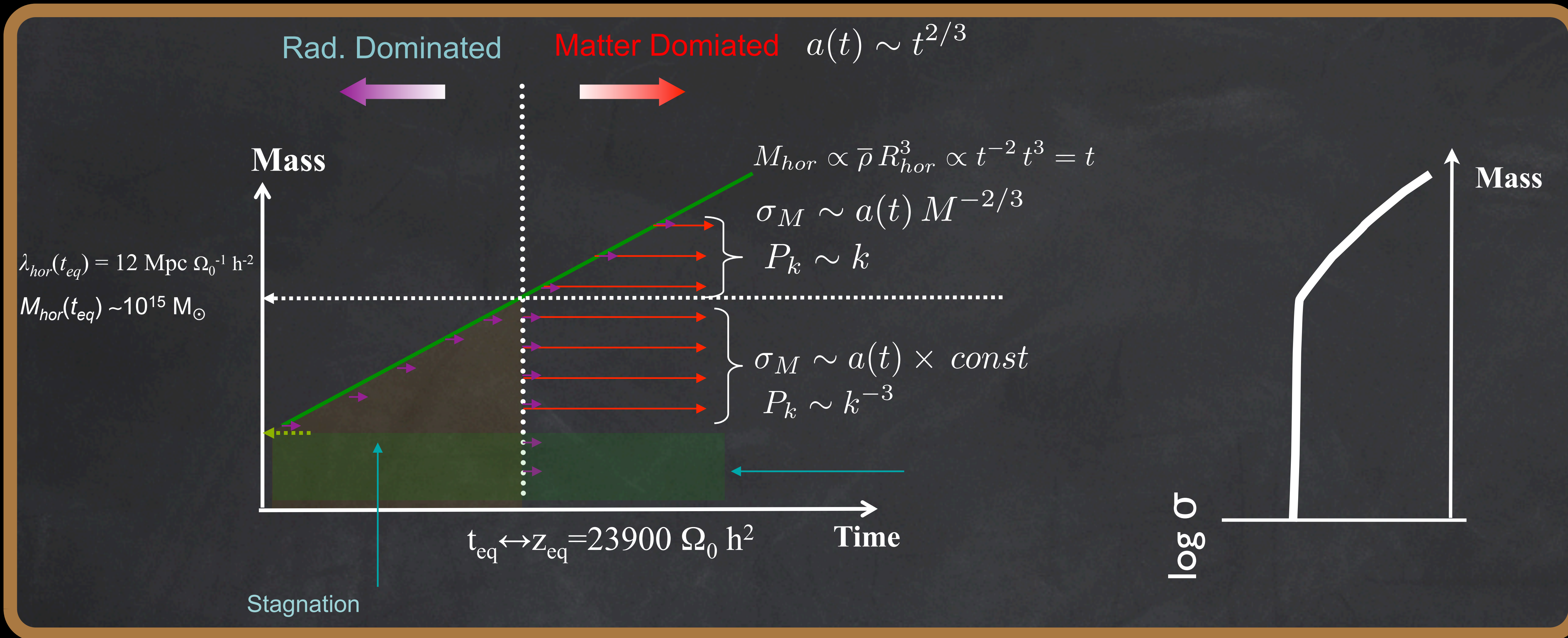

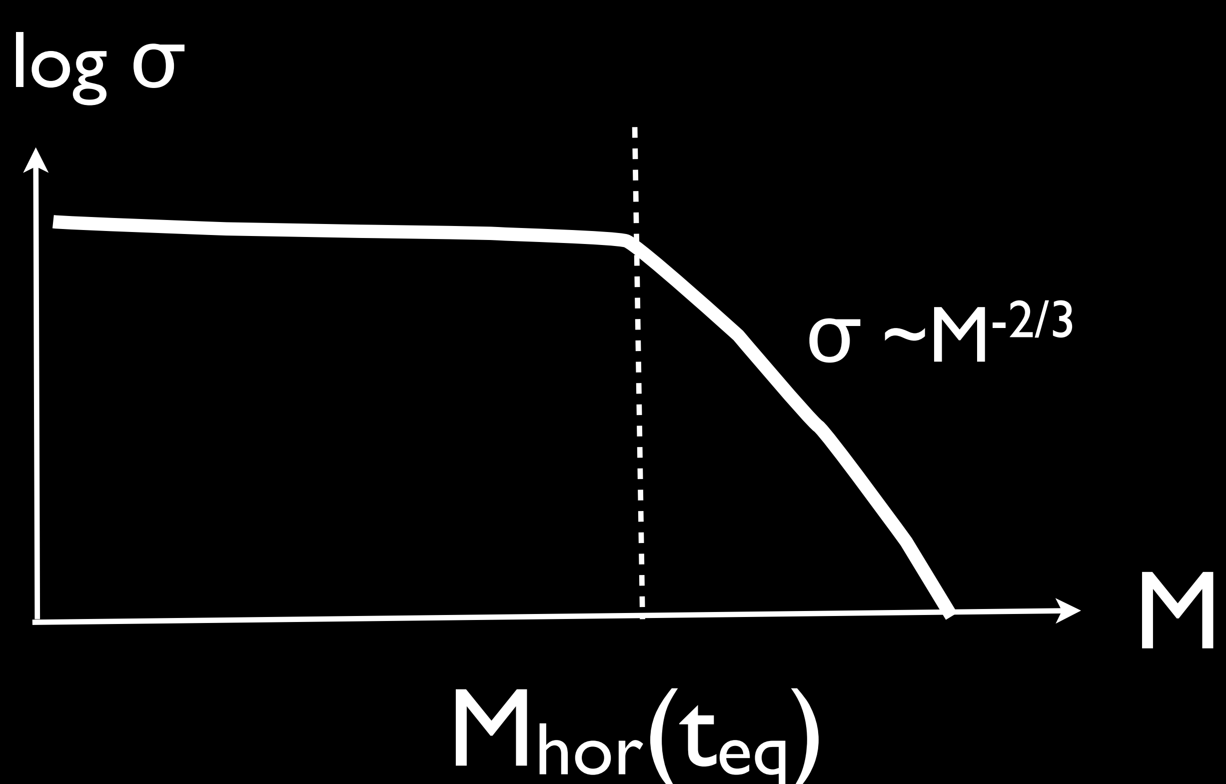

Perturbations involving scales larger than that of the horizon at the equivalence start to grow later

$R_{hor} = 2c\, t_{hor} = 13\, h^{-2}\, Mpc$
$= 110$ Mpc for $\sigma_0 = 0.3\ h = 0.7$

In terms of wavenumber k→Power Spectrum

$$\sigma_M^2 = \frac{1}{(2\pi)^3 V} \int^{M \leftrightarrow k} dk\, k^2\, P(k)$$

$$P(k) = \langle |\delta_k|^2 \rangle$$

$$\sigma_M \propto M^{-2/3} \qquad P(k) \propto k$$

$$\sigma_M = const \qquad P(k) \propto k^{-3}$$

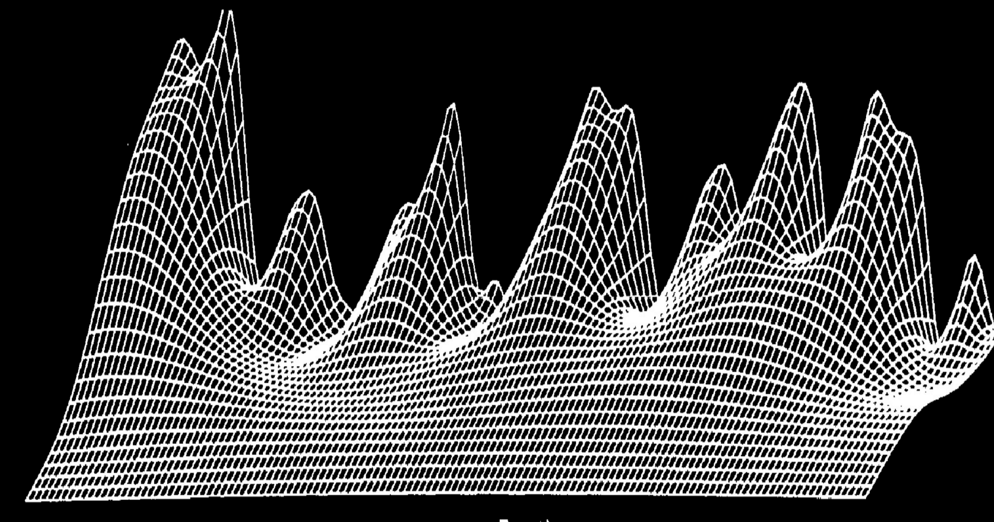

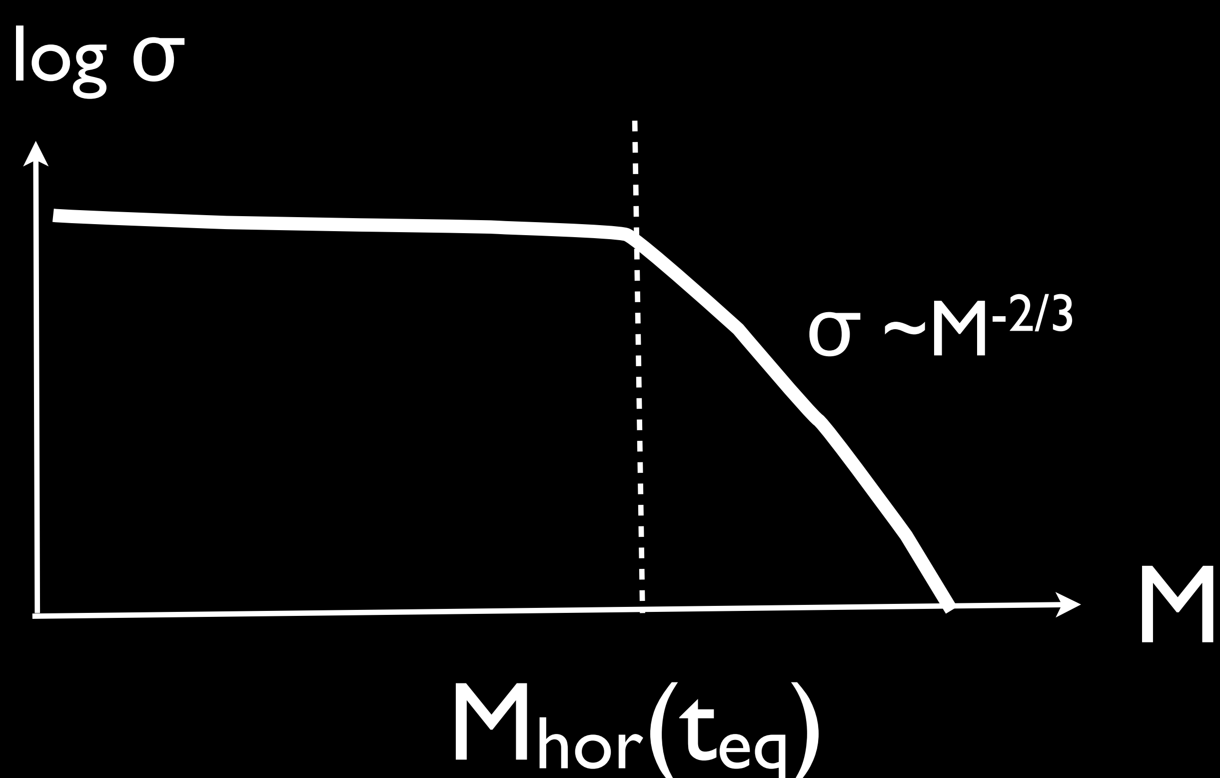

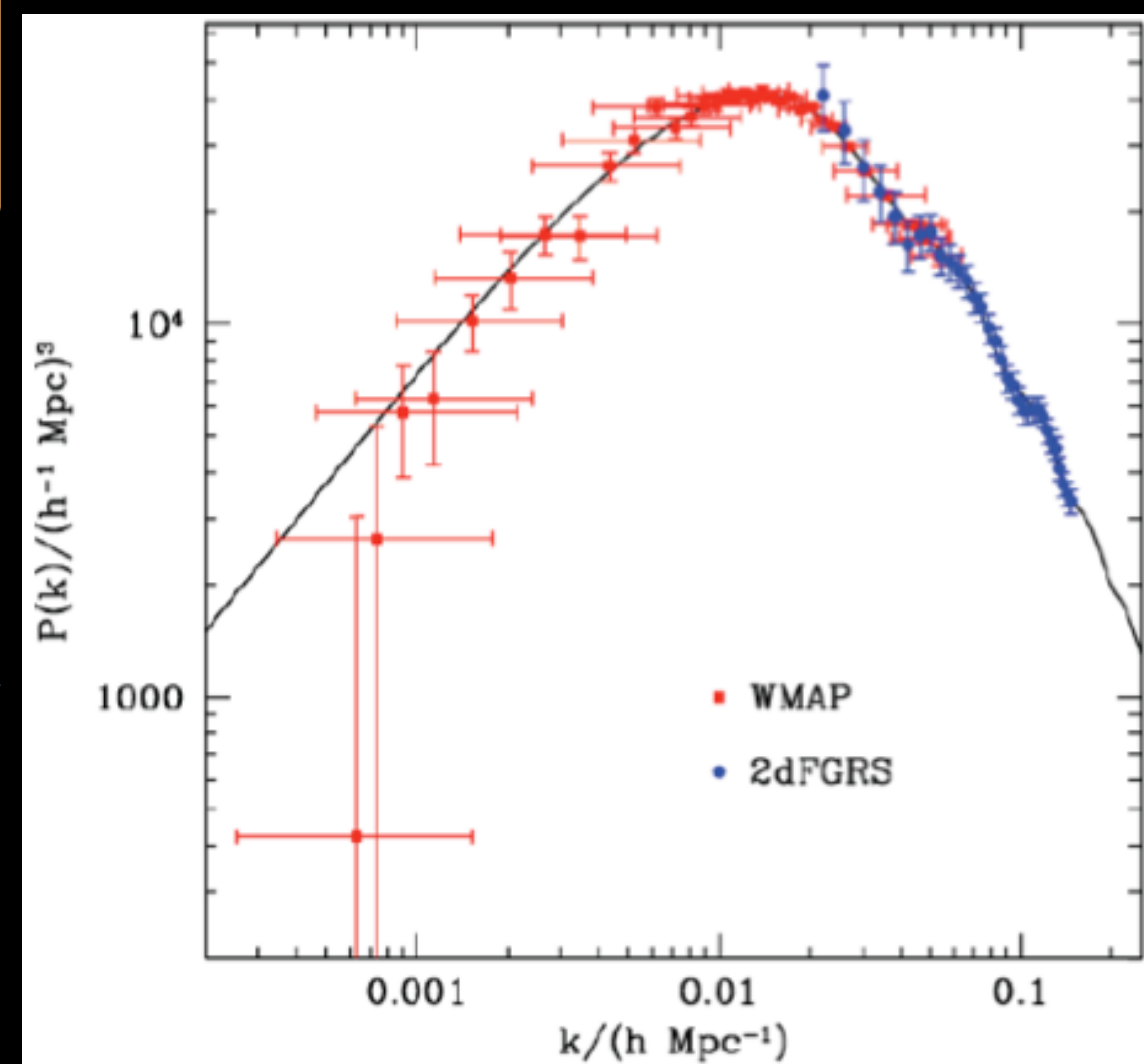

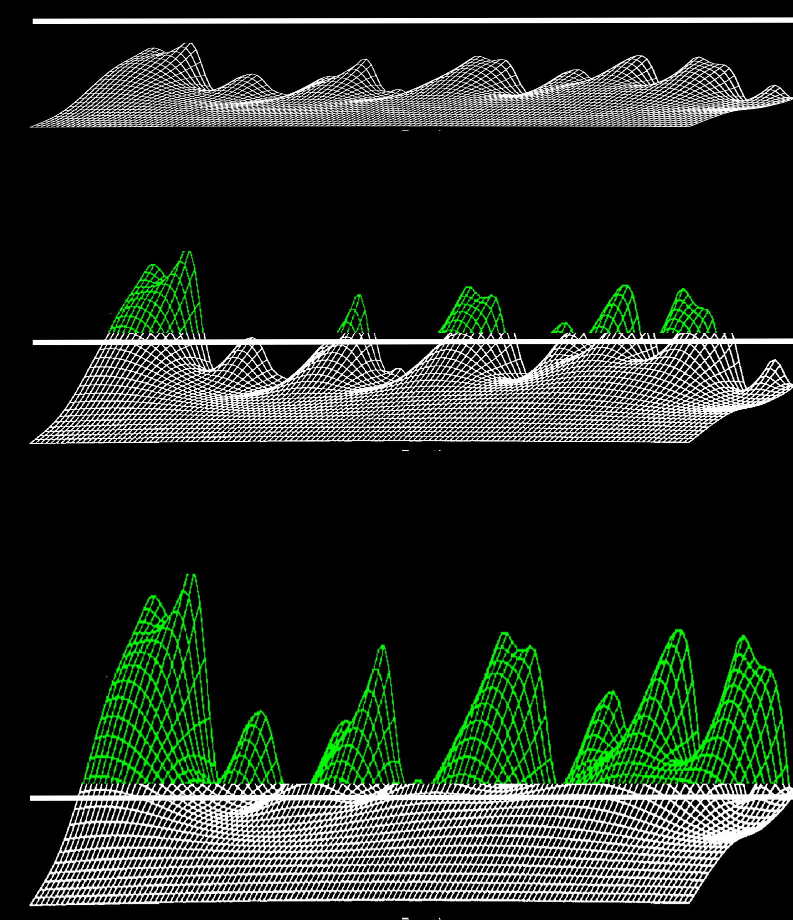

Mass Function: counting the peaks over collapse threshold δ_c

$$N(M)MdM = \overline{\rho}\frac{d}{dM}\left[\int_{\delta_c}^{\infty} d\delta \frac{1}{\sqrt{2\pi}\,\sigma(M,t)} e^{-\frac{\delta^2}{2\sigma^2(M,t)}}\right]$$

$$N(M) = \sqrt{\frac{2}{\pi}}\,\frac{\overline{\rho}}{M^2}\,\frac{\delta_c}{\sigma(M)}\,\frac{dln\sigma}{dlnM}\,e^{-\frac{\delta_c^2}{\sigma(M)^2}}$$

Press & Scechter 1974
Steep Log Slope at
low masses

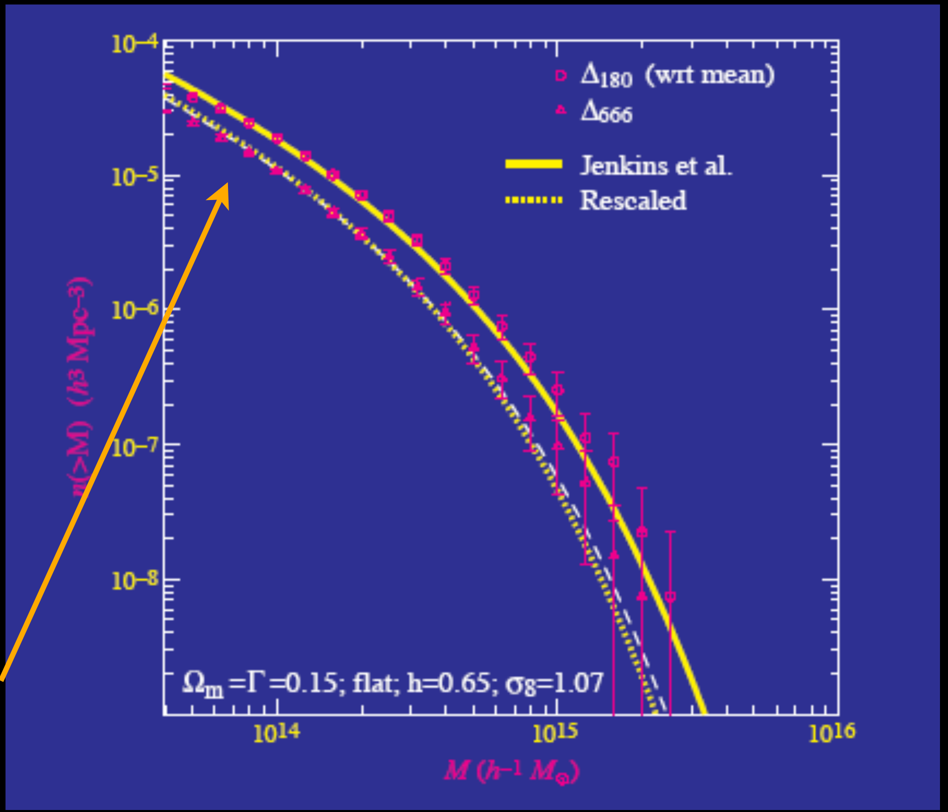

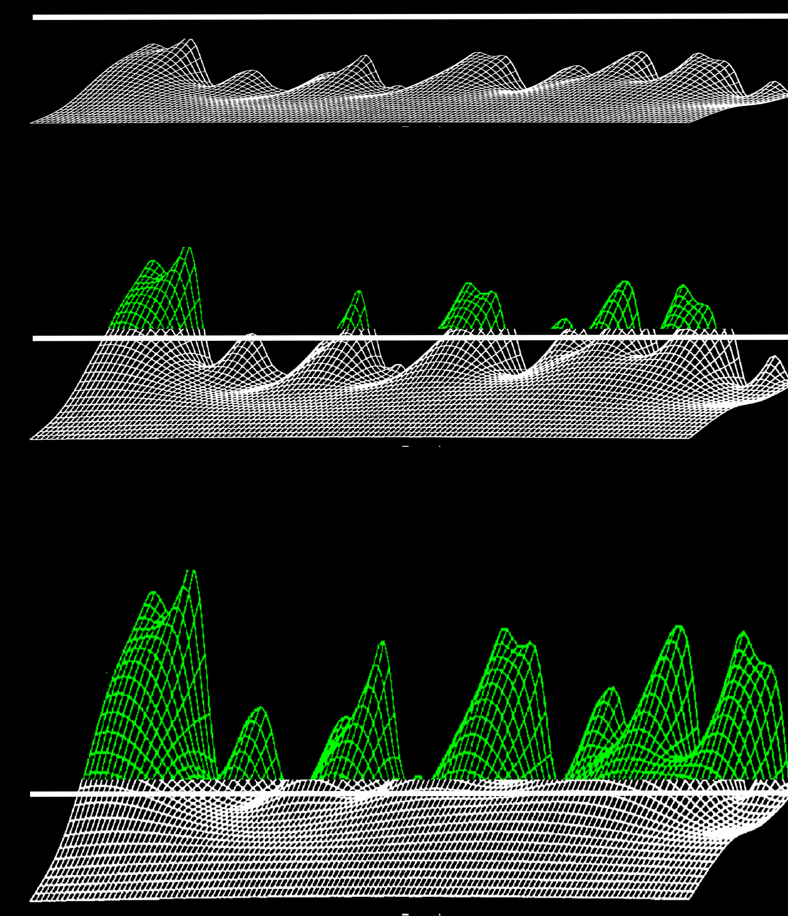

Mass Function: counting the peaks over collapse threshold δ_c

$$N(M)MdM = \overline{\rho}\frac{d}{dM}\left[\int_{\delta_c}^{\infty} d\delta \frac{1}{\sqrt{2\pi}\,\sigma(M,t)} e^{-\frac{\delta^2}{2\sigma^2(M,t)}}\right]$$

$$N(M) = \sqrt{\frac{2}{\pi}}\,\frac{\overline{\rho}}{M^2}\,\frac{\delta_c}{\sigma(M)}\,\frac{dln\sigma}{dlnM}\,e^{-\frac{\delta_c^2}{\sigma(M)^2}}$$

Press & Scechter 1974
Steep Log Slope at
low masses

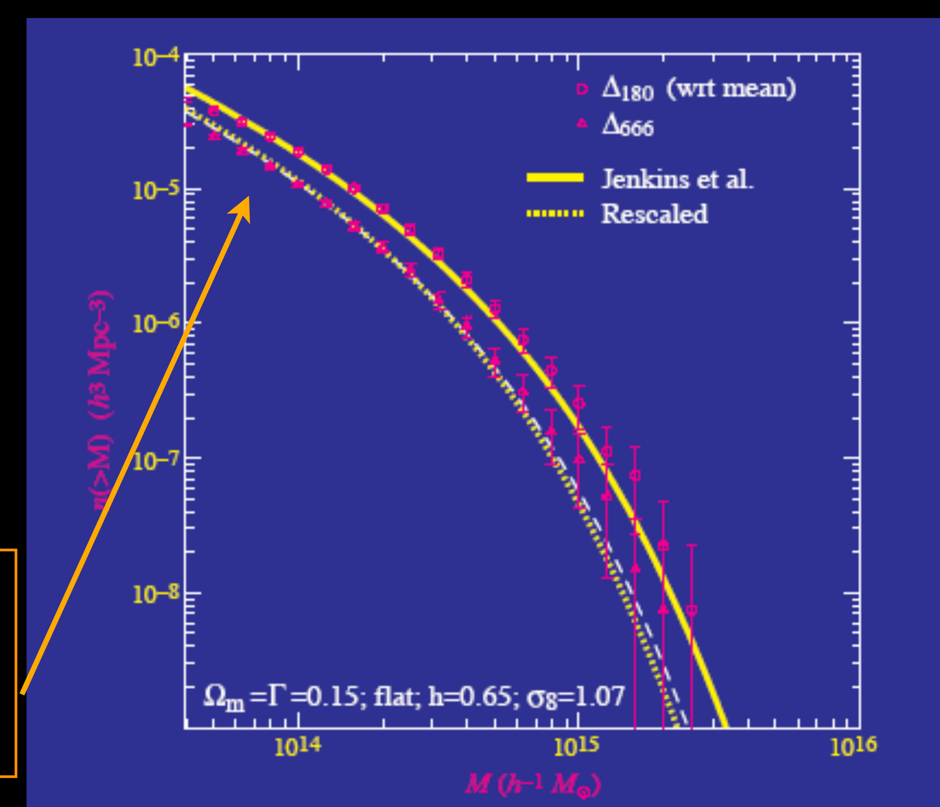

Dissipation, free-streaming scale

$$r_{fs} = \int_0^t \frac{v(t)}{R(t)}$$

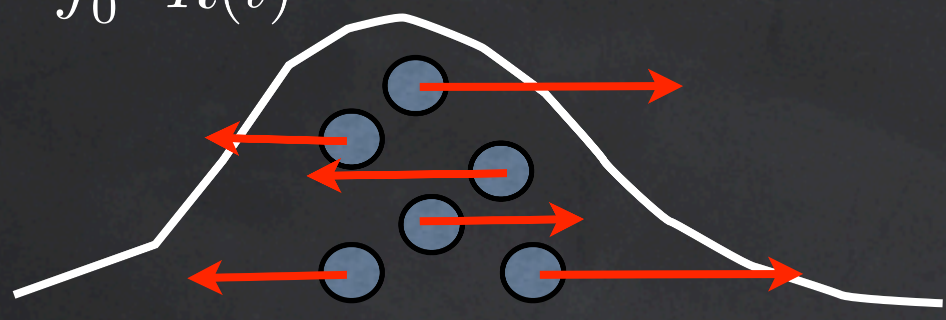

$$\sigma_\chi \propto a^{-1}\, m_\chi^{-1/2}$$

$$M_{fs} = 4 \times 10^{15} \left(\frac{m_\nu}{30\ \mathrm{eV}}\right)^{-2} M_\odot$$

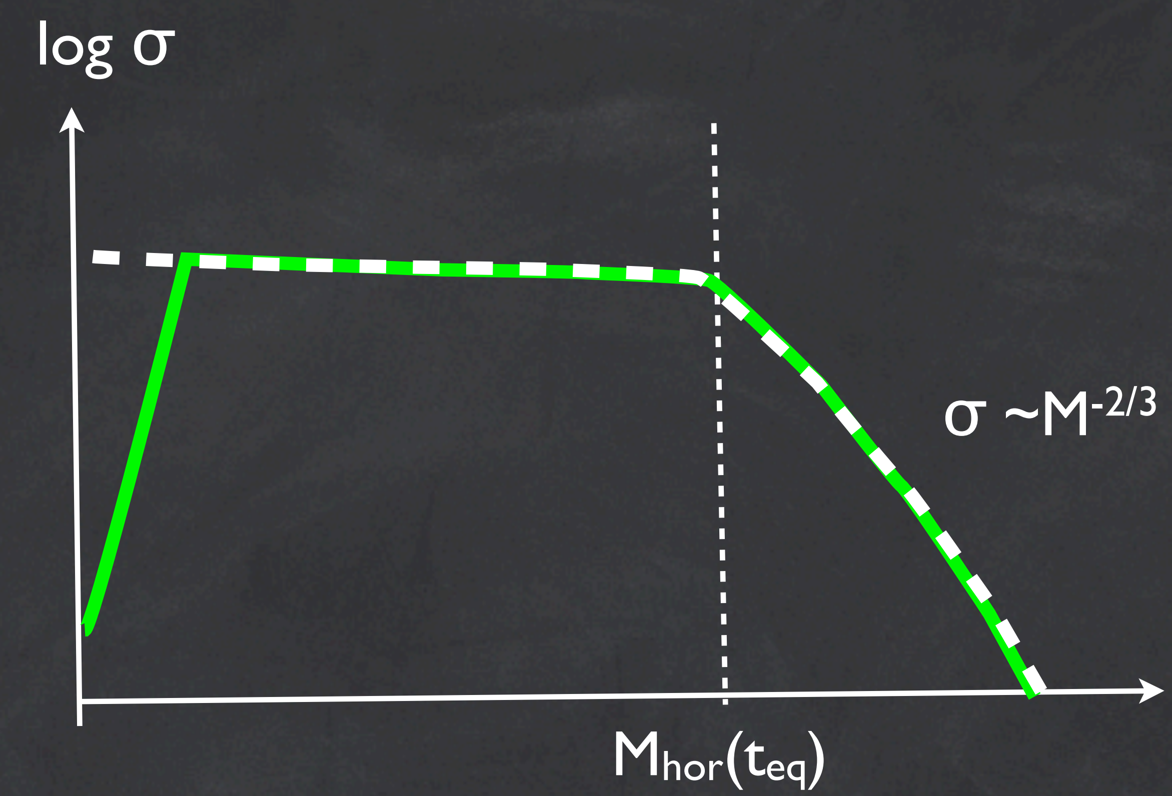

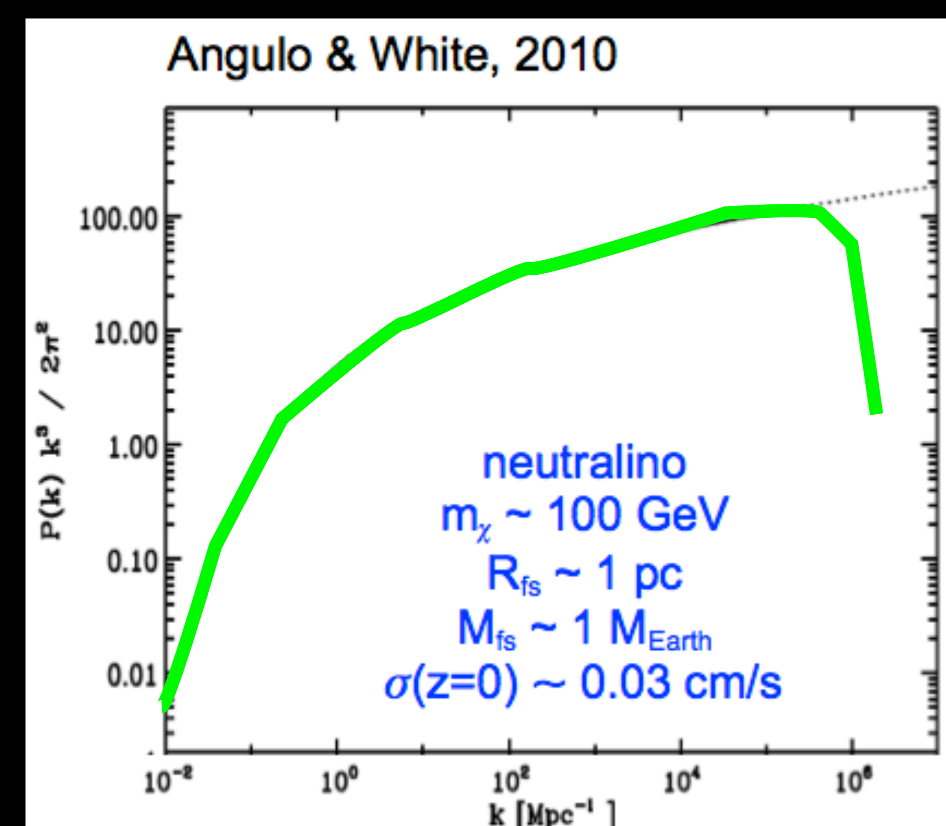

Dissipation, free-streaming scale

$$r_{fs} = \int_0^t \frac{v(t)}{R(t)}$$

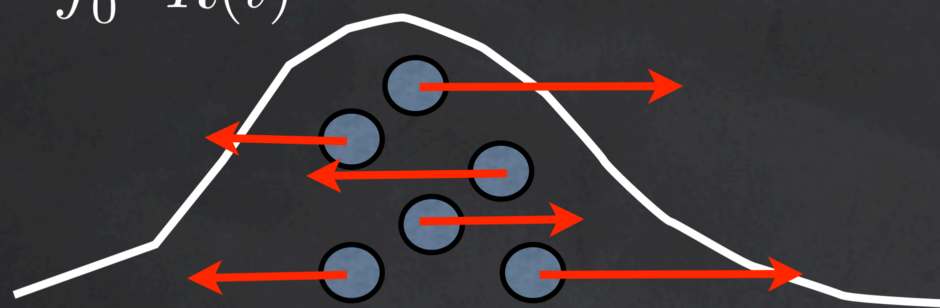

$$\sigma_\chi \propto a^{-1}\, m_\chi^{-1/2}$$

$$M_{fs} = 4 \times 10^{15} \left(\frac{m_\nu}{30\ \mathrm{eV}}\right)^{-2} M_\odot$$

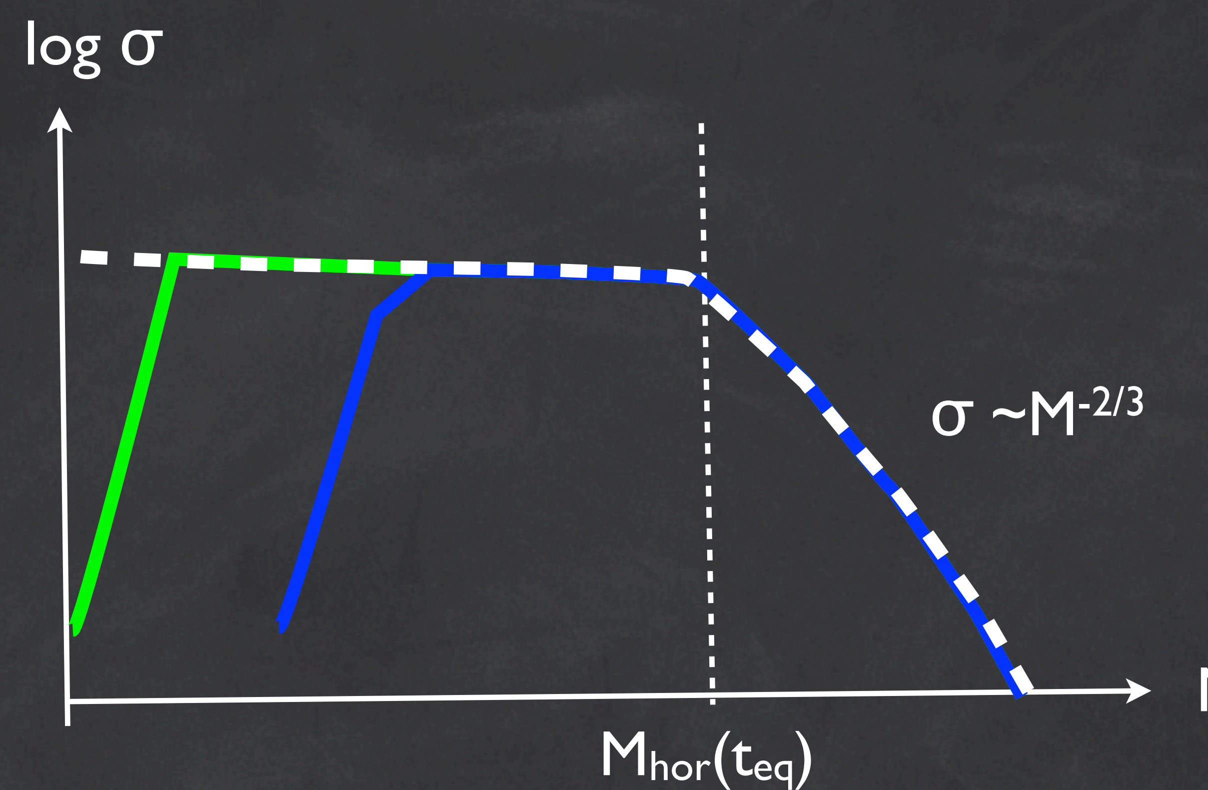

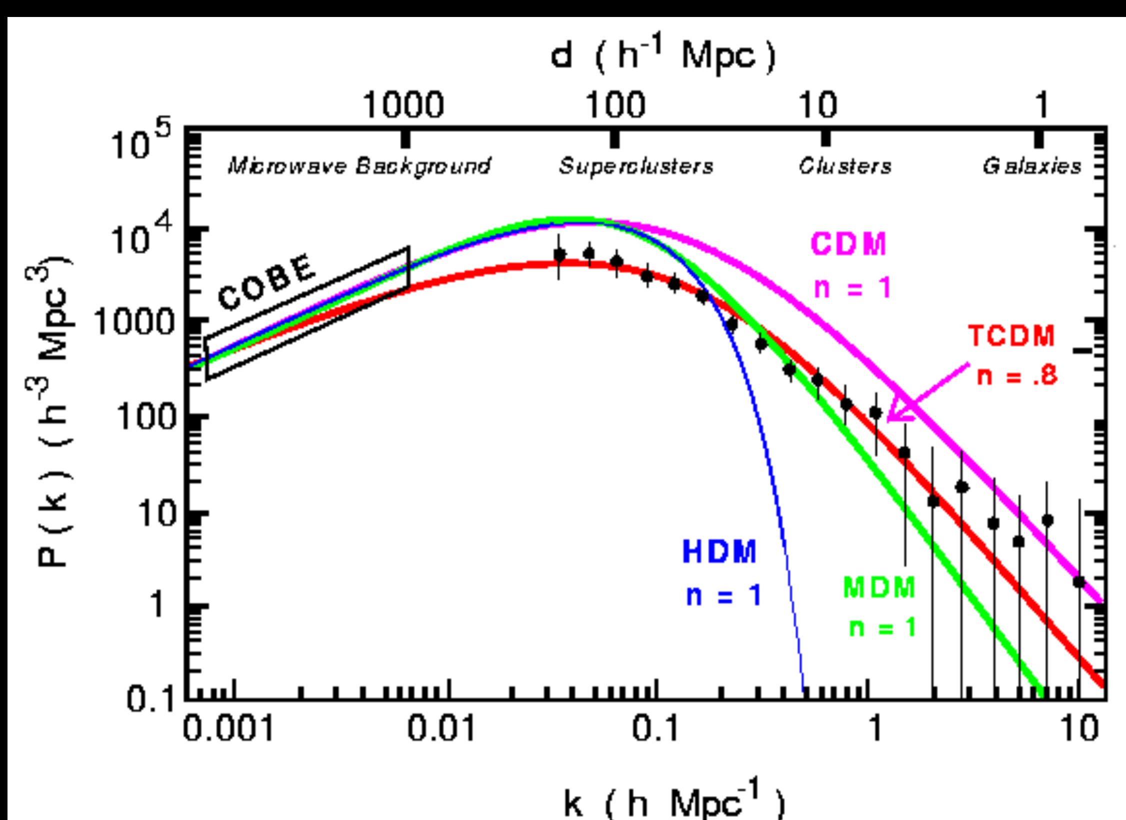

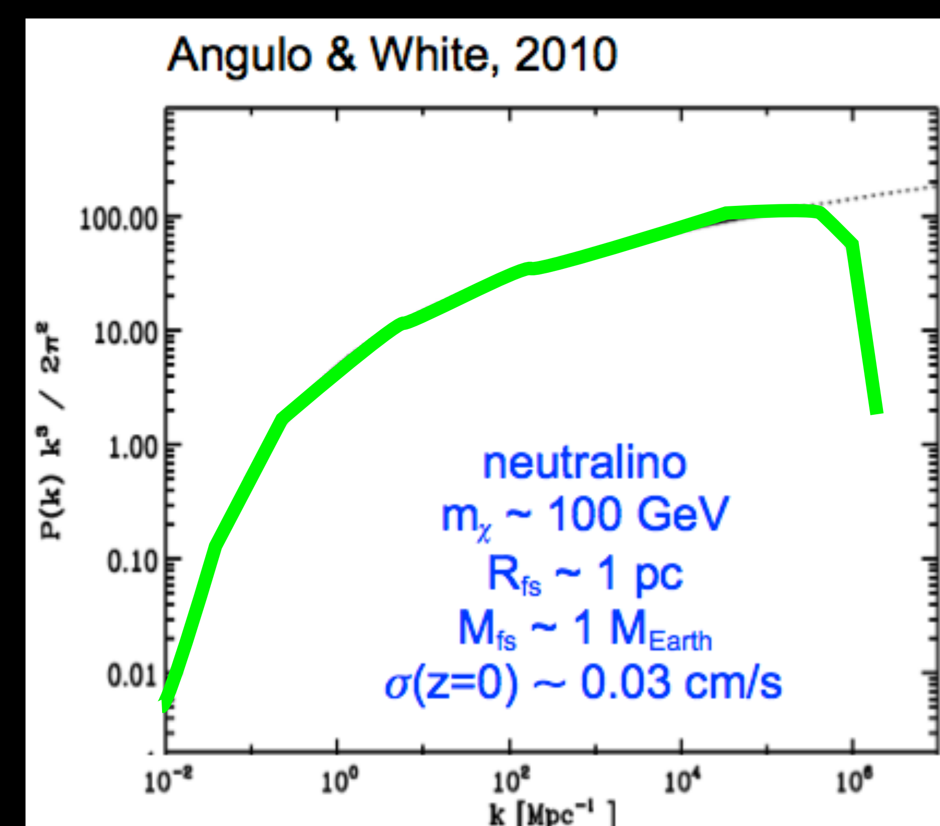

Varying the particle mass

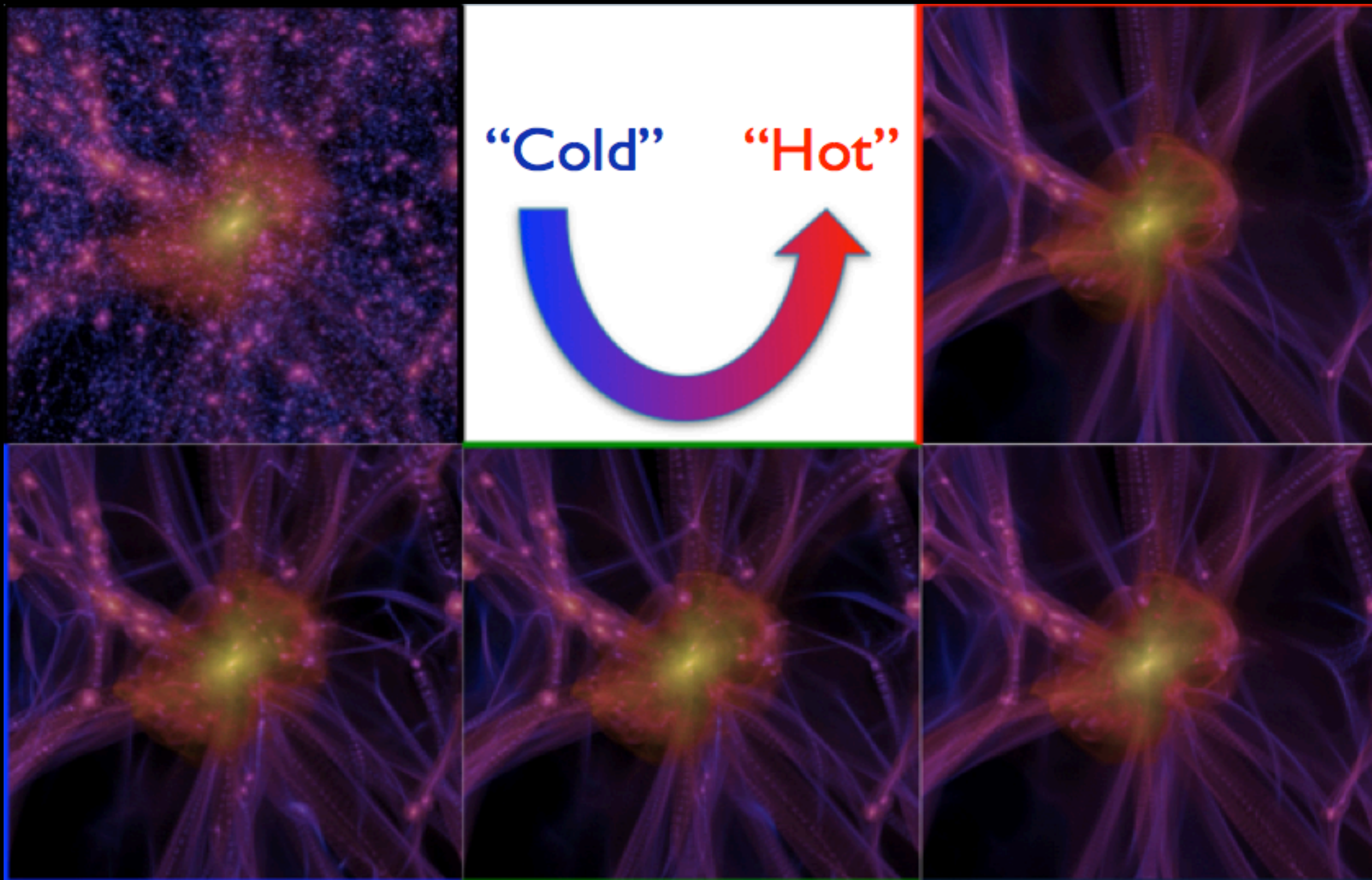

Lovell et al. 2012

Testing the DARK MATTER scenarios against observations: the evolution of galaxies

Requires modelling of baryon physics inside evolving DM potential wells

- gas physis (cooling, heating)
- disk formation
- star formation
- evolution of the stellar population
- injection of energy into the gas
  from SNae

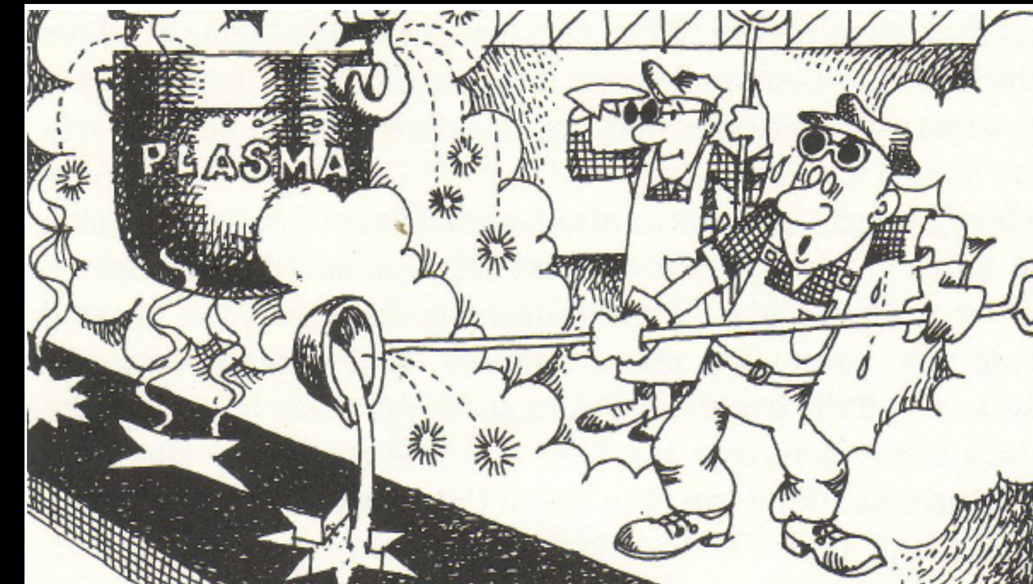

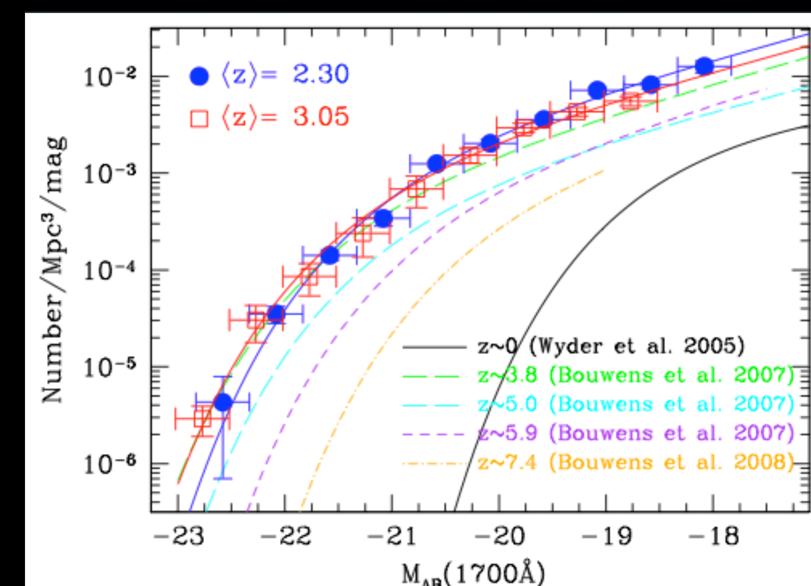

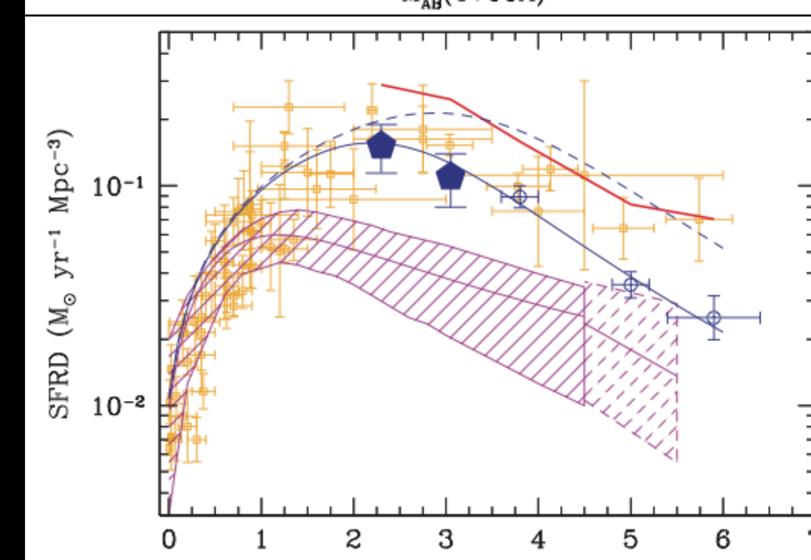

Testing the DARK MATTER scenarios against observations: the evolution of galaxies

Requires modelling of baryon physics inside evolving DM potential wells

- gas physis (cooling, heating)
- disk formation
- star formation
- evolution of the stellar population
- injection of energy into the gas from SNae

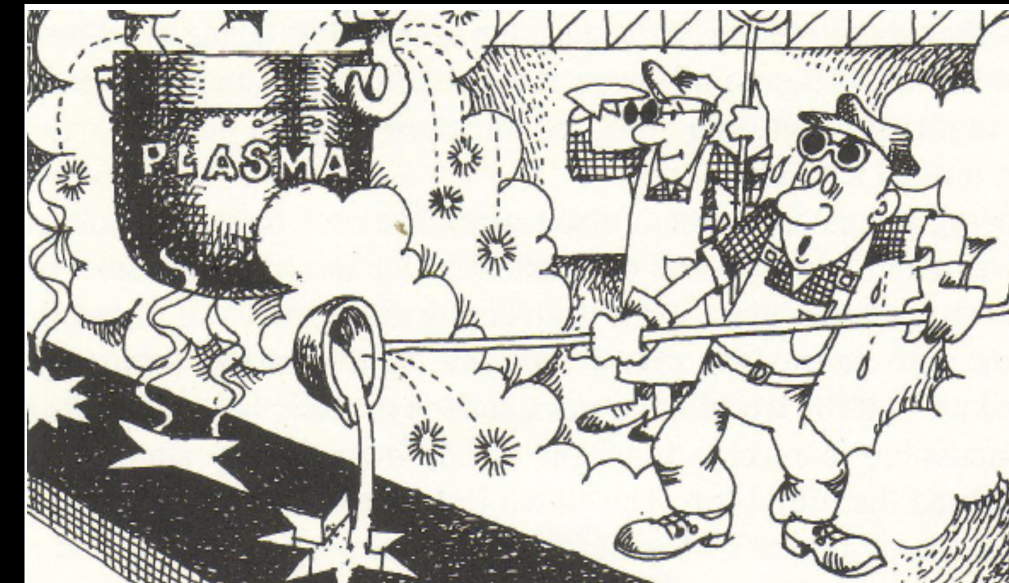

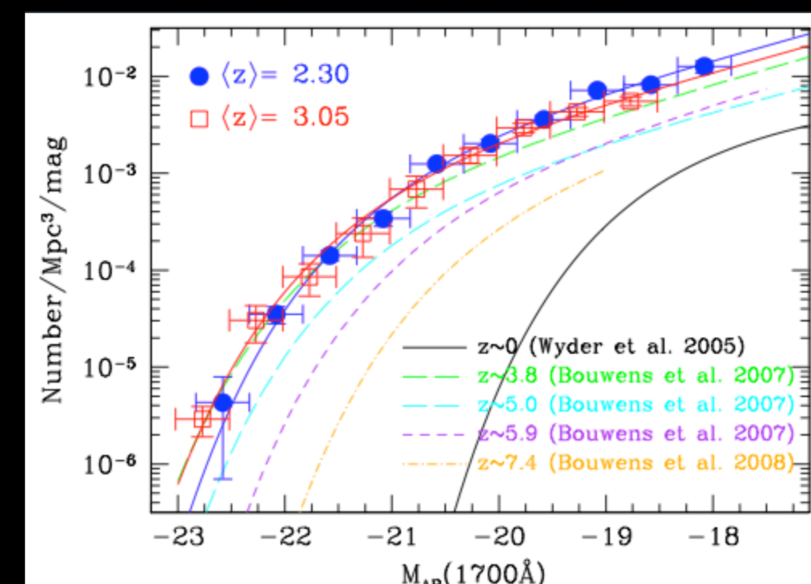

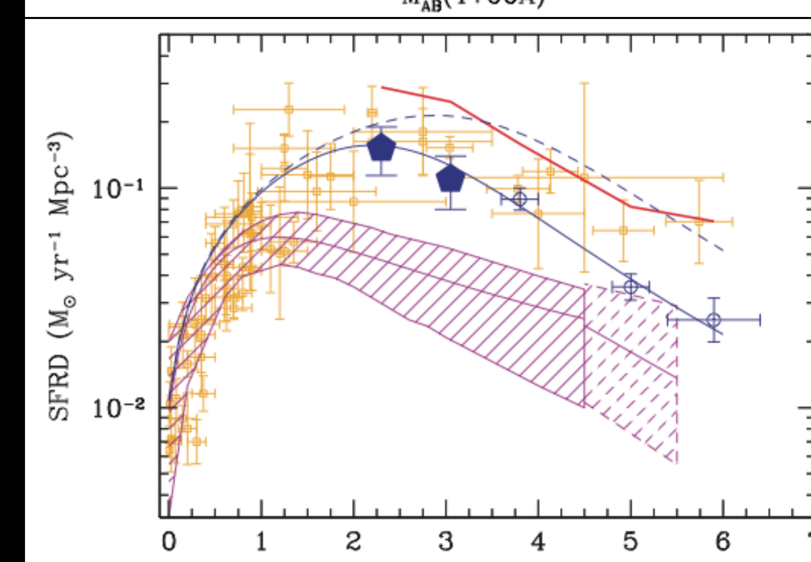

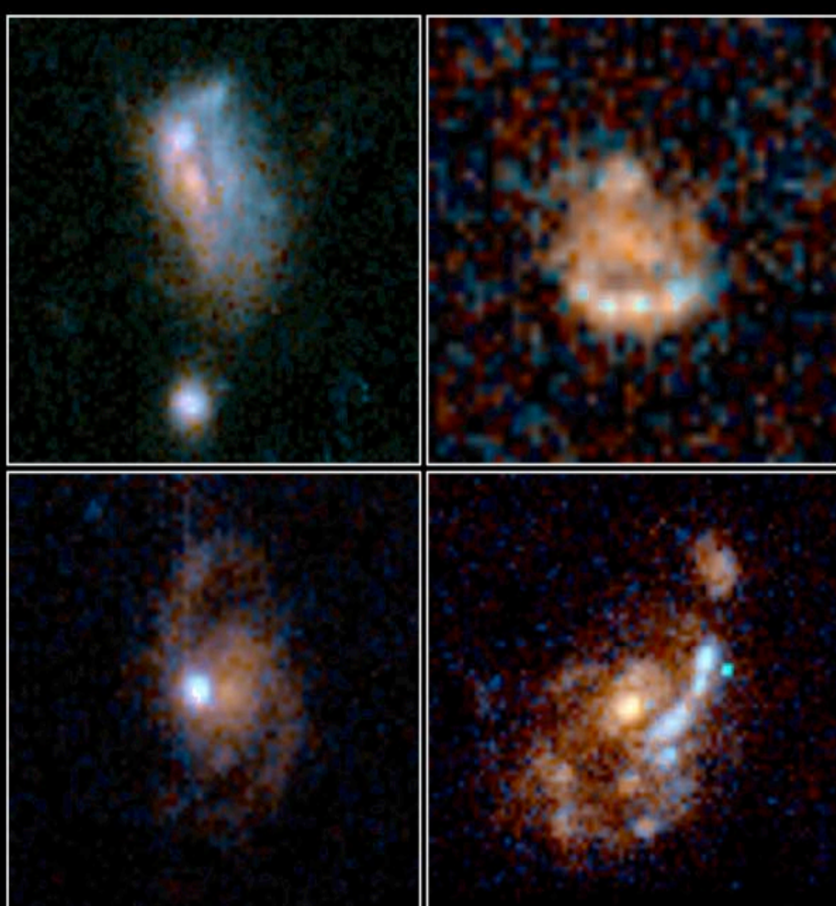

Medium Deep Survey HST • WFPC2

PRC94-39b • ST ScI OPO • R. Griffiths (JHU), NASA

Galaxy Formation in a Cosmological Context

Hydrodynamcal N-body simulations

<u>Pros</u>
include hydrodynamics of gas
contain spatial information
<u>Cons</u>
numerically expensive
(limited exploration of parameter space)
requires sub-grid physics

Semi-Analytic Models Monte-Carlo realization of collapse and merging histories

<u>Pros</u>
Physics of baryons linked to DM halos through scaling laws, allows a fast spanning of parameter space
<u>Cons</u>
Simplified description of gas physics
Do not contain spatial informations

Galaxy Formation in a Cosmological Context

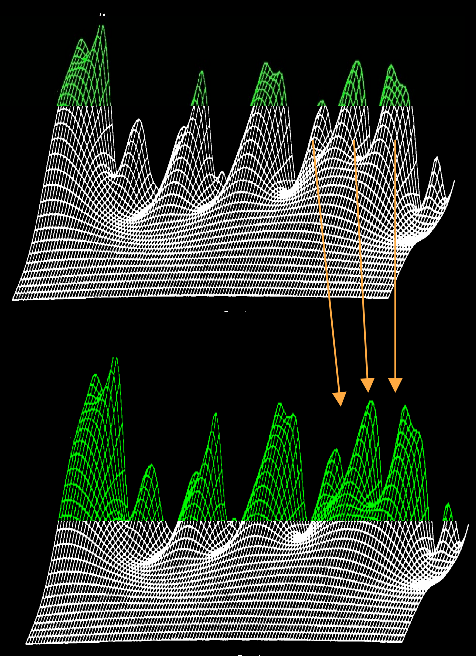

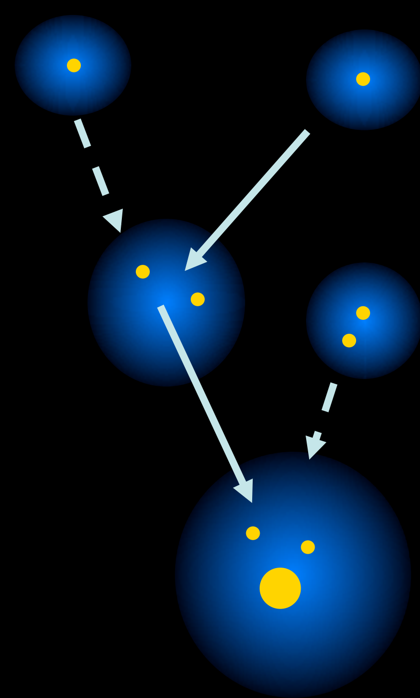

Semi-Analytic Models
Monte-Carlo realization of collapse and merging histories

<u>Pros</u>

Physics of baryons linked to DM halos through scaling laws, allows a fast spanning of parameter space

<u>Cons</u>

Simplified description of gas physics
Do not contain spatial informations

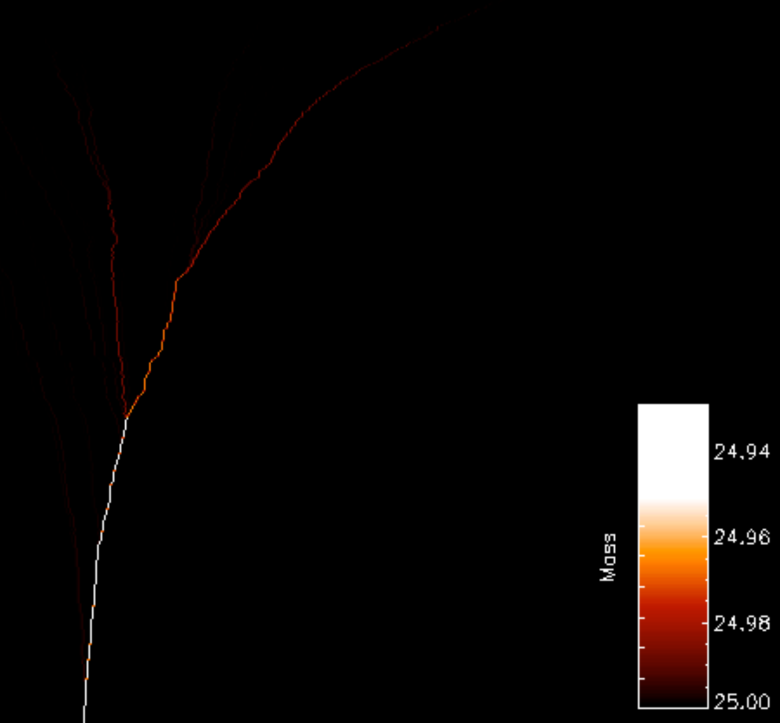

Sub-Halo dymanics:
dynamical friction, binary aggregation

Halo Properties
Density Profiles
Virial Temperature

Gas Properties
Profiles
Cooling - Heating Processes
Collapse, disk formation

Star Formation Rate

Gas Heating (feedback)
SNae
UV background

Evolution of stellar populations

Growth of Supermassive BHs
Evolution of AGNs

Properties of merging trees

Simulation
by Governato 04

Initial ($z \approx 4$-6) merging events involve small clumps with comparable size

Rapid merging, frequent encounters

Last major merging at $z \approx 3$ for $M \approx 3 \, 10^{12} \, M_\odot$

At later times, merging rate declines

Accretion of smaller lumps onto the main progenitor

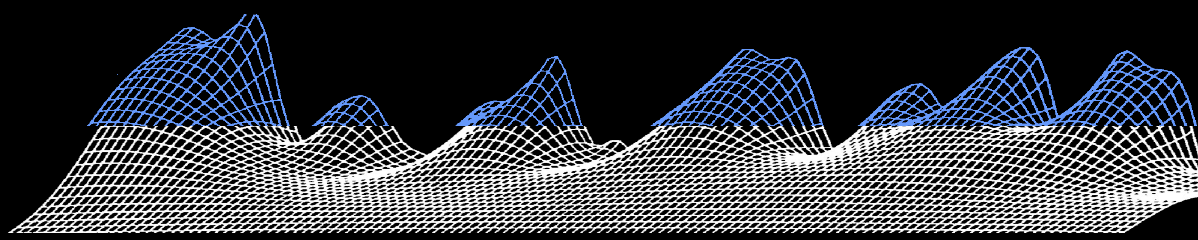

NM et al. 06

Baryonic Processes

Frequent galaxy encounters

Rapid cooling (high gas density)

Starbursts with large fraction of Gas converted into stars

$z \gtrsim 2$

Decline of cooling rate

Drop of encounter rate

Quiescent and declining star formation

$z \lesssim 2$

z

Properties of merging trees

Simulation
by Governato 04

Initial ($z \approx 4$-6) merging events involve small clumps with comparable size

Rapid merging, frequent encounters

Last major merging at $z \approx 3$ for $M \approx 310^{12}\ M_{\odot}$

At later times, merging rate declines

Accretion of smaller lumps onto the main progenitor

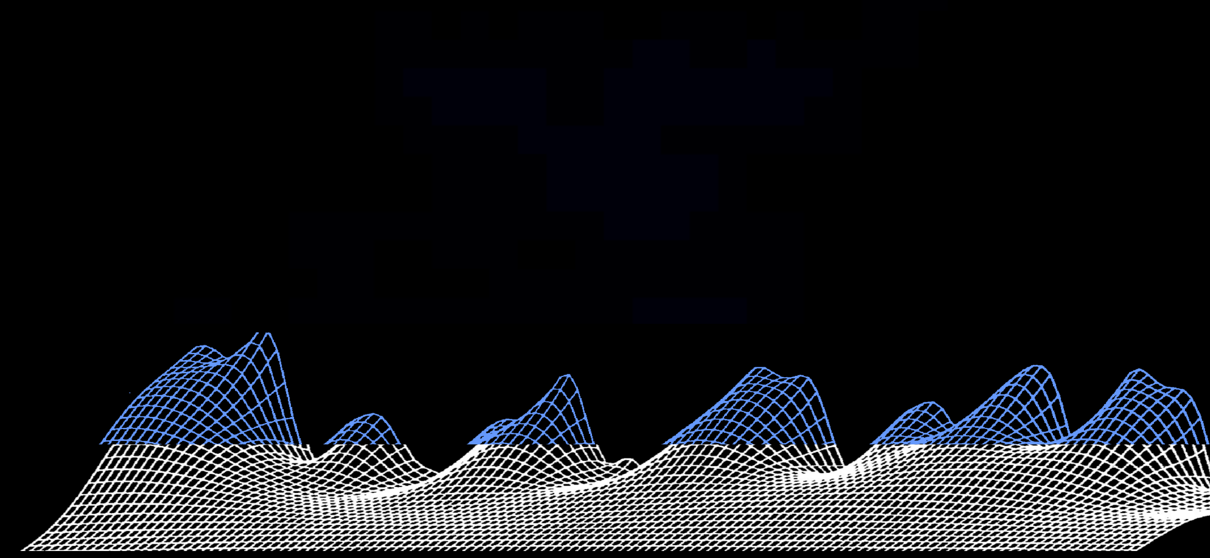

Baryonic Processes

NM et al. 06

Frequent galaxy encounters

Rapid cooling (high gas density)

Starbursts with large fraction of Gas converted into stars

$z \gtrsim 2$

Decline of cooling rate

Drop of encounter rate

Quiescent and declining star formation

$z \lesssim 2$

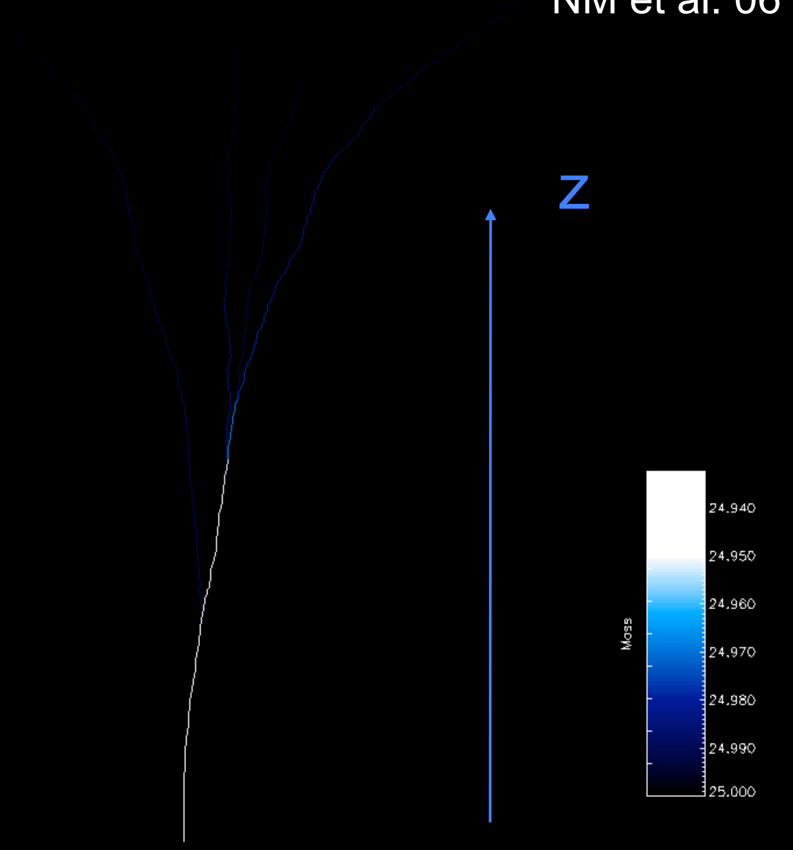

Properties of merging trees

Simulation
by Governato 04

Initial ($z \approx 4$-6) merging events involve small clumps with comparable size

Rapid merging, frequent encounters

Last major merging at $z \approx 3$ for $M \approx 3\,10^{12}\ M_\odot$

At later times, merging rate declines

Accretion of smaller lumps onto the main progenitor

Phase 1

Zhao et al. 2003
Diemand et al. 2007
Hoffman et al. 2007
Ascasibar & Gottloeber 2008

Phase 2

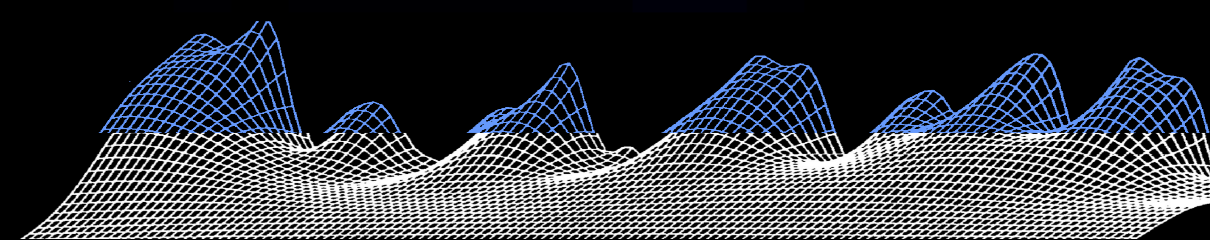

Baryonic Processes

Frequent galaxy encounters

Rapid cooling (high gas density)

Starbursts with large fraction of Gas converted into stars

$z \gtrsim 2$

Decline of cooling rate

Drop of encounter rate

Quiescent and declining star formation

$z \lesssim 2$

NM et al. 06

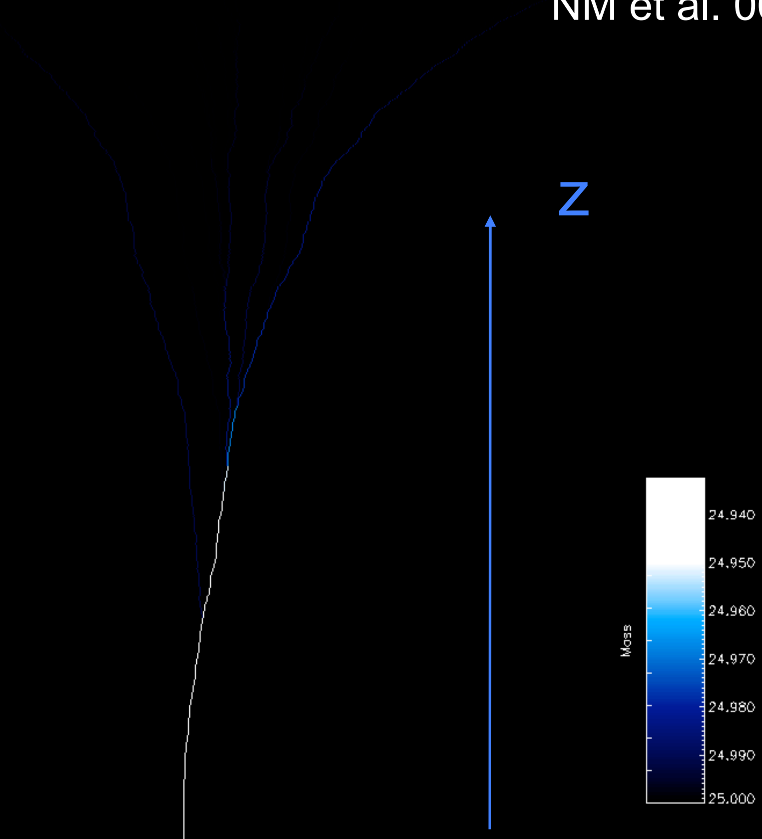

Properties of merging trees

Simulation
by Governato 04

Initial ($z\approx4$-6) merging events involve small clumps with comparable size

Rapid merging, frequent encounters

Last major merging at $z\approx3$ for $M\approx3\,10^{12}\ M_\odot$

At later times, merging rate declines

Accretion of smaller lumps onto the main progenitor

Phase 1

Zhao et al. 2003
Diemand et al. 2007
Hoffman et al. 2007
Ascasibar & Gottloeber 2008

Phase 2

Baryonic Processes

Frequent galaxy encounters

Rapid cooling (high gas density)

Starbursts with large fraction of Gas converted into stars

$z \gtrsim 2$

Decline of cooling rate

Drop of encounter rate

Quiescent and declining star formation

$z \lesssim 2$

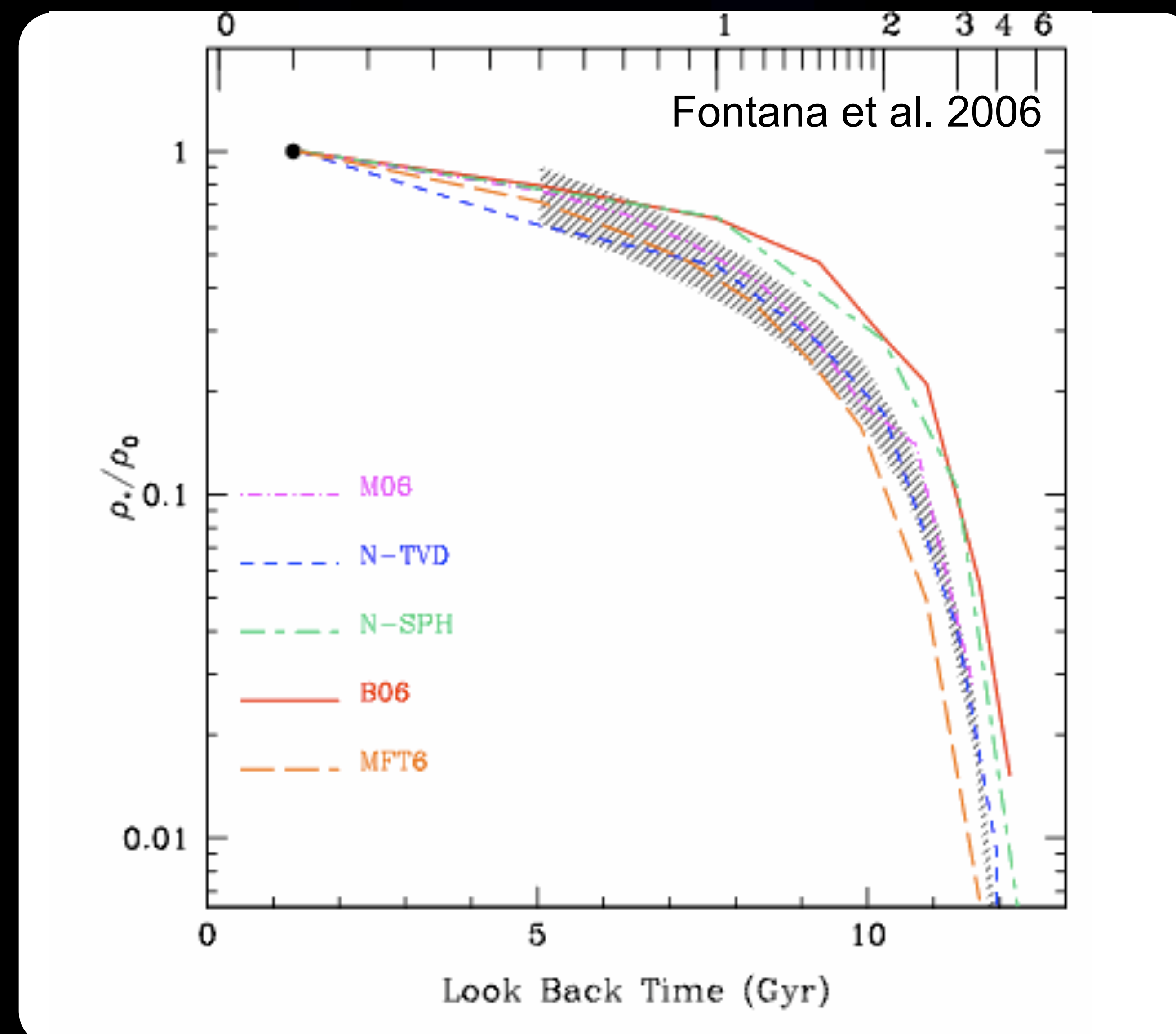

Galaxy Formation models in CDM scenario

Local properties:

gas content
luminosity distribution
disk sizes
distribution of the stellar mass content

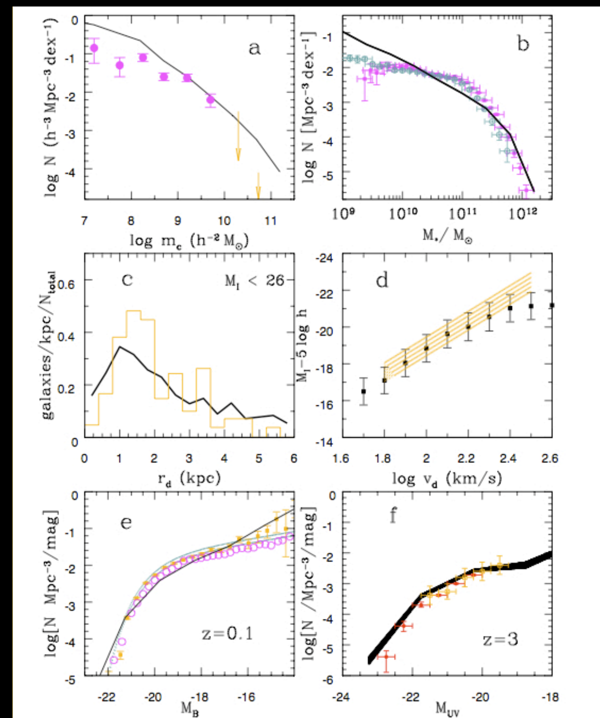

NM et al. 2006

properties of distant galaxies:

luminosity distribution
evolution of the star formation rate

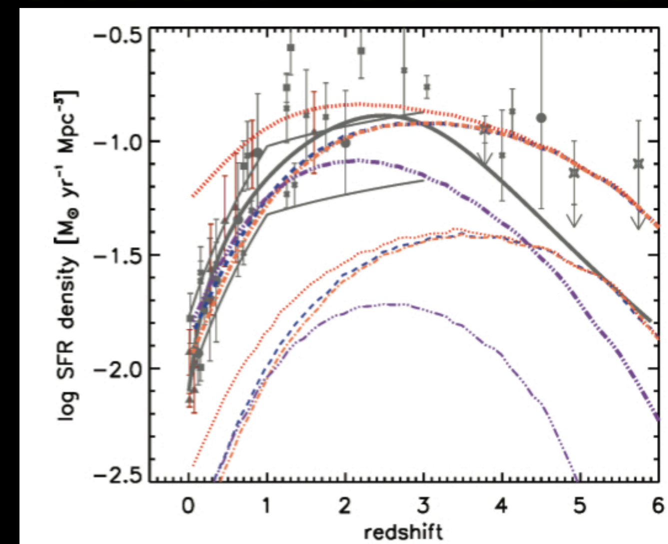

Somerville et al. 2010

NM et al. 2006

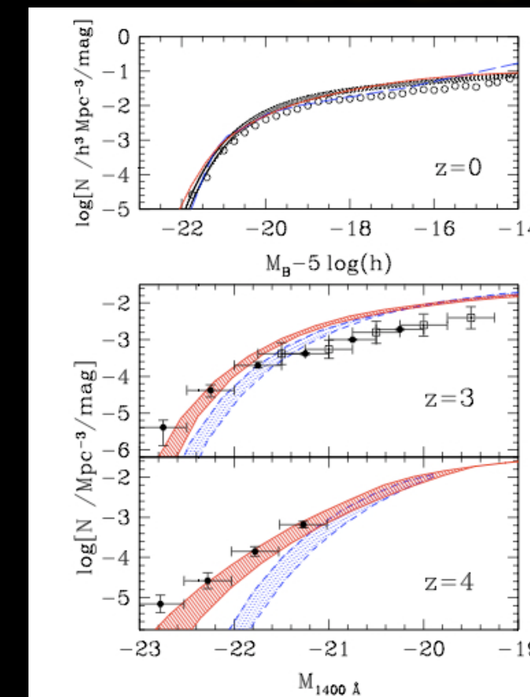

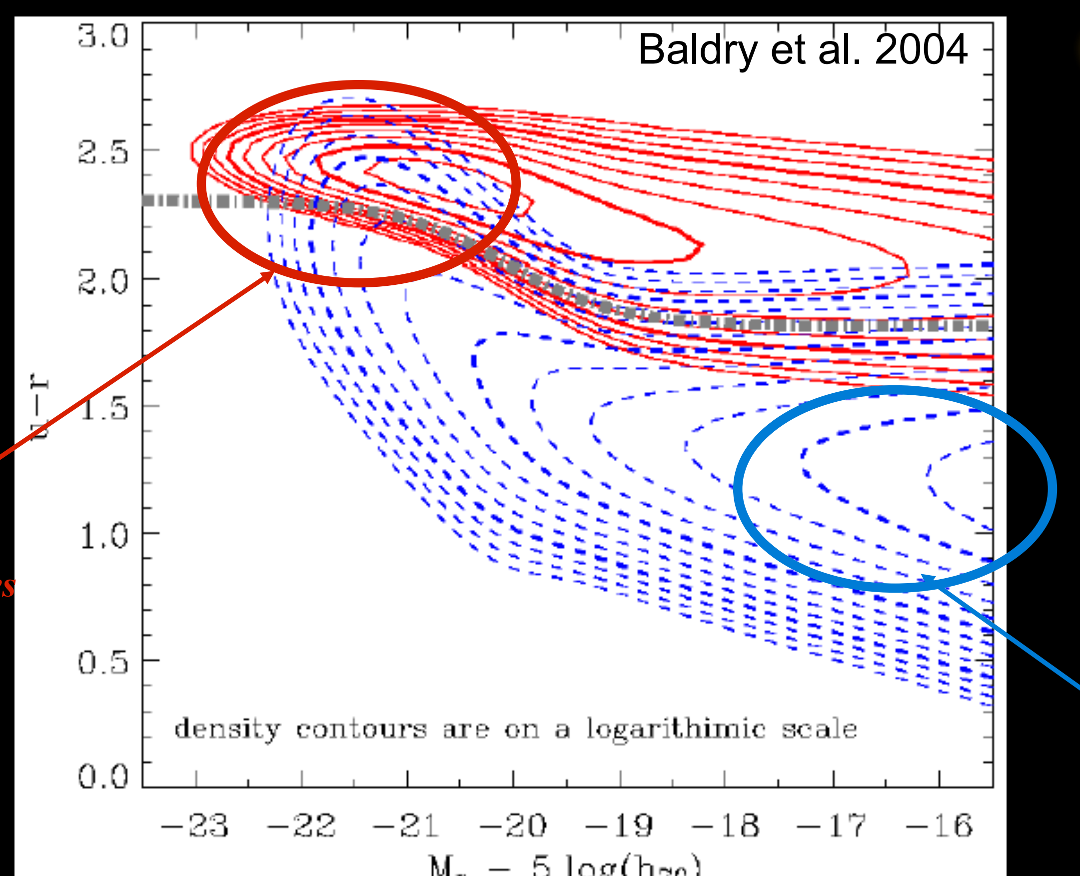

Color Distributions: bimodal distribution (early type vs late type)

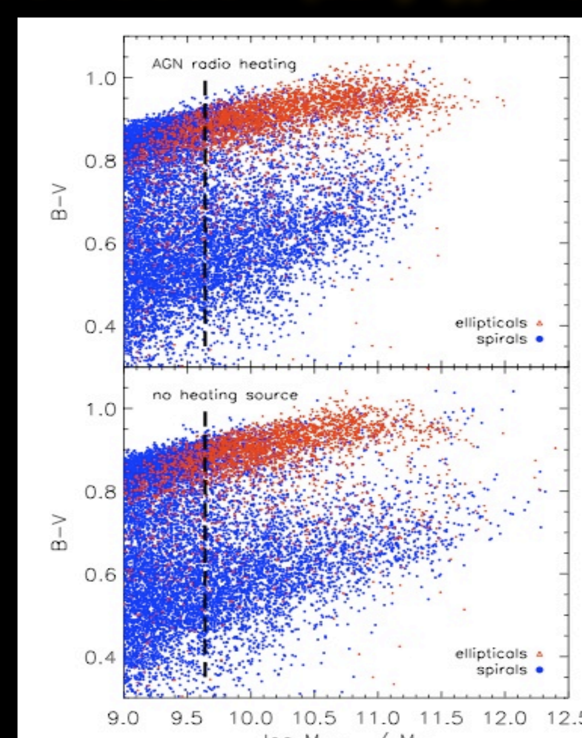

Croton et al. 2006

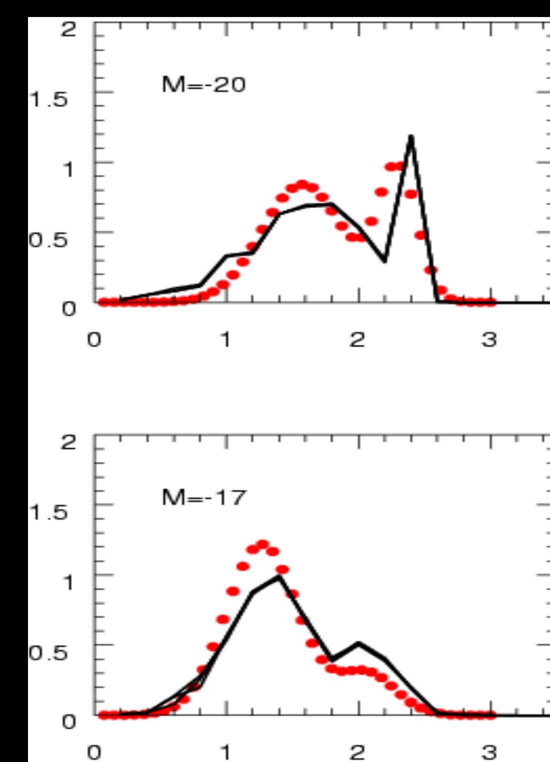

NM et al. 2008

Critical Issues

Overabundance of low-mass objects

i) abundance of satellite DM haloes
ii) density profiles
iii) abundance of faint galaxies
iv) abundance of faint AGN
v) star formation histories of satellites
vi) the v_{max}-M_* relation

1) Dependence on specific theoretical model
2) Dependence on star formation and feedback effects
3) Solution in WDM scenario

Critical Issues

i) satellite DM haloes

CDM Substructure in simulated cluster and galaxy haloes look similar.

Expected number of satellites in Milky Way- like galaxies in CDM largely exceeds the observed abundance.

Via Lactea simulation of a Milky Way - like galaxy
Diemand et al. 2008

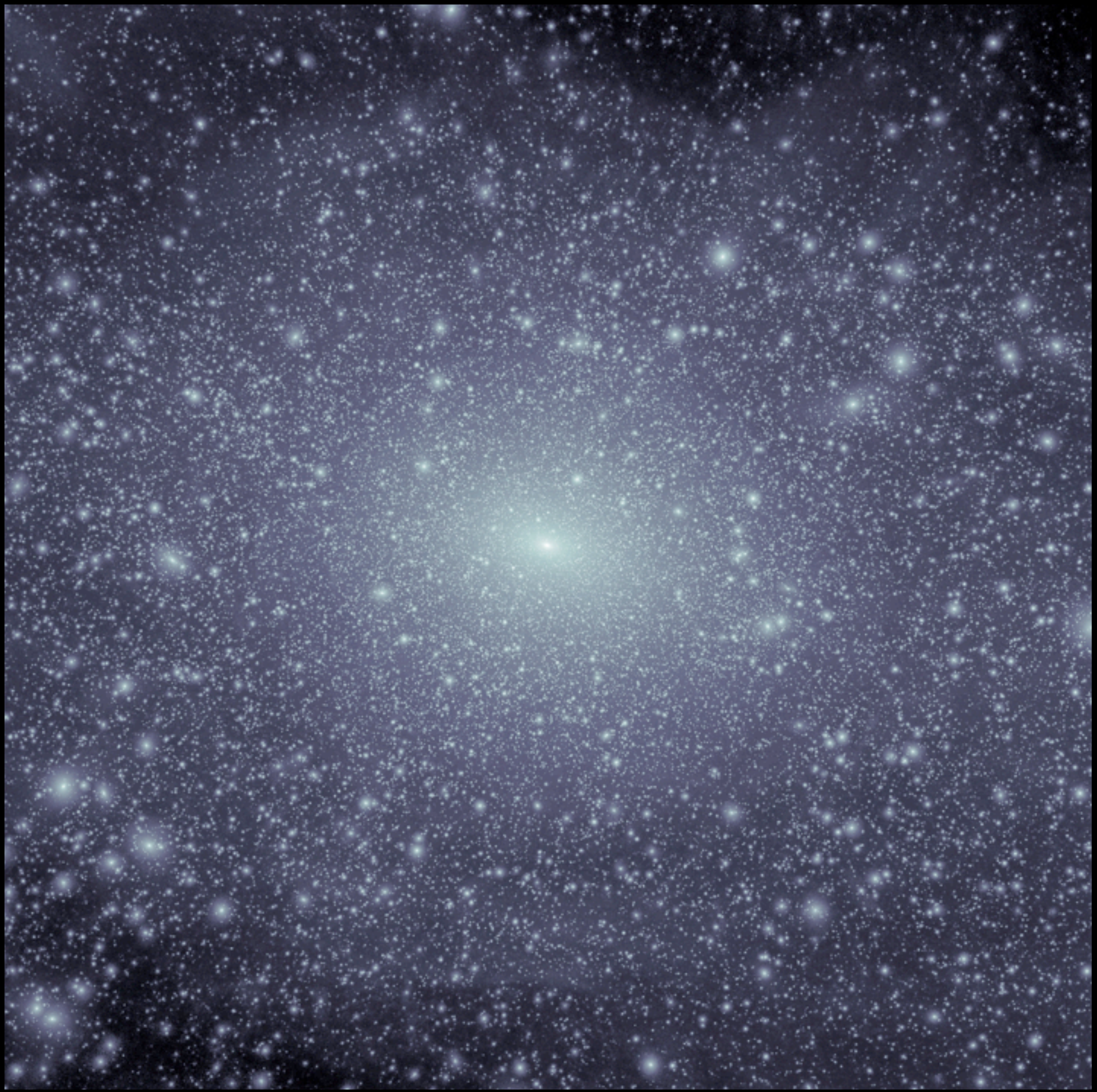

Critical Issues

CDM Substructure in simulated cluster and galaxy haloes look similar.

Expected number of satellites in Milky Way- like galaxies in CDM largely exceeds the observed abundance.

i) satellite DM haloes

Kravtsov, Klypin, Gnedin 2004

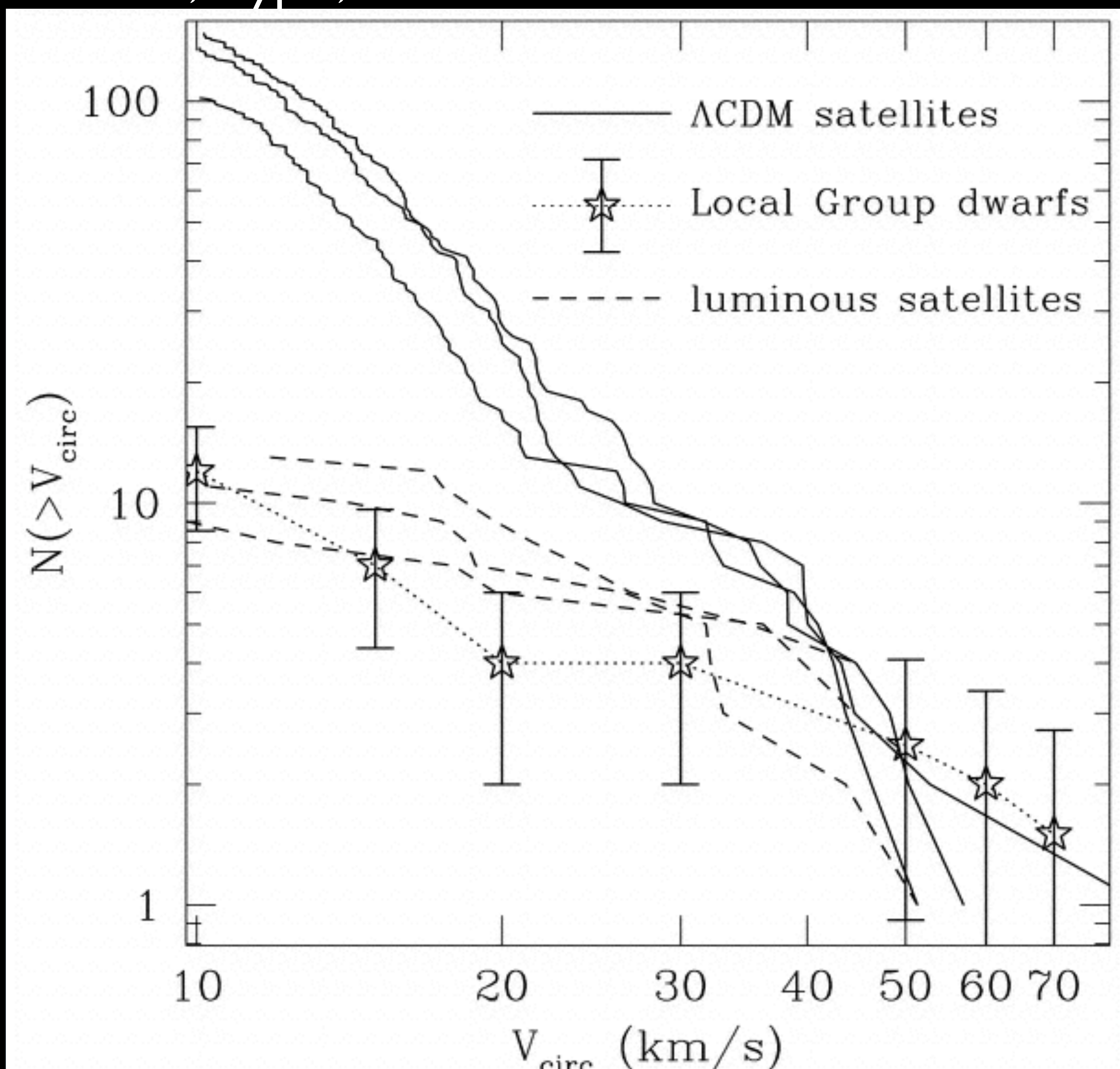

Critical Issues

ii) density profiles

Most observed dwarf galaxies consist of a rotating stellar disk embedded in a massive dark-matter halo with a near-constant-density core. Models based on the dominance of CDM, however, invariably form galaxies with dense spheroidal stellar bulges and steep central dark-matter profiles, because low-angular- momentum baryons and dark matter sink to the centres of galaxies through accretion and repeated mergers.

NFW
circular velocity profile

Moore et al. 2002

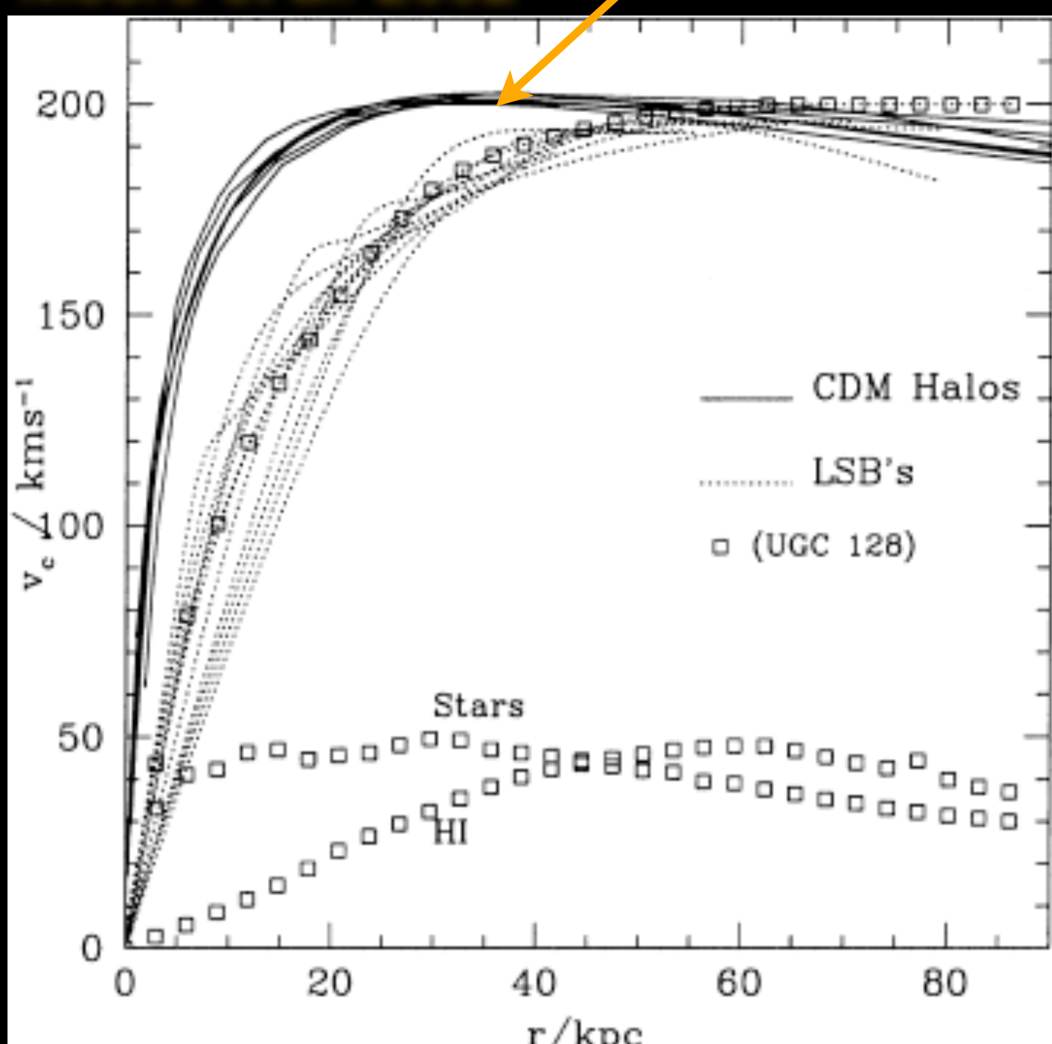

The effect of adopting a cutoff
in the power spectrum for r<8 Mpc

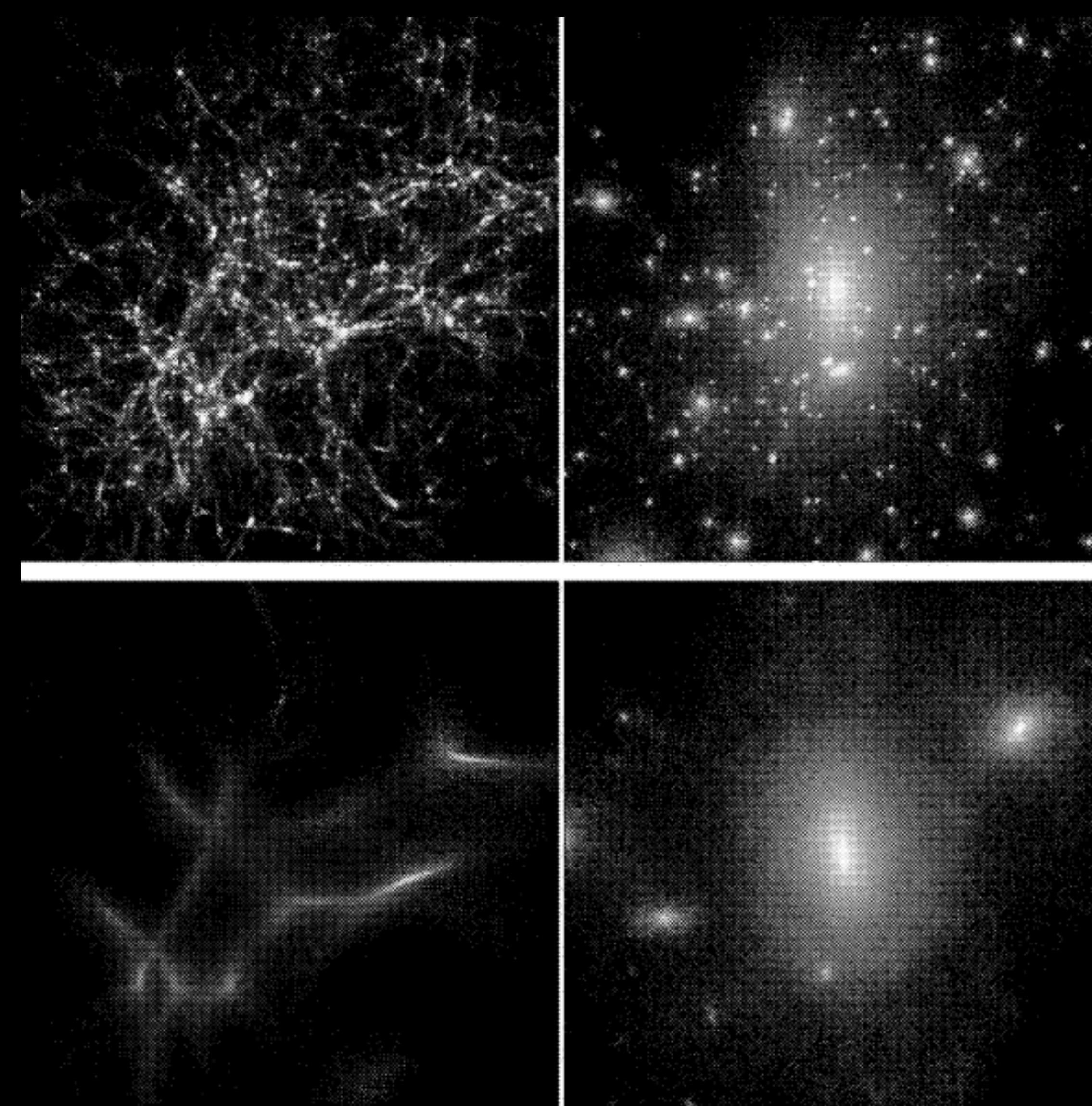

Critical Issues

iii)over-prediction of faint galaxies

In all first-generation SAM the number density of faint (low-mass) galaxies was over-predicted

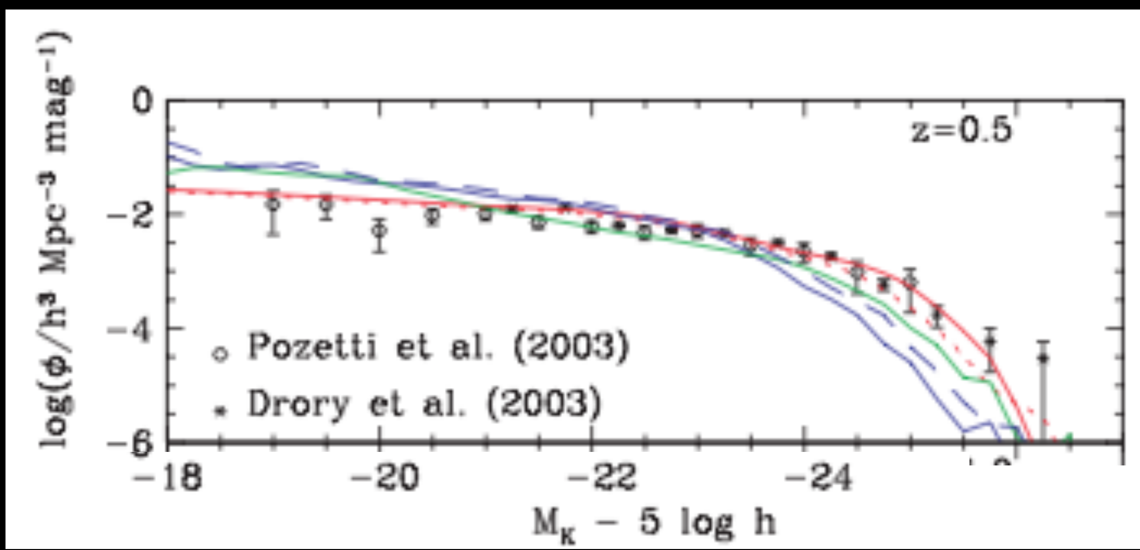

Bower et al. 2006

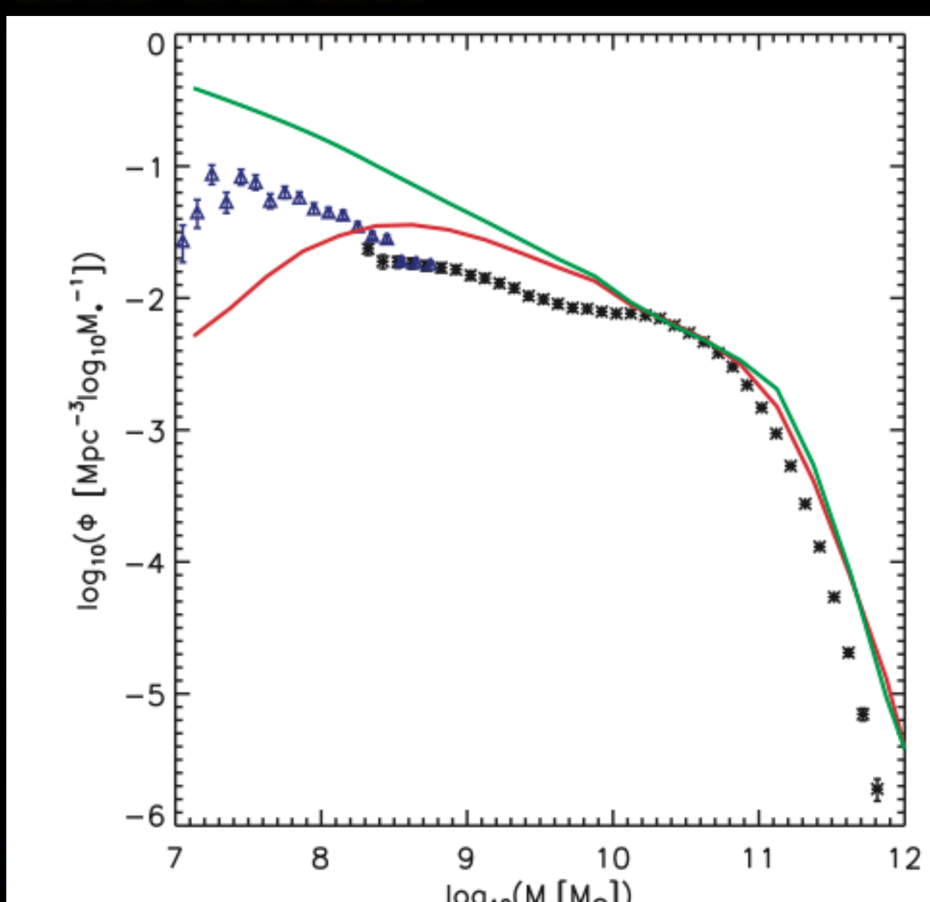

The Stellar Mass Function in the De Lucia et al. SAM based on Millenium merger trees

The K-Band Luminosity Function in the Somerville et al. SAM

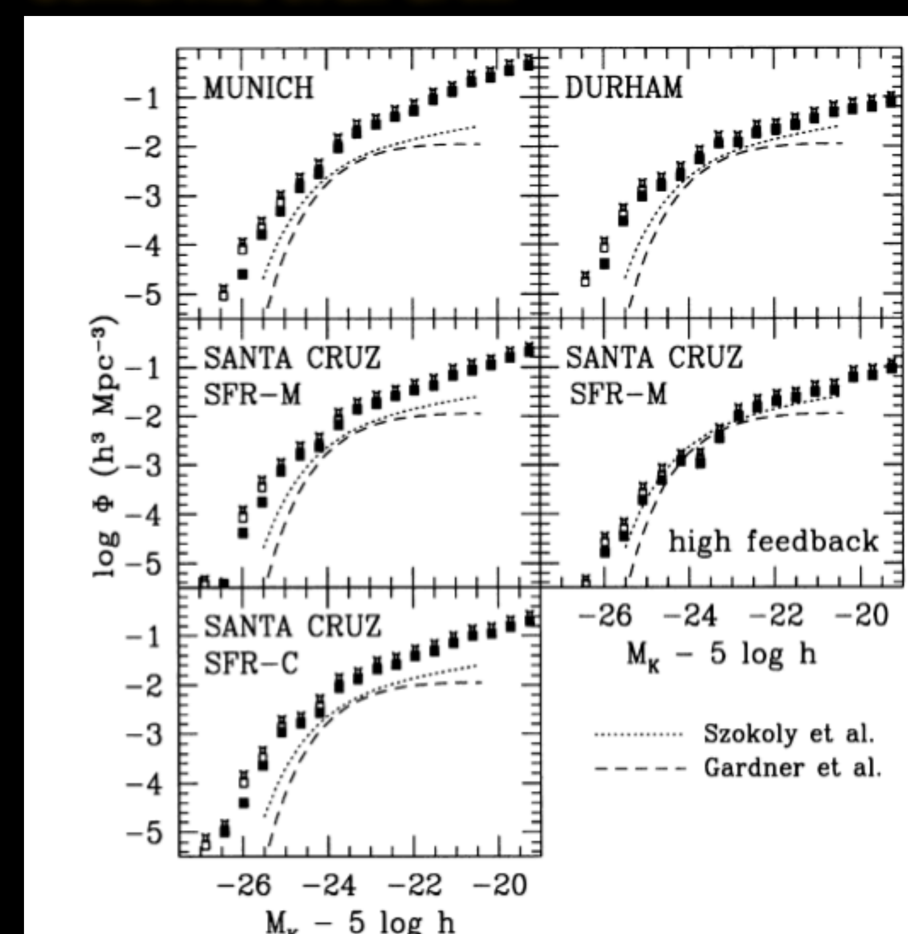

A first-order solution: feedback and UV background

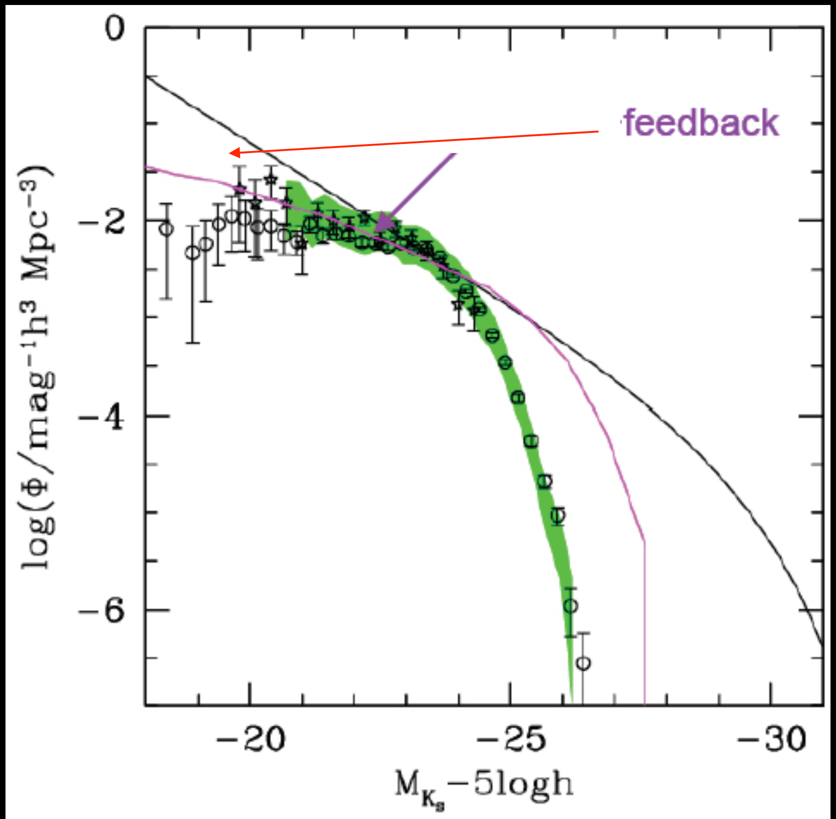

The origin of the problem:
The DM halo Mass function has a steep log slope $N \sim M^{-1.8}$
While the Observed Galaxy Luminosity Function
has a much flattter slope $N \sim L^{-1.2}$

A Possible Solution:
Suppress luminosity (star formation) in low-mass haloes $L/M \sim M^{\beta}$ $\beta=1$ - 3
Heat - Expell Gas from shallow potential wells
- Enhanced SN feedback
- UV background

$$E_{SN} \approx 10^{51}\,\eta_0\eta_{IMF}\,\Delta M_* erg/s$$

$$v_{SN} = \sqrt{E_{SN}/M_{gas}} \approx 100 \;\; km/s$$

At Z=0 the mass scale at which SN can effectively espell gas from DM potential wells

$$M_{SN} \sim 10^{10}\, M_{\odot}$$

at low z, at higher redshift the density is higher an M_{SN} increases

Vogelsberger et al. 2014

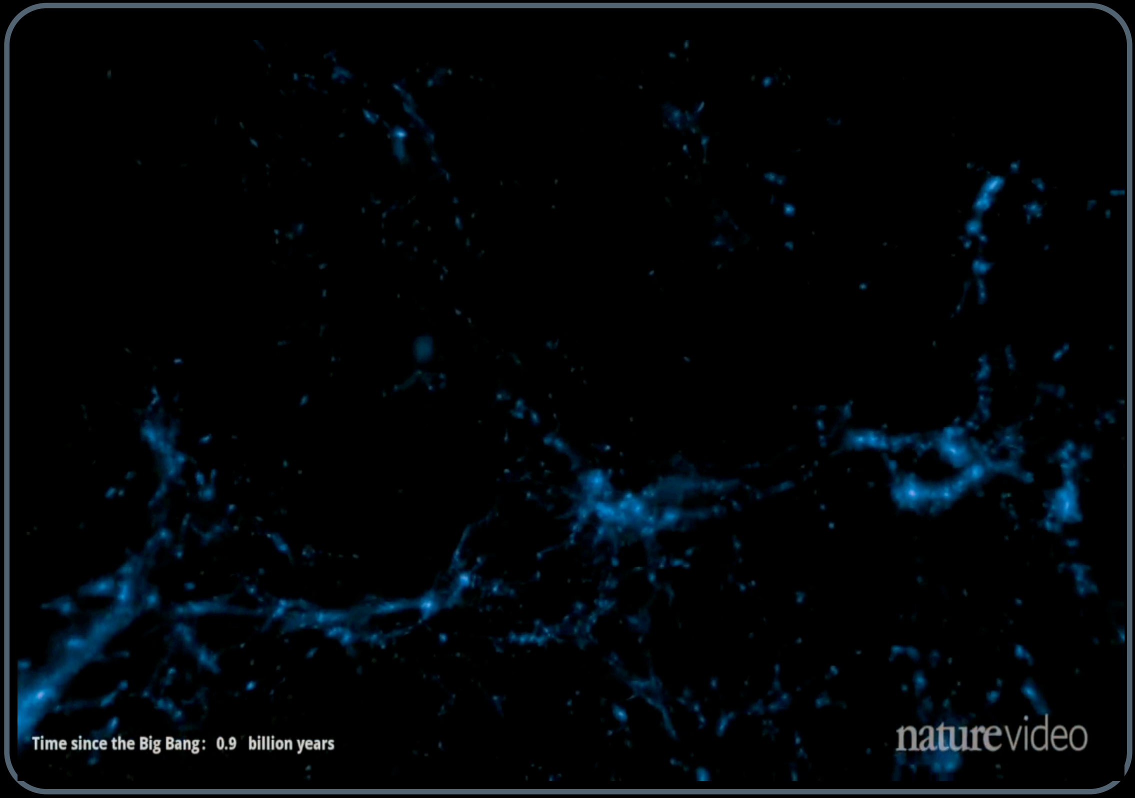

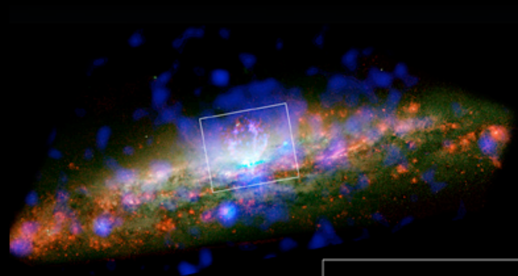

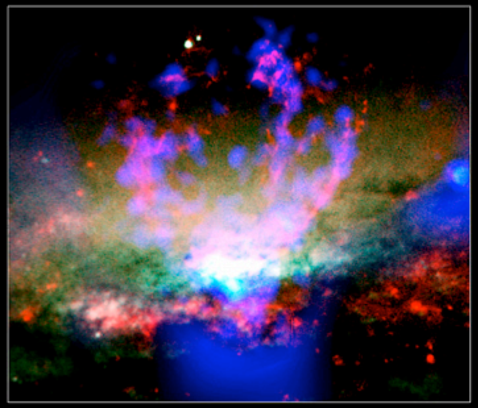

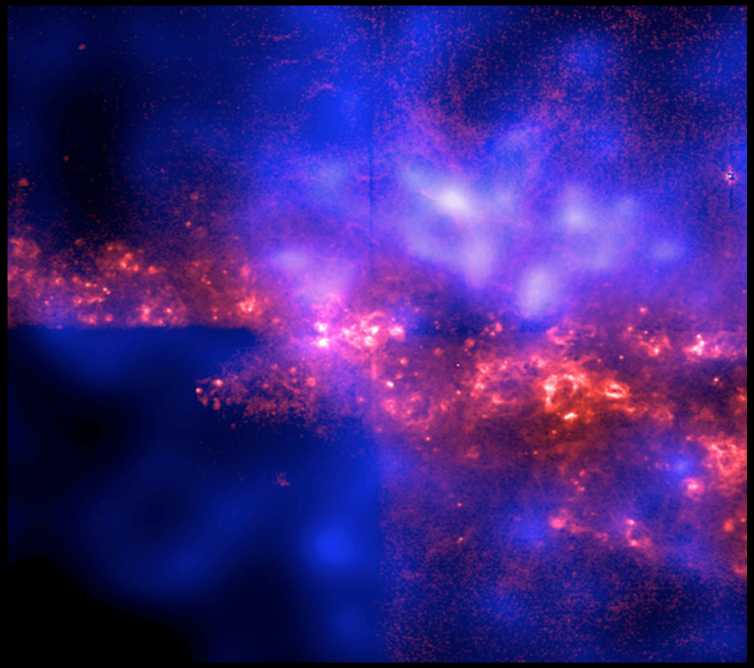

A first-order solution: feedback and UV background

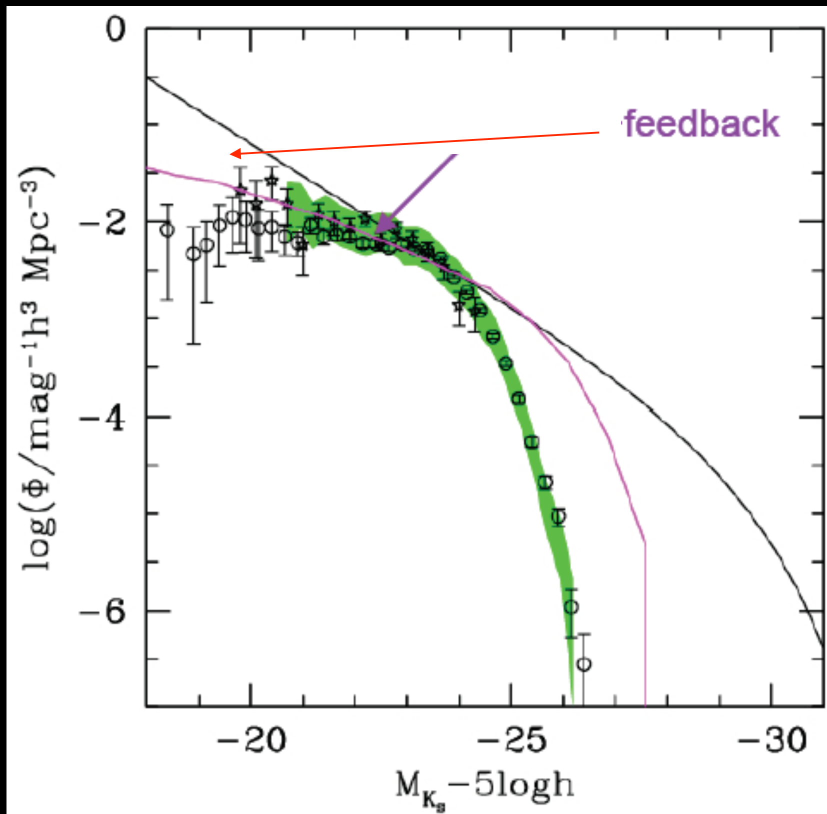

The origin of the problem:

The DM halo Mass function has a steep log slope $N \sim M^{-1.8}$

While the Observed Galaxy Luminosity Function

has a much flattter slope $N \sim L^{-1.2}$

A Possible Solution:

Suppress luminosity (star formation) in low-mass haloes $L/M \sim M^{\beta}$ $\beta = 1 - 3$

Heat - Expell Gas from shallow potential wells

- Enhanced SN feedback
- UV background

$$E_{SN} \approx 10^{51}\, \eta_0 \eta_{IMF}\, \Delta M_* erg/s$$

$$v_{SN} = \sqrt{E_{SN}/M_{gas}} \approx 100 \;\; km/s$$

At Z=0 the mass scale at which SN can effectively espell gas from DM potential wells

$$M_{SN} \sim 10^{10}\, M_{\odot}$$

at low z, at higher redshift the density is higher an M_{SN} increases

Vogelsberger et al. 2014

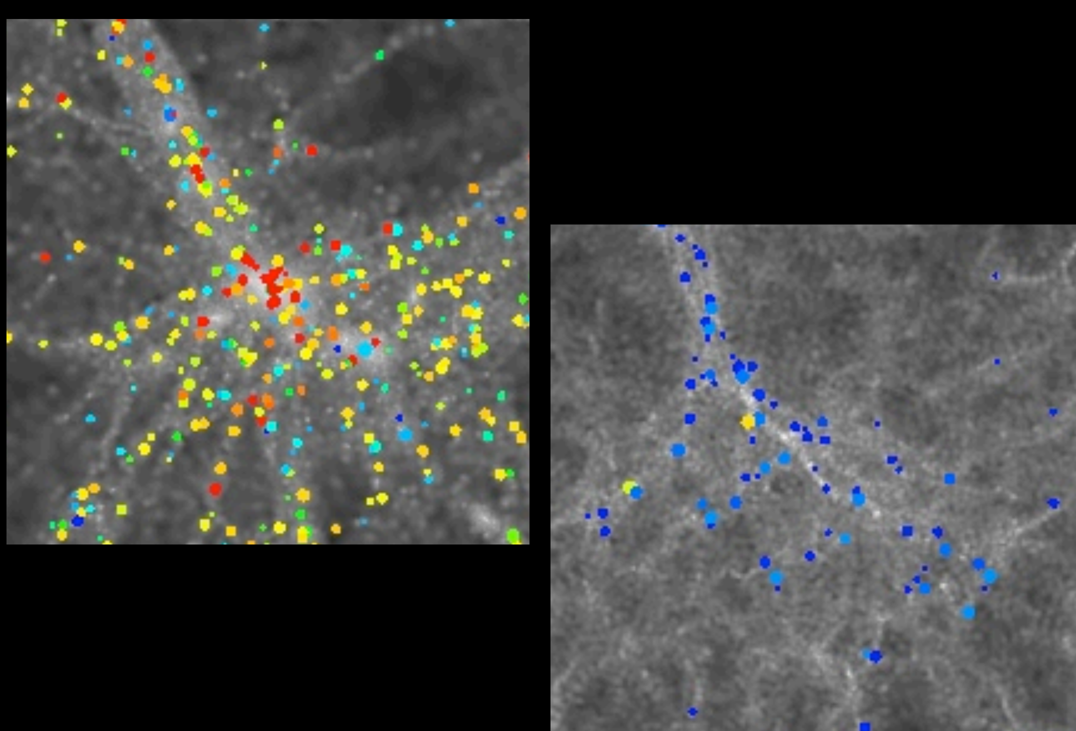

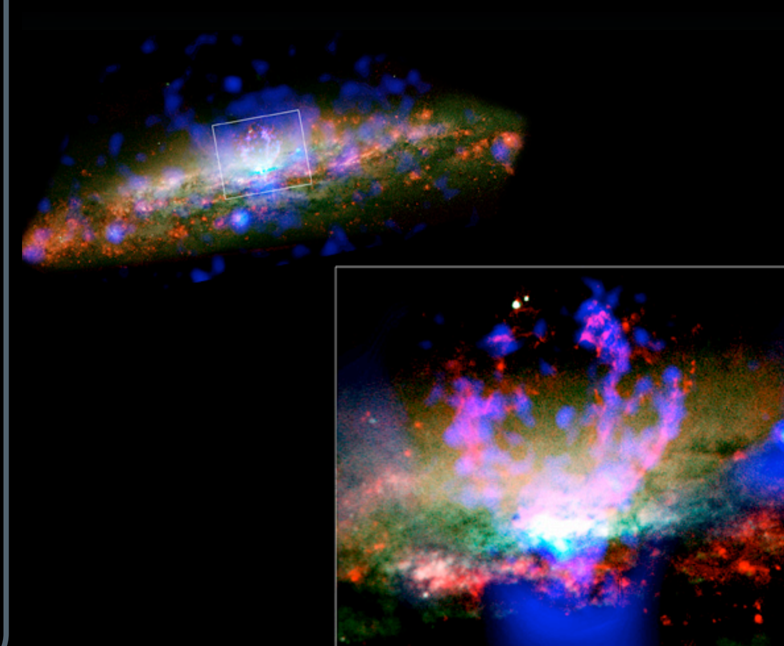

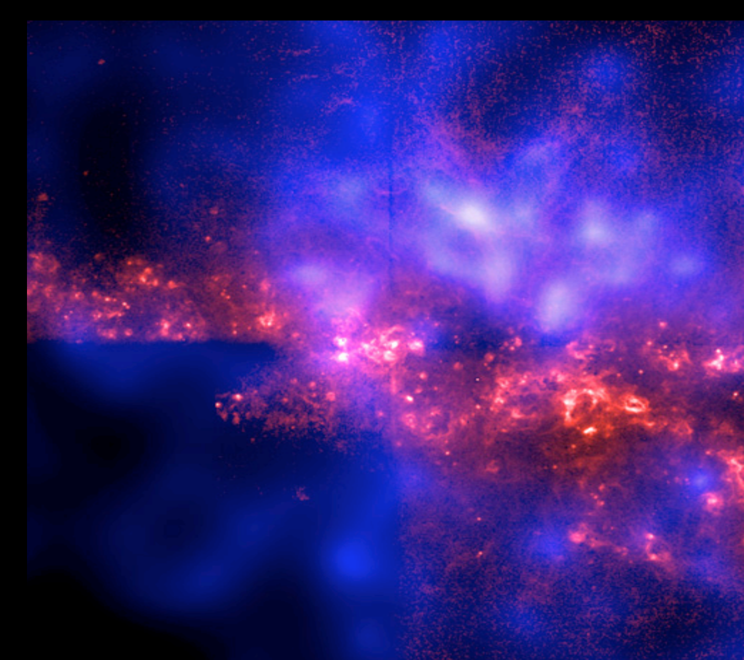

A first-order solution: feedback and UV background

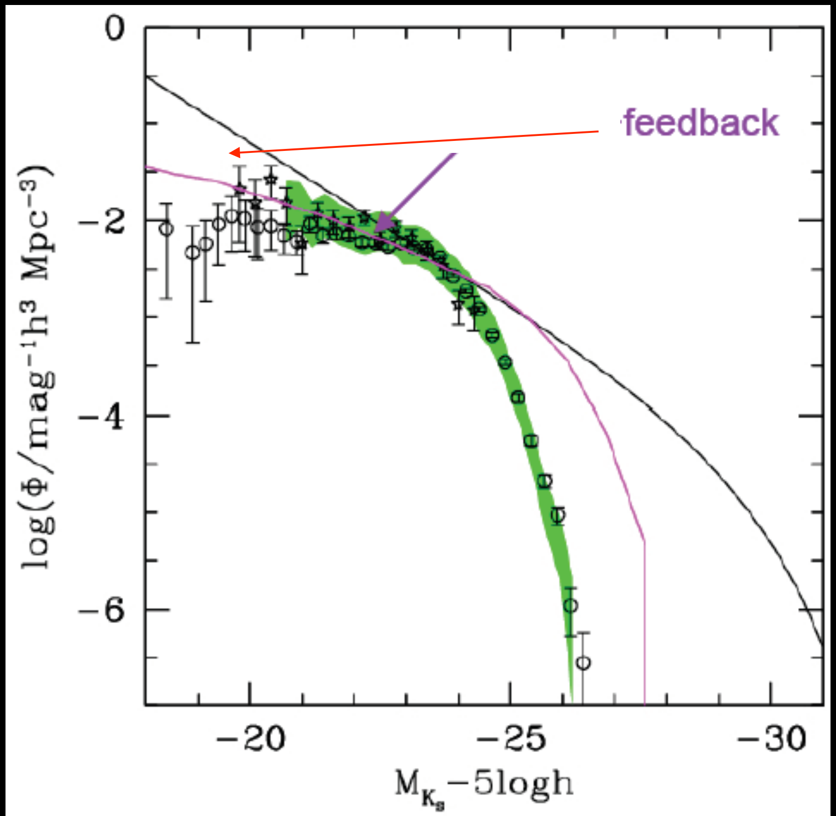

The origin of the problem:
The DM halo Mass function has a steep log slope $N \sim M^{-1.8}$
While the Observed Galaxy Luminosity Function
has a much flattter slope $N \sim L^{-1.2}$

A Possible Solution:
Suppress luminosity (star formation) in low-mass haloes $L/M \sim M^{\beta}$ $\beta = 1 - 3$
Heat - Expell Gas from shallow potential wells
- Enhanced SN feedback
- UV background

$$E_{SN} \approx 10^{51}\, \eta_0 \eta_{IMF}\, \Delta M_* erg/s$$

$$v_{SN} = \sqrt{E_{SN}/M_{gas}} \approx 100 \quad km/s$$

At Z=0 the mass scale at which
SN can effectively espell gas from
DM potential wells

$$M_{SN} \sim 10^{10}\, M_{\odot}$$

at low z, at higher redshift the
density is higher an M_{SN} increases

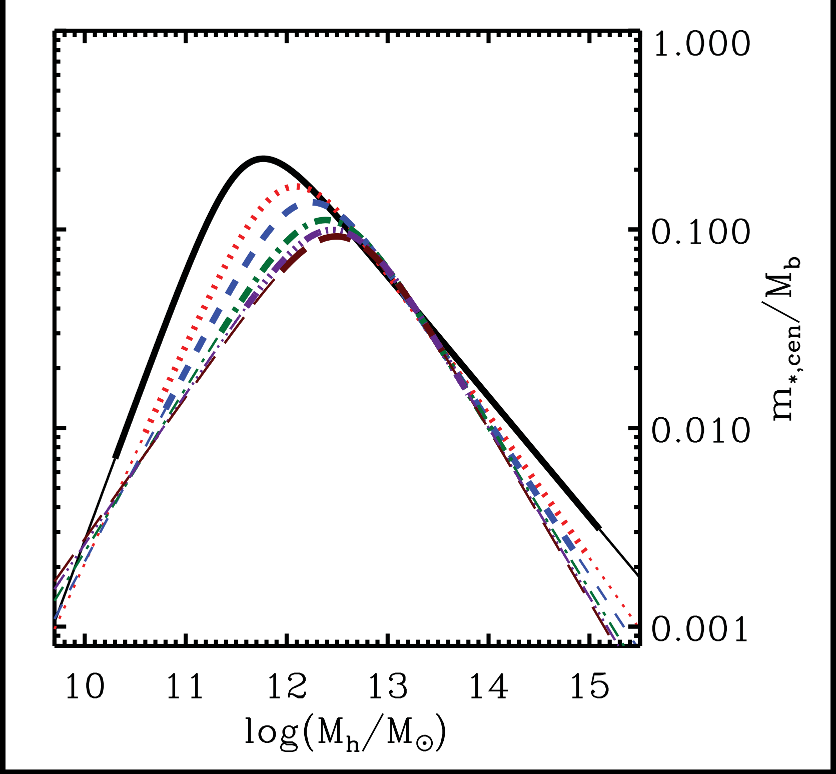

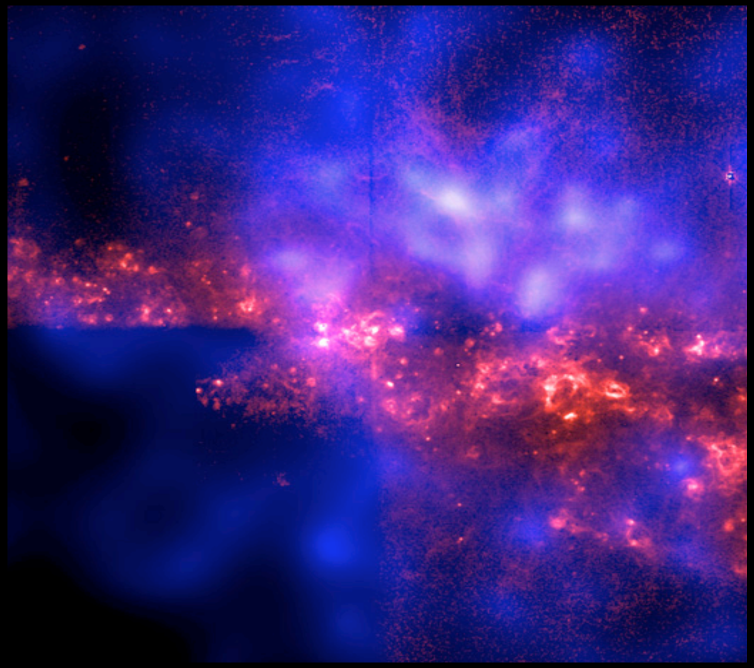

Moster et al. 2014

Feedback and UV background

i) the abundance of satellites

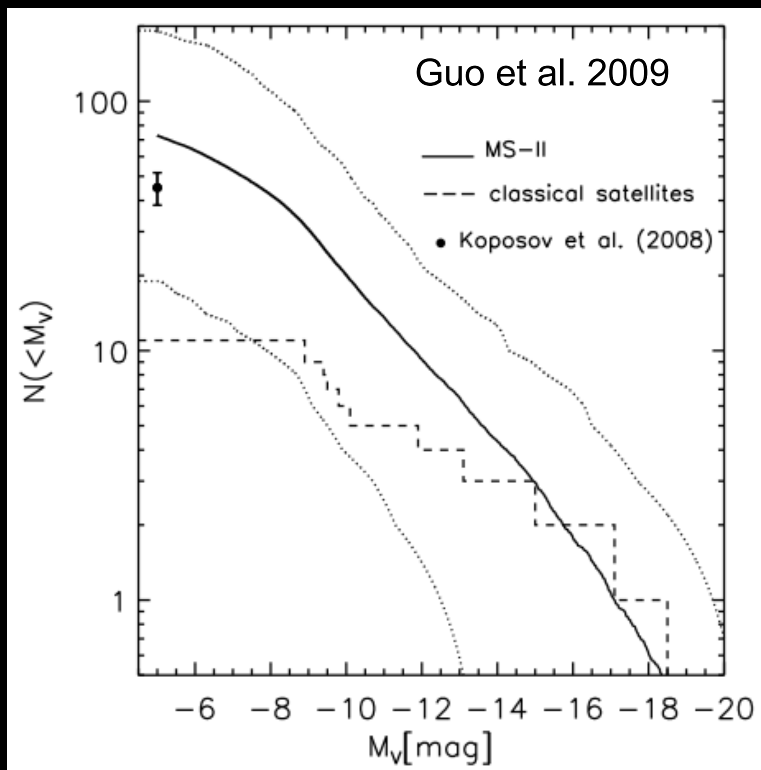

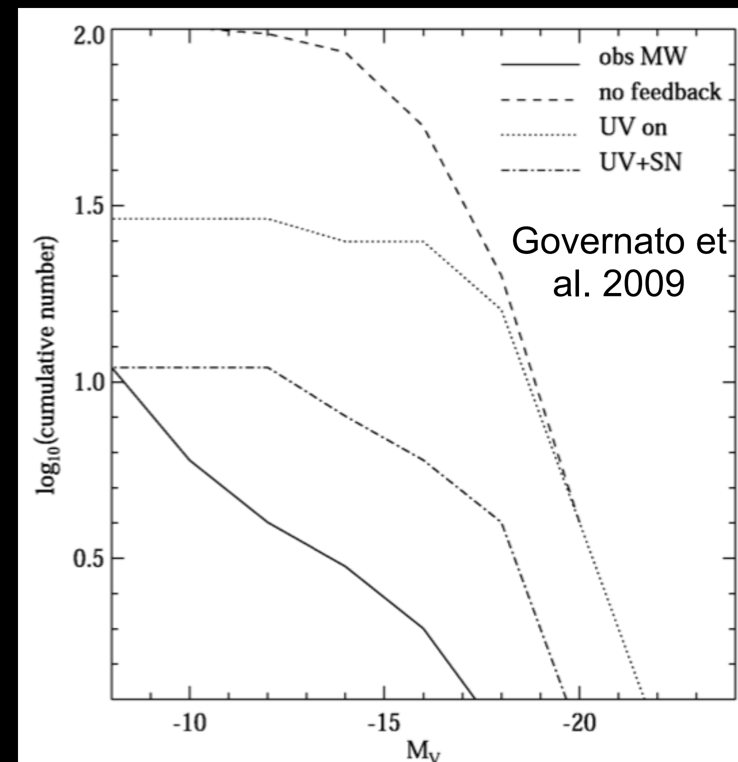

Brooks & Zolotov 2014

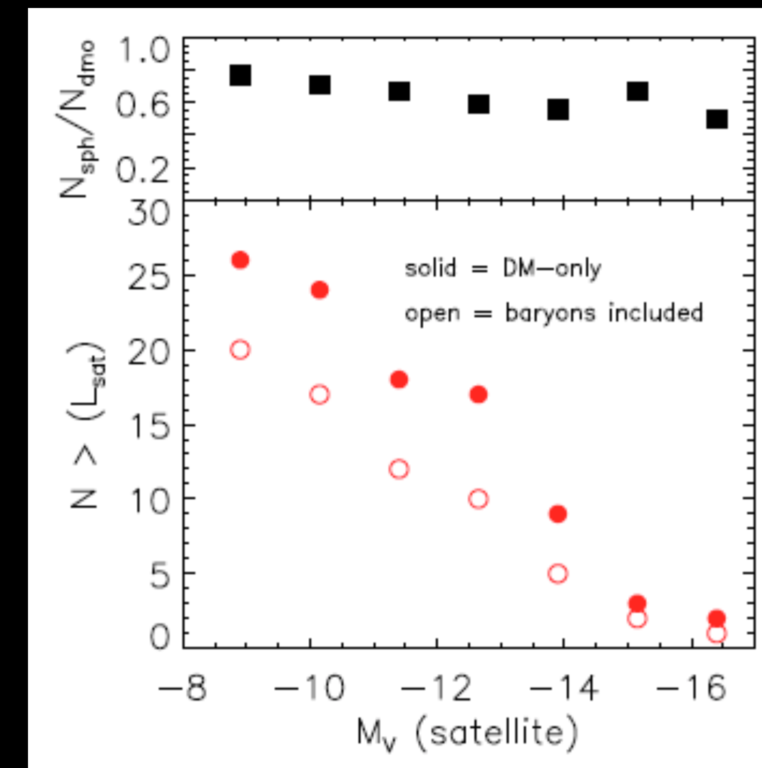

ii) the abundance of faint galaxies

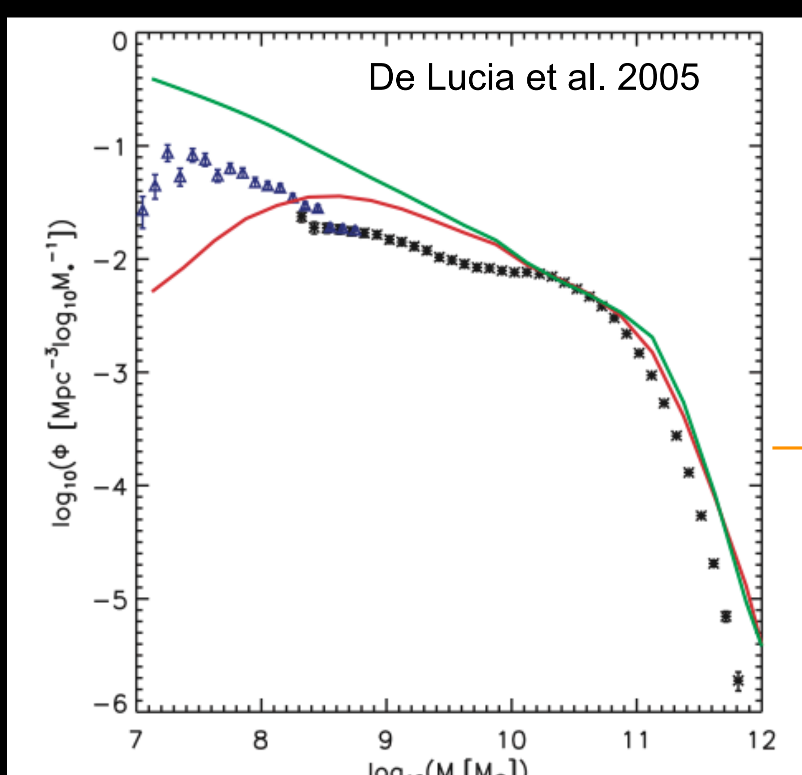

Refined treatment of Gas and Stellar Stripping

Enhanced (tuned) feedback dependence on the circular velocity of the DM halo

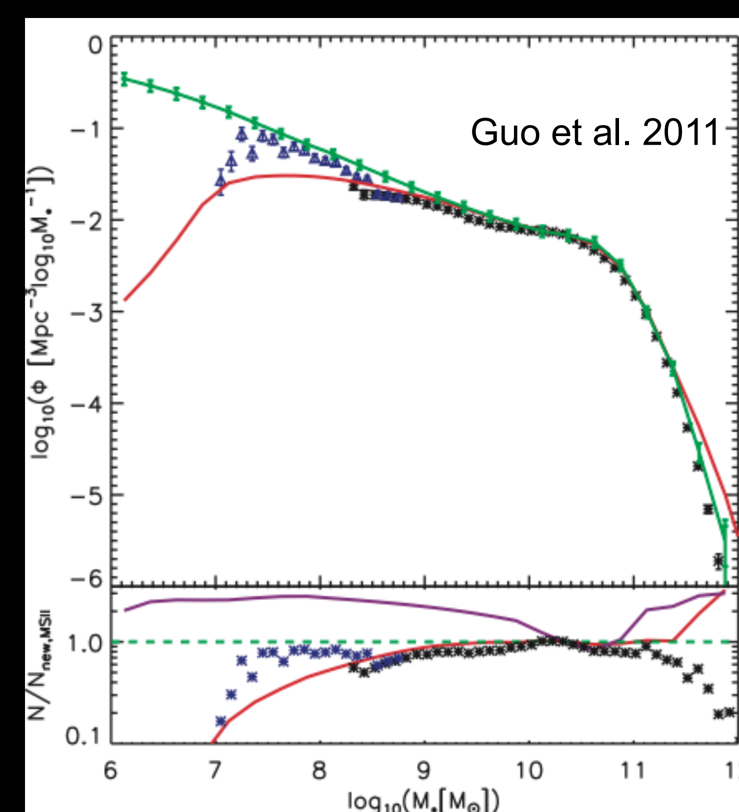

Feedback and UV background

iii) the density profiles

A proposed solution at low redshift

"… The rapid fluctuations caused by episodic feedback progressively pump energy into the DM particle orbits, so that they no longer penetrate to the centre of the halo" (Weinberg et al. 2013, Governato et al. 2012)

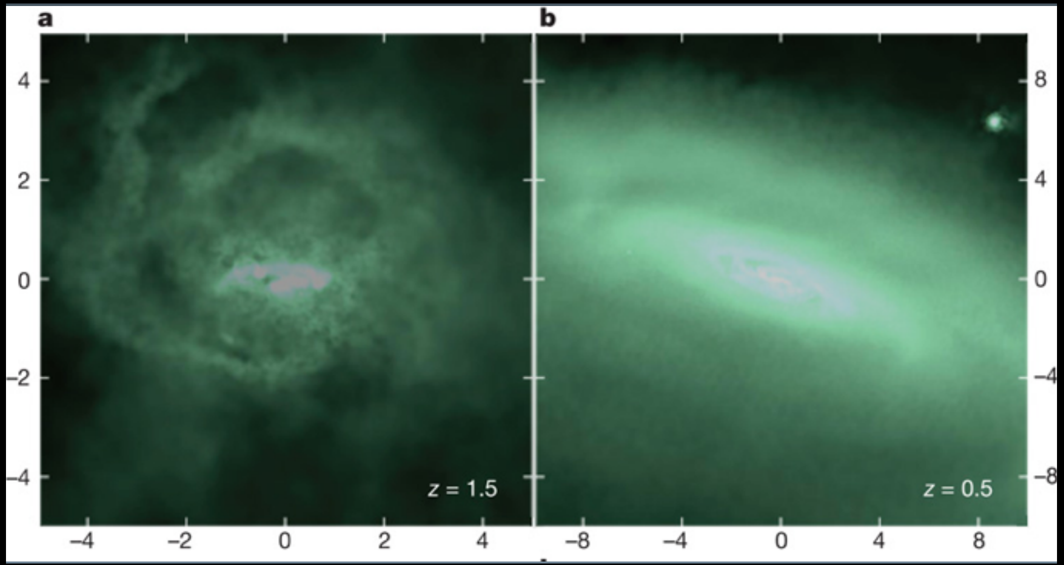

Governato et al. 2012

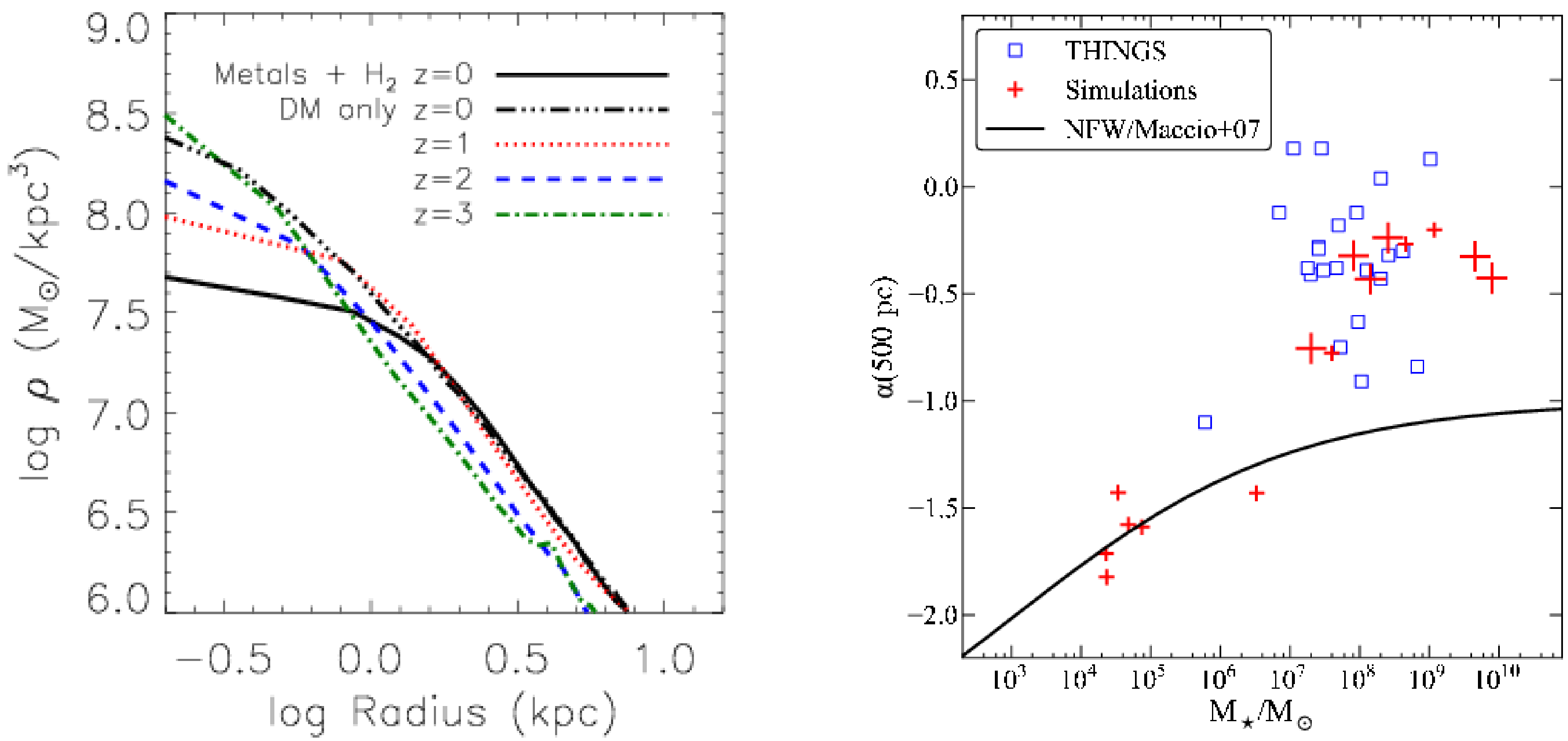

Fig. 3. Baryonic effects on CDM halo profiles in cosmological simulations, from Governato et al. (2012). *(Left)* The upper, dot-dash curve shows the cuspy dark matter density profile resulting from from a collisionless N-body simulation. Other curves show the evolution of the dark matter profile in a simulation from the same initial conditions that includes gas dynamics, star formation, and efficient feedback. By $z = 0$ (solid curve) the perturbations from the fluctuating baryonic potential have flattened the inner profile to a nearly constant density core. *(Right)* Logarithmic slope of the dark matter profile α measured at 0.5 kpc, as a function of galaxy stellar mass. Crosses show results from multiple hydrodynamic simulations. Squares show measurements from rotation curves of observed galaxies. The black curve shows the expectation for pure dark matter simulations, computed from NFW profiles with the appropriate concentration. For $M_* > 10^7 M_\odot$, baryonic effects reduce the halo profile slopes to agree with observations.

The problem persists at high redshifts

Governato et al. 2012

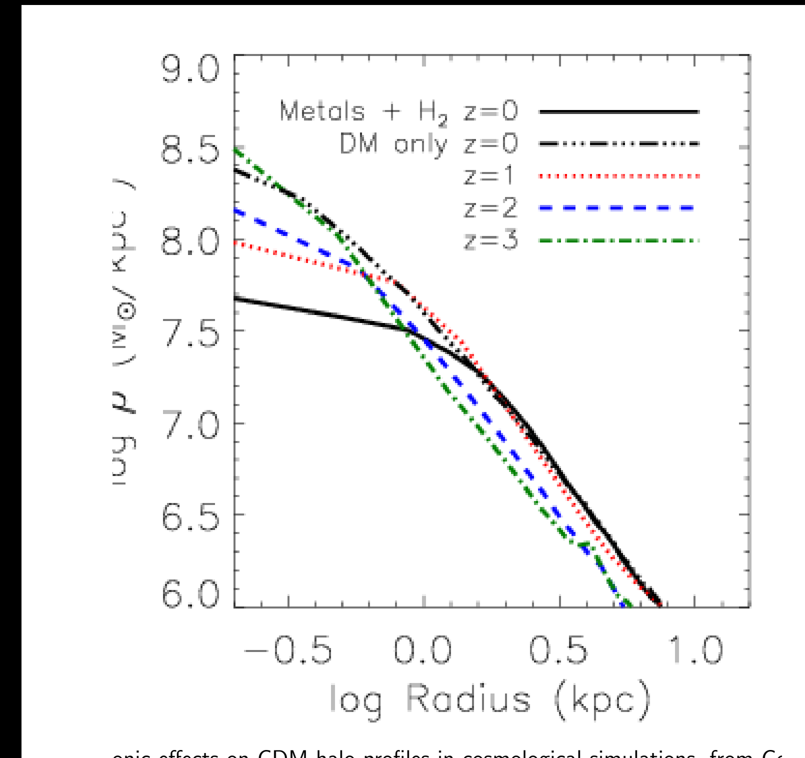

NM et al. 2006

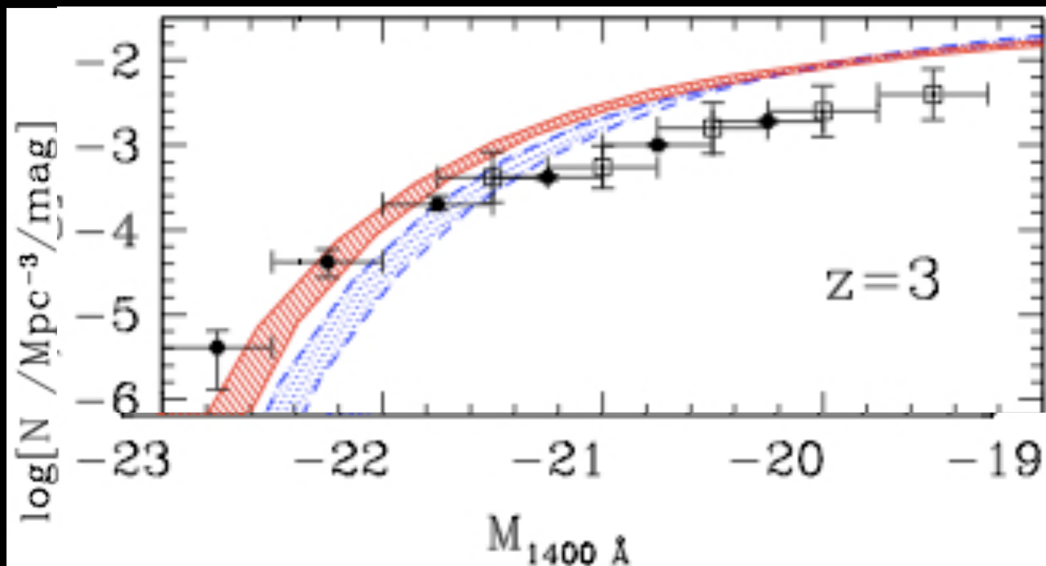

Guo et al. 2011

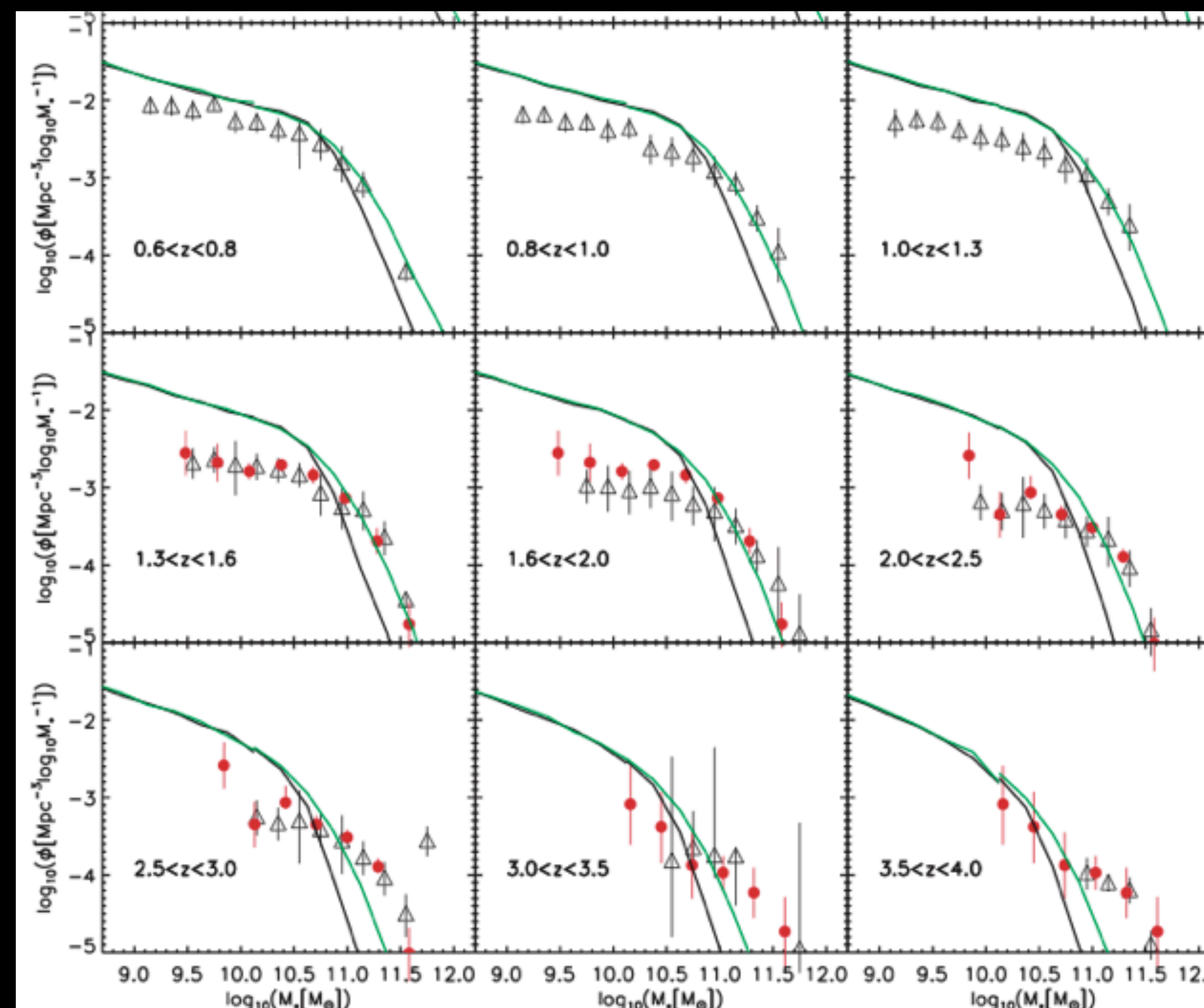

Lo Faro et al. 2009

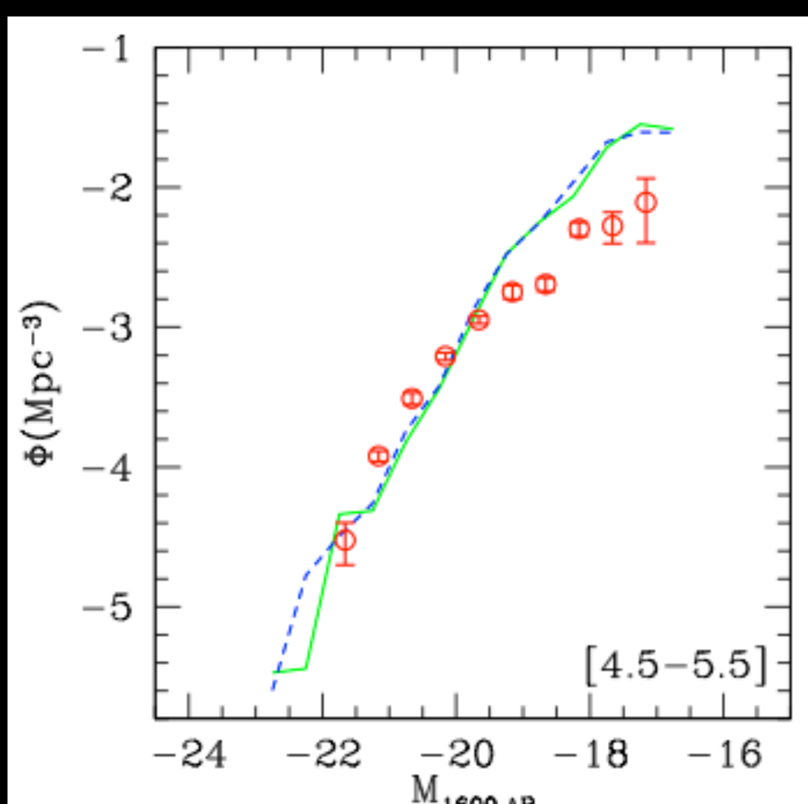

The problem persists at high redshifts

Corresponds to a mass scale affected by non-gravitational SN energy injection

$$M \approx (v_{esc}^2/G)\,r$$

$$M \approx A\,v_{esc}^3\,(1+z)^{-3/2}$$

$$r \propto (M/\rho)^{1/3}$$

$$\rho = 180\,\rho_u = 180\,\rho_u\,(1+z)^3$$

$$A \equiv \sqrt{3/G^3\,4\,\pi\,\rho_u}$$

$v_{esc} = v_{SN} \rightarrow \quad M_{SN} \approx A\,v_{SN}^3\,(1+z)^{-3/2}$

at $z \approx 0$ $\quad M_{SN} \sim 10^{10}\,M_\odot$

At high-z
larger densities imply
larger escape velocity
even for low-mass galaxies
feedback increasingly
ineffective

Lo Faro et al. 2009

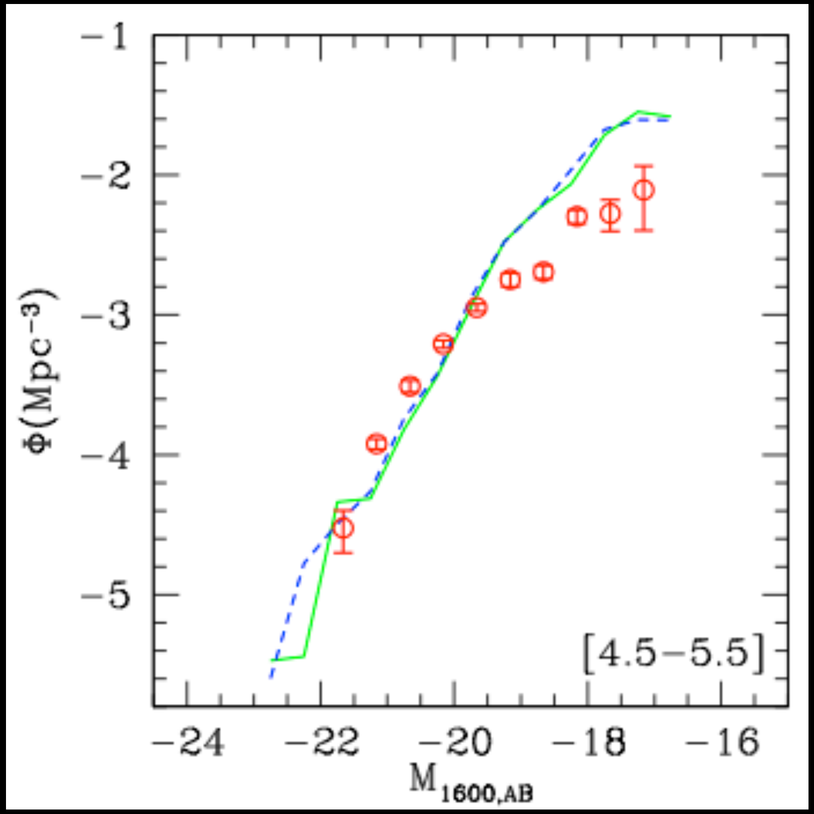

Guo et al. 2011

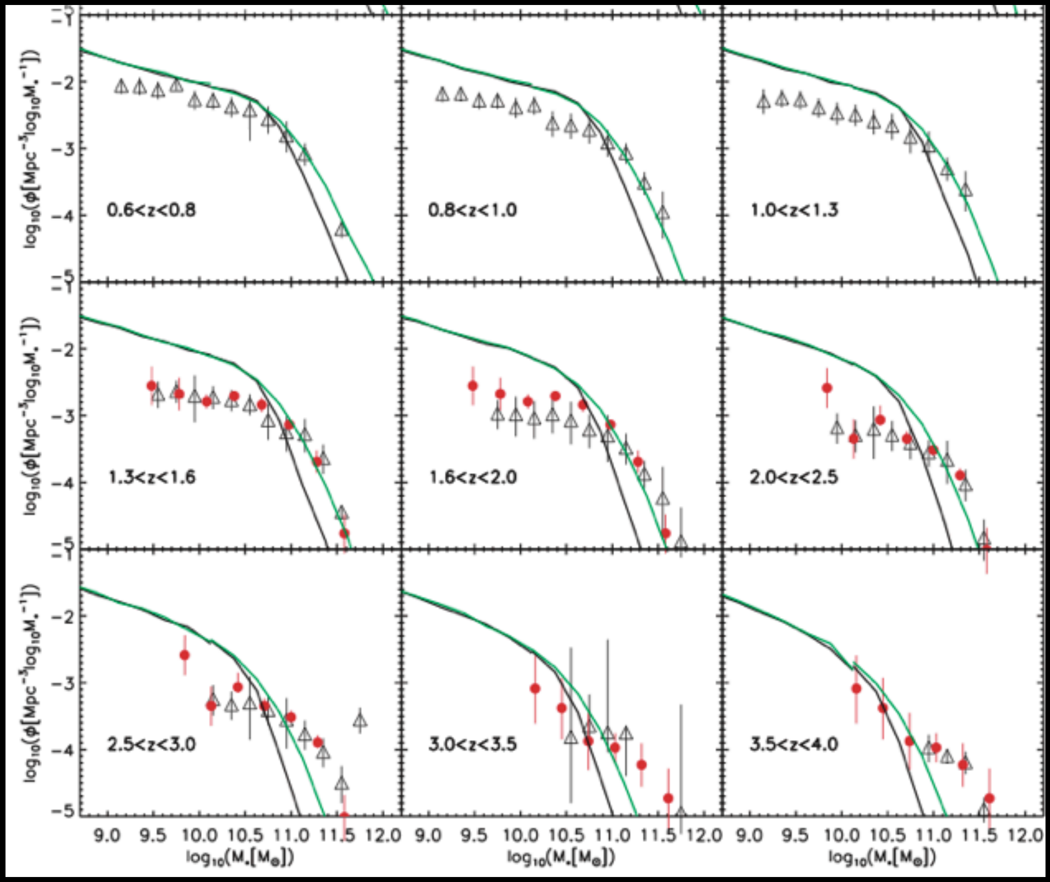

Galaxy formation in WDM Cosmology

Problem Persists at high redshifts

Too many low-mass structures

Need to suppress Power Spectrum at small scales ?

can WDM solve all problems simultaneously ?

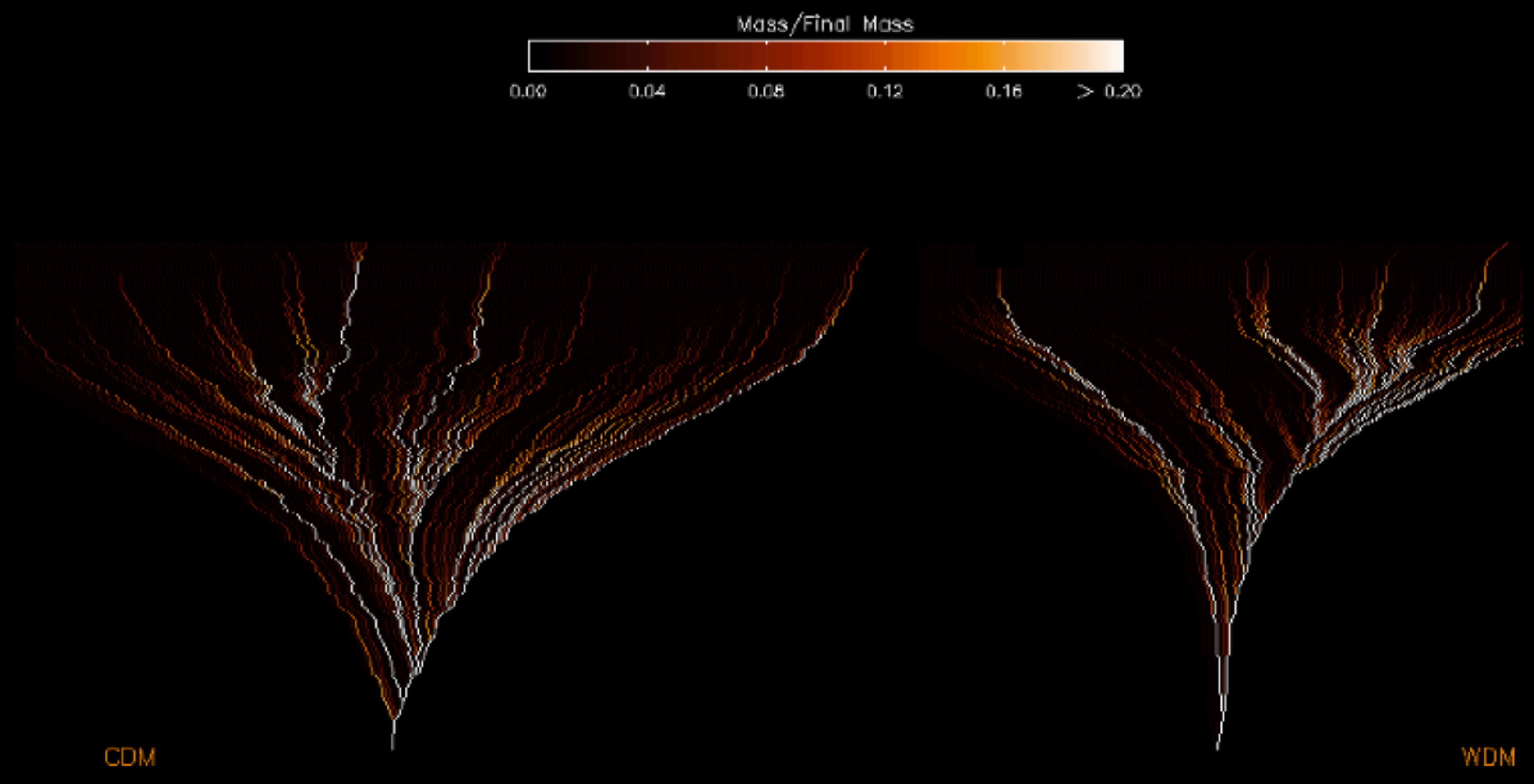

Galaxy formation in WDM Cosmology

Problem Persists at high redshifts

Too many low-mass structures

Need to suppress Power Spectrum at small scales ?

can WDM solve all problems simultaneously ?

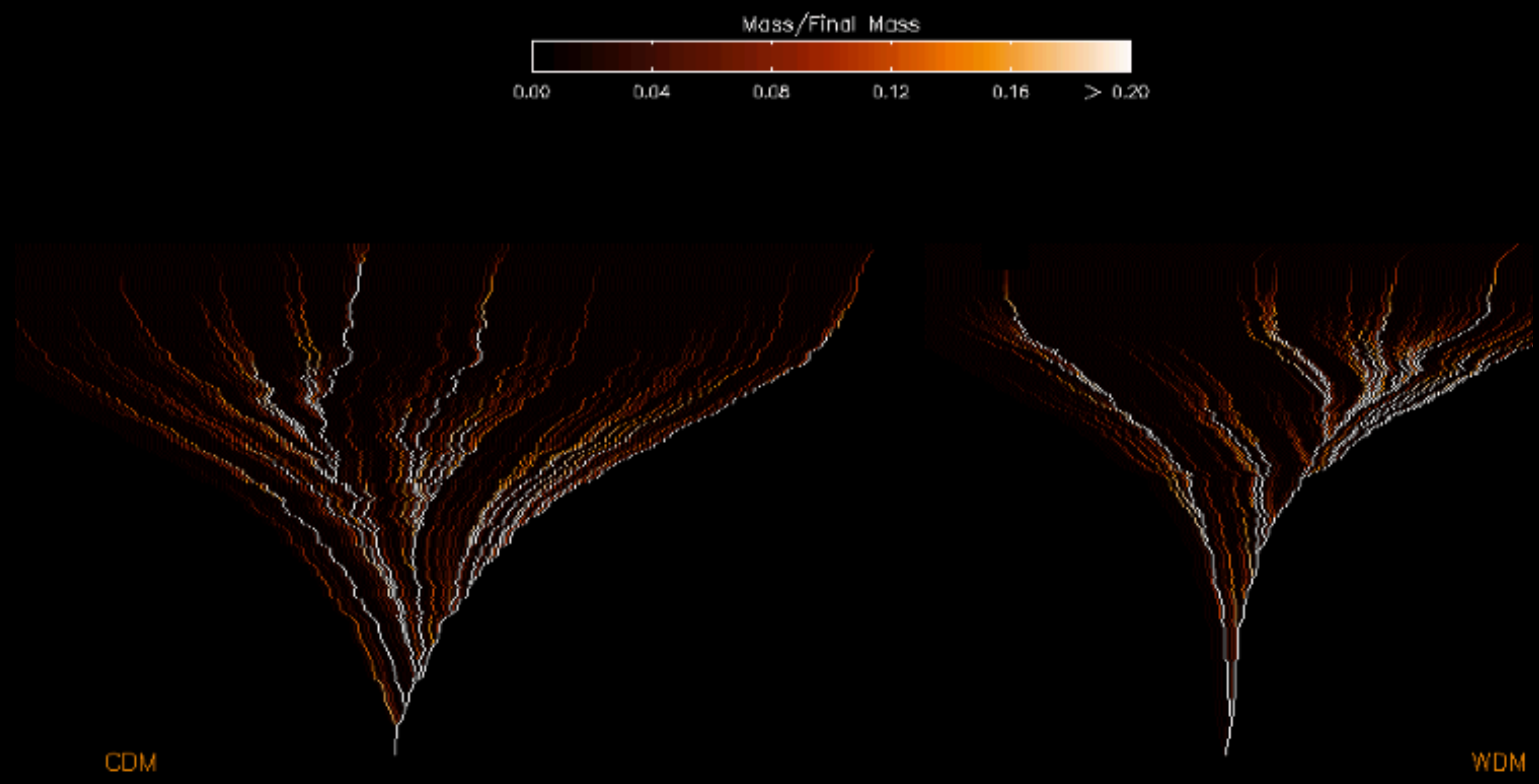

Rome PANDA model

NM, A. Lamstra

Implementing WDM power spectrum in the galaxy formation model

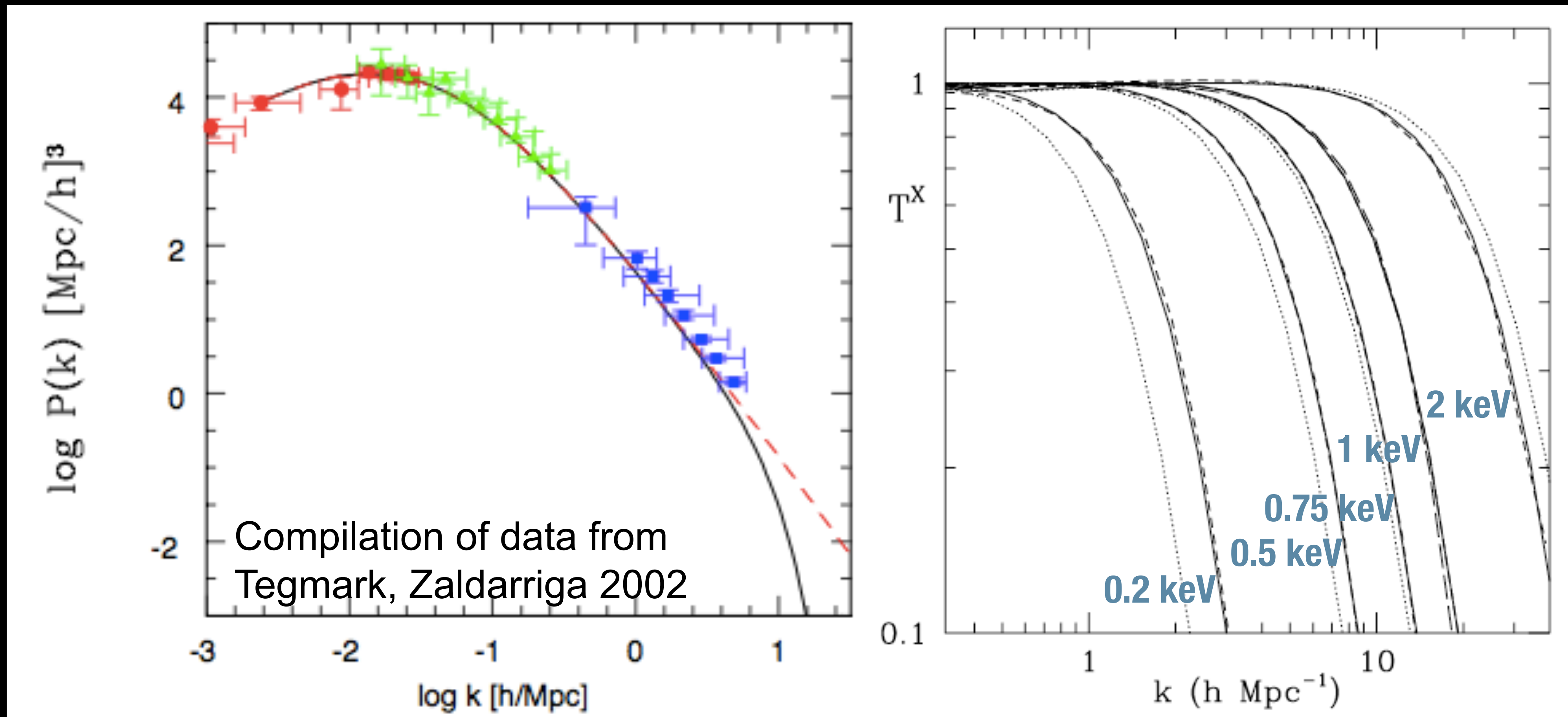

To explore the maximal effect of a power-spectrum cutoff on galaxy formation, we consider a cutoff at scales just below 0.2 Mpc, where data from Lyman-α systems (compared to N-body simulations) yields stringer upper limits on power suppression. This corresponds to mass scales M_{fs}~5 10^8 $M_\odot$

$$r_{fs} \approx 0.2 \left[\frac{\Omega_X h^2}{0.15}\right]^{1/3} \left[\frac{m_X}{rmkeV}\right]^{-4/3} \text{Mpc} \qquad \frac{P_{WDM}(k)}{P_{CDM}(k)} = \left[1 + (\alpha\, k)^{2\,\mu}\right]^{-5\,\mu}$$

$$\alpha = 0.049 \left[\frac{\Omega_X}{0.25}\right]^{0.11} \left[\frac{m_X}{\text{keV}}\right]^{-1.11} \left[\frac{h}{0.7}\right]^{1.22} h^{-1}\ \text{Mpc}$$

WDM
particle mass
1 kev

Implementing WDM power spectrum in the galaxy formation model

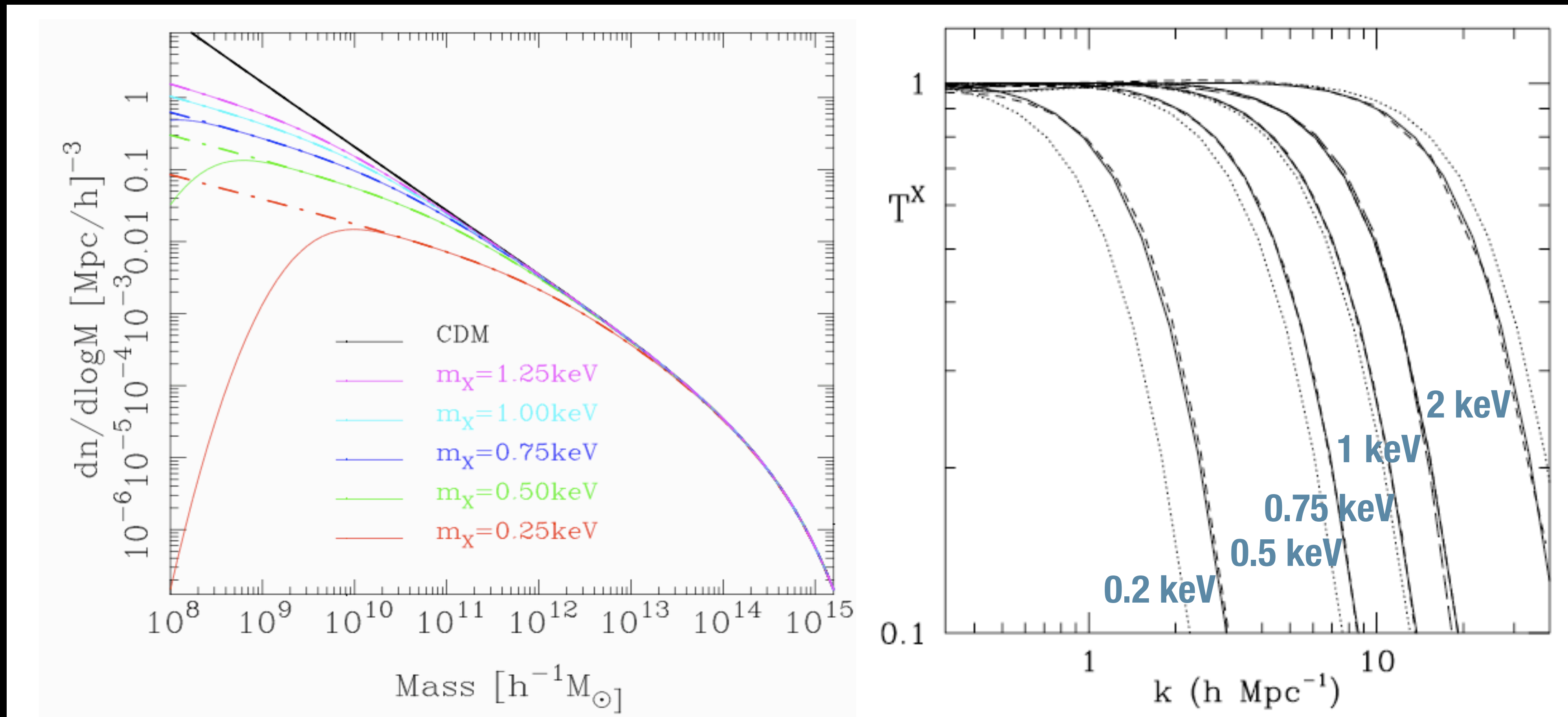

To explore the maximal effect of a power-spectrum cutoff on galaxy formation, we consider a cutoff at scales just below 0.2 Mpc, where data from Lyman-α systems (compared to N-body simulations) yields stringer upper limits on power suppression. This corresponds to mass scales M_{fs}~5 10^8 $M_\odot$

$$r_{fs} \approx 0.2 \left[\frac{\Omega_X\, h^2}{0.15}\right]^{1/3} \left[\frac{m_X}{rmkeV}\right]^{-4/3} \mathrm{Mpc} \qquad \frac{P_{WDM}(k)}{P_{CDM}(k)} = \left[1 + (\alpha\, k)^{2\,\mu}\right]^{-5\,\mu}$$

$$\alpha = 0.049 \left[\frac{\Omega_X}{0.25}\right]^{0.11} \left[\frac{m_X}{\mathrm{keV}}\right]^{-1.11} \left[\frac{h}{0.7}\right]^{1.22} h^{-1}\ \mathrm{Mpc}$$

WDM
particle mass
1 kev

Implementing WDM power spectrum in the galaxy formation model

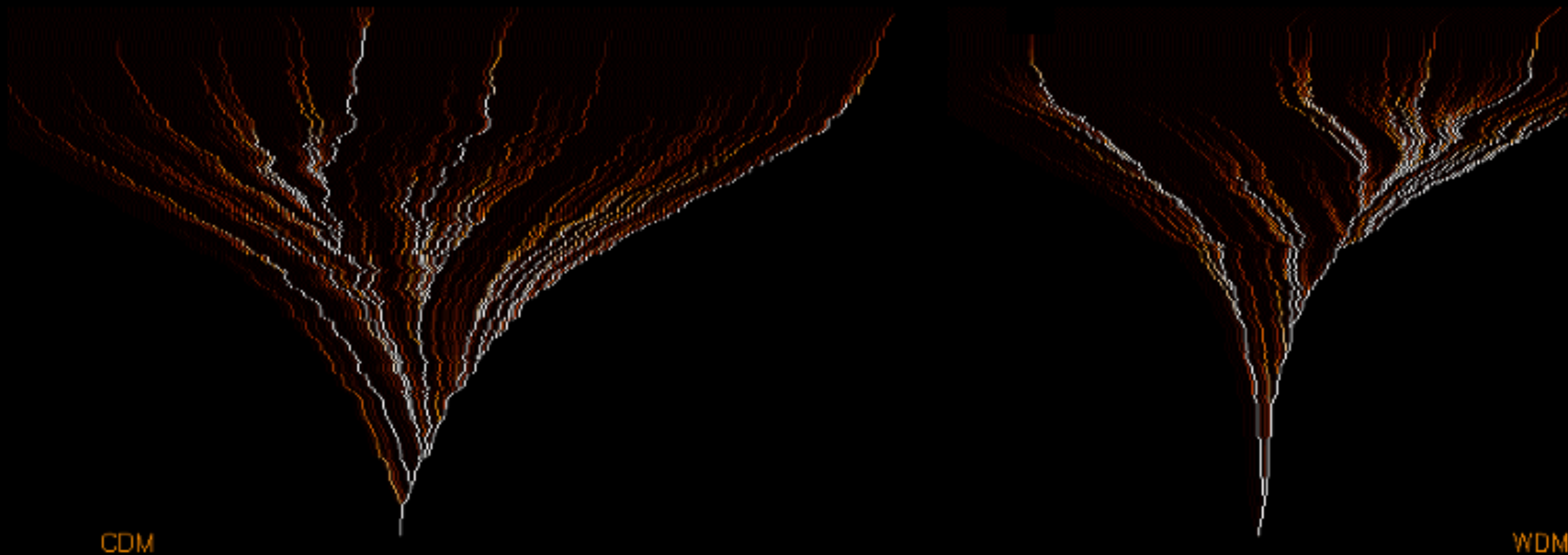

To explore the maximal effect of a power-spectrum cutoff on galaxy formation, we consider a cutoff at scales just below 0.2 Mpc, where data from Lyman-α systems (compared to N-body simulations) yields stringer upper limits on power suppression. This corresponds to mass scales M_{fs}~5 10^8 $M_\odot$

$$r_{fs} \approx 0.2 \left[\frac{\Omega_X h^2}{0.15}\right]^{1/3} \left[\frac{m_X}{rmkeV}\right]^{-4/3} \mathrm{Mpc} \qquad \frac{P_{WDM}(k)}{P_{CDM}(k)} = \left[1 + (\alpha\, k)^{2\,\mu}\right]^{-5\,\mu}$$

$$\alpha = 0.049 \left[\frac{\Omega_X}{0.25}\right]^{0.11} \left[\frac{m_X}{\mathrm{keV}}\right]^{-1.11} \left[\frac{h}{0.7}\right]^{1.22} h^{-1}\ \mathrm{Mpc}$$

WDM
particle mass
1 kev

Implementing WDM power spectrum in the galaxy formation model

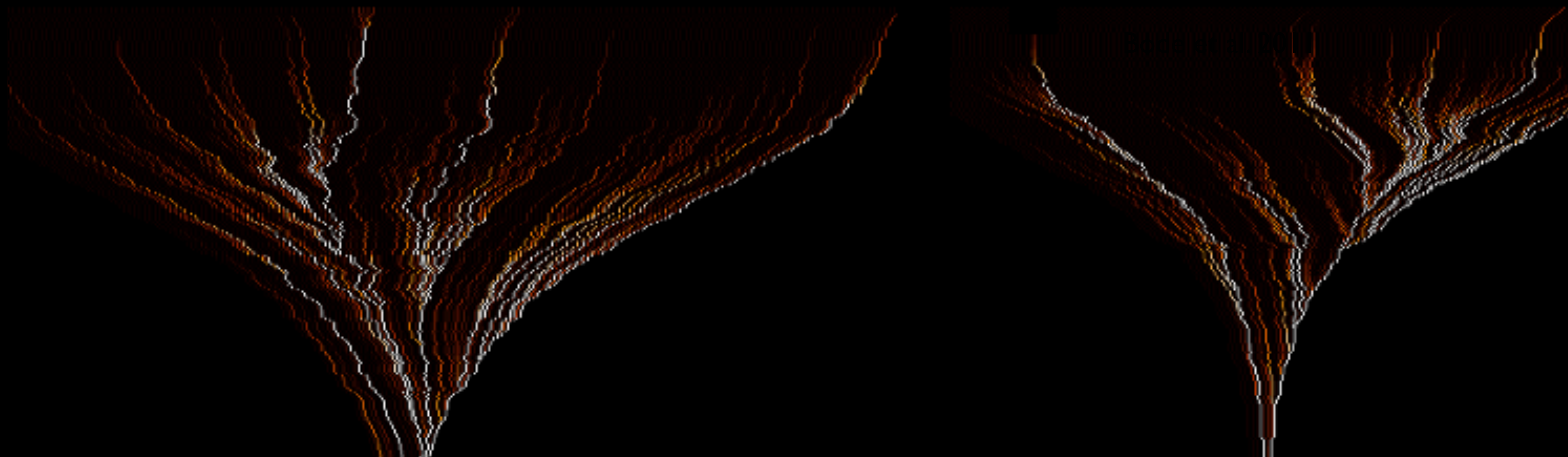

WDM

Halo Properties	Gas Properties	Star Formation	Gas Heating (feedback)	Evolution of stellar populations
Density Profiles Virial Temperature	Profiles Cooling - Heating Collapse Disk formation		SNae UV background	

Galaxy formation in WDM implies computing how modifications of the power spectrum propagate to the above processes

$$r_{fs} \approx 0.2 \left[\frac{\Omega_X\, h^2}{0.15}\right]^{1/3} \left[\frac{m_X}{rmkeV}\right]^{-4/3} \mathrm{Mpc} \qquad \frac{P_{WDM}(k)}{P_{CDM}(k)} = \left[1+(\alpha\, k)^{2\,\mu}\right]^{-5\,\mu}$$

$$\alpha = 0.049 \left[\frac{\Omega_X}{0.25}\right]^{0.11} \left[\frac{m_X}{\mathrm{keV}}\right]^{-1.11} \left[\frac{h}{0.7}\right]^{1.22} h^{-1}\ \mathrm{Mpc}$$

WDM
particle mass
1 kev

Galaxy Formation in WDM cosmology (m_{WDM}~1 keV)

NM et al. 2012-2013

local lum. and stell. mass distributions

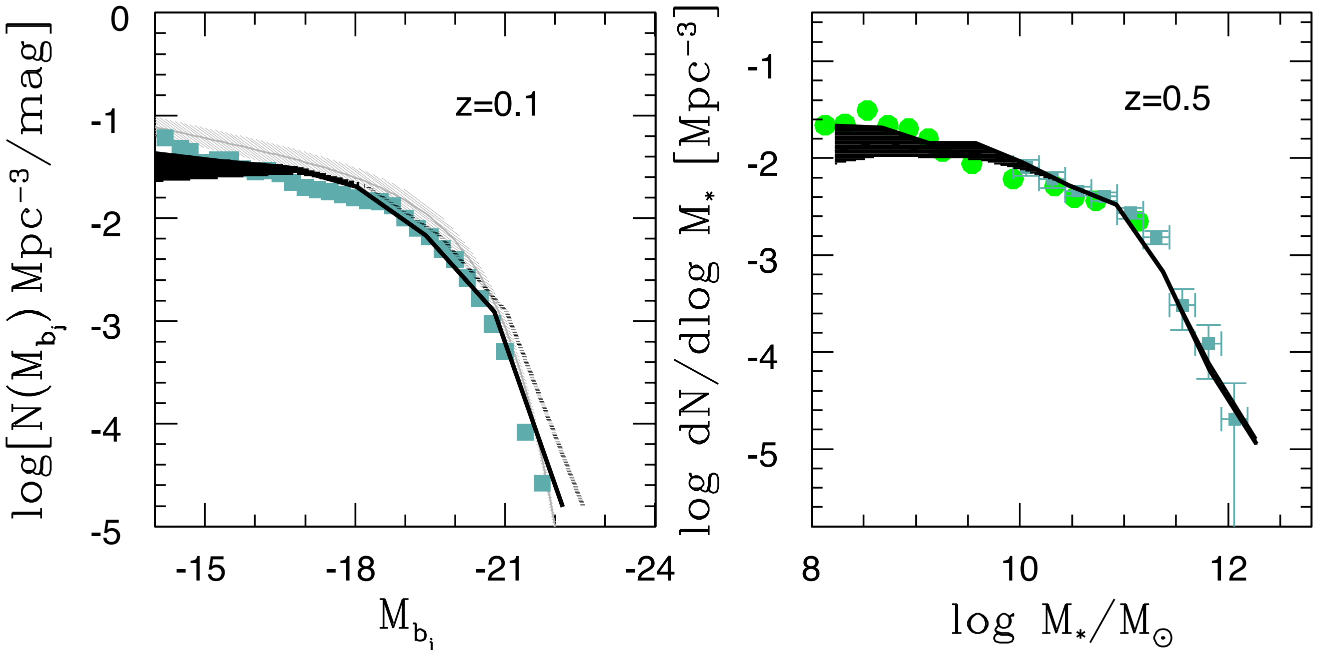

Evolution

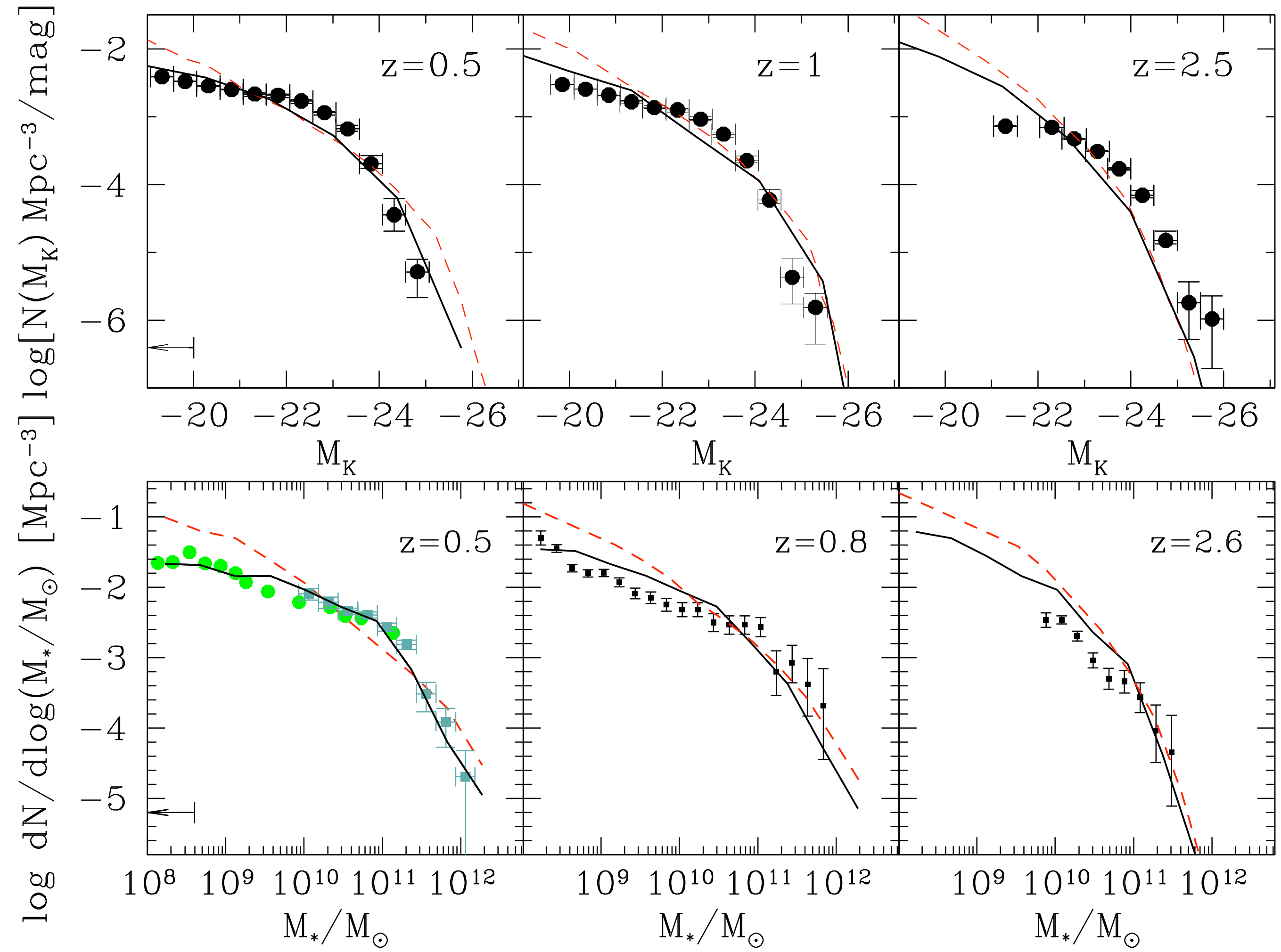

High-z (z=4) lum. distributions

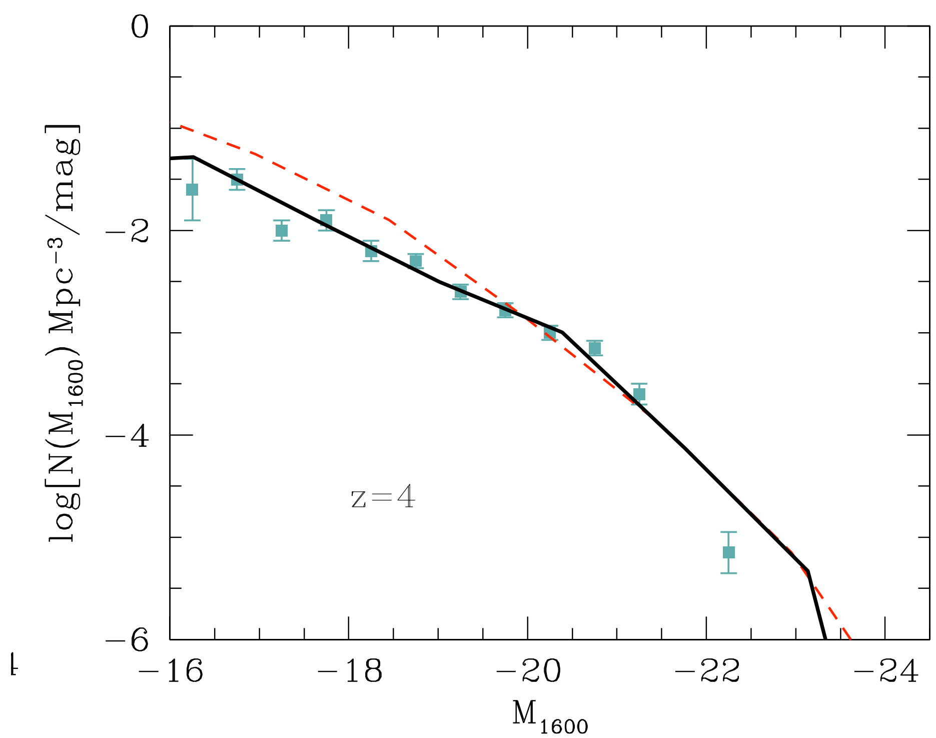

color distributions

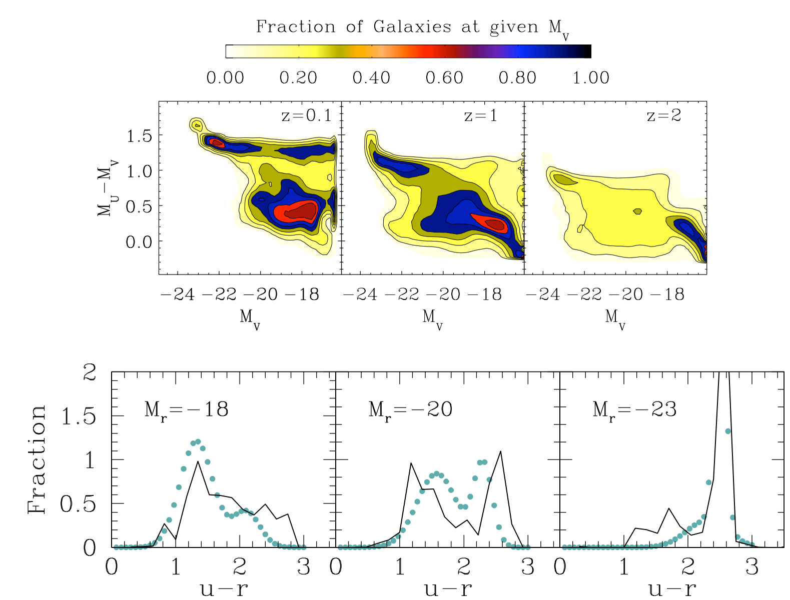

CDM models overestimate faint AGN abundance at high z

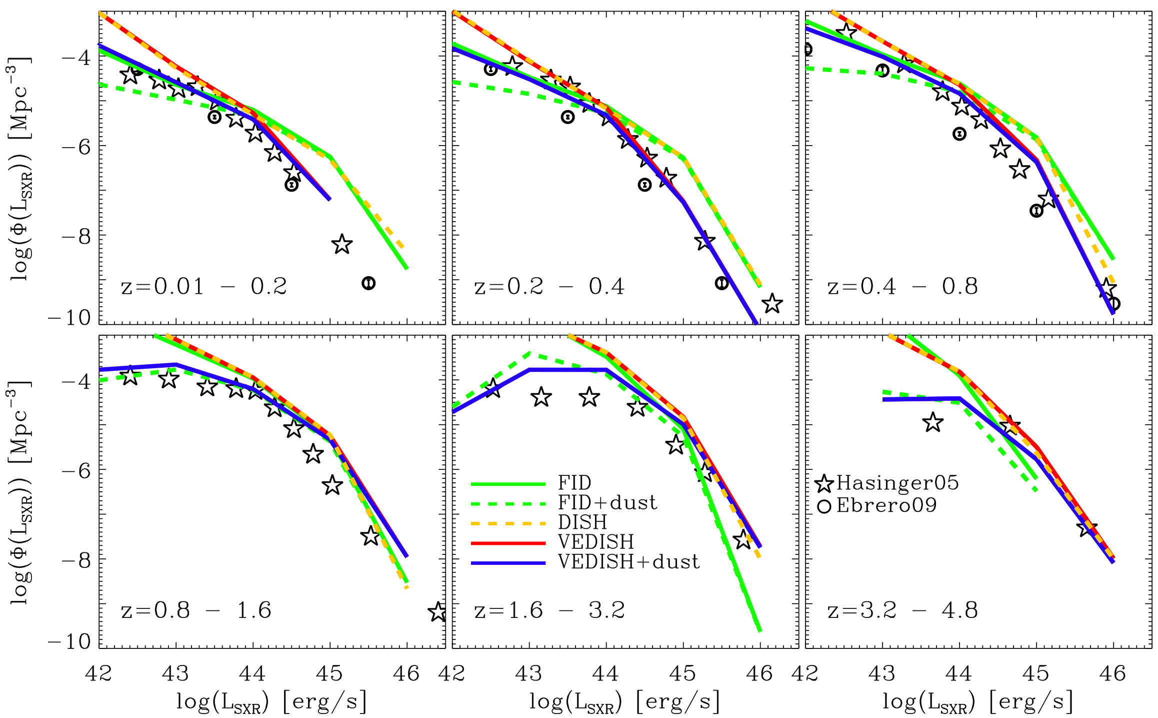

Hirschmann et al. 2012

NM, Fiore, Lamastra 2013

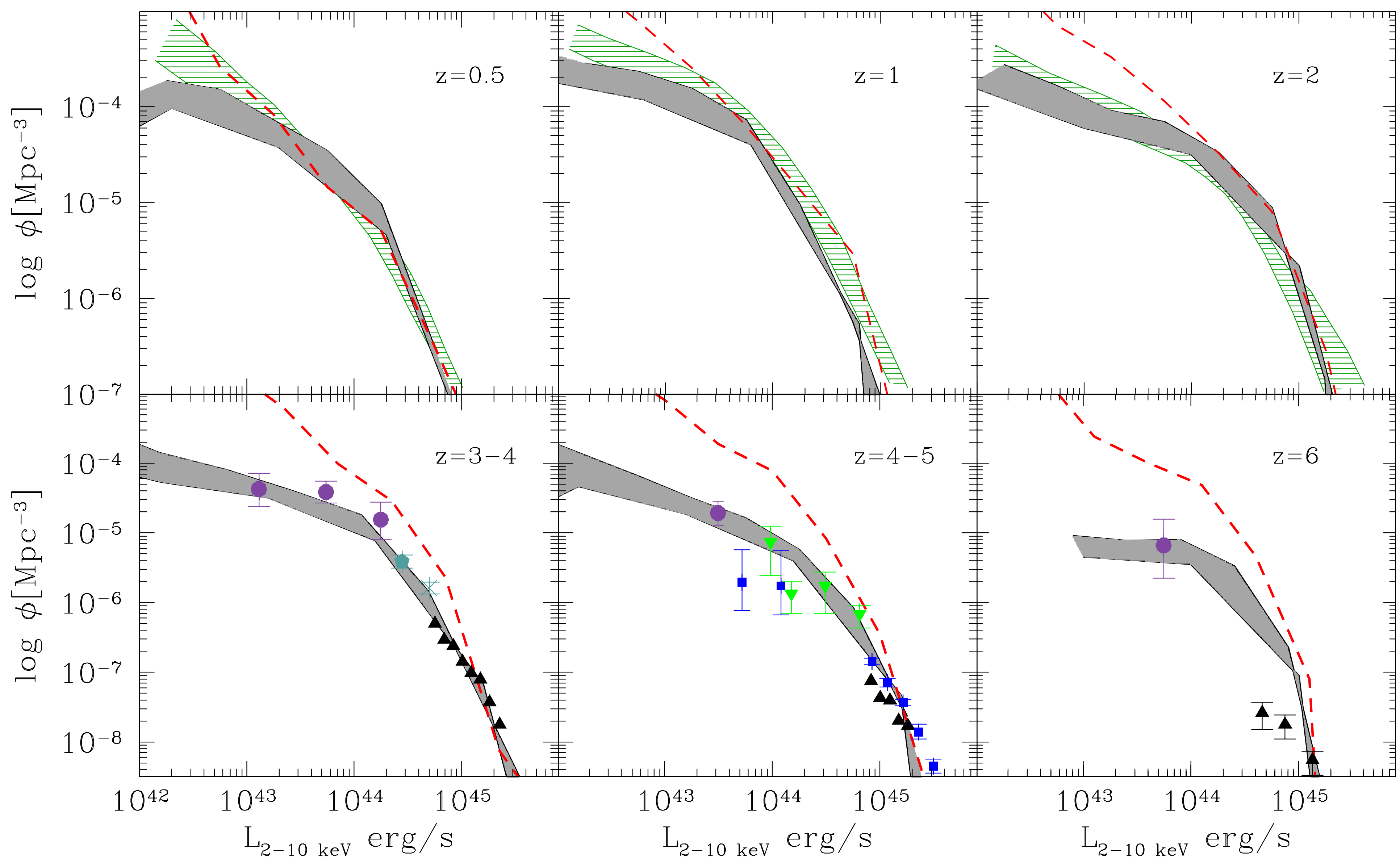

Abundance of galaxies as a function of their velocity width (gas rotation velocity)

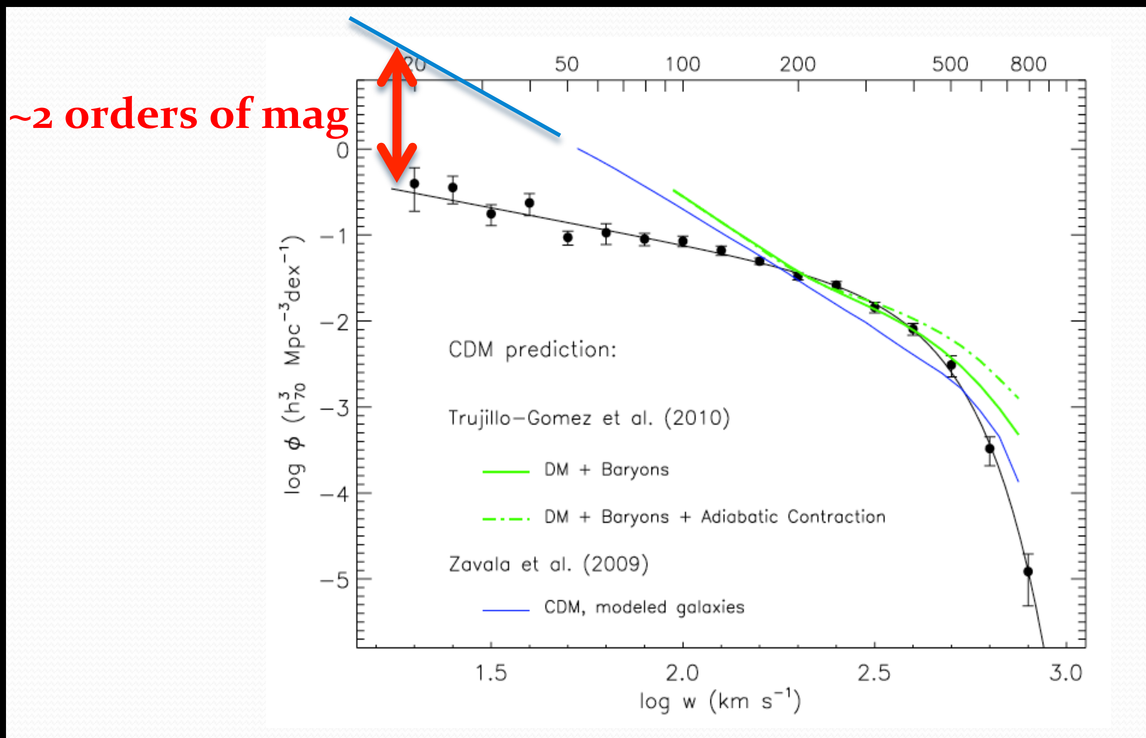

Papastergis+ (2011)

21-cm survey done with Arecibo Telescope: 3000 deg^2; 11000 detections
measures: redshift, velocity width, integrated flux
No spatial resolution (size, inclination, shape)

Directly measures
the <u>depth of the potential well</u>:
less prone to physics of gas (feedback)

Solutions within CDM scenario ?
- large fraction of galaxies with low gas content (below the sensitivity)
-large fraction of galaxies with rising rotation curve

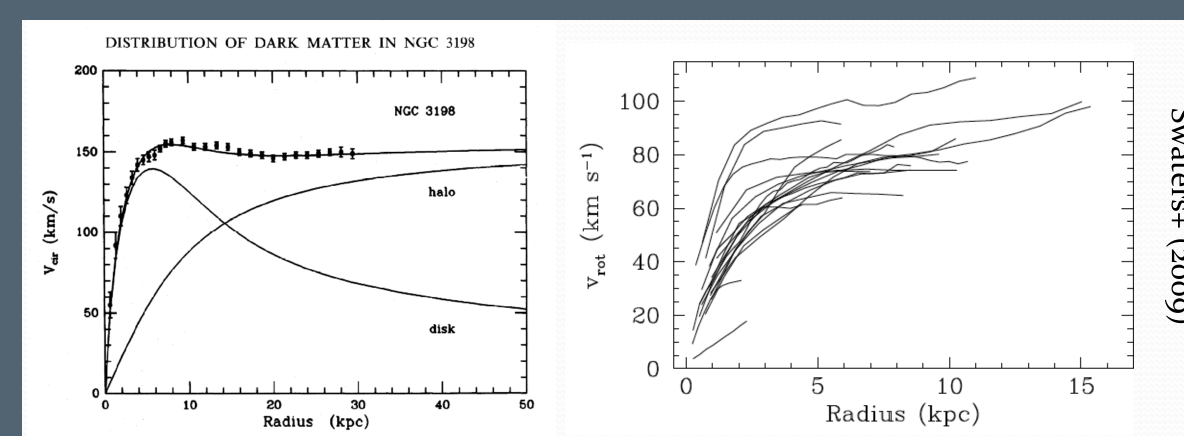

'flat' rotation curve

'rising' rotation curves

Abundance of galaxies as a function of their velocity width (gas rotation velocity)

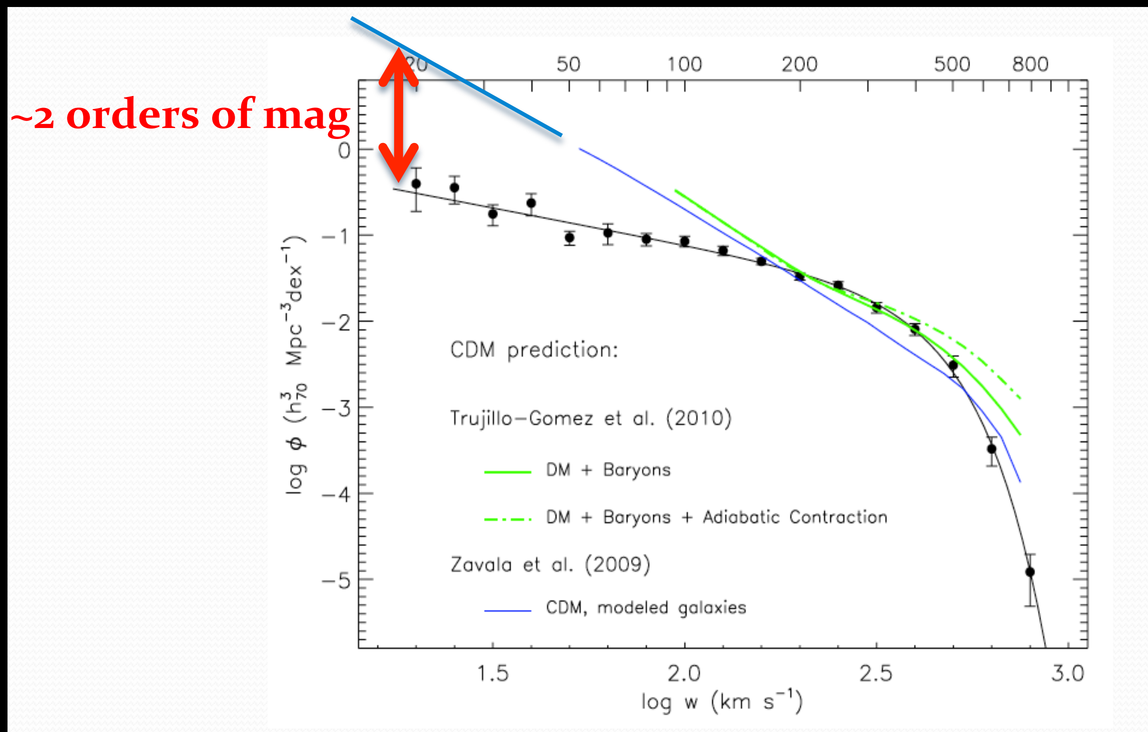

Papastergis+ (2011)

21-cm survey done with Arecibo Telescope: 3000 deg^2; 11000 detections
measures: redshift, velocity width, integrated flux
No spatial resolution (size, inclination, shape)

Directly measures
the depth of the potential well:
less prone to physics of gas (feedback)

At high redshift, galaxies are denser

Difficult to expel gas from such compact objects

Even with maximized feedback, current models still over estimate the number of small mass galaxies

Abundance of galaxies as a function of their velocity width (gas rotation velocity)

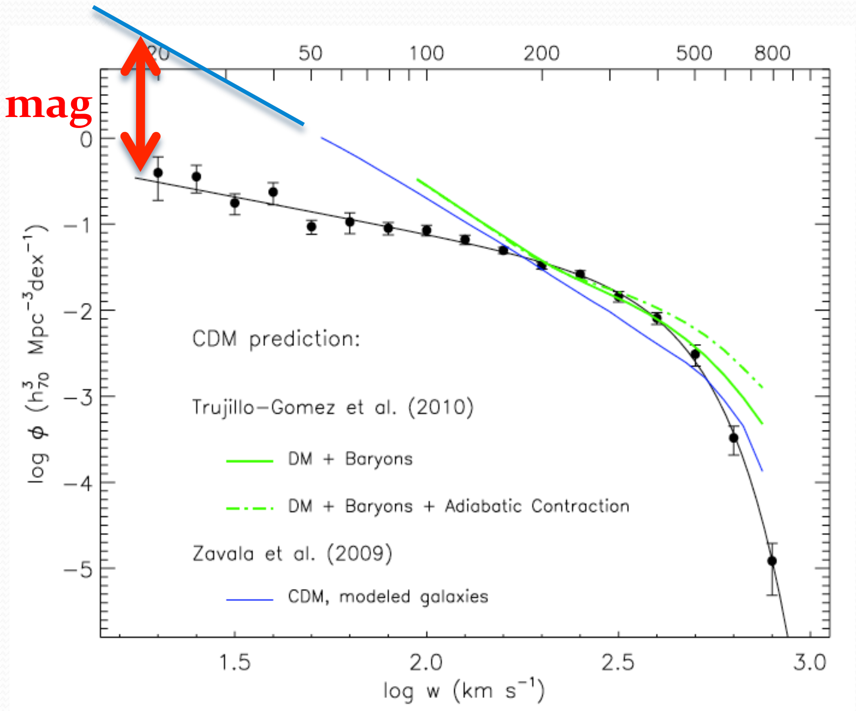

Papastergis+ (2011)

21-cm survey done with Arecibo Telescope: 3000 deg^2; 11000 detections
measures: redshift, velocity width, integrated flux
No spatial resolution (size, inclination, shape)

Directly measures
the depth of the potential well:
less prone to physics of gas (feedback)

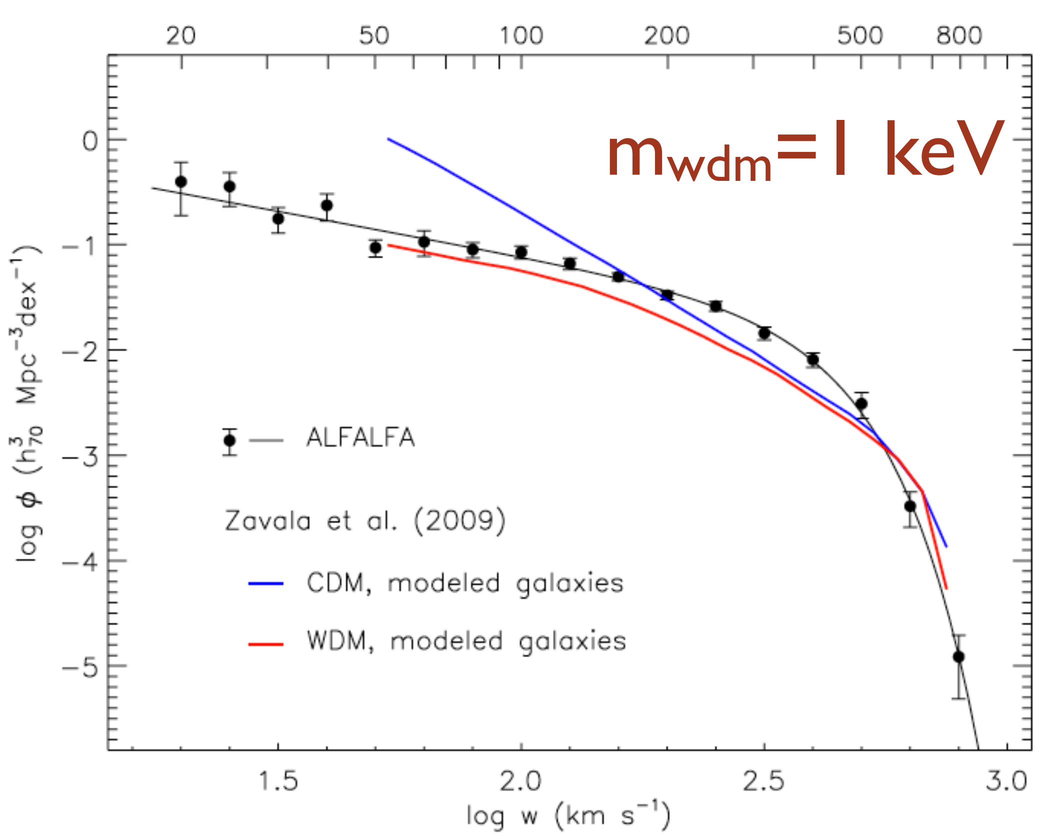

Papastergis+ (2011)

modeling: Zavala+ (2009)

WDM naturally yields a flat distribution
Zavala et al. 2009

Substructures, Density profiles, Rotation curves in WDM

Density Profiles

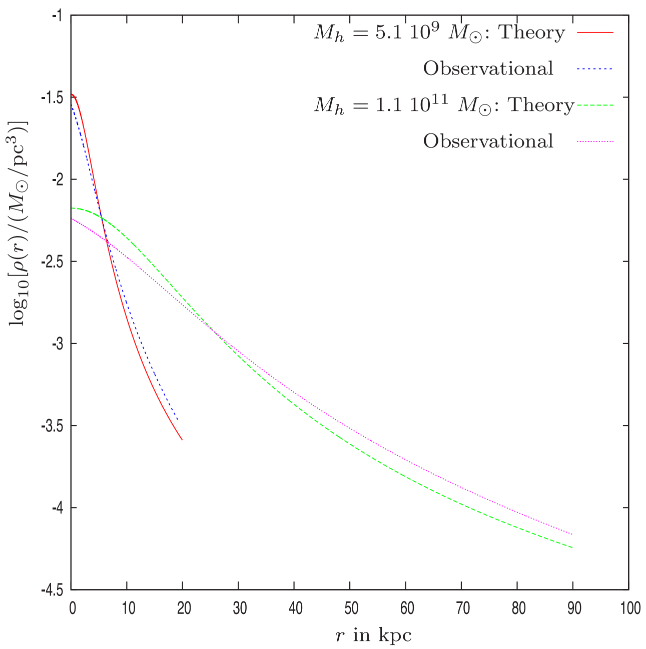

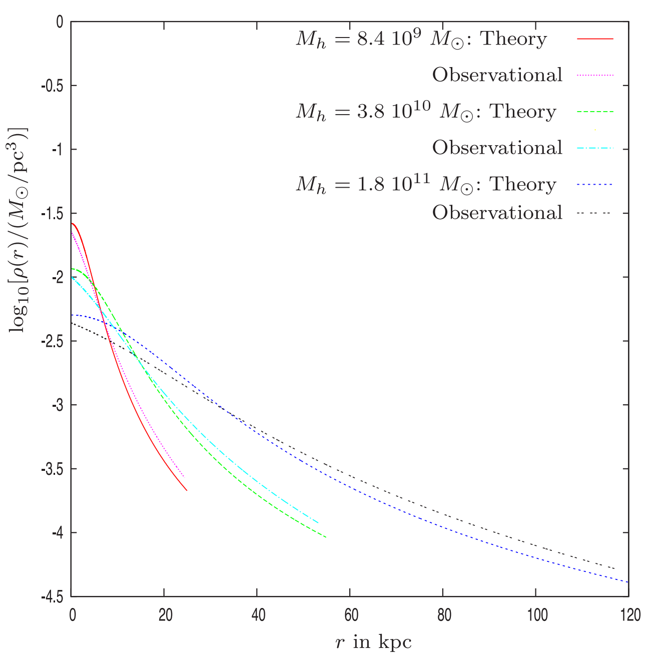

De Vega, Salucci, Sanchez 2014
Fermionic WDM

Rotation Curves

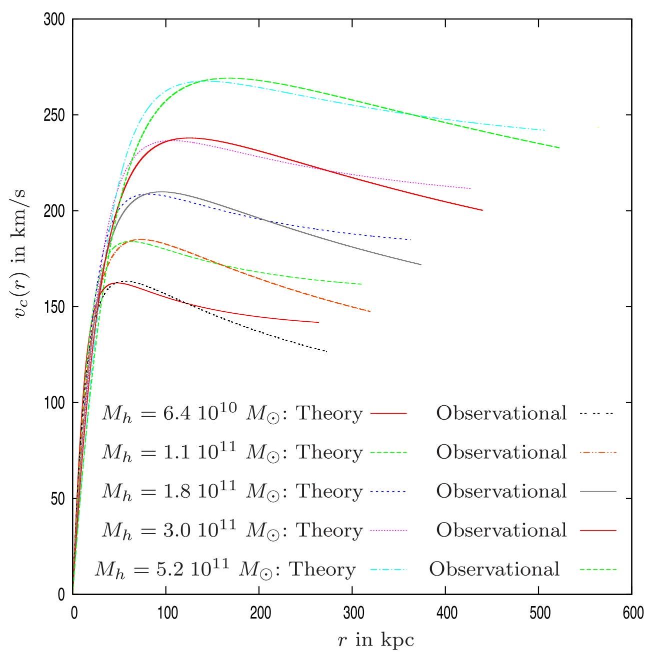

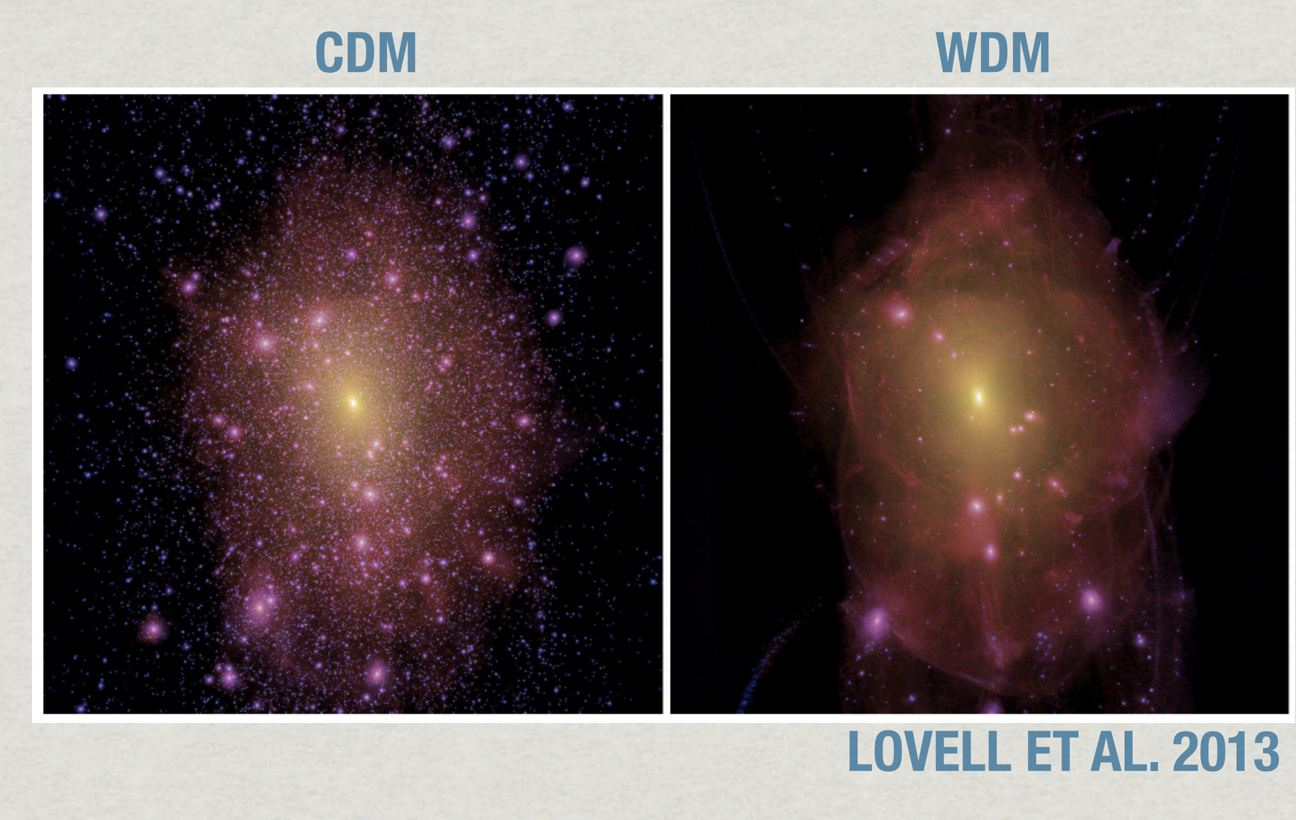

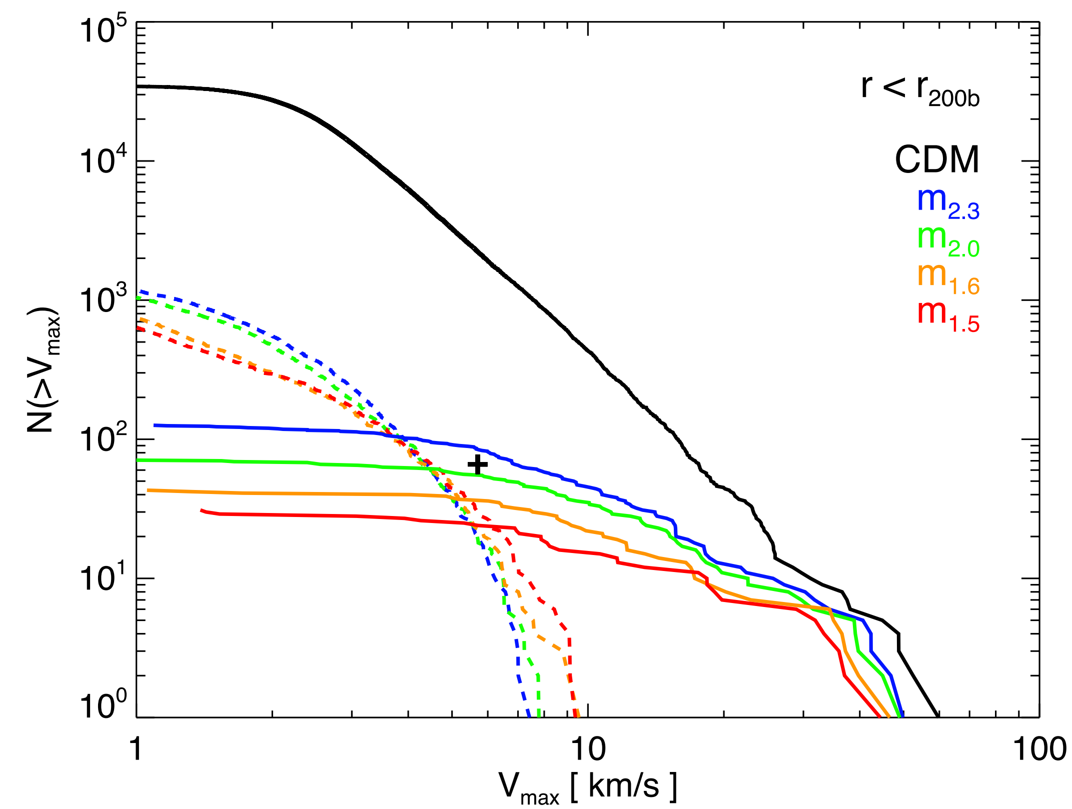

Figure 11. Cumulative subhalo mass, M_{sub}, (top panel) and V_{max} (bottom panel) functions of subhaloes within $r < r_{200b}$ of the main halo centre in the HRS at $z = 0$. Solid lines correspond to genuine subhaloes and dashed lines to spurious subhaloes. The black line shows results for CDM-W7 and the coloured lines for the WDM models, as in Fig. 1. The black cross in the lower panel indicates the expected number of satellites of $V_{max} > 5.7\ \mathrm{km\,s^{-1}}$ as derived in the text.

Disentangling feedback effects from WDM

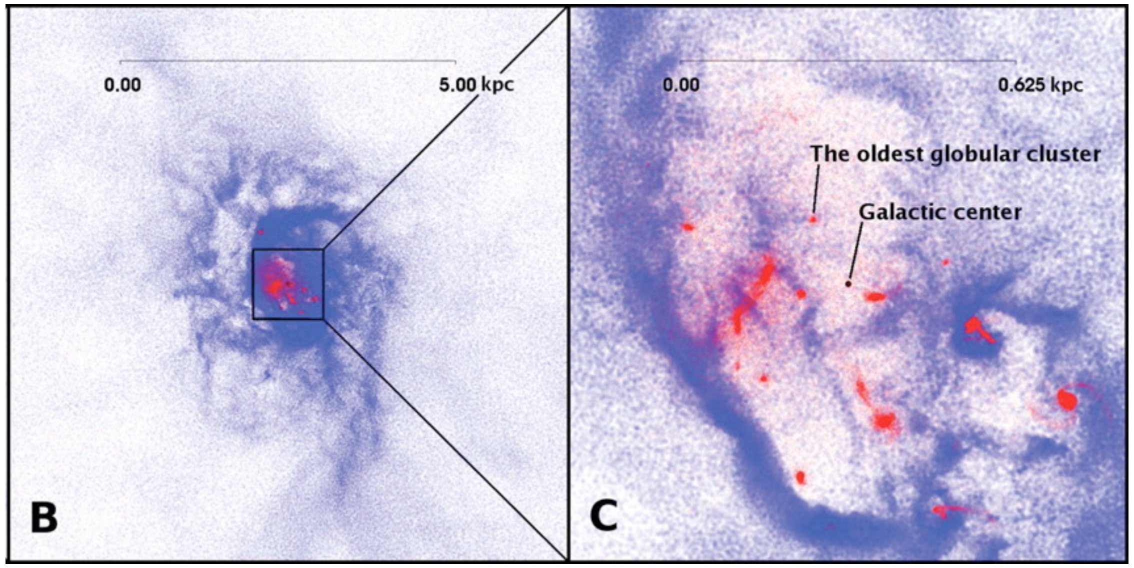

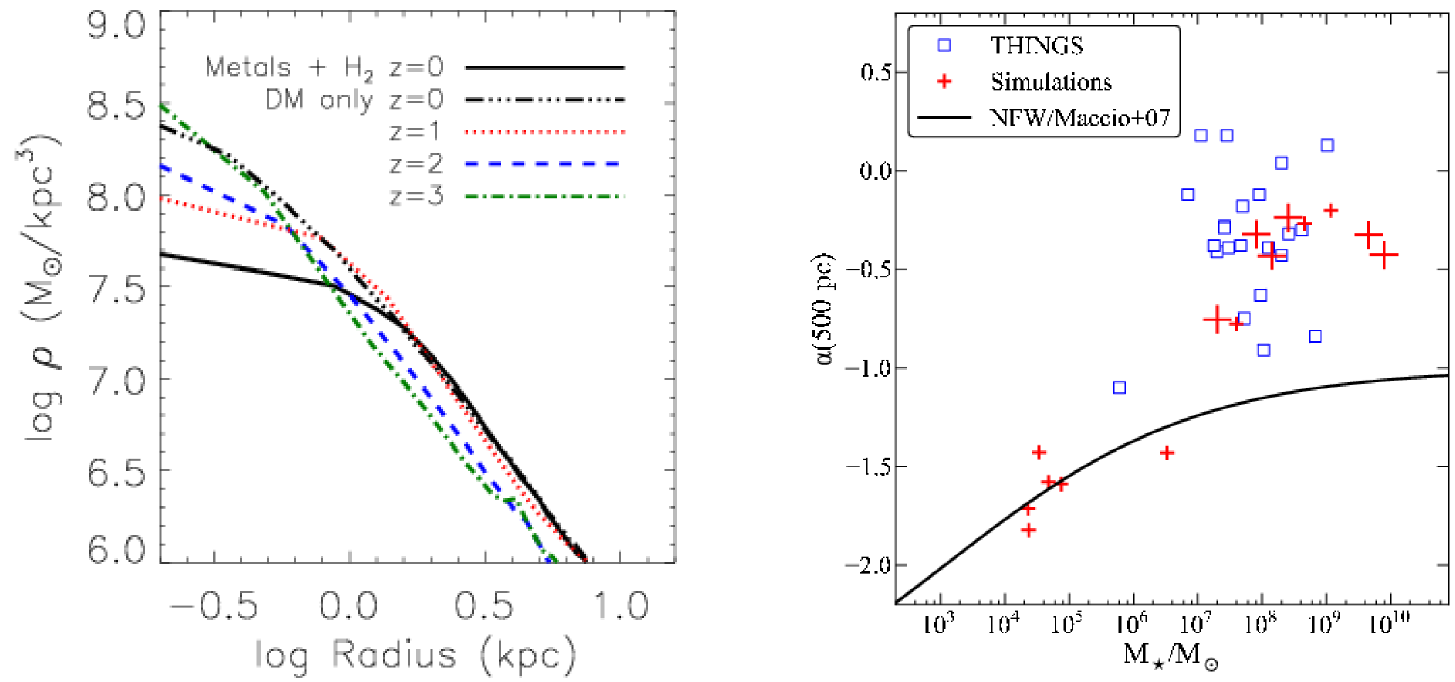

Fig. 3. Baryonic effects on CDM halo profiles in cosmological simulations, from Governato et al. (2012). *(Left)* The upper, dot-dash curve shows the cuspy dark matter density profile resulting from from a collisionless N-body simulation. Other curves show the evolution of the dark matter profile in a simulation from the same initial conditions that includes gas dynamics, star formation, and efficient feedback. By $z = 0$ (solid curve) the perturbations from the fluctuating baryonic potential have flattened the inner profile to a nearly constant density core. *(Right)* Logarithmic slope of the dark matter profile α measured at 0.5 kpc, as a function of galaxy stellar mass. Crosses show results from multiple hydrodynamic simulations. Squares show measurements from rotation curves of observed galaxies. The black curve shows the expectation for pure dark matter simulations, computed from NFW profiles with the appropriate concentration. For $M_* > 10^7 M_\odot$, baryonic effects reduce the halo profile slopes to agree with observations.

In the outer region profiles with feedback are close to CDM NFW

Feedback acts in the inner regions

Shankar+ 2014

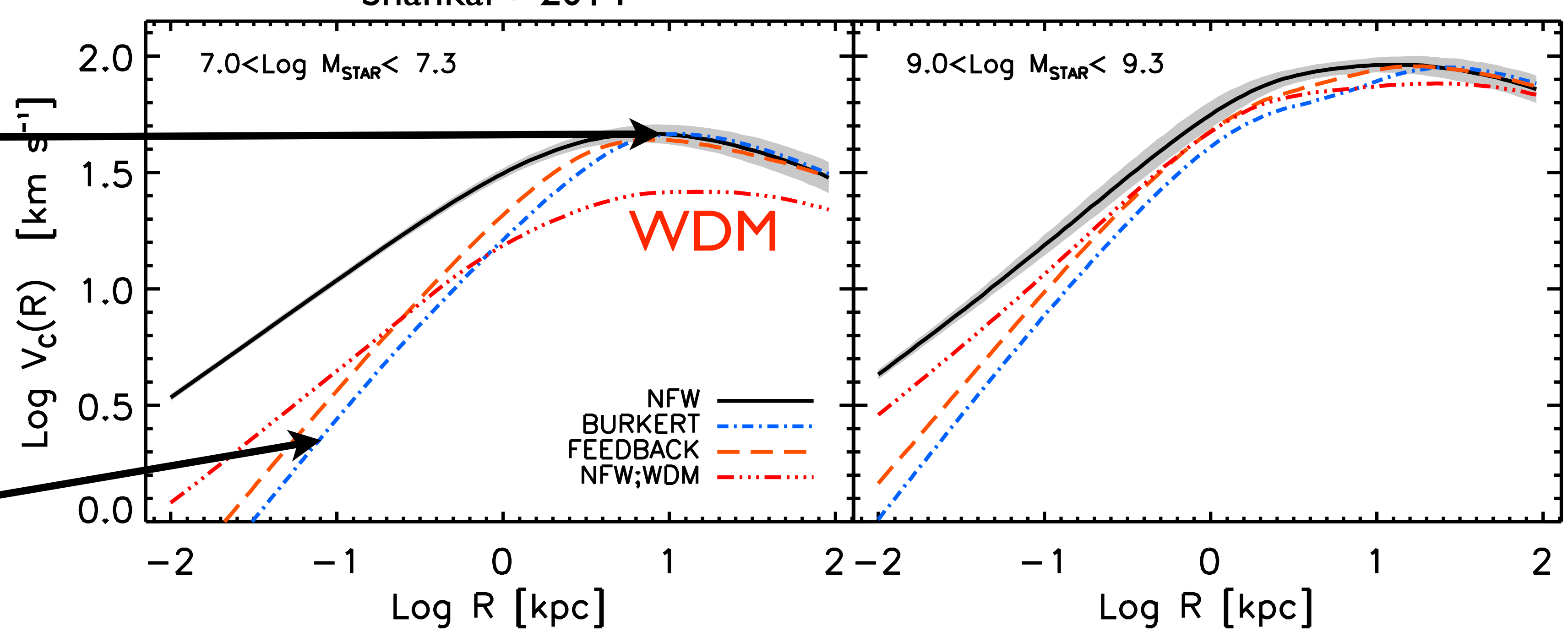

Matching the V_{max}-M_* relation

A semi-empirical approach (Shankar et al. 2014)

1. select a sample of DM haloes
2. associate to each halo a galaxy of a given stellar mass according to an abundance matching relation
3. compute rotation velocity curves for each DM halo (for WDM adopt the $c(M_h)$ relation by Schneider et al 2012 for 1 keV thermal relic DM)
4. infer predicted V_{MAX}-M_* relation (computed at maximum of the rotation curve)

Matching the V_{max}-M_* relation

A semi-empirical approach (Shankar et al. 2014)

1. select a sample of DM haloes
2. associate to each halo a galaxy of a given stellar mass according to an abundance matching relation
3. compute rotation velocity curves for each DM halo (for WDM adopt the $c(M_h)$ relation by Schneider et al 2012 for 1 keV thermal relic DM)
4. infer predicted V_{MAX}-M_* relation (computed at maximum of the rotation curve)

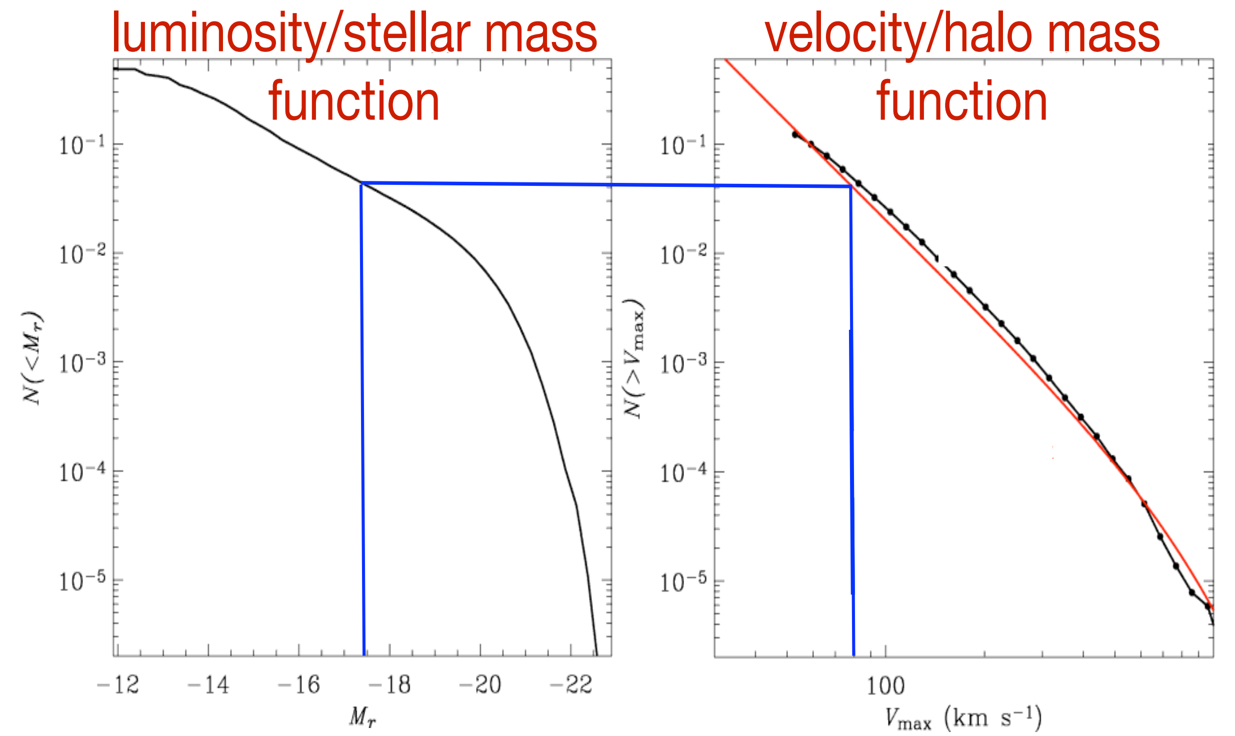

Matching the V_{max}-M_* relation

A semi-empirical approach (Shankar et al. 2014)

1. select a sample of DM haloes
2. associate to each halo a galaxy of a given stellar mass according to an abundance matching relation
3. compute rotation velocity curves for each DM halo (for WDM adopt the $c(M_h)$ relation by Schneider et al 2012 for 1 keV thermal relic DM)
4. infer predicted V_{MAX}-M_* relation (computed at maximum of the rotation curve)

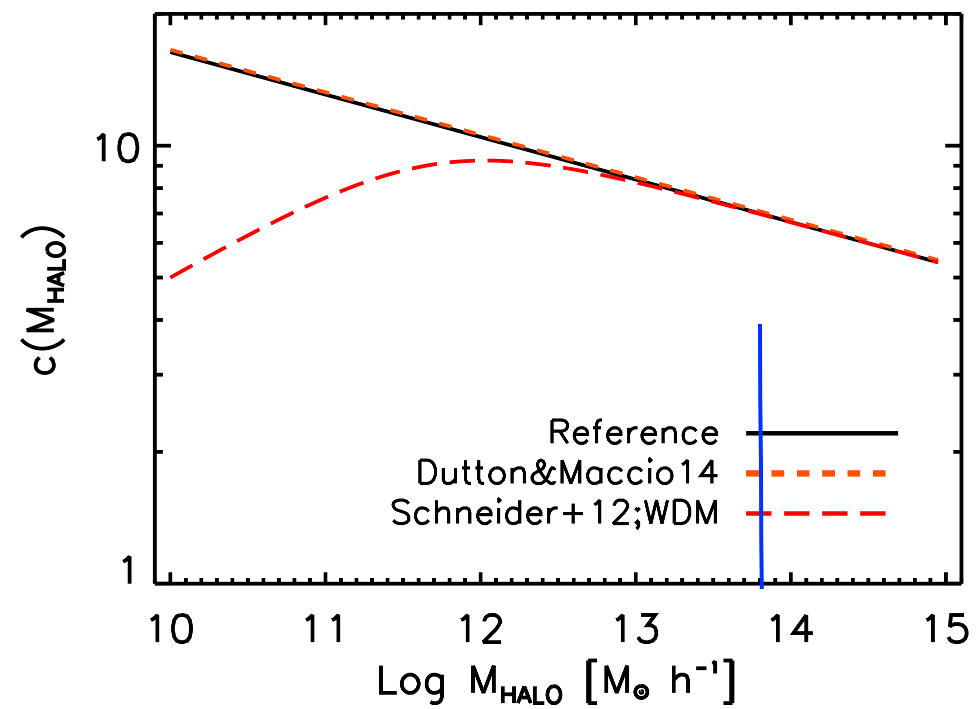

Matching the V_{max}-M_* relation

A semi-empirical approach (Shankar et al. 2014)

1. select a sample of DM haloes
2. associate to each halo a galaxy of a given stellar mass according to an abundance matching relation
3. compute rotation velocity curves for each DM halo (for WDM adopt the $c(M_h)$ relation by Schneider et al 2012 for 1 keV thermal relic DM)
4. infer predicted V_{MAX}-M_* relation (computed at maximum of the rotation curve)

Feedback profile from Di Cintio et al. 2014
hydro-simulations baryons+stellar feedback

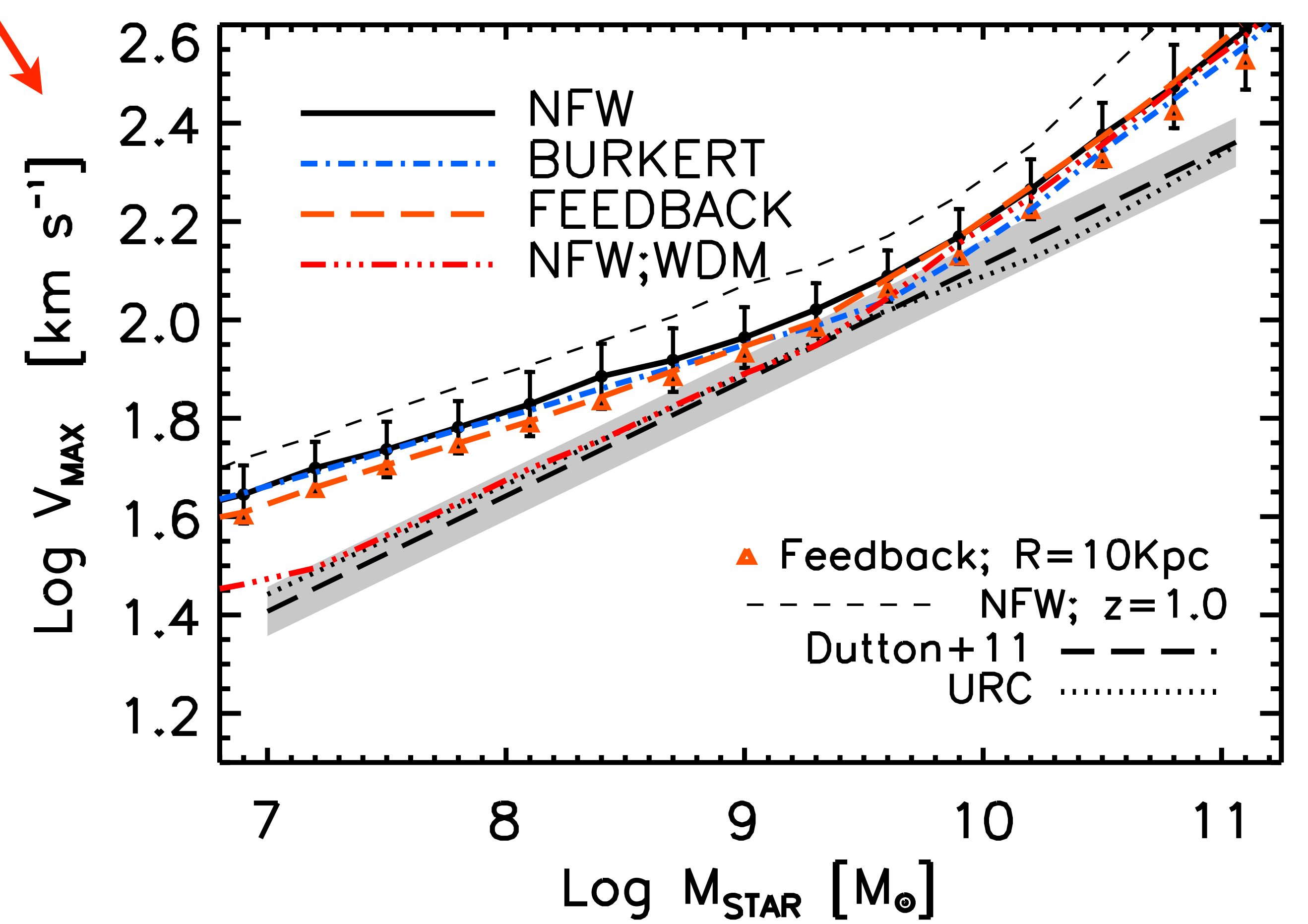

Solution in CDM scenario

most low-mass haloes do not contain galaxies due to the effect or UV background, feedback and reionization(assuming no self-shielding and H_2 cooling)

Sawala et al. 2015

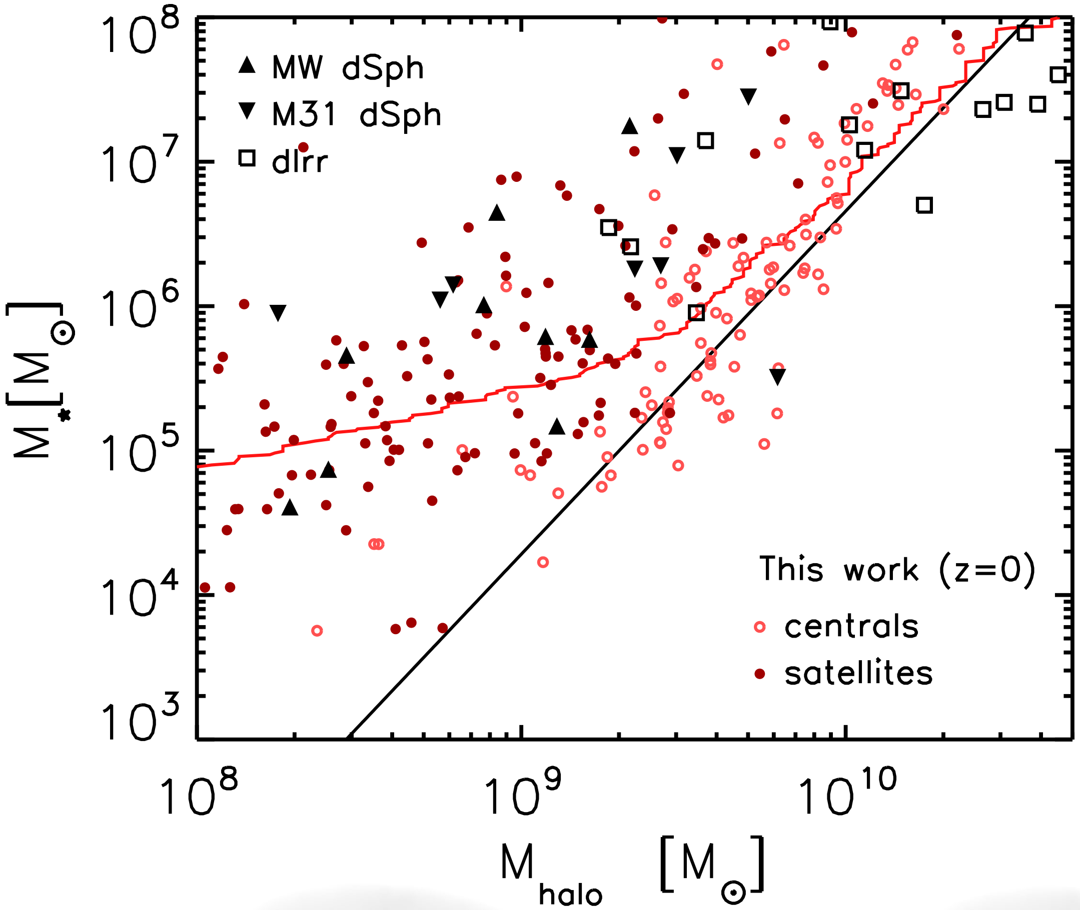

Milky-Way like haloes should contain thousands of dark halos (with no stars or gas)

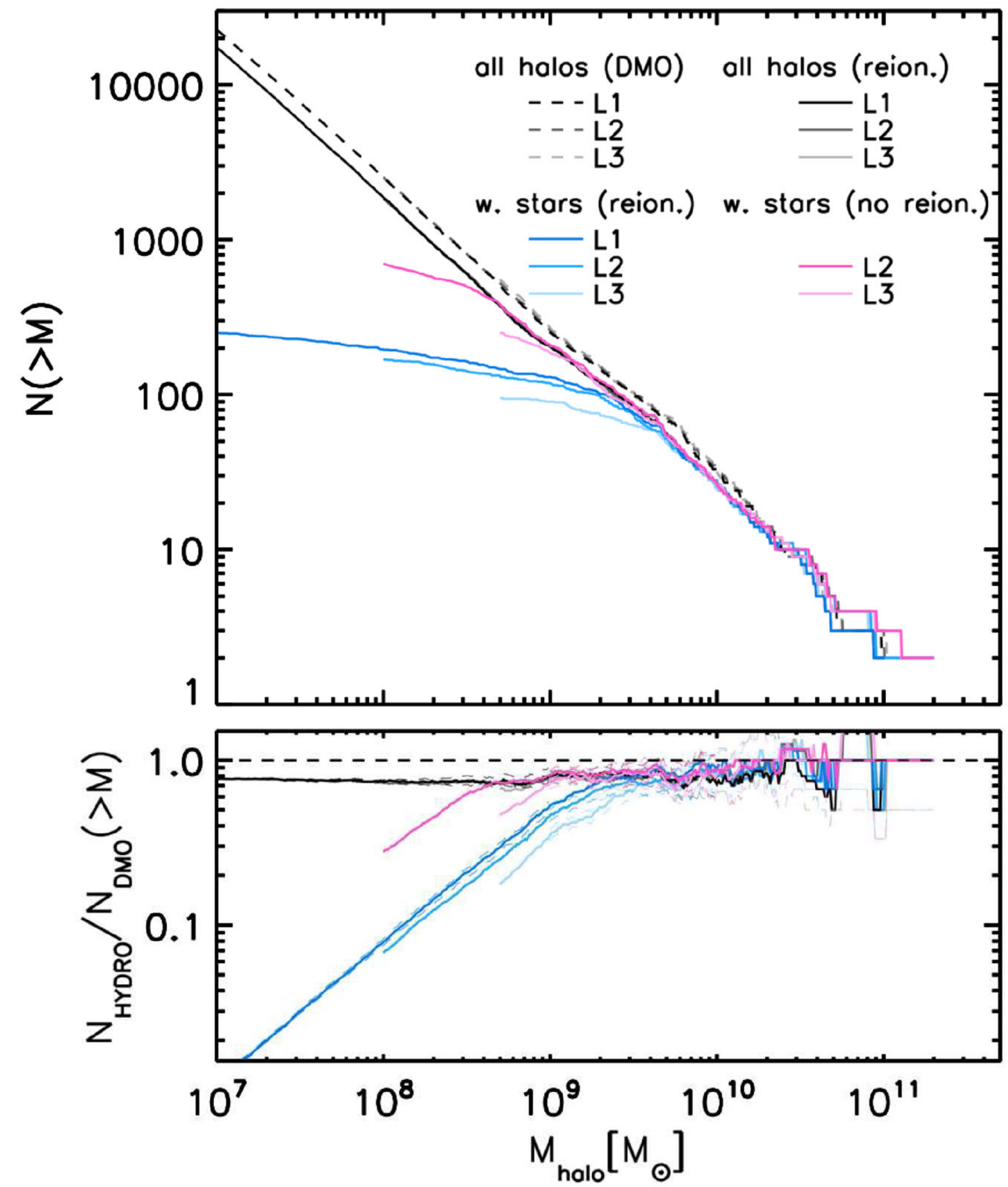

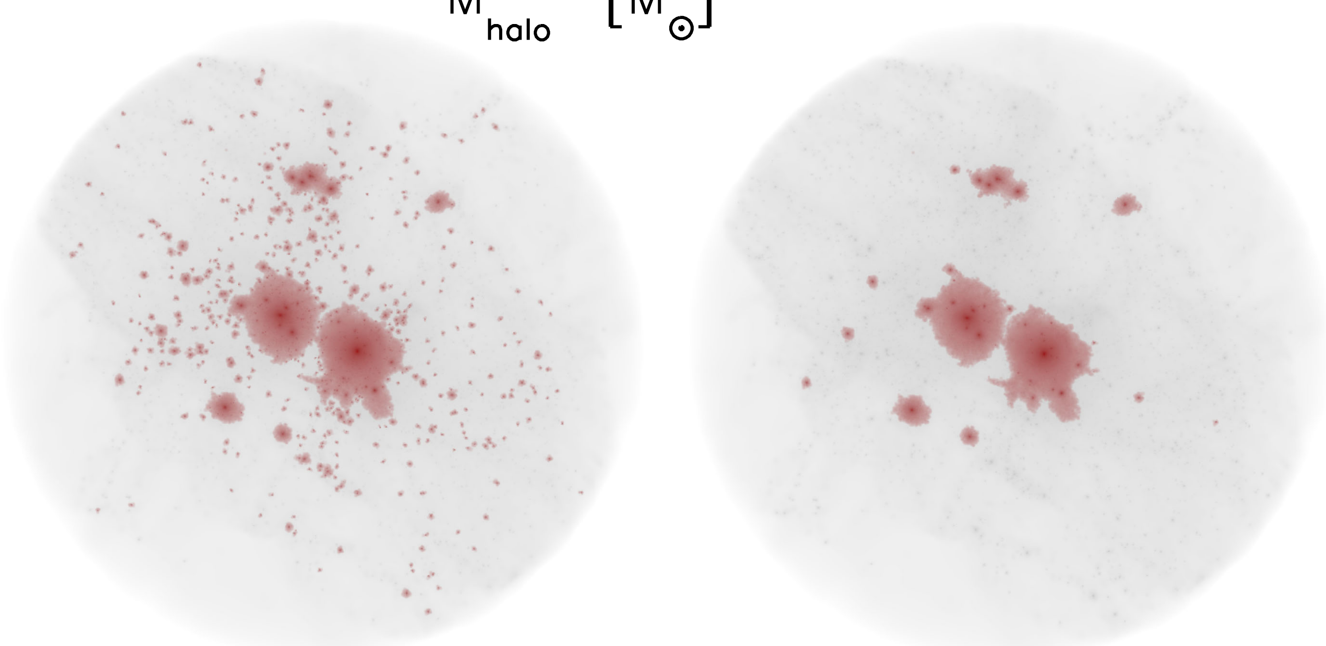

Figure 1. Projected density distribution of dark matter within 2 Mpc around the simulated Milky Way – M31 barycentre at $z = 0$ from one of our simulation volumes. Highlighted in red on top of the total mass distribution are particles in haloes above $5 \times 10^7\ M_\odot$ (left-hand panel), and particles in just those haloes that contain stars (right-hand panel).

Luminosity Function of Satellite Galaxies

Is Milky Way representative of $M_{halo} \approx 10^{12}\ M_{\odot}$?

Compare with a wide set of satellites/host halos through the satellite luminosity function

ACS F814W imaging of the COSMOS field,

identify satellites as much as a thousand times fainter than their host galaxies and as close as 0.3 (1.4) arcsec (kpc)and as close as 0.3 (1.4) arcsec (kpc)

Hundreds of hosts

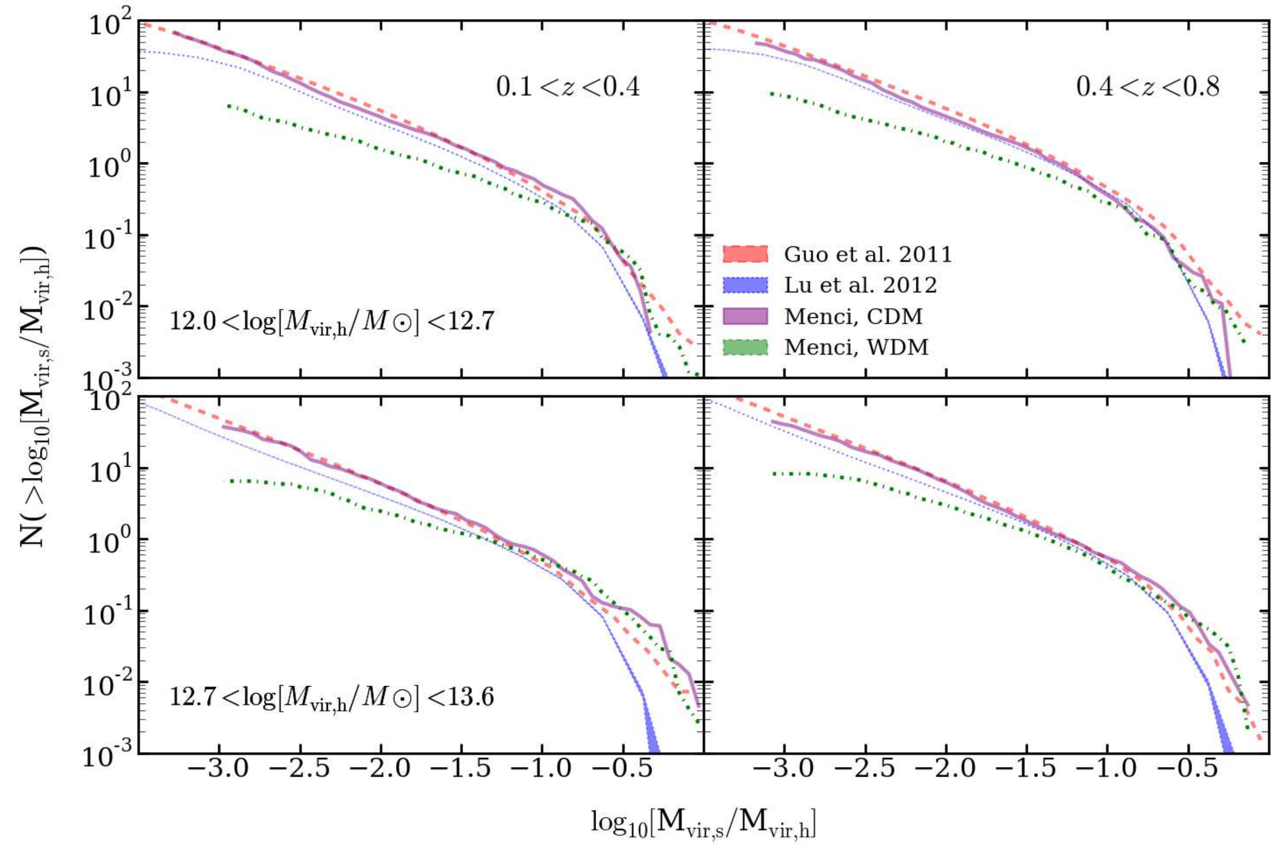

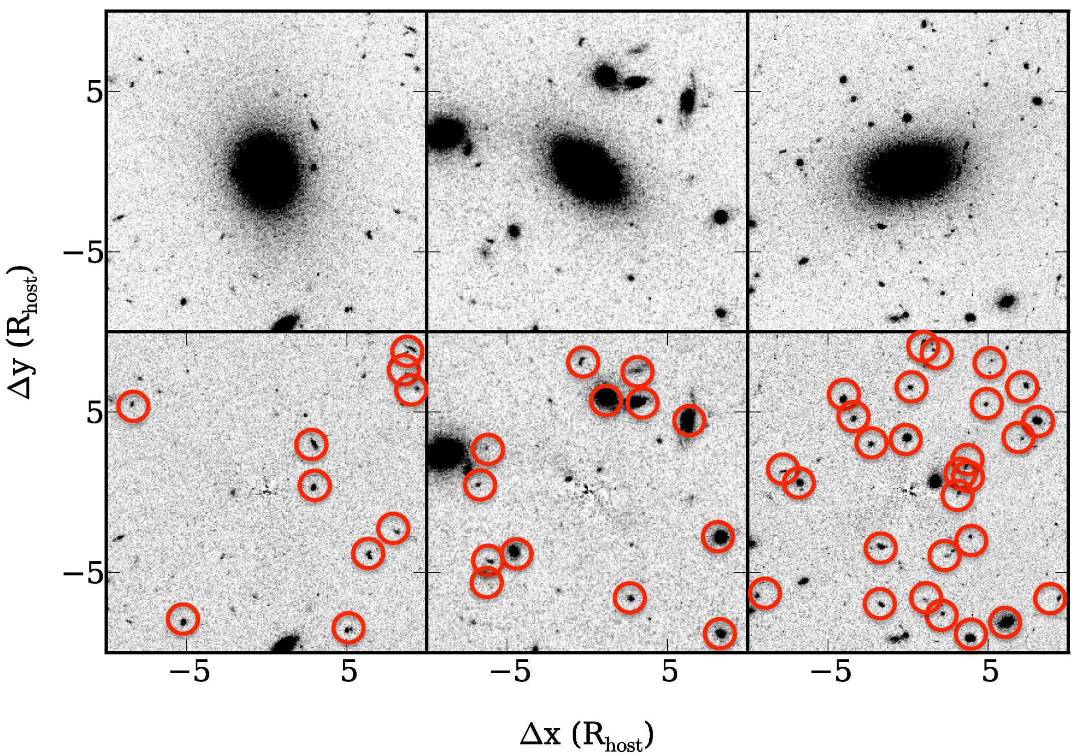

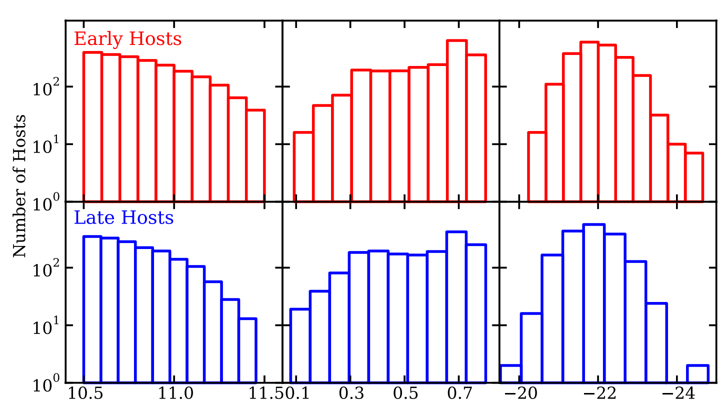

The luminosity distribution of Satellite Galaxies
Nierenberg, Treu, NM 2013

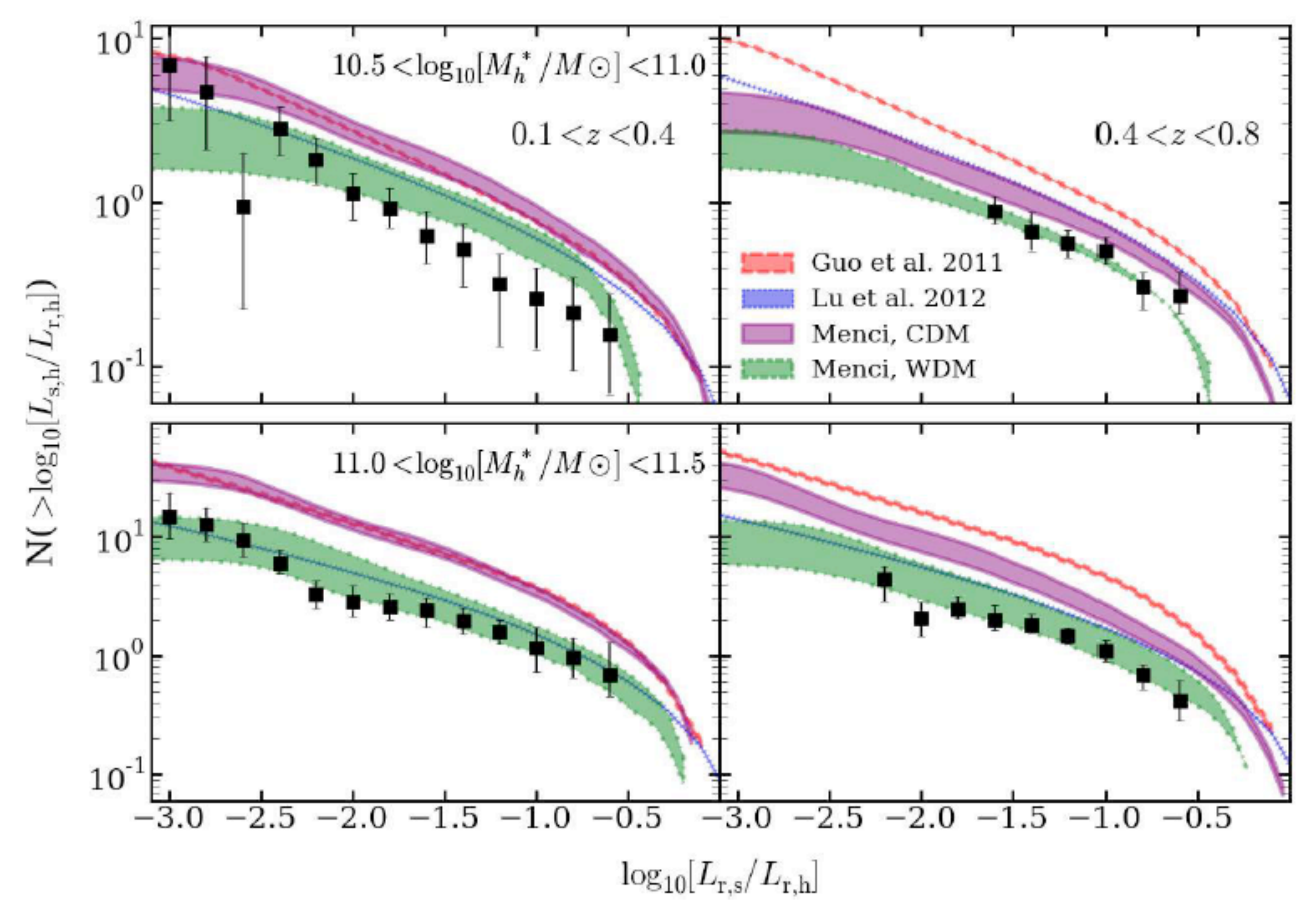

SATELLITE GALAXIES

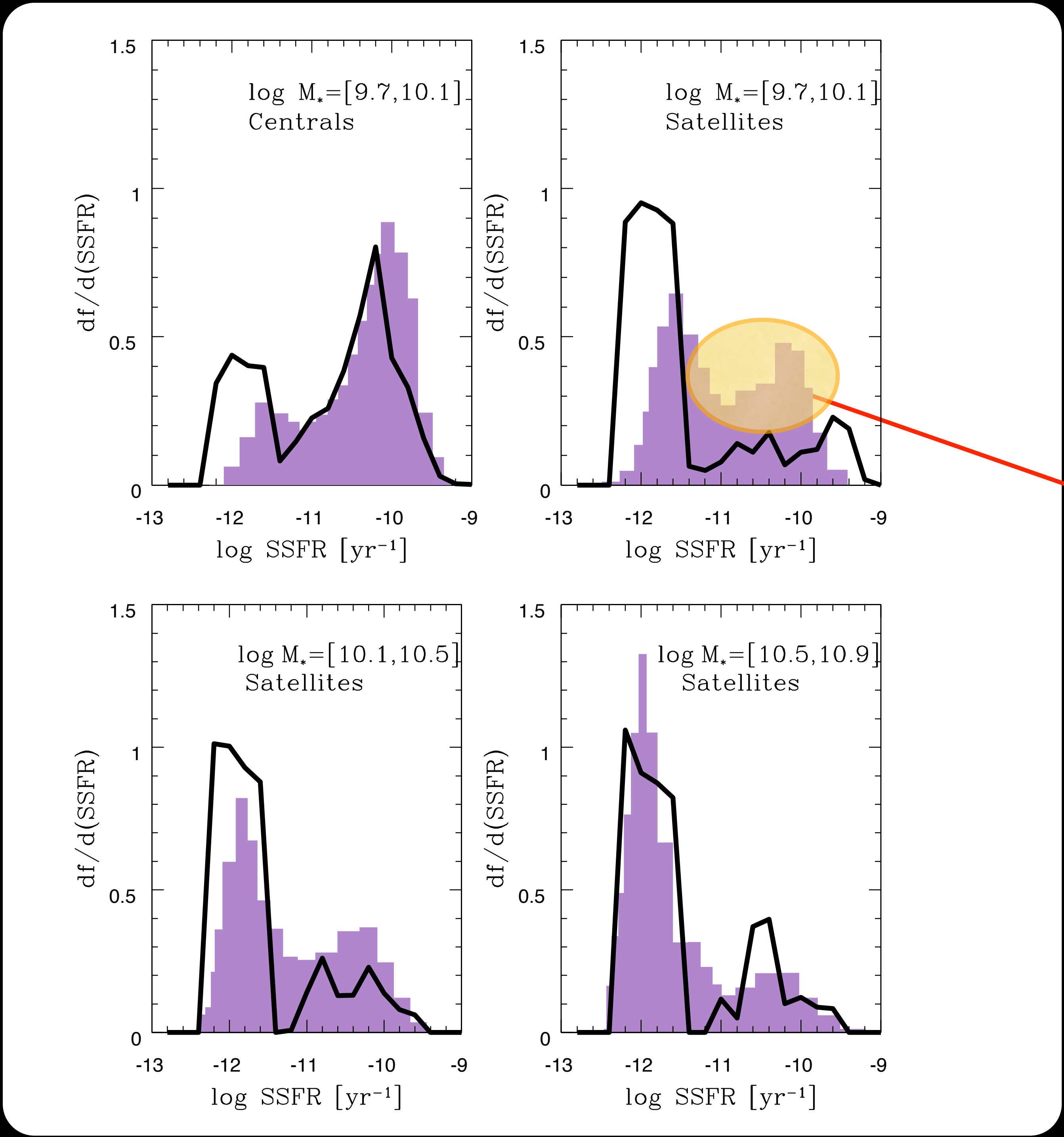

Specific Star Formation Rate SSFR
measures the current star formation activity with respect to the past

$$SSFR = \dot{M}_*/M*$$

Population of active satellites missing in CDM models
Model satellites undergo passive evolution

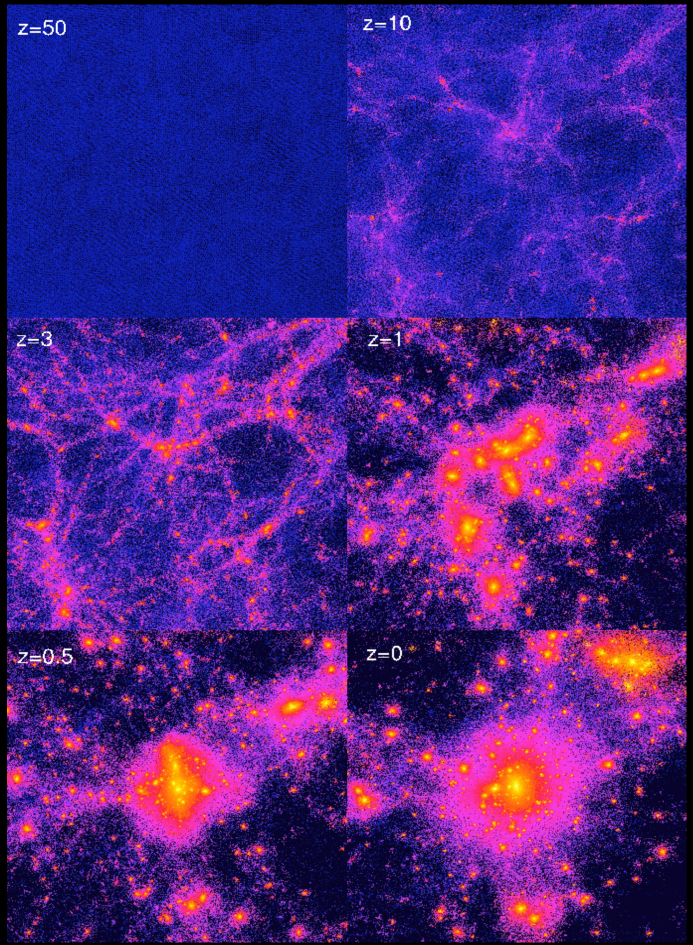

NM 2014;
Data from Wetzel et al. 2013

THE FRACTION OF QUIESCENT SATELLITE GALAXIES

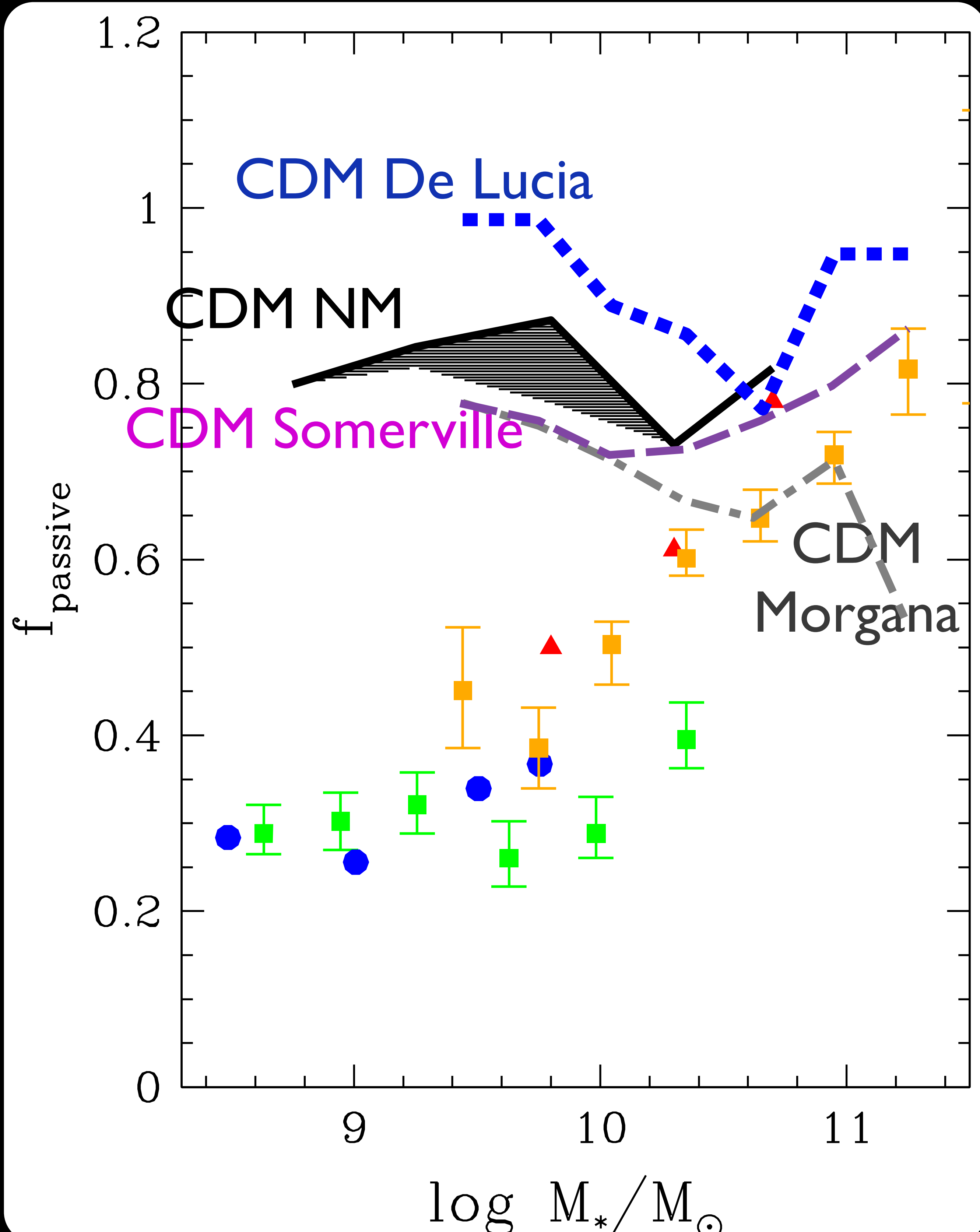

NM 2014;
Data from Wetzel et al. 2013
Kimm et al. 2014
Phillips 2014
Geha 2012

Quiescent Fraction

Measures the fract.ion of quescent satellites

Threshold SSFR<10^{-11} yrs
corresponds to minimum in the SSFR distribution
correspond to $\Delta t=3\ t_H$
(to form M_* it would need $3t_H$ at current SF rate)

$$SSFR = \dot{M}_*/M* = 10^{-11}\ \mathrm{yrs} \rightarrow M_* = 3\,t_H\,\dot{M}_*$$

Result robust with respect to different CDM models with different feedback modelling

Due to the large number of dense DM clumps collapsed at high redshifts
gas rapidly converted into stars at high-redshifts

- Cold gas converted into stars at high z
- Hot gas stripped when they were incorporated into larger DM haloes

No further star formation at low redhsift

THE FRACTION OF QUIESCENT SATELLITE GALAXIES

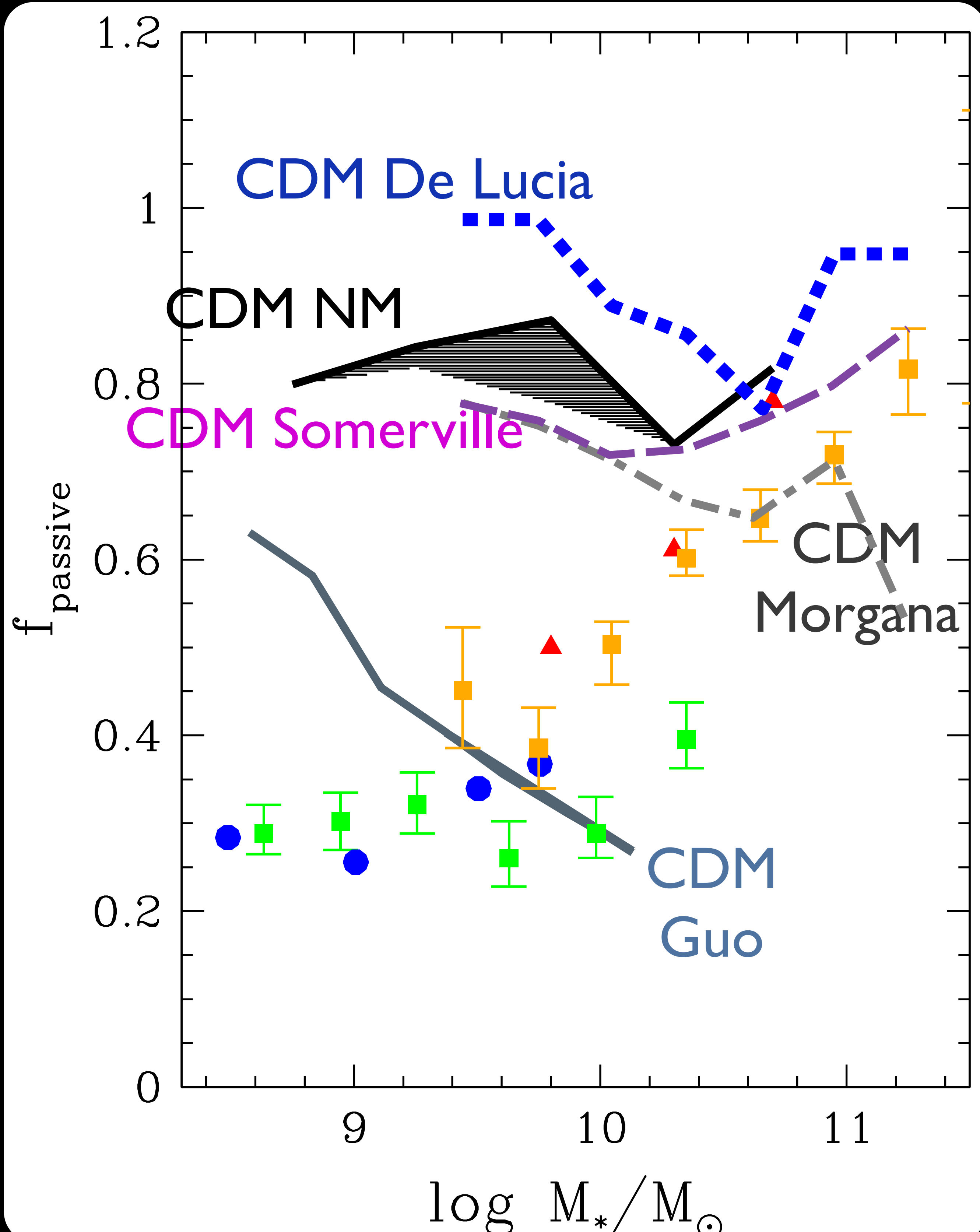

NM 2014;
Data from Wetzel et al. 2013
Kimm et al. 2014
Phillips 2014
Geha 2012

Quiescent Fraction

Measures the fract.ion of quescent satellites

Threshold SSFR<10^{-11} yrs
corresponds to minimum in the SSFR distribution
correspond to $\Delta t = 3\ t_H$
(to form M* it would need $3t_H$ at current SF rate)

$$SSFR = \dot{M}_*/M* = 10^{-11}\ \mathrm{yrs} \rightarrow M_* = 3\, t_H\, \dot{M}_*$$

Result robust with respect to different CDM models with different feedback modelling

Due to the large number of dense DM clumps collapsed at high redshifts
gas rapidly converted into stars at high-redshifts

- Cold gas converted into stars at high z
- Hot gas stripped when they were incorporated into larger DM haloes

No further star formation at low redhsift

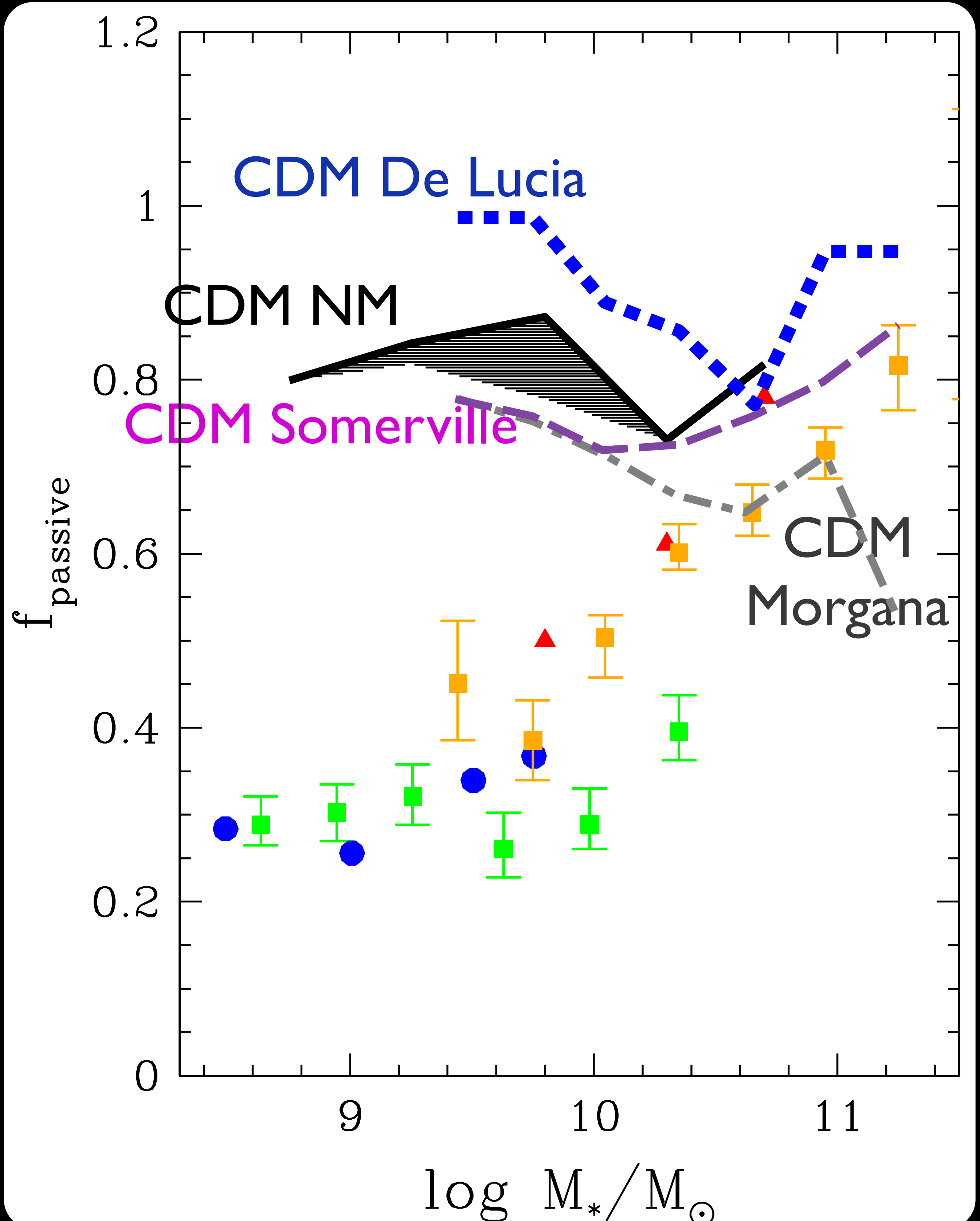

NM 2014;
Data from Wetzel et al. 2013
Kimm et al. 2014
Phillips 2014
Geha 2012

THE FRACTION OF QUIESCENT SATELLITE GALAXIES

Quiescent Fraction

Measures the fract.ion of quescent satellites

Threshold SSFR<10^{-11} yrs
corresponds to minimum in the SSFR distribution
correspond to Δt=3 t_H
(to form M_* it would need 3t_H at current SF rate)

$$SSFR = \dot{M}_*/M* = 10^{-11}\ \text{yrs} \rightarrow M_* = 3\,t_H\,\dot{M}_*$$

Result robust with respect to different CDM models with different feedback modelling

Due to the large number of dense DM clumps collapsed at high redshifts
gas rapidly converted into stars at high-redshifts

- Cold gas converted into stars at high z
- Hot gas stripped when they were incorporated into larger DM haloes

No further star formation at low redhsift

THE FRACTION OF QUIESCENT SATELLITE GALAXIES

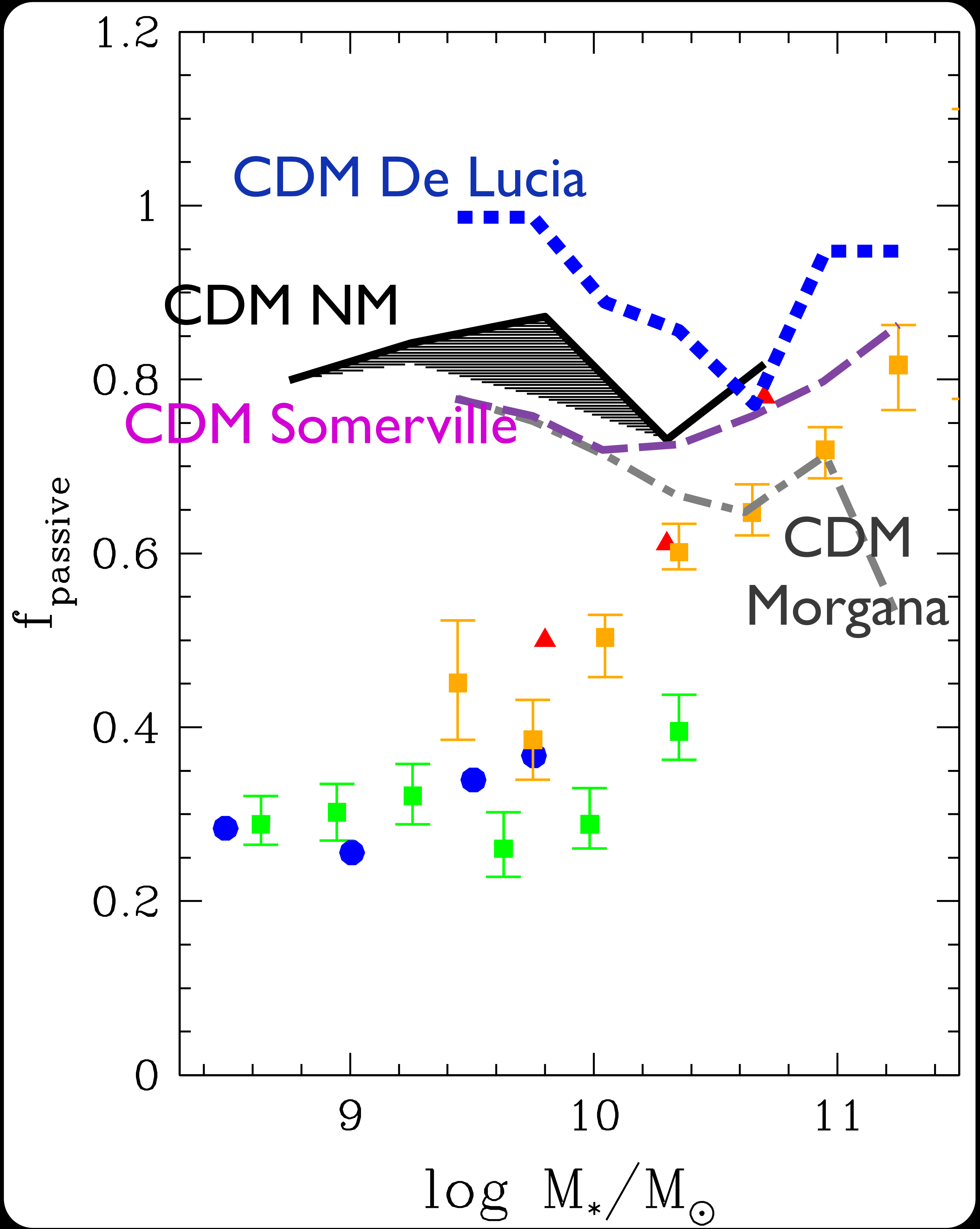

NM 2014;
Data from Wetzel et al. 2013
Kimm et al. 2014
Phillips 2014
Geha 2012

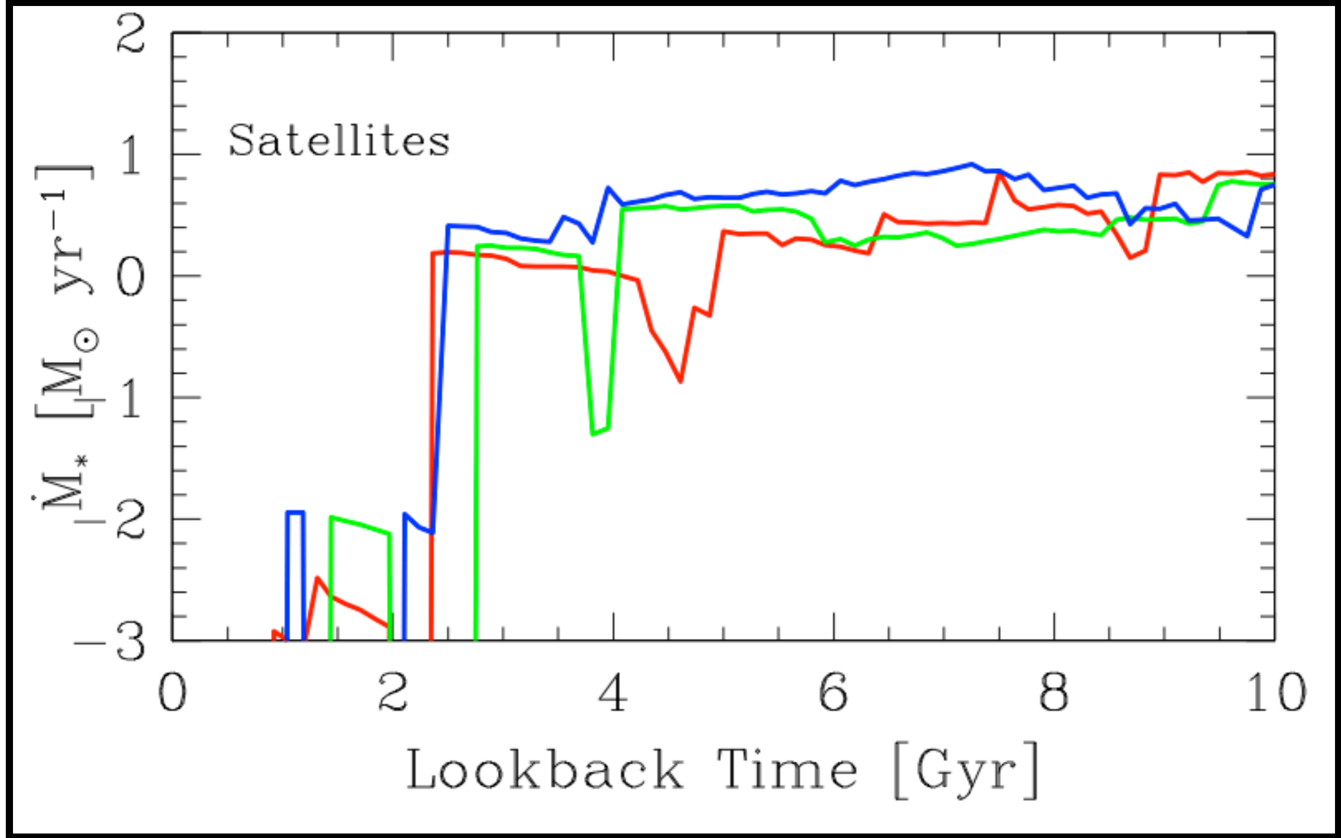

Result robust with respect to different CDM models with different feedback modelling

Due to the large number of dense DM clumps collapsed at high redshifts
gas rapidly converted into stars at high-redshifts

- Cold gas converted into stars at high z
- Hot gas stripped when they were incorporated into larger DM haloes

No further star formation at low redhsift

THE FRACTION OF QUIESCENT SATELLITE GALAXIES

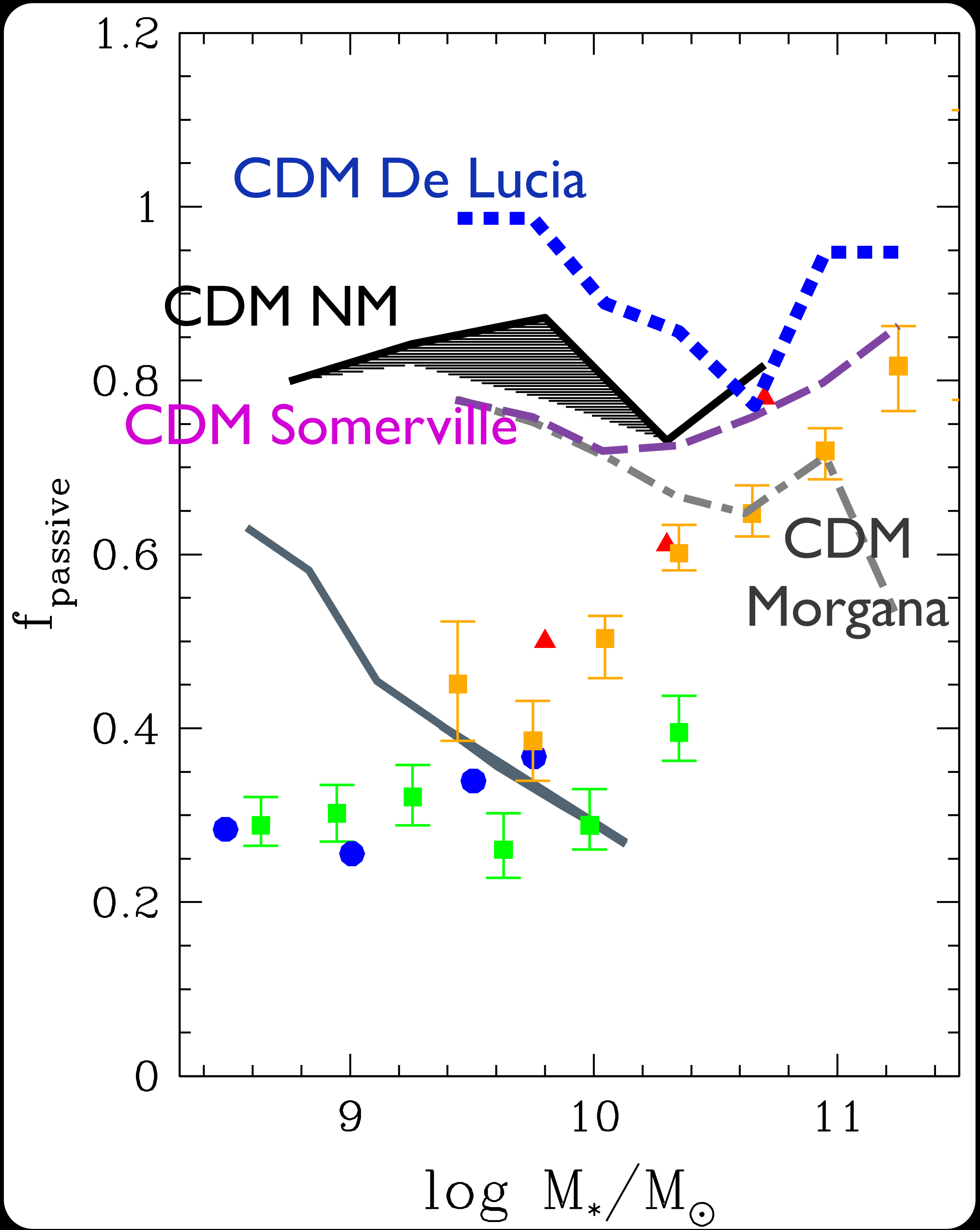

NM 2014;
Data from Wetzel et al. 2013
Kimm et al. 2014
Phillips 2014
Geha 2012

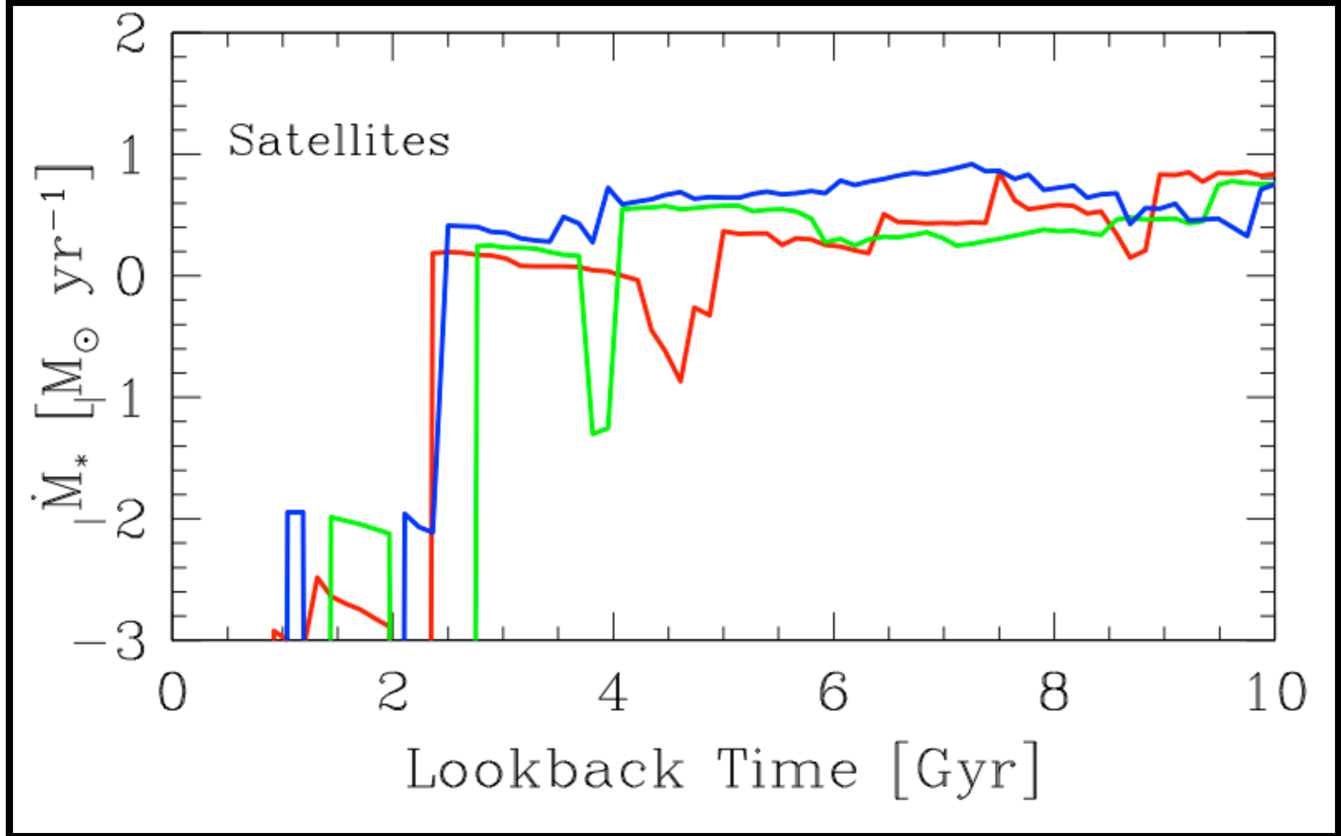

Result robust with respect to different CDM models with different feedback modelling

Due to the large number of dense DM clumps collapsed at high redshifts
gas rapidly converted into stars at high-redshifts

- Cold gas converted into stars at high z
- Hot gas stripped when they were incorporated into larger DM haloes

No further star formation at low redhsift

THE FRACTION OF QUIESCENT SATELLITE GALAXIES

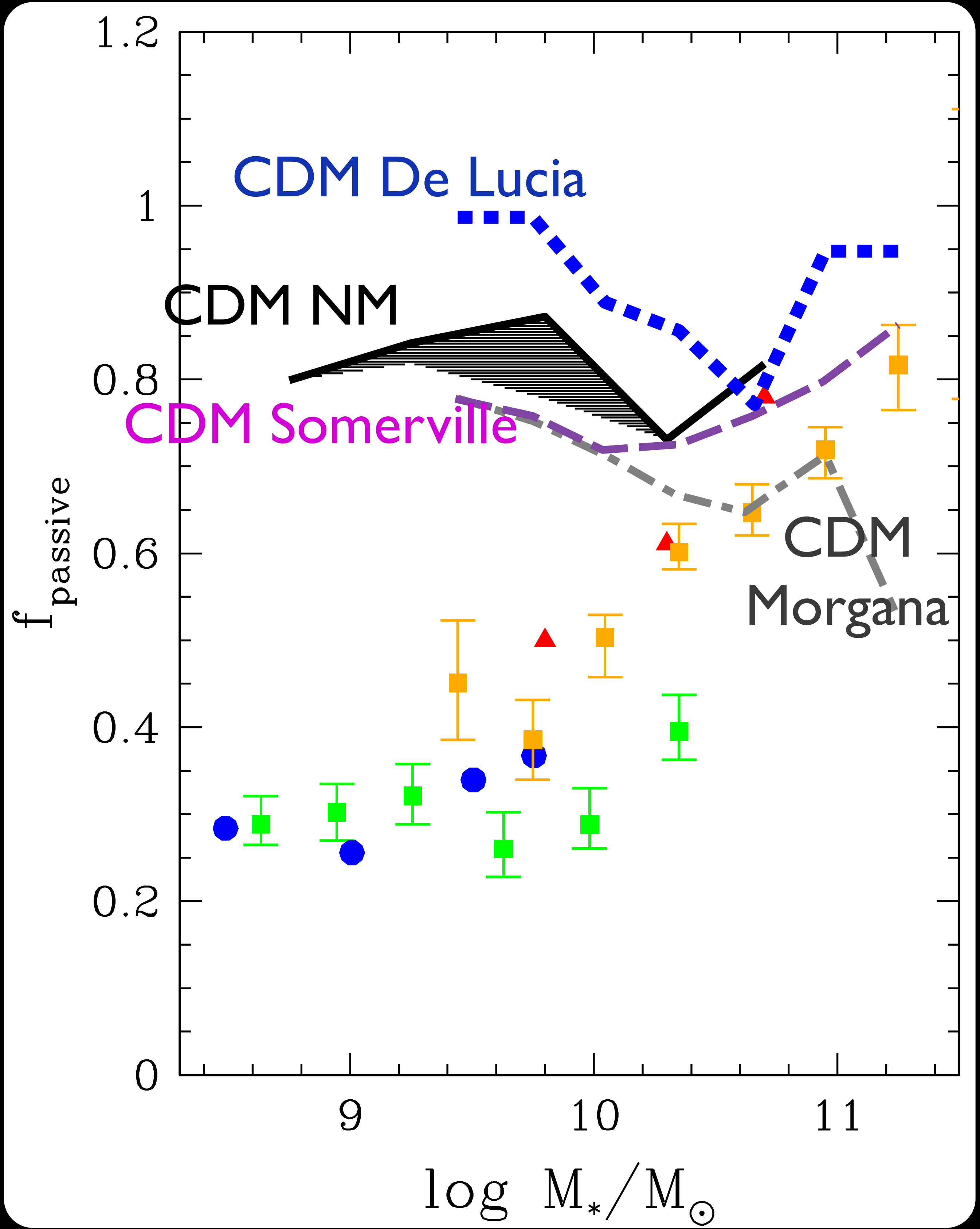

NM 2014;
Data from Wetzel et al. 2013
Kimm et al. 2014
Phillips 2014
Geha 2012

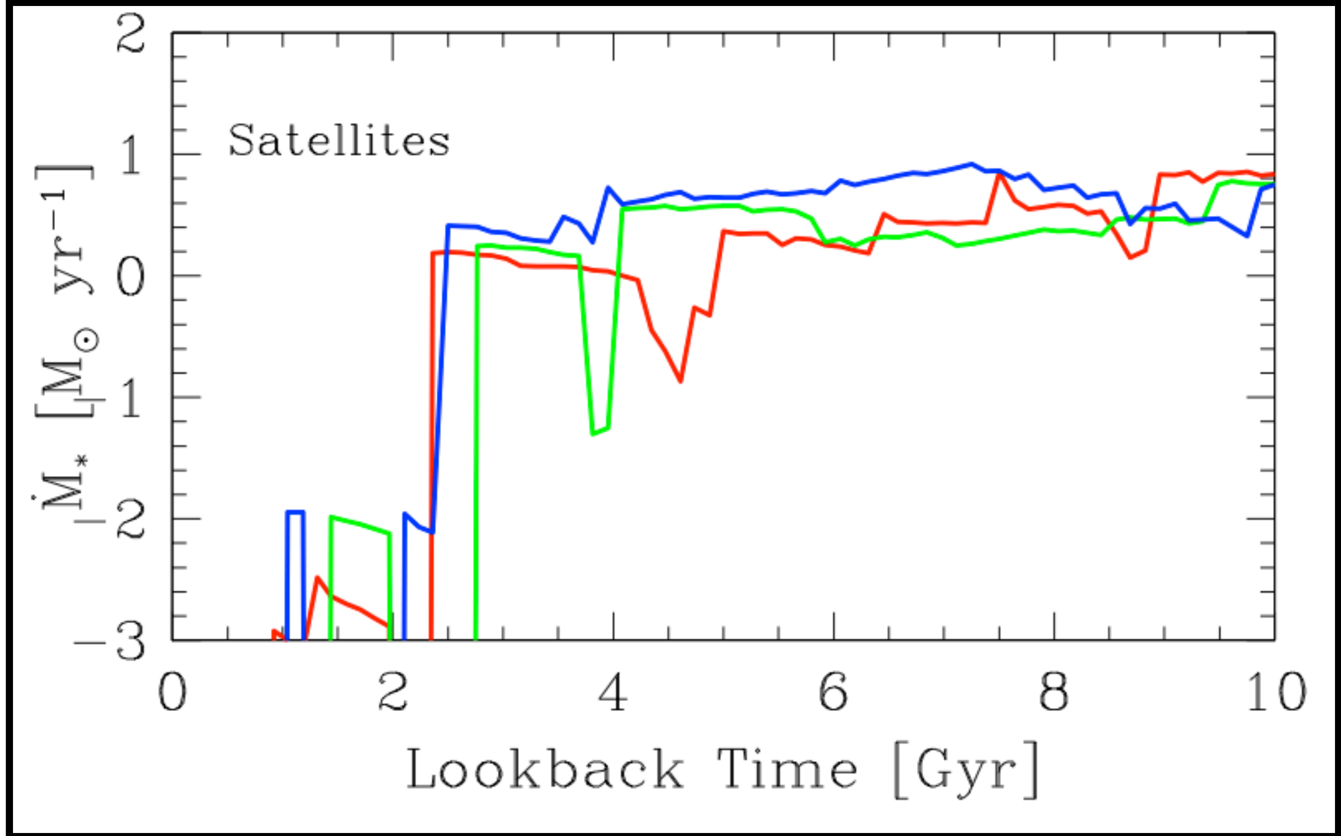

Result robust with respect to different CDM models with different feedback modelling

Due to the large number of dense DM clumps collapsed at high redshifts
gas rapidly converted into stars at high-redshifts

- Cold gas converted into stars at high z
- Hot gas stripped when they were incorporated into larger DM haloes

No further star formation at low redhsift

THE FRACTION OF QUIESCENT SATELLITE GALAXIES

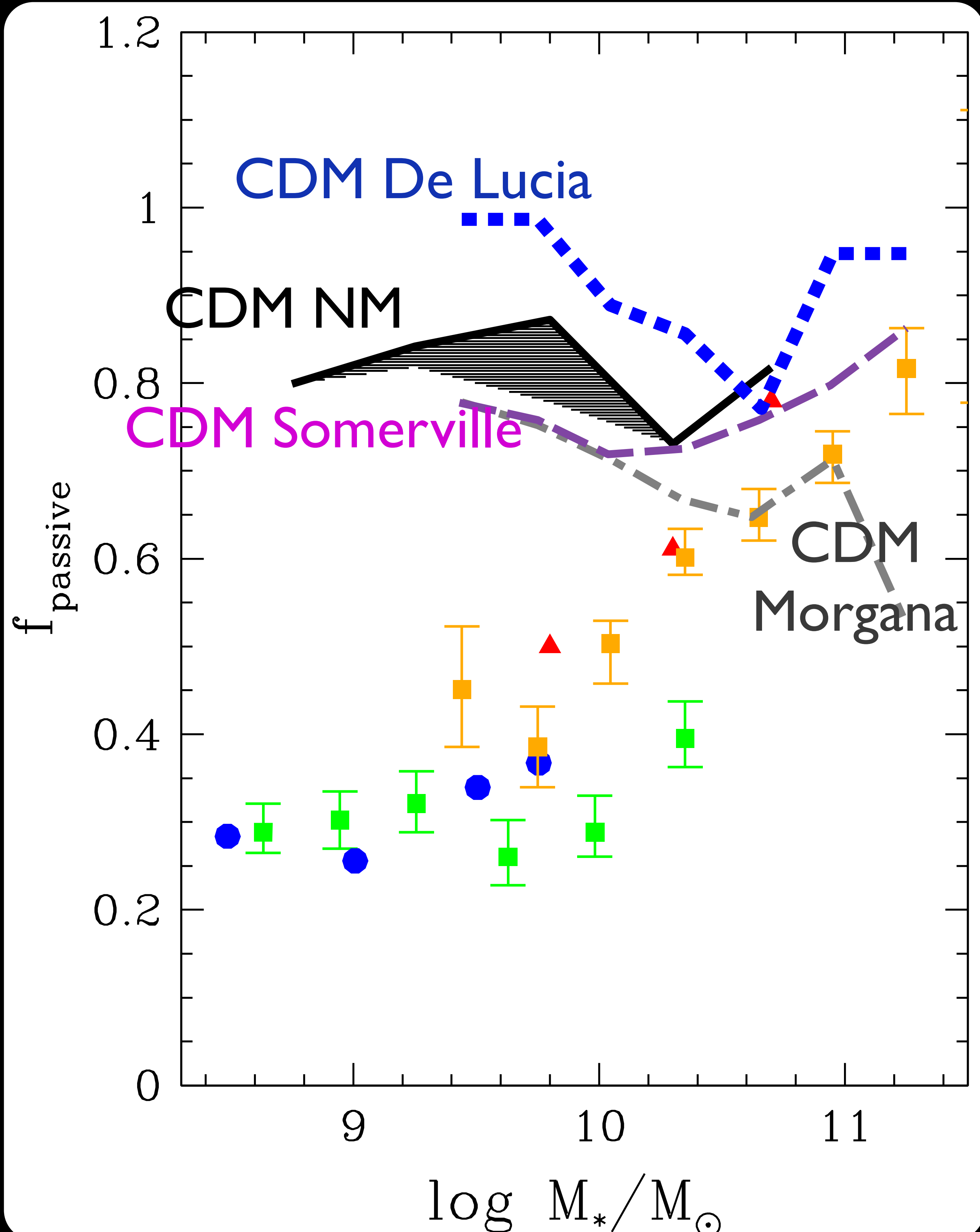

NM 2014;
Data from Wetzel et al. 2013
Kimm et al. 2014
Phillips 2014
Geha 2012

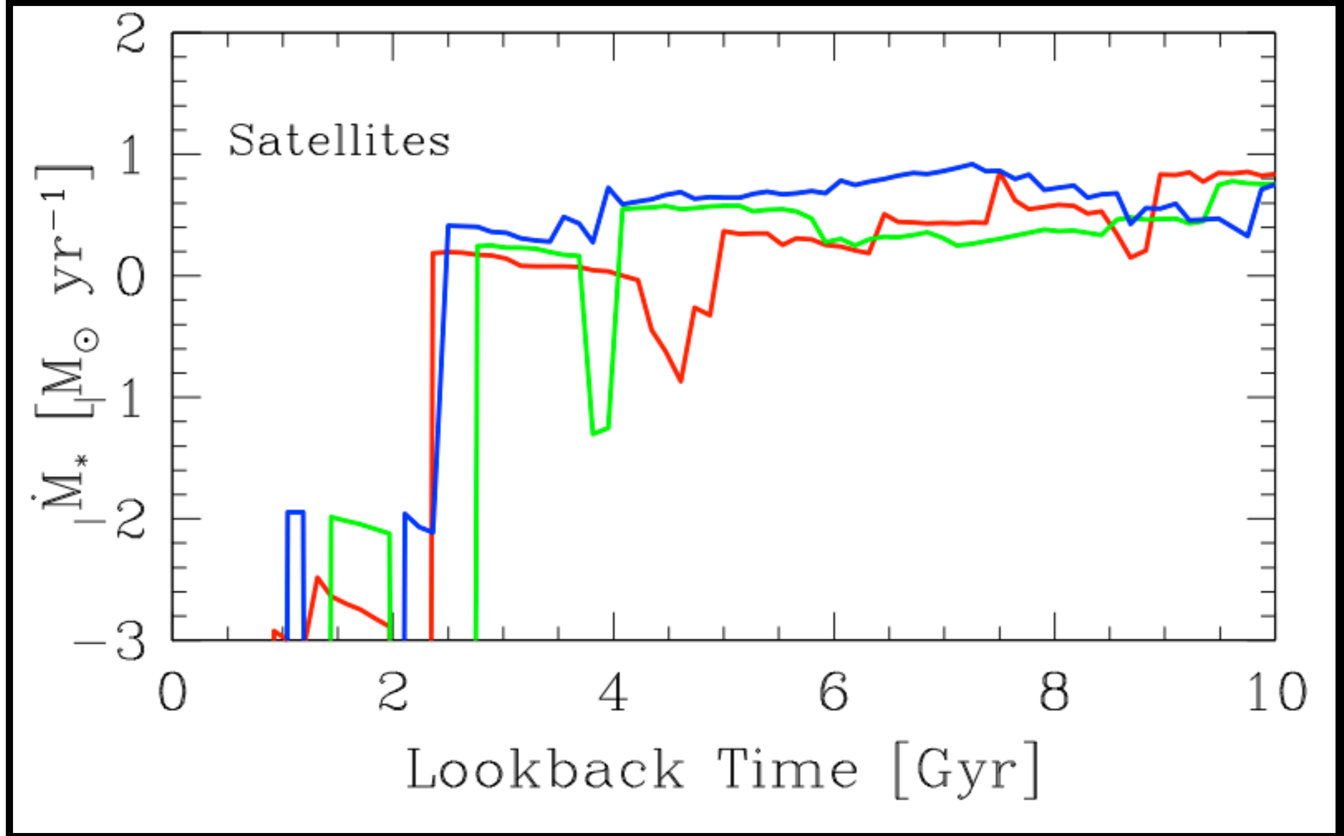

Result robust with respect to different CDM models with different feedback modelling

Due to the large number of dense DM clumps collapsed at high redshifts
gas rapidly converted into stars at high-redshifts

- Cold gas converted into stars at high z
- Hot gas stripped when they were incorporated into larger DM haloes

No further star formation at low redhsift

Star Formation histories of satellites in WDM

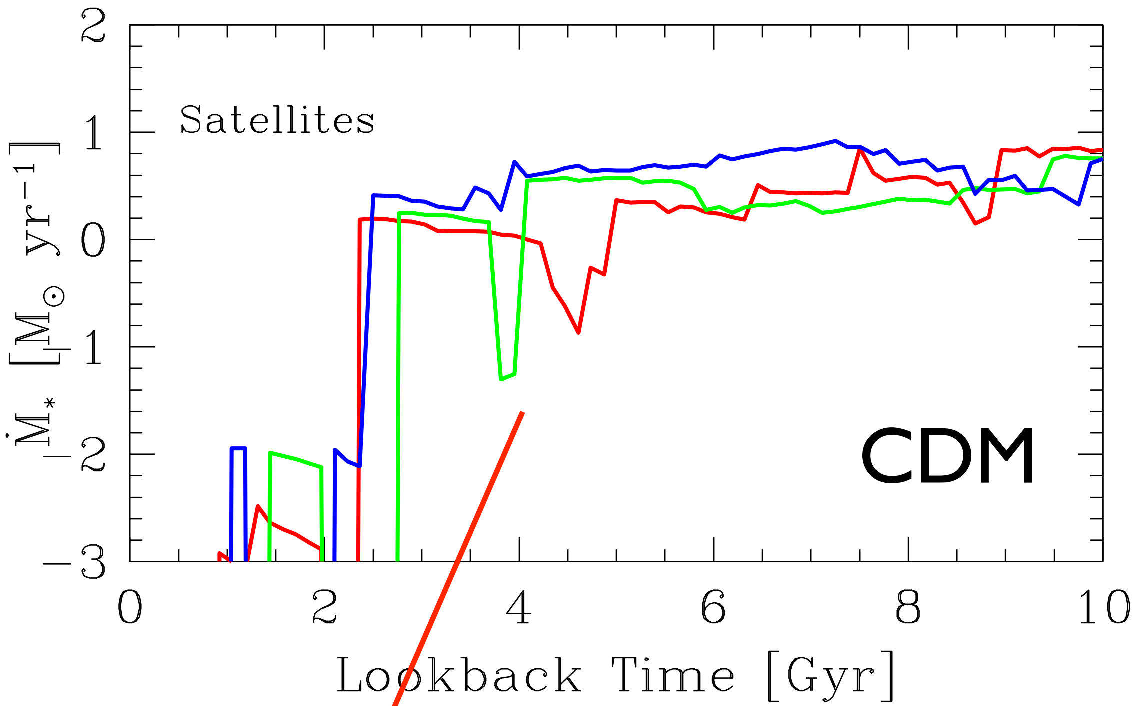

Passive Satellites in CDM at low redshift

- Cold gas converted into stars at high z
- Hot gas stripped when they were incorporated into larger DM haloesNo further star formation

CDM

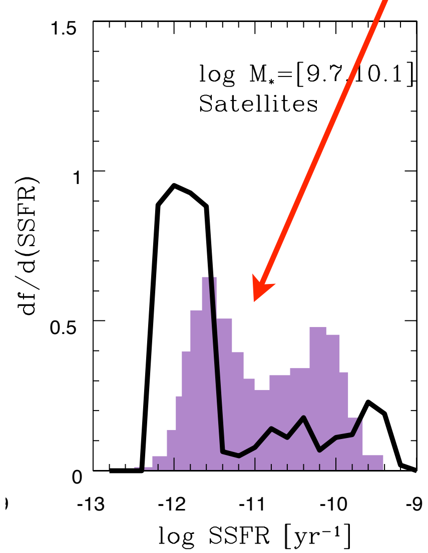

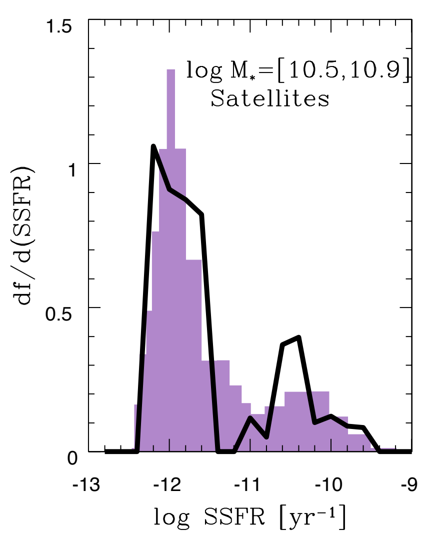

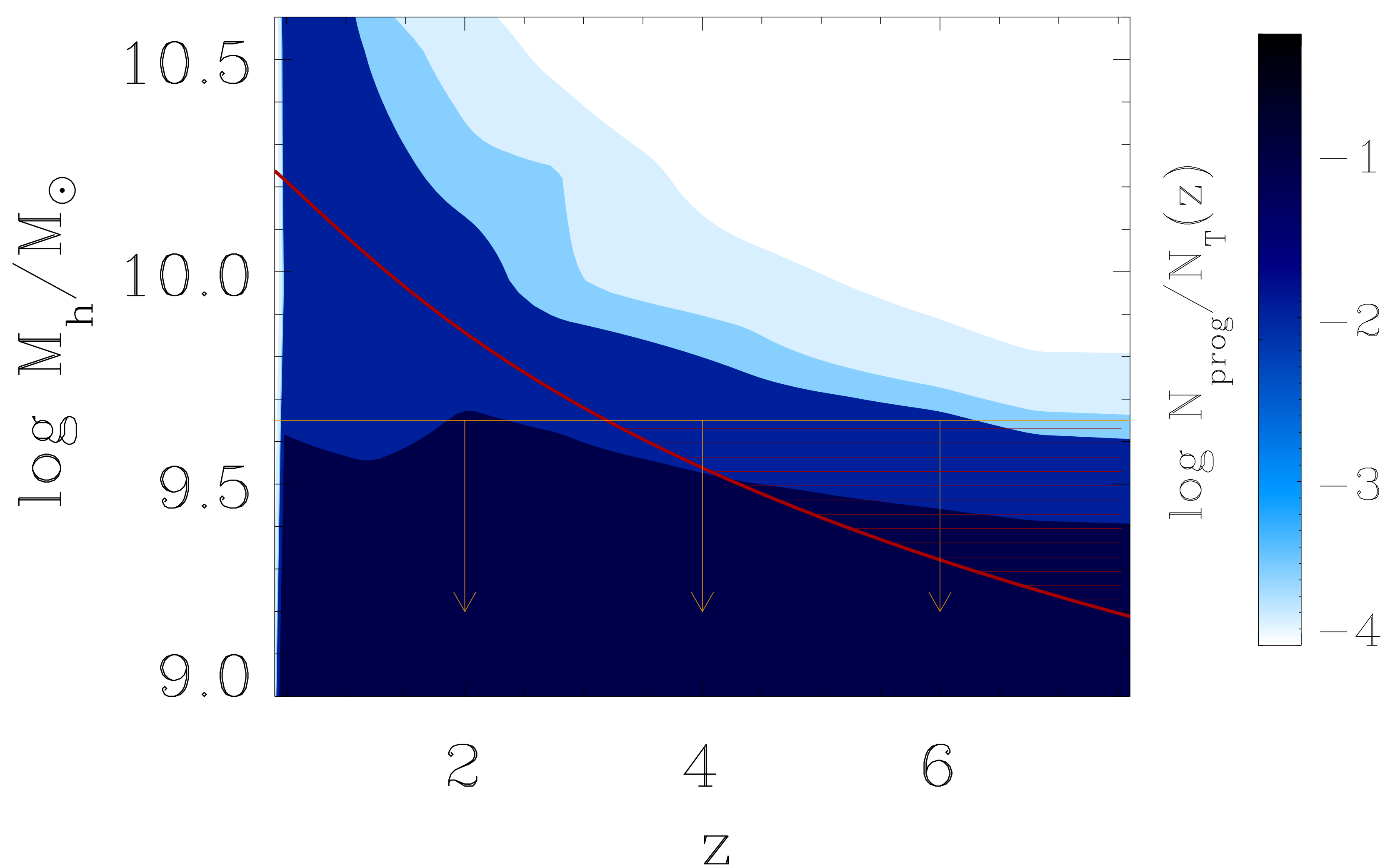

Star Formation histories of satellites in WDM

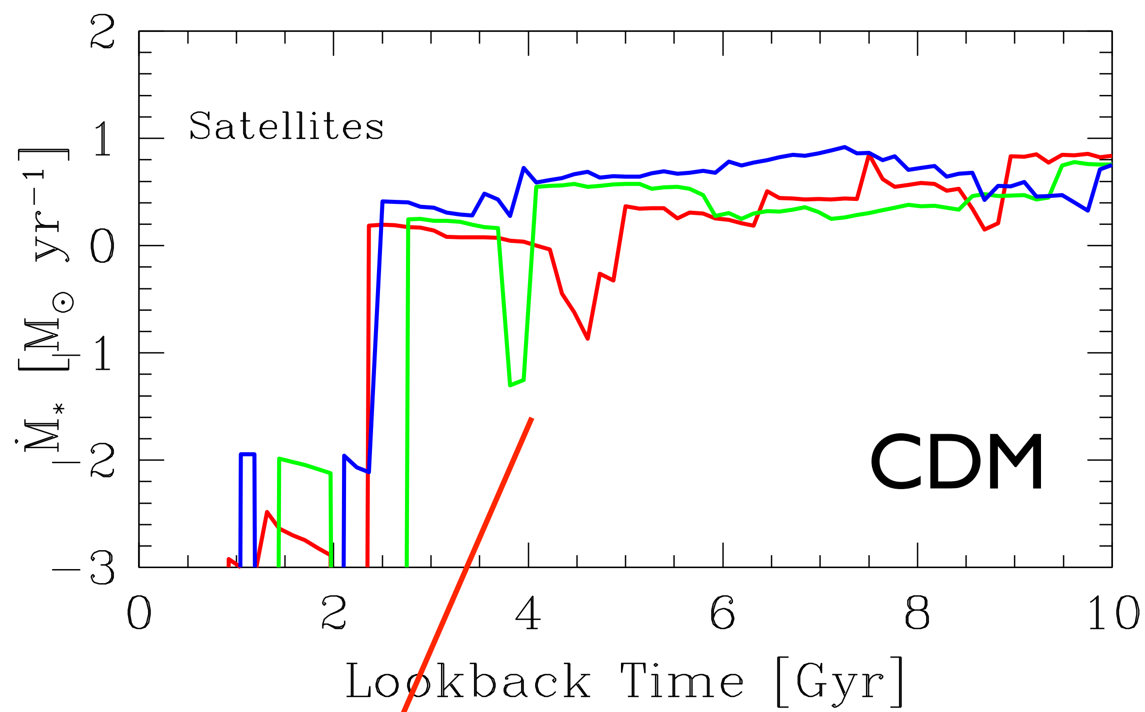

Passive Satellites in CDM at low redshift
- Cold gas converted into stars at high z
- Hot gas stripped when they were incorporated into larger DM haloesNo further star formation

CDM

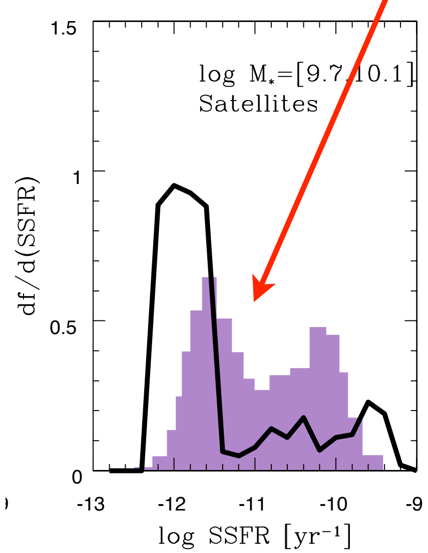

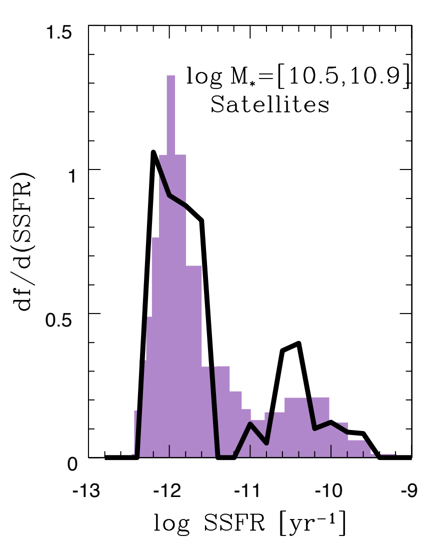

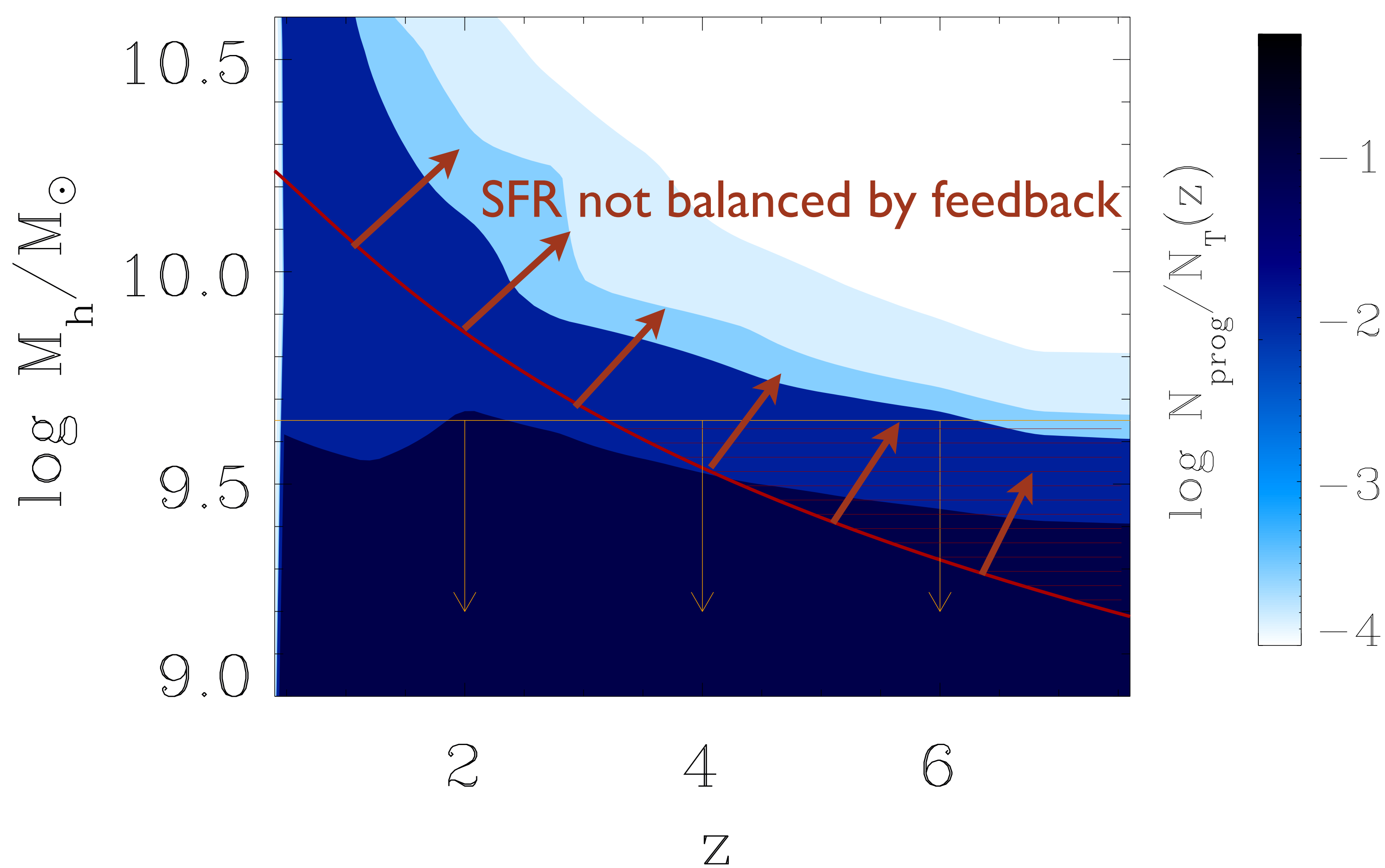

Star Formation histories of satellites in WDM

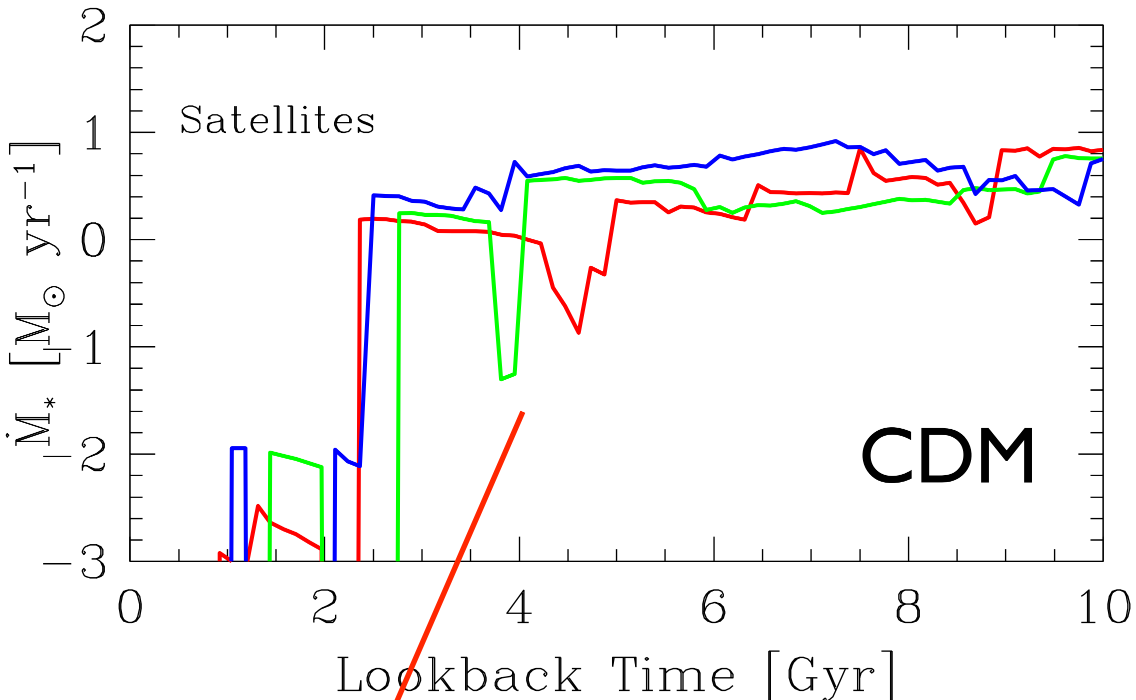

Passive Satellites in CDM at low redshift

- Cold gas converted into stars at high z
- Hot gas stripped when they were incorporated into larger DM haloesNo further star formation

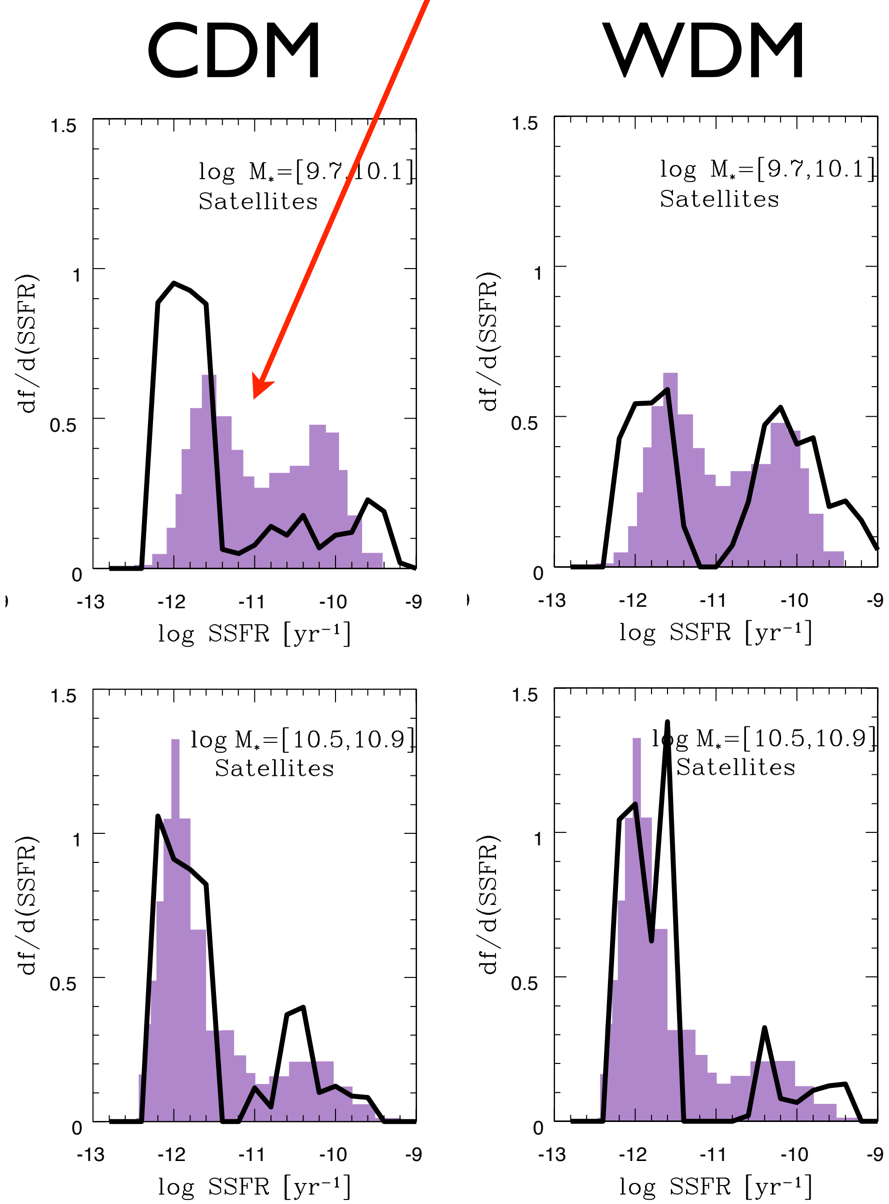

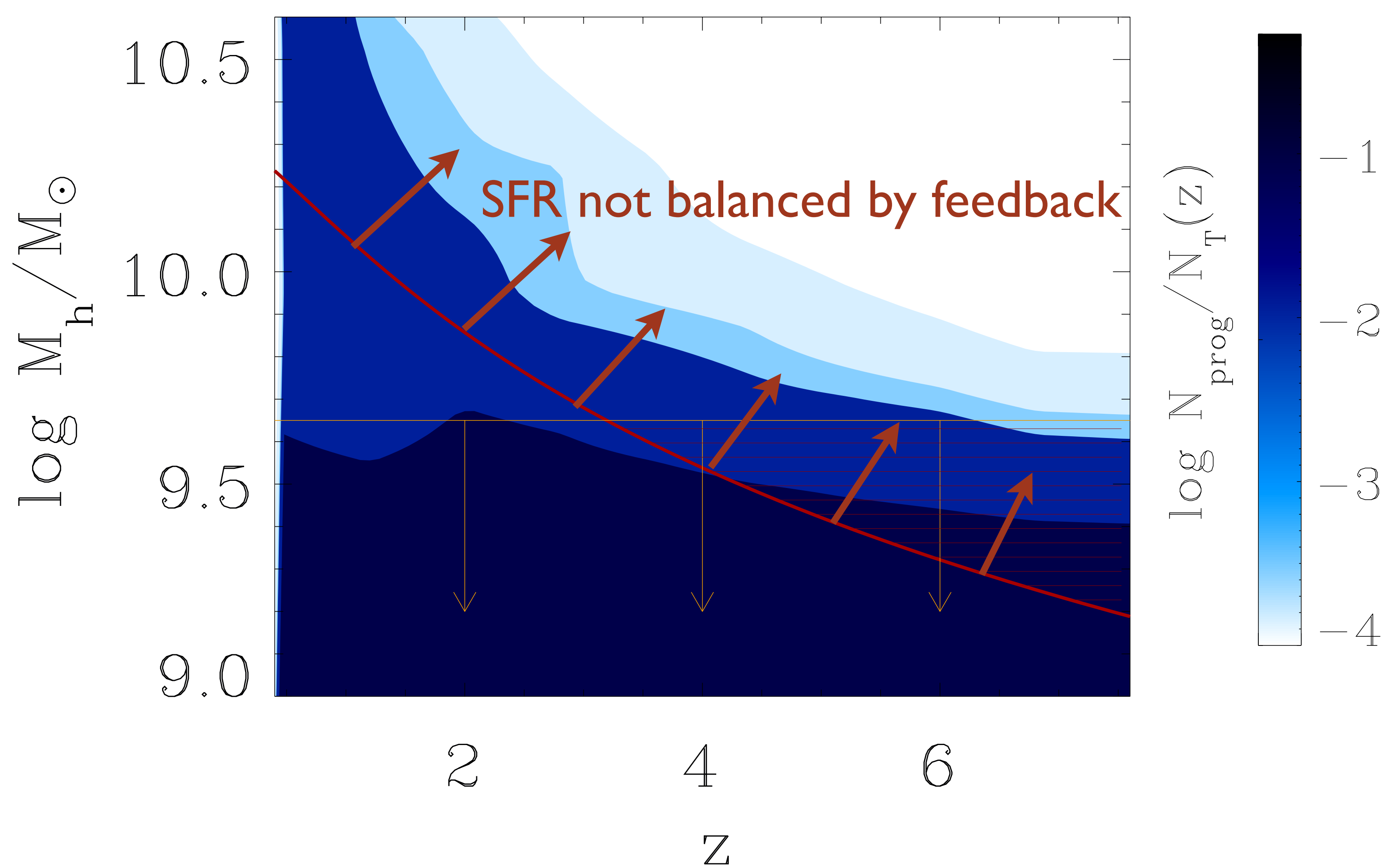

Star Formation histories of satellites in WDM

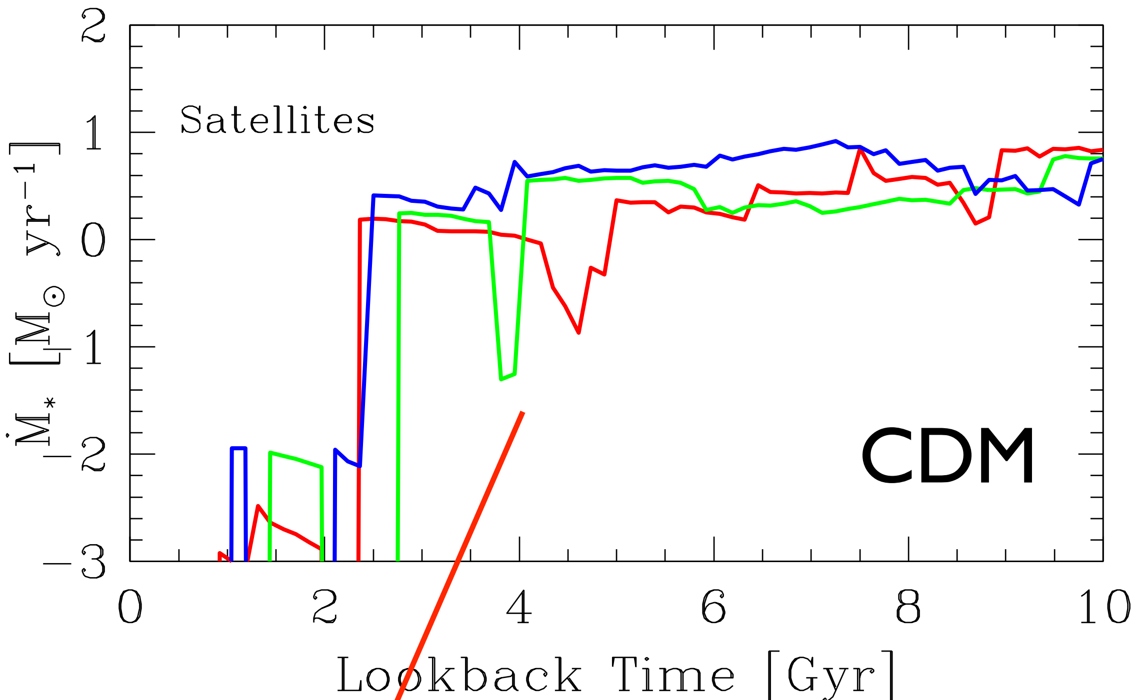

Passive Satellites in CDM at low redshift

- Cold gas converted into stars at high z
- Hot gas stripped when they were incorporated into larger DM haloesNo further star formation

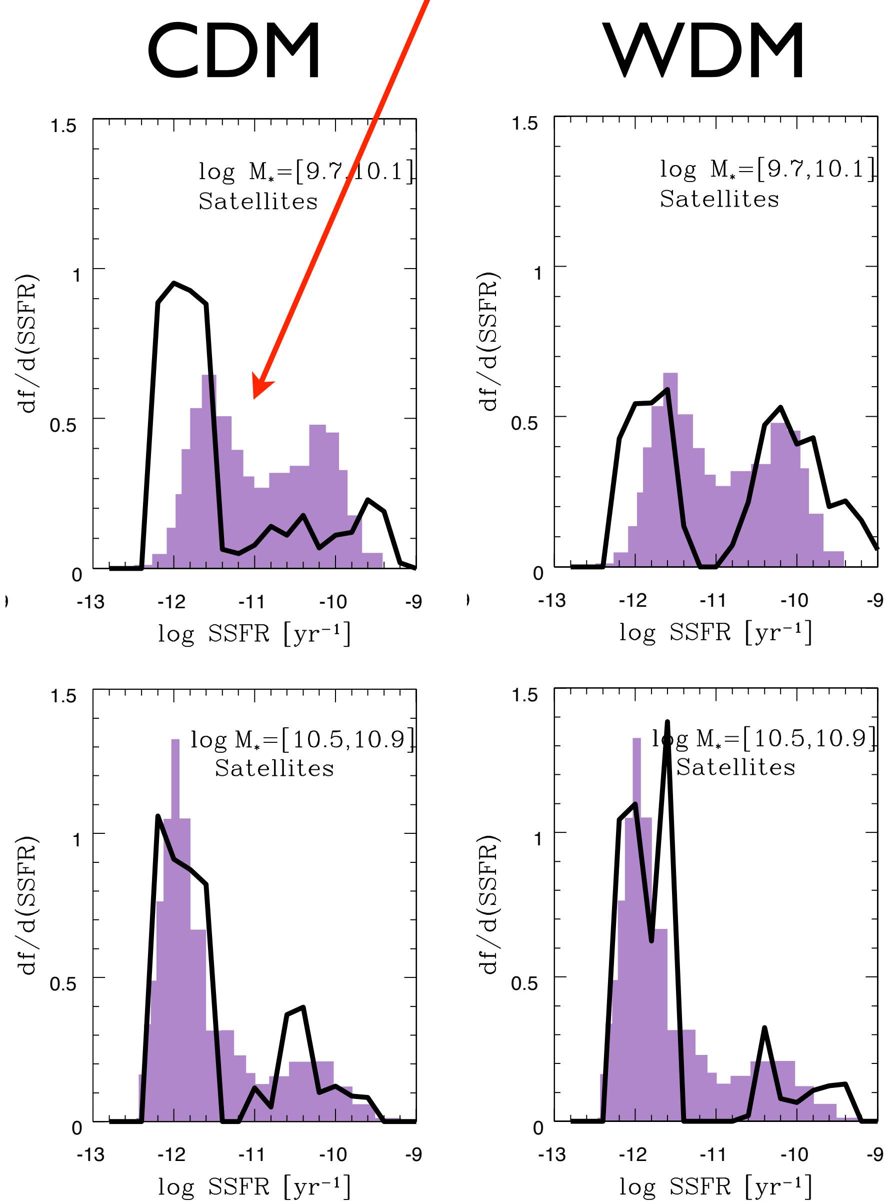

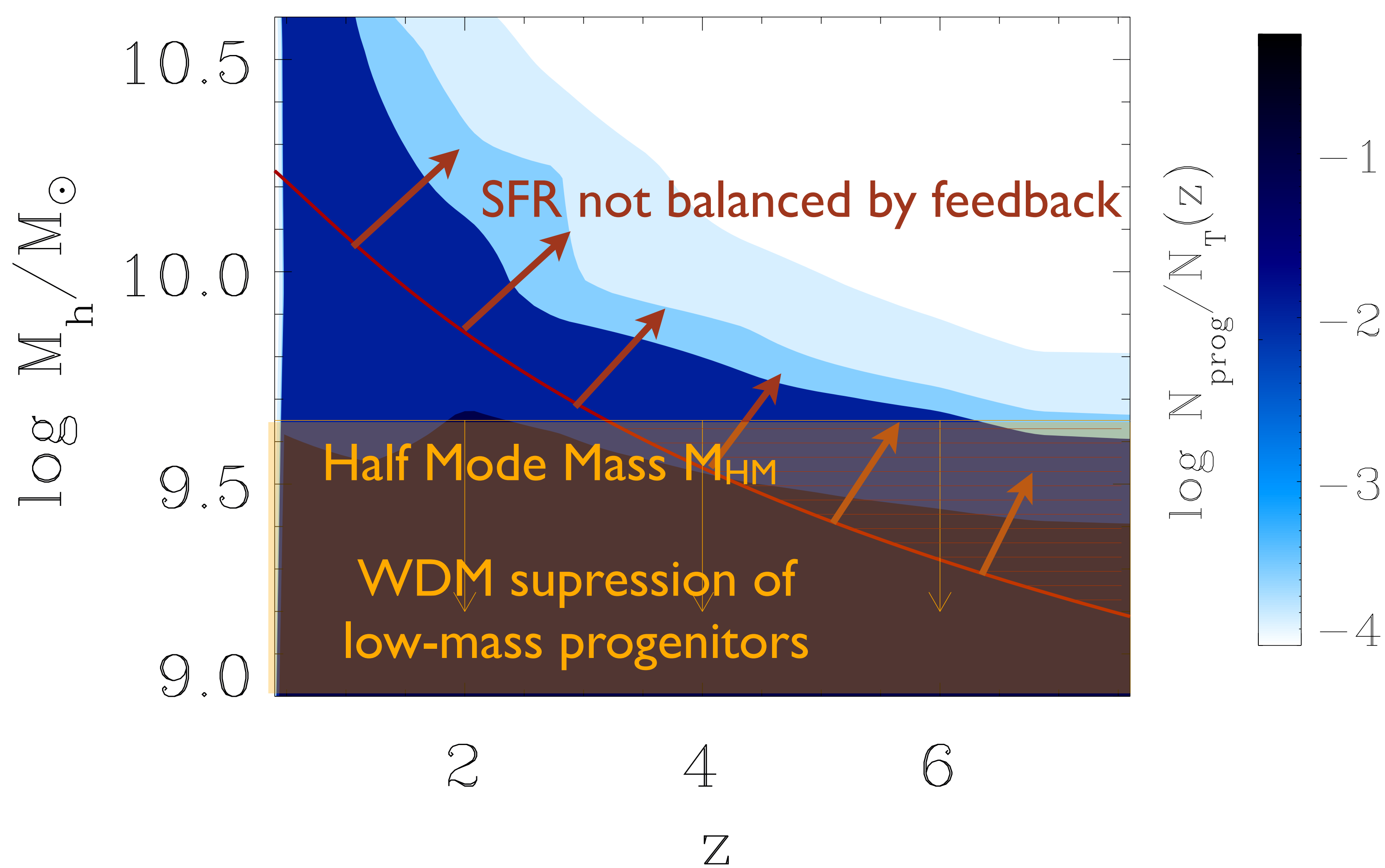

Star Formation histories of satellites in WDM

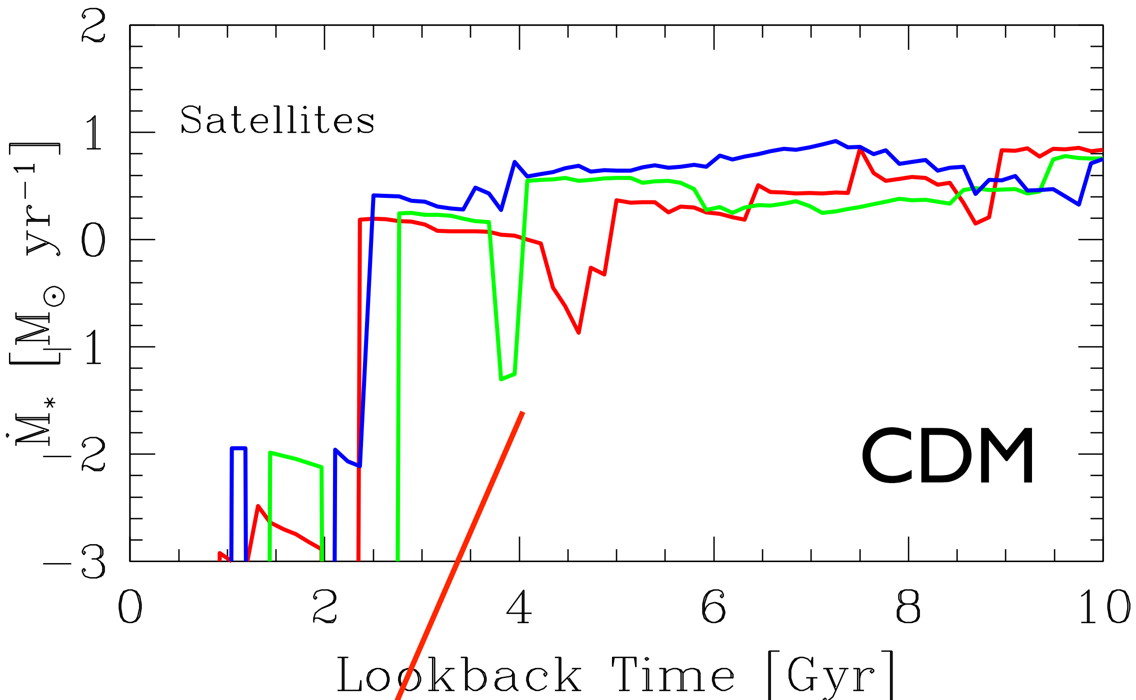

Passive Satellites in CDM at low redshift

- Cold gas converted into stars at high z
- Hot gas stripped when they were incorporated into larger DM haloesNo further star formation

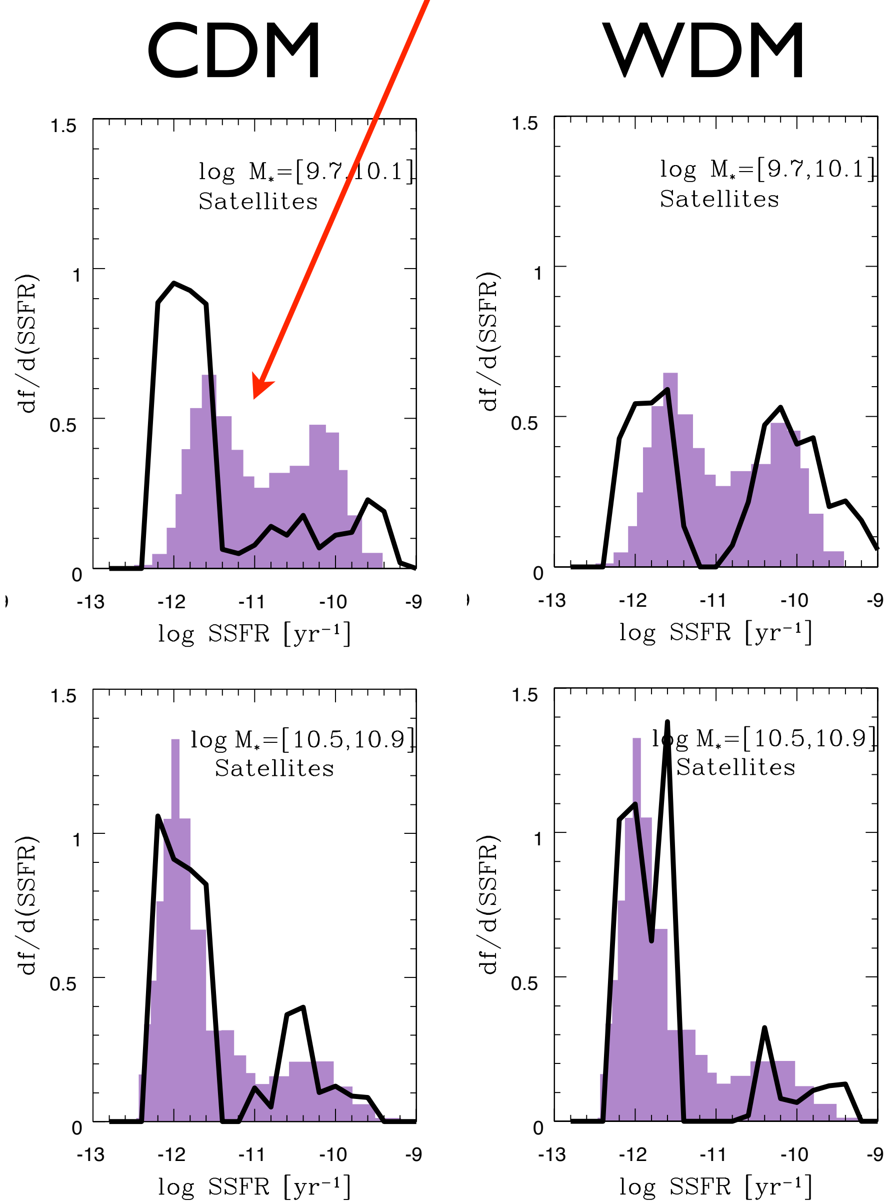

Reduction in the number of progenitors with high SFR at high redshifts

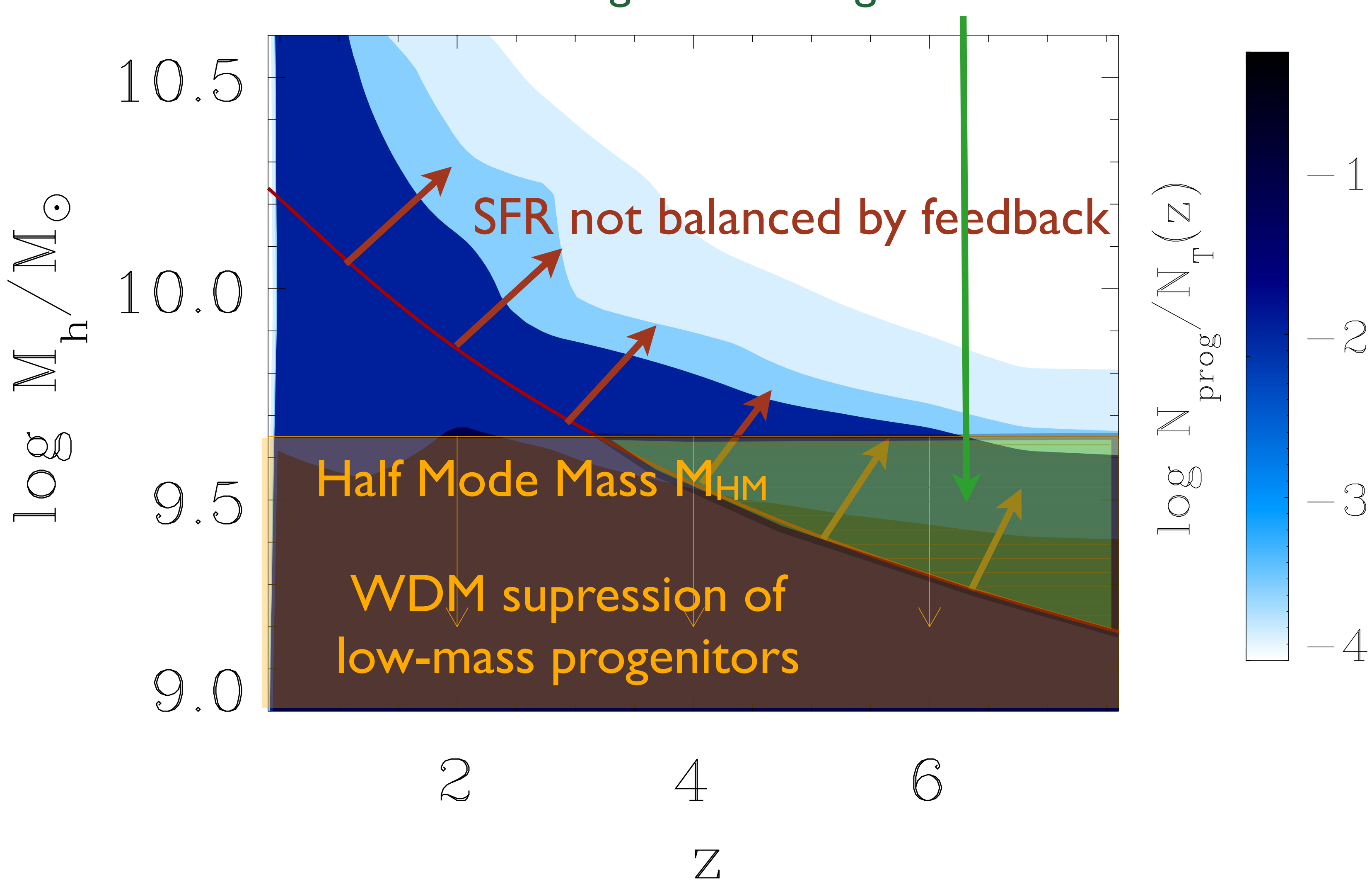

Growth of Stellar Mass for Satellite Galaxies

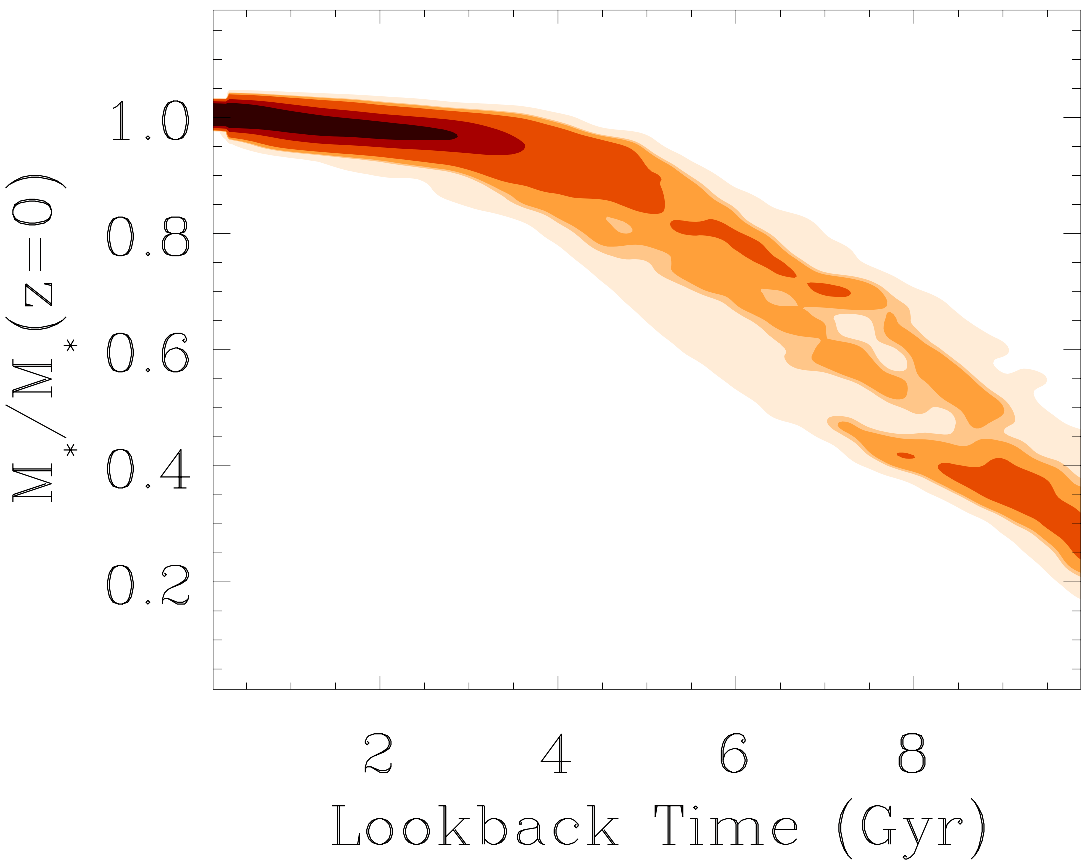

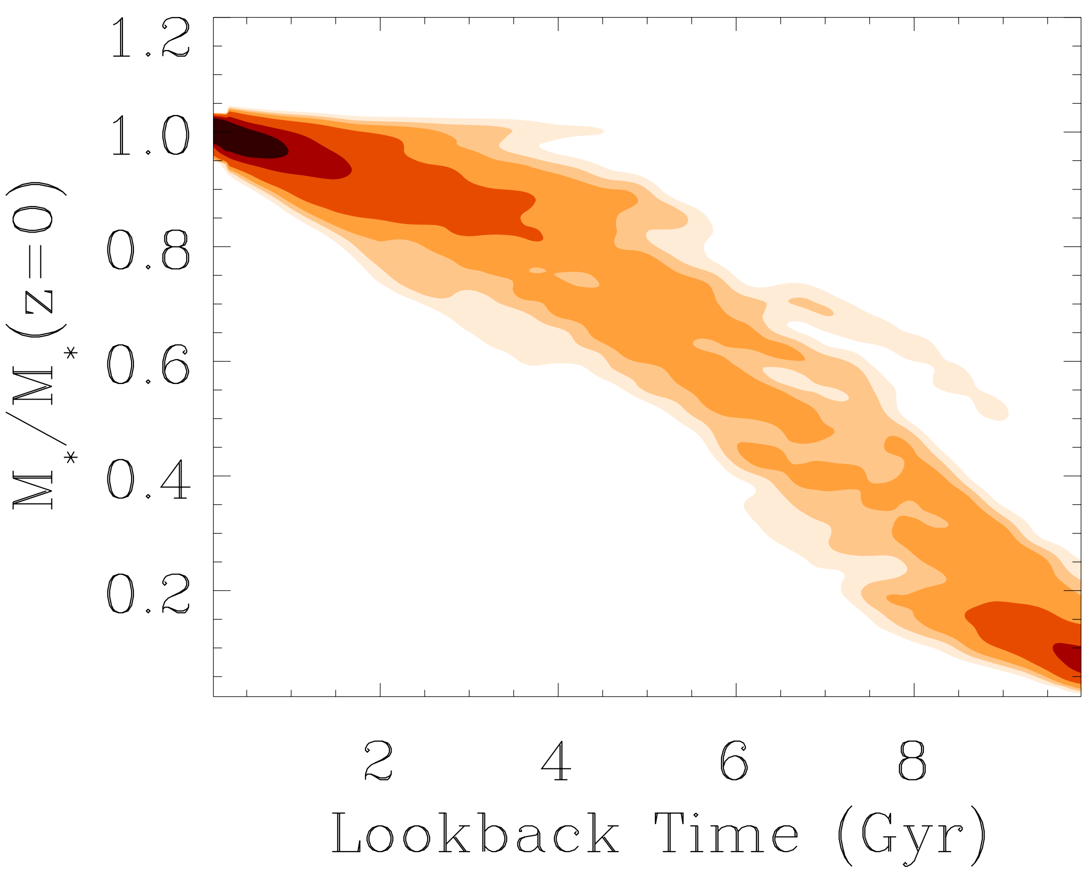

The suppression of progenitors of satellite galaxies with high SFR (those characterized by ineffective feedback) yields Slower growth of stella mass in WDM

Growth of Stellar Mass for Satellite Galaxies

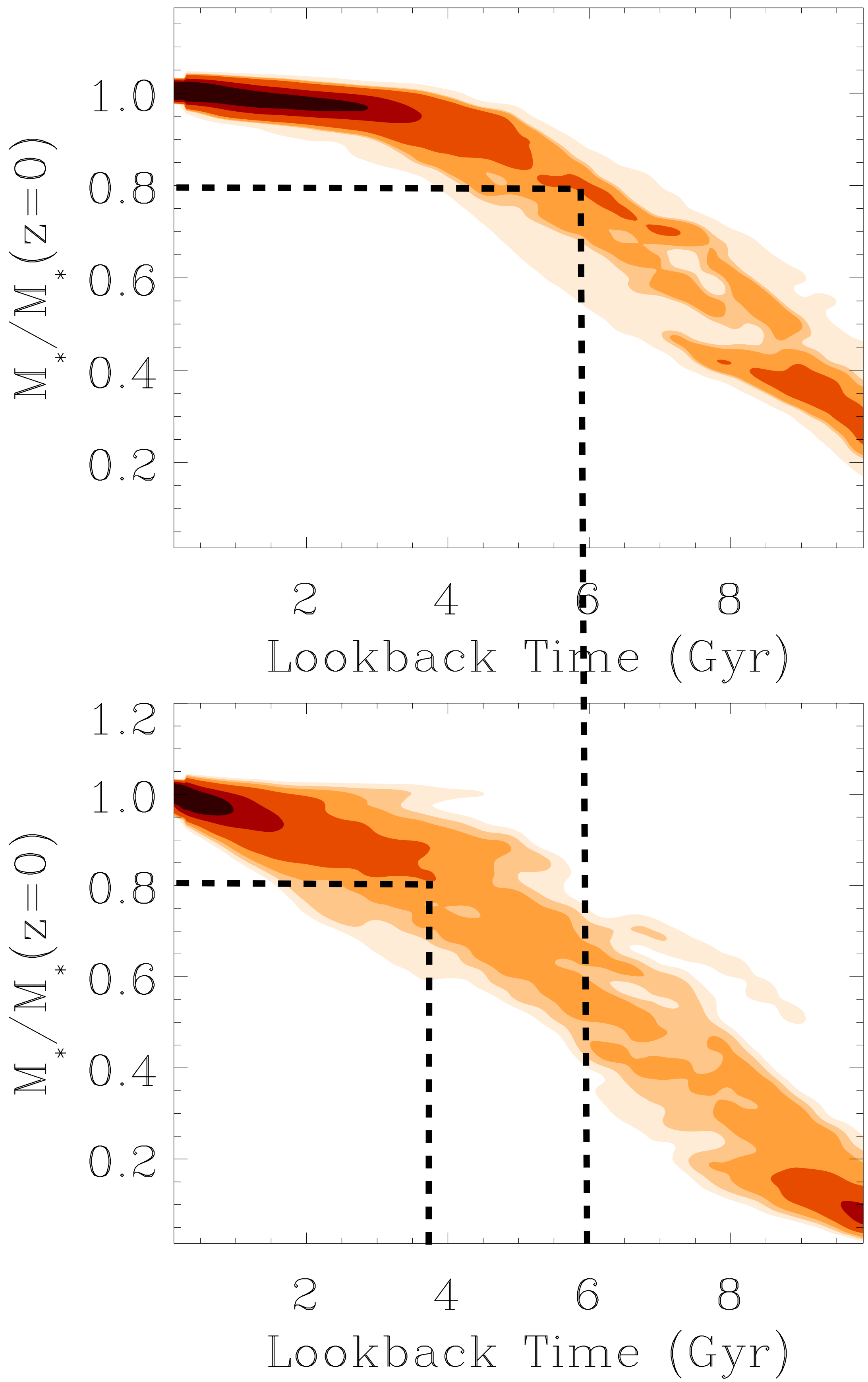

The suppression of progenitors of satellite galaxies with high SFR (those characterized by ineffective feedback) yields Slower growth of stella mass in WDM

CDM: 80 % of mass formed 6 Gyr ago
WDM: 80 % of mass formed 4 Gyr ago

Approx. delay ~ 2 Gyr

Fraction of Quiescent Satellite Galaxies

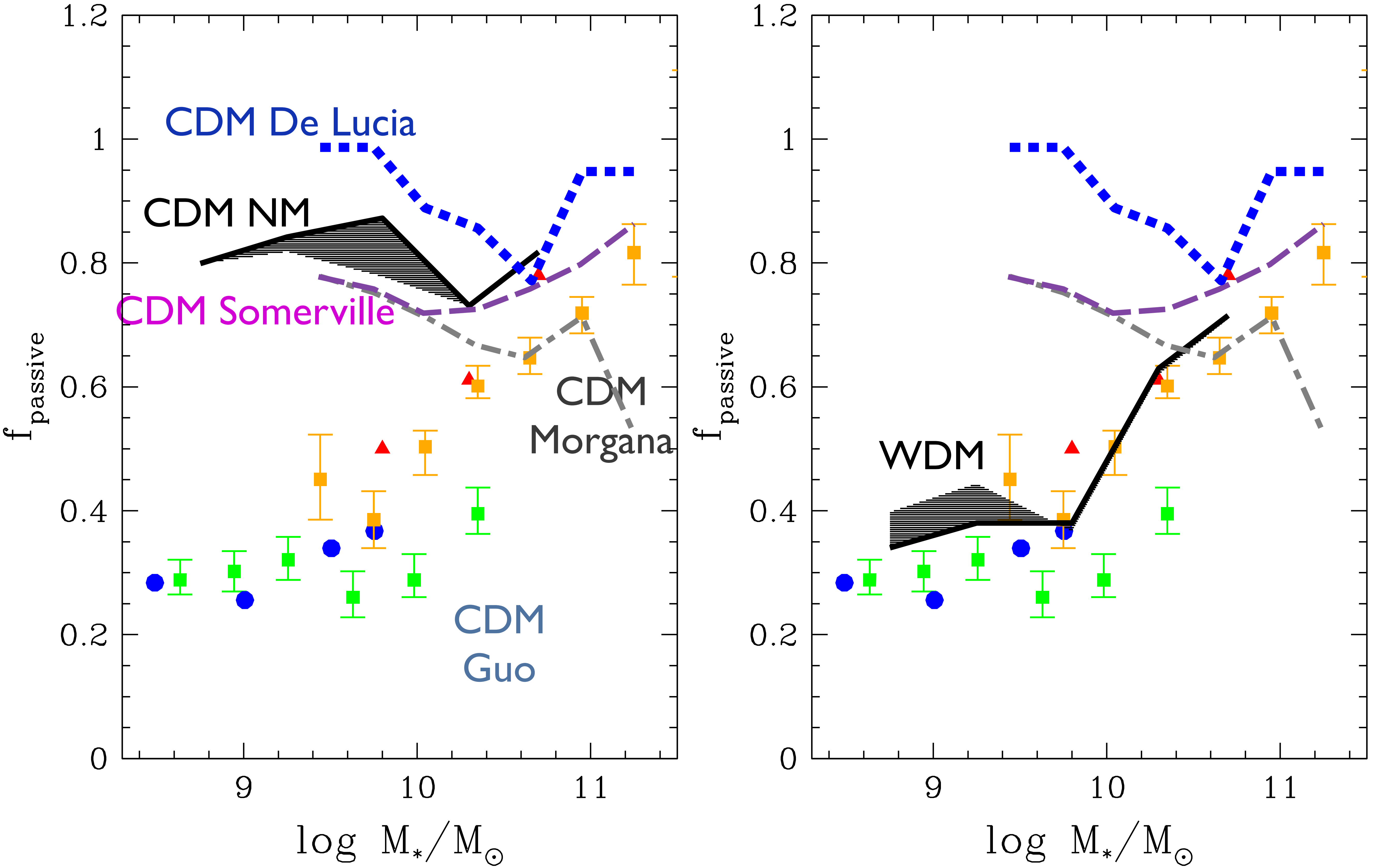

The Age of stellar populations in low-mass galaxies

CDM predicts early collapse of a huge number of low-mass halos, which remain isolated at later times retaining the early-formed stellar populations; as a result, CDM-based SAMs generally provide flat age-mass relations (Fontanot et al. 2009; Pasquali et al. 2010; De Lucia & Borgani 2012).

Increasing the stellar feedback worsen the problem

Early SF: WDM induces delay in star formation, affects small-mass objects(see, e.g., Angulo et al. 2013)

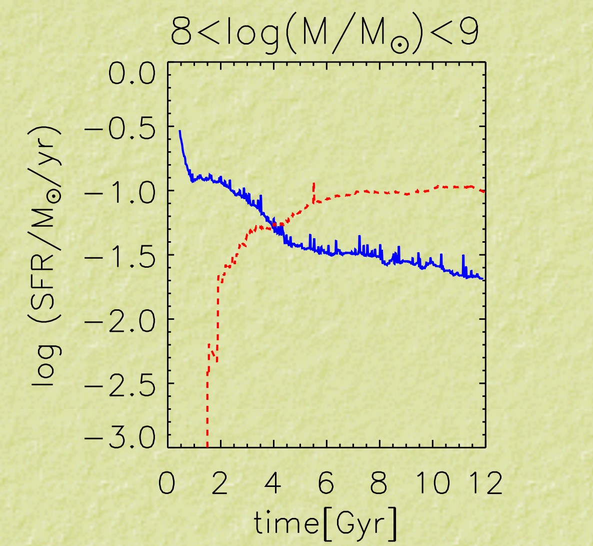

$$Age(t_0) = \frac{\int_0^{t_0} (t_0 - t)\,\psi(t)\,dt}{\int_0^{t_0} \psi(t)\,dt}$$

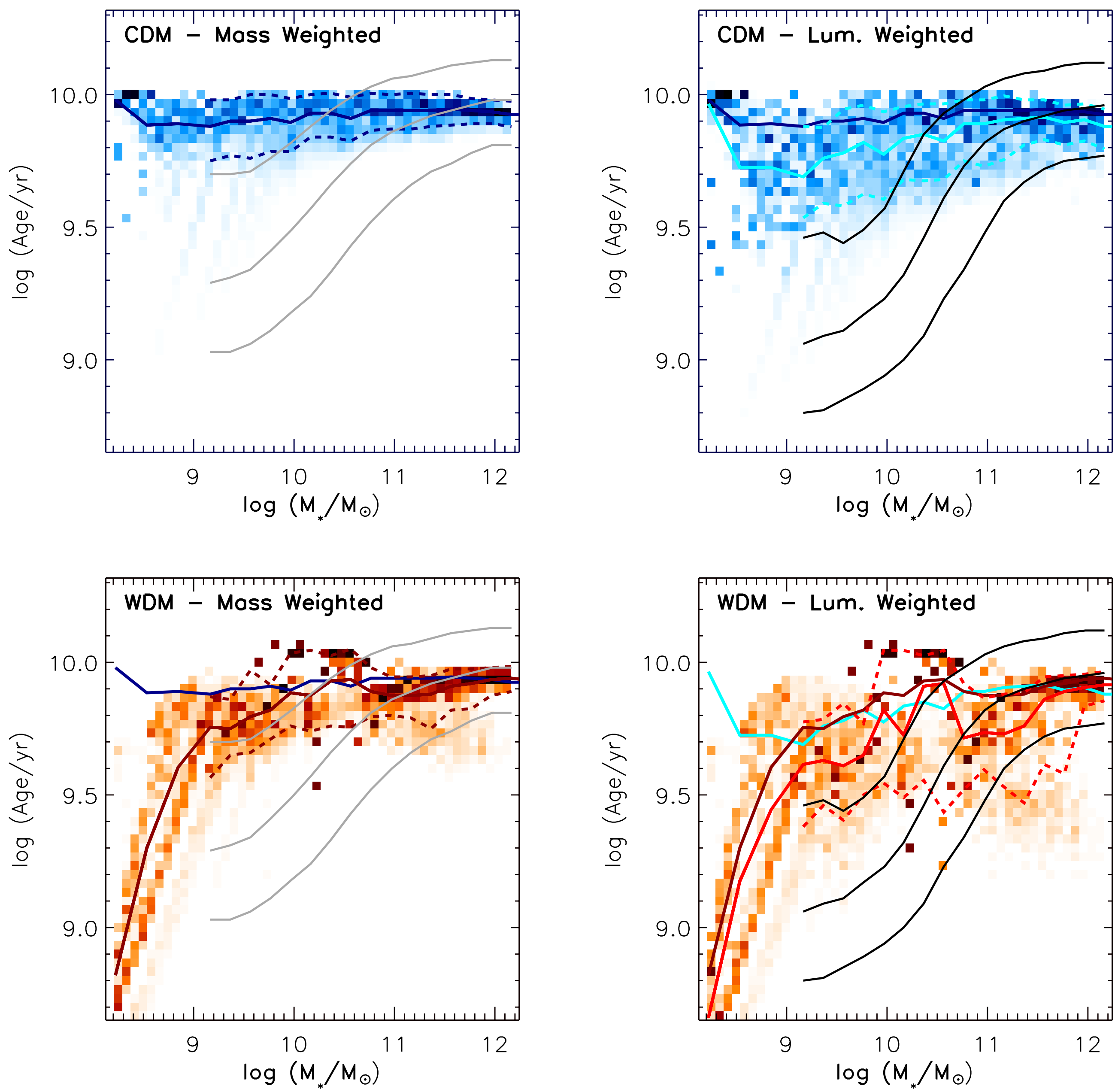

Calura, NM, Gallazzi 2014

The upper, the middle and the lower grey (black) curves represent the 16th, the 50th (median) and the 84th percentiles of the observed distribution in mass-(light-)weighted stellar age (Gallazzi et al. 2008)

Constraining the WDM candidate mass through the abundance of low-mass galaxies

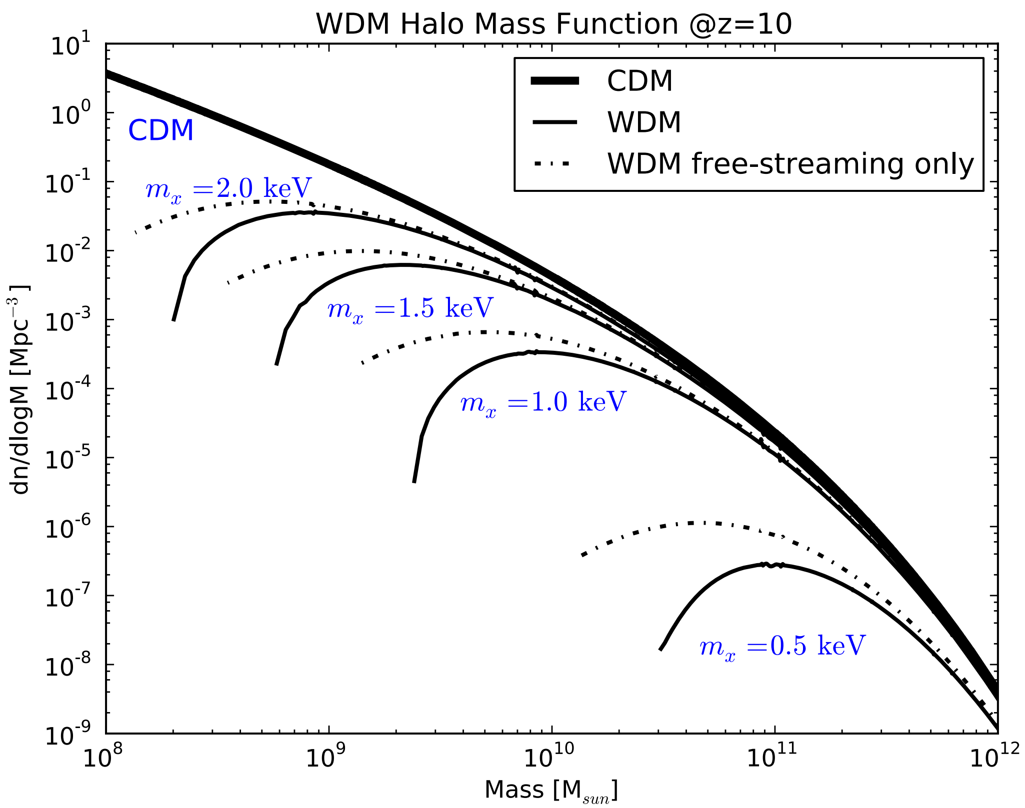

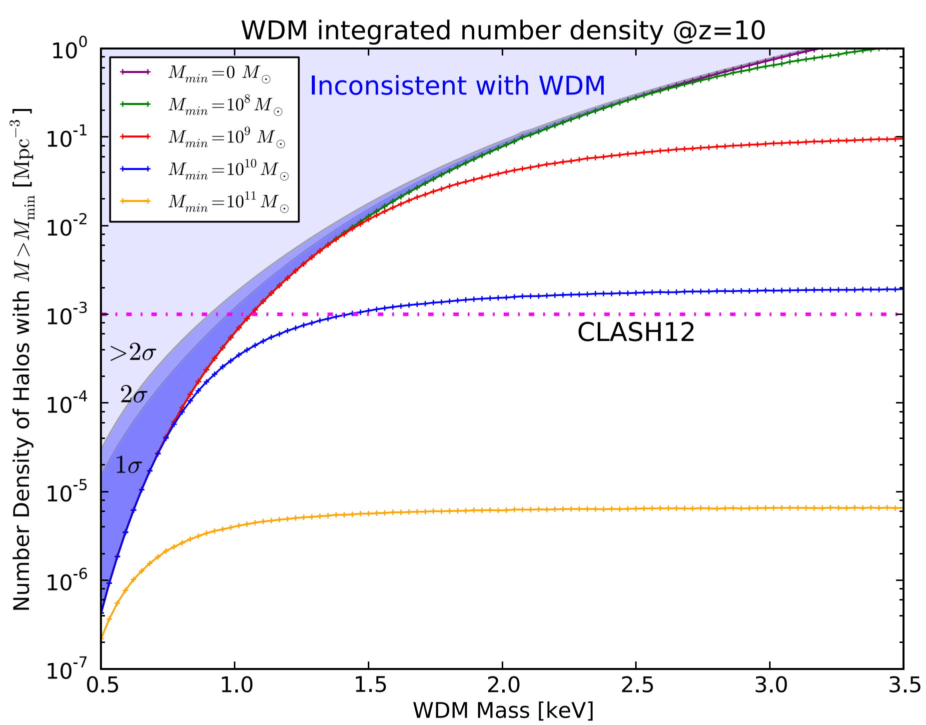

Several works compare with MW satellite abundance.
But results are subject to strong halo-to-halo variance

Pacucci, Mesinger, Haiman 2013

show that the two z ≈ 10 galaxies already detected by the Cluster Lensing And Supernova survey with Hubble (CLASH) survey are sufficient to constrain the WDM particle mass to $m_x > 1$

Schultz et al. 2014
Use abundance matching at the bright end of the the high-z luminosity functions to compute L-M_h relation.

Comparing the observed and the predicted densities of faint galaxies they derive a lower mass limit m_X>1 keV

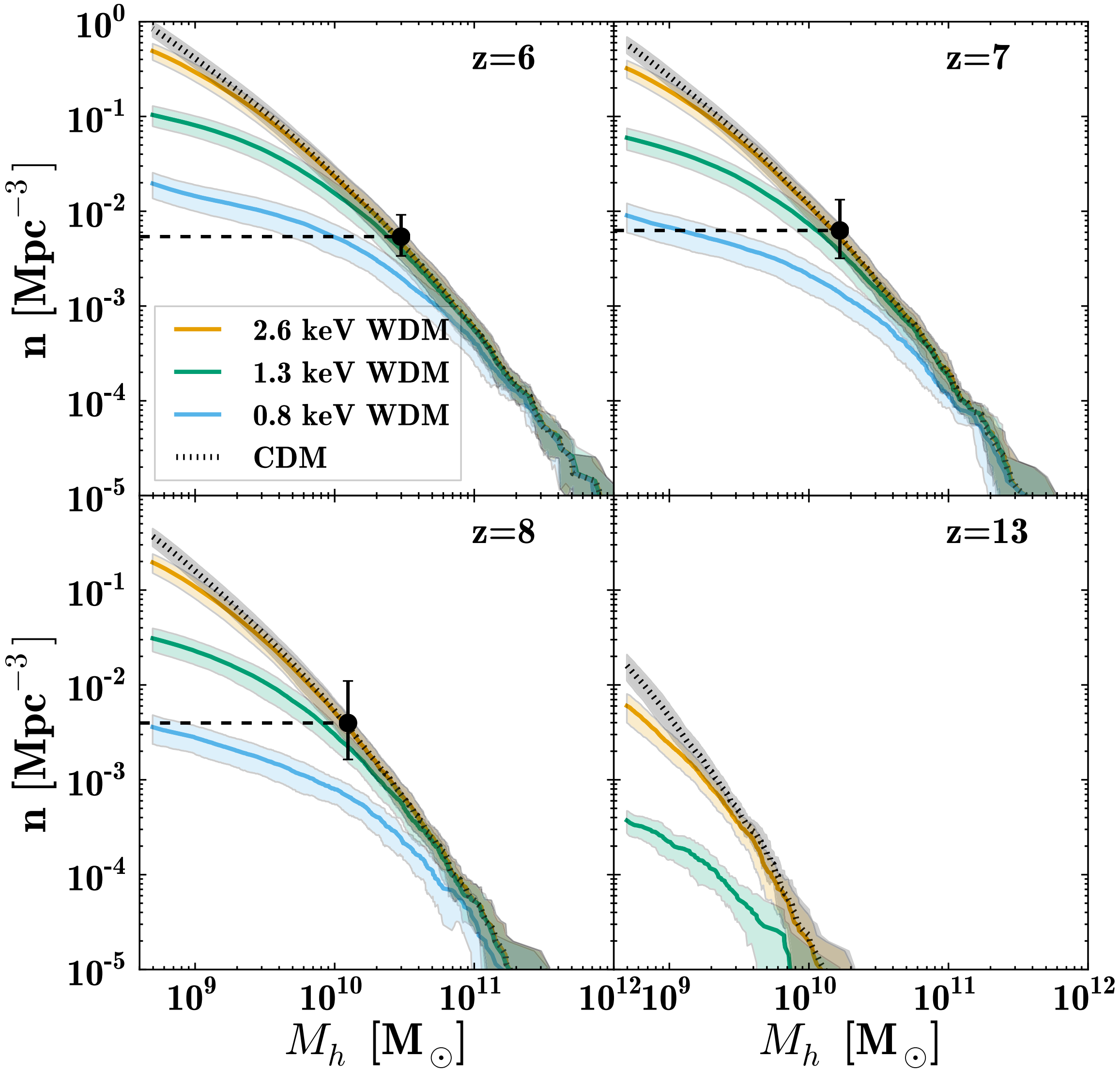

Schultz et al. 2014

Use abundance matching at the bright end of the the high-z luminosity functions to compute L-M_h relation.

Comparing the observed and the predicted densities of faint galaxies they derive a lower mass limit m_X>1 keV

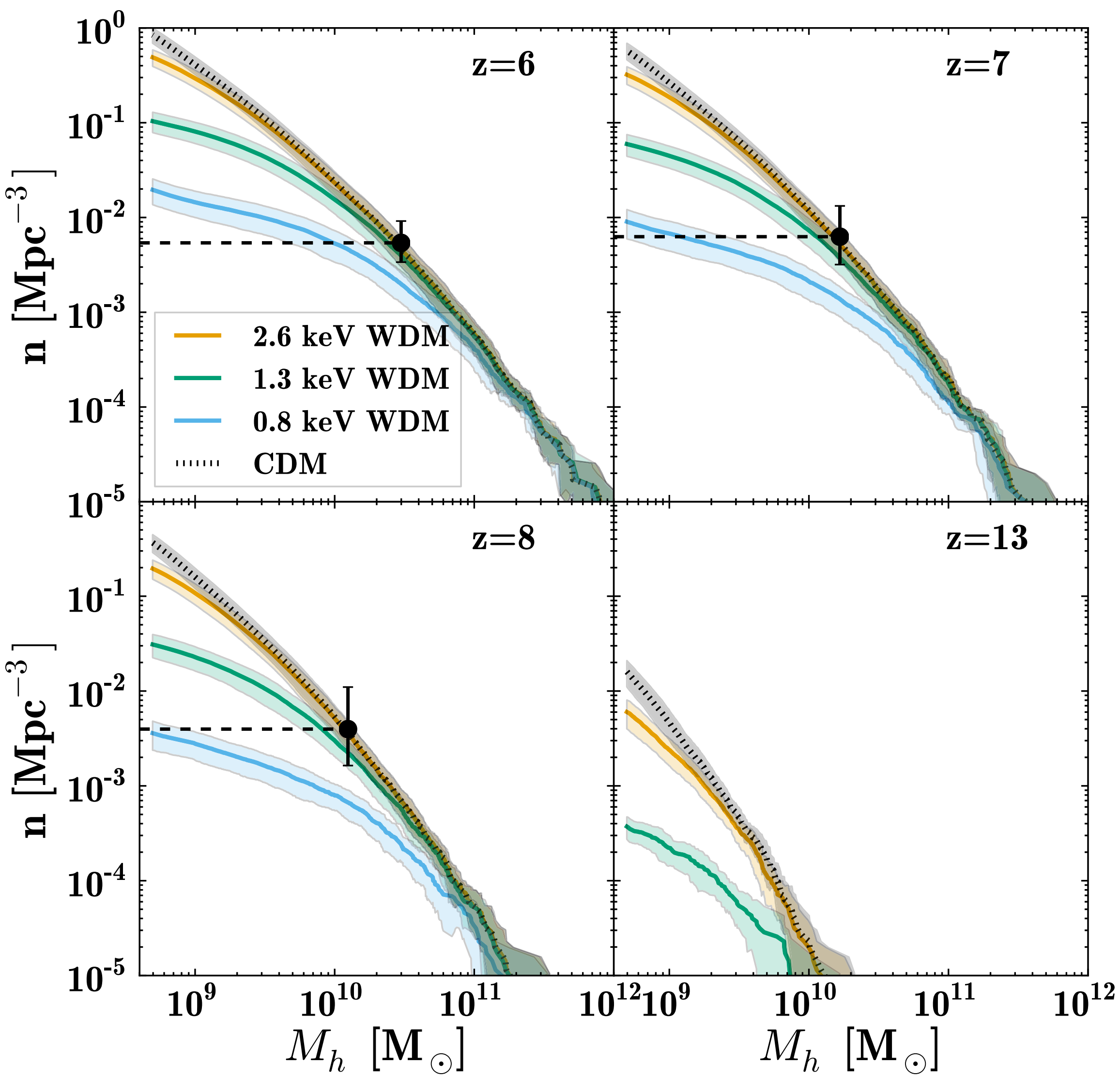

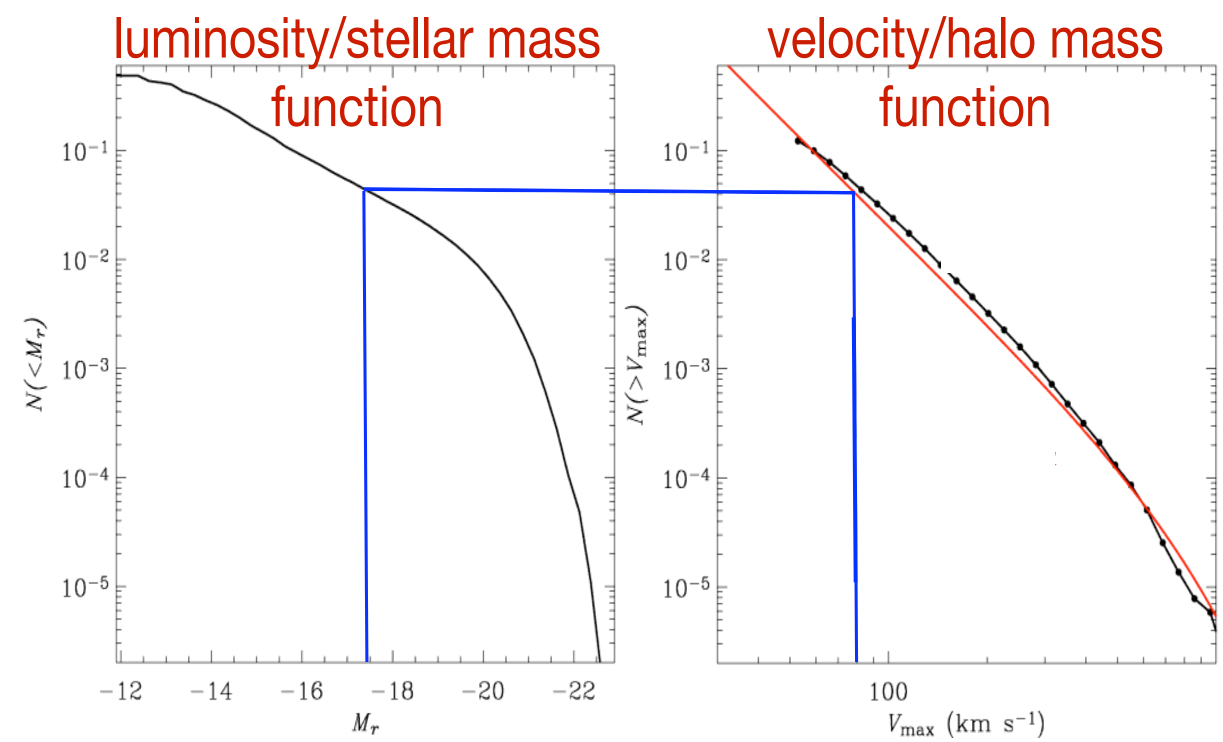

Schultz et al. 2014

Use abundance matching at the bright end of the the high-z luminosity functions to compute L-M_h relation.

Comparing the observed and the predicted densities of faint galaxies they derive a lower mass limit m_X>1 keV

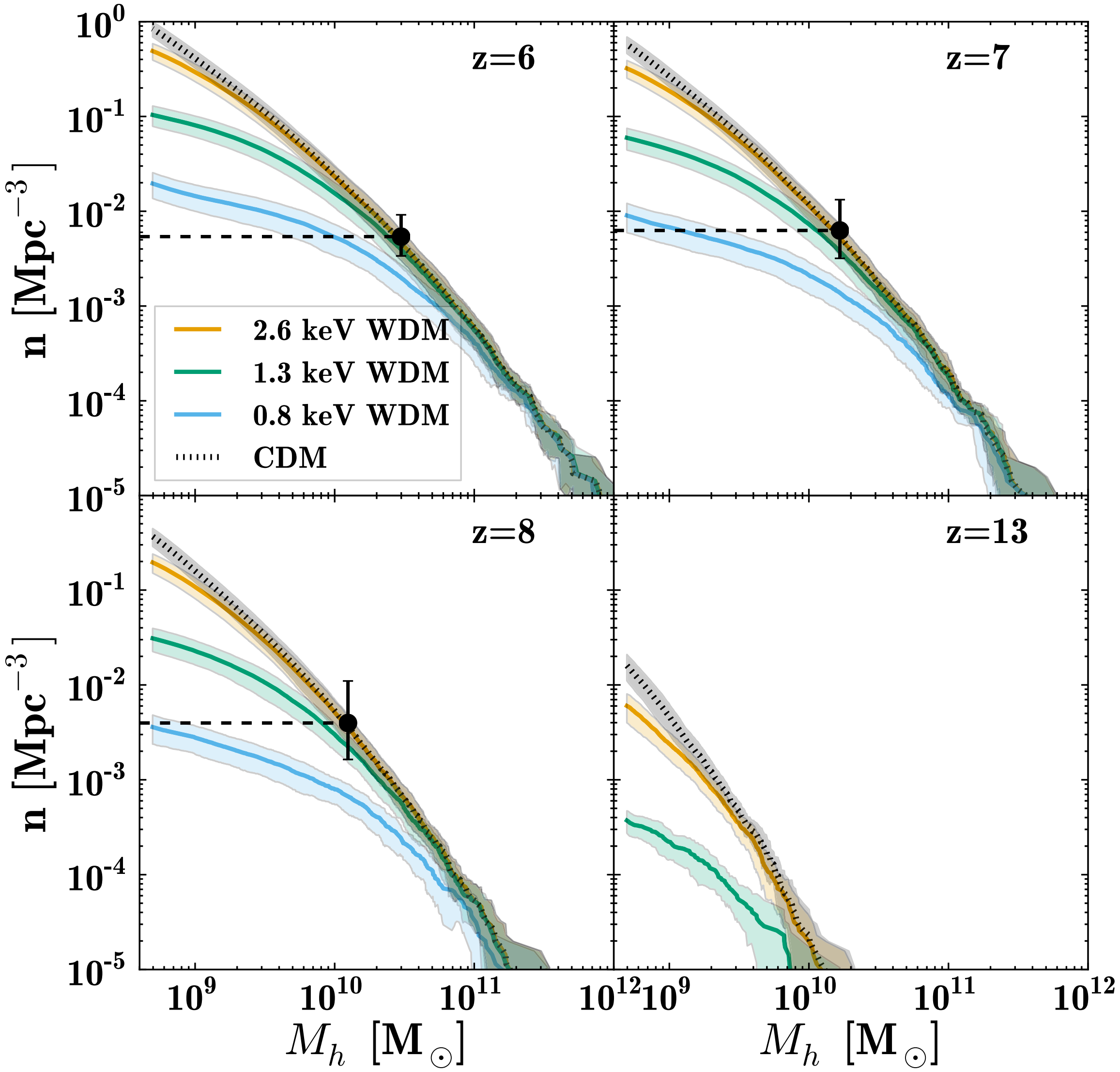

A different approach
focus on lower redshift but deeper observations

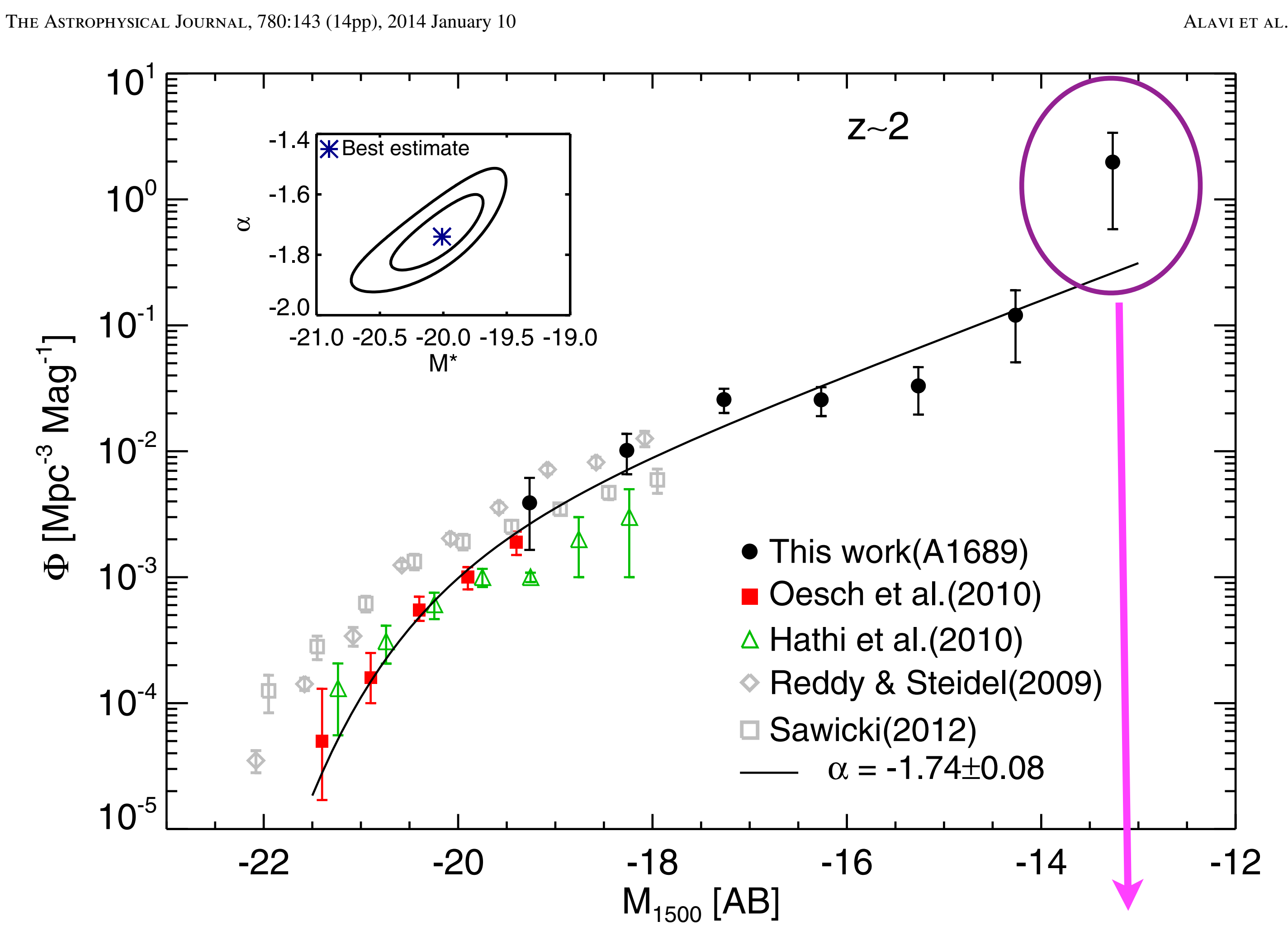

To connect M_{1500} to DM mass M

1) UV luminosity is directly linked to SFR
log SFR=1-2.5(M_{1500}+20.5)

Deepest
Luminosity
Function measured
so far

A different approach
focus on lower redshift but deeper observations

Santini et al. 2014

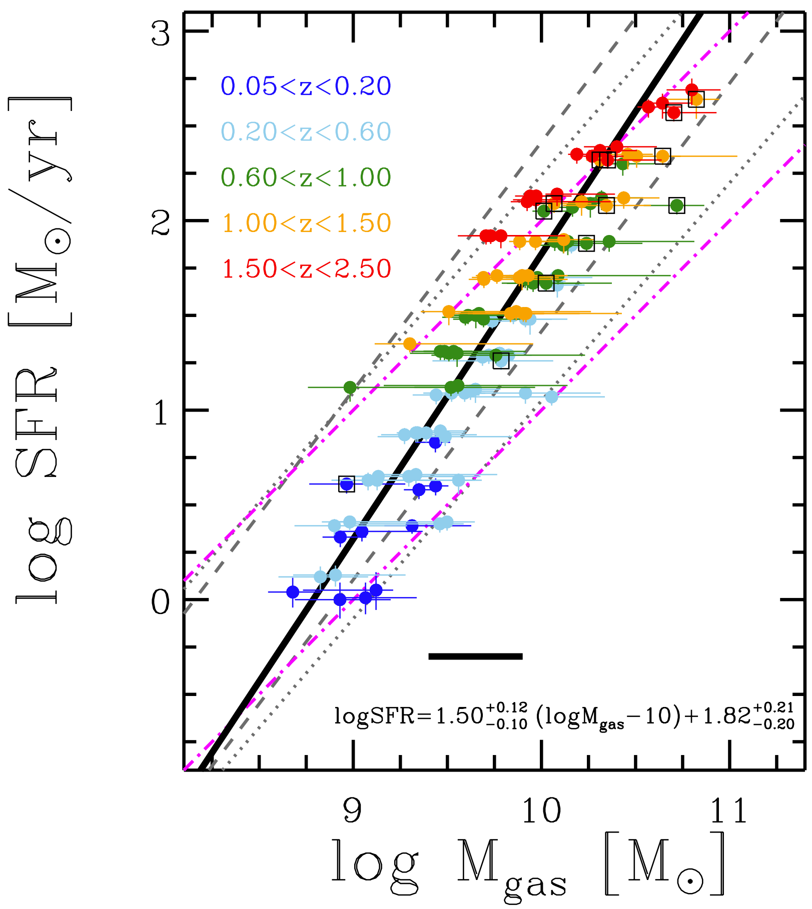

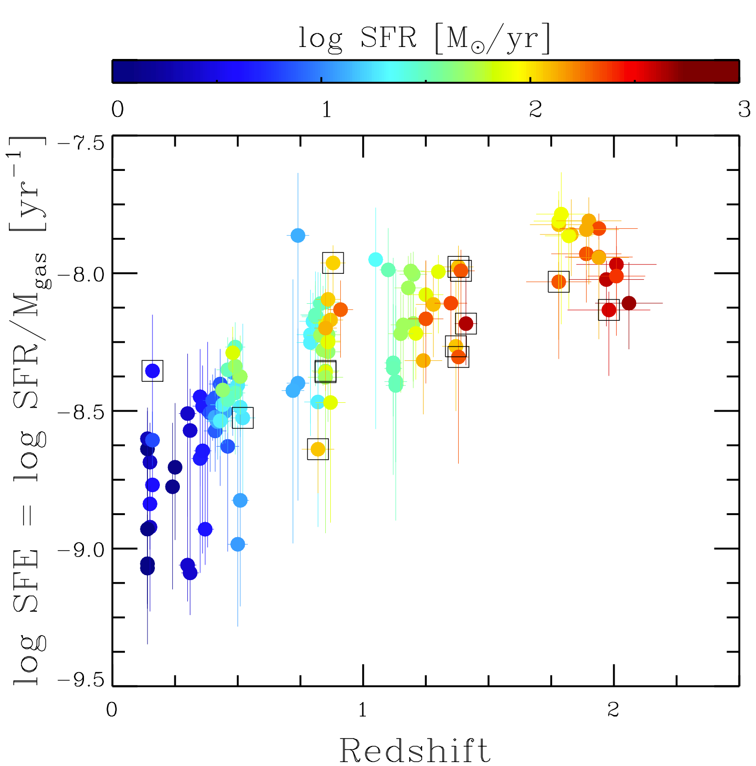

The slope of the SFR - M_{gas} relation yields the gas-to-star conversion timescale at z=2
$\tau_* = 3\ 10^7 - 2\ 10^8$ yrs

To connect M_{1500} to DM mass M

1) UV luminosity is directly linked to SFR
log SFR=1-2.5(M_{1500}+20.5)

2) SFR=M_{gas}/τ_*

A different approach
focus on lower redshift but deeper observations

To connect M_{1500} to DM mass M

1) UV luminosity is directly linked to SFR
$\log SFR = 1 - 2.5(M_{1500} + 20.5)$

2) $SFR = M_{gas}/\tau_*$

3) $M_{gas} = f_g\ (\Omega_b/\Omega_{DM})M_{DM}$

write M_{gas} as a fraction of the baryonic content of DM halo

4) $SFR = (f_g/\tau_*)\ (\Omega_b/\Omega_{DM})M_{DM}$

A different approach
focus on lower redshift but deeper observations

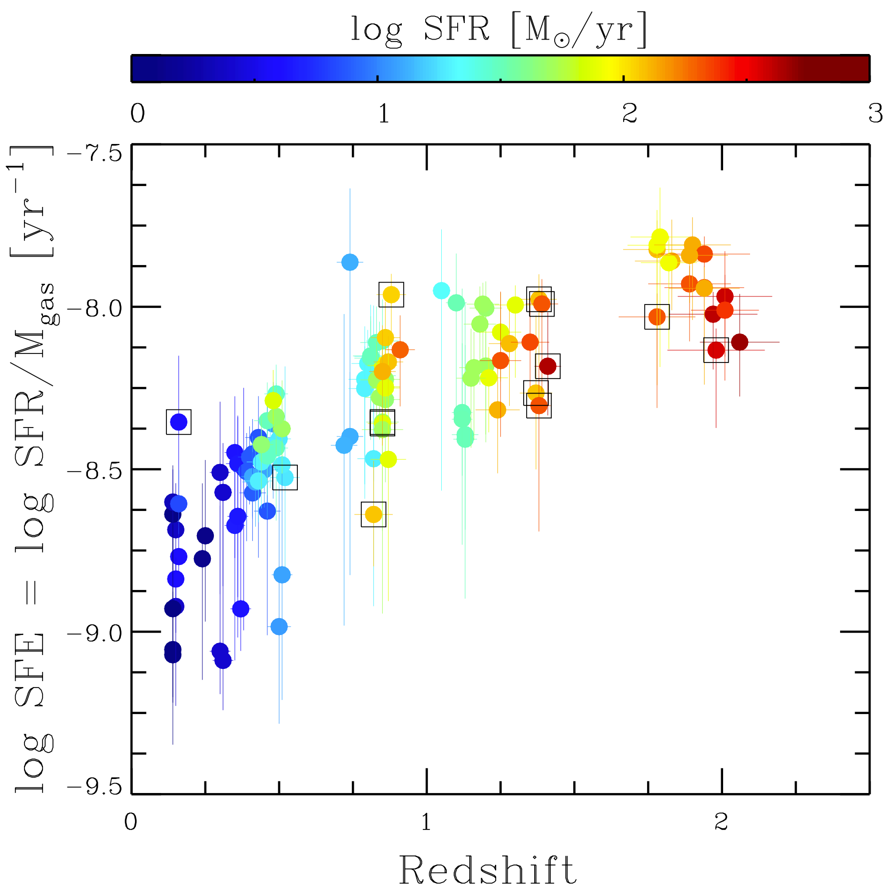

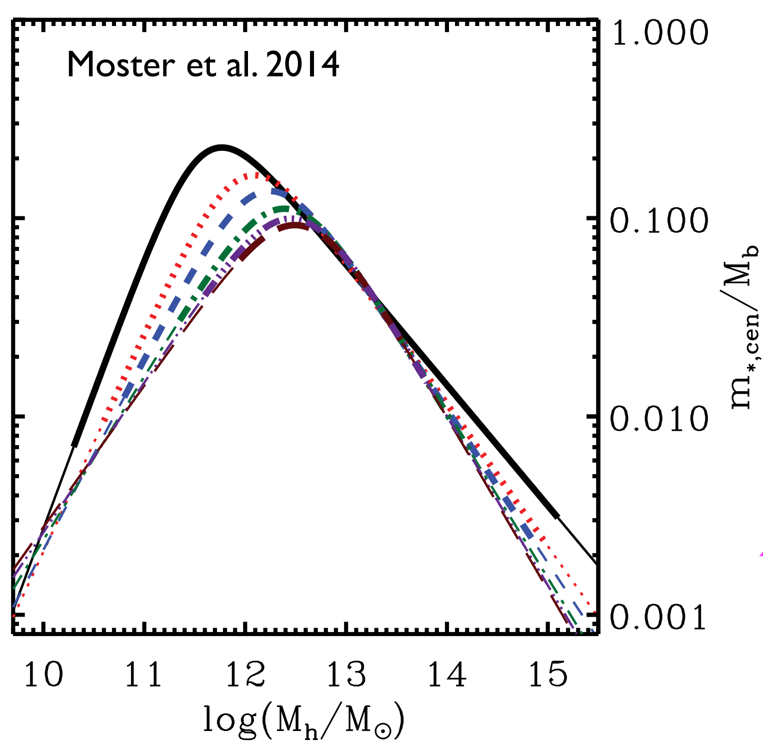

To connect M_{1500} to DM mass M

1) UV luminosity is directly linked to SFR
log SFR=1-2.5(M_{1500}+20.5)

2) SFR=M_{gas}/τ_*

3) $M_{gas}=f_g\ (\Omega_b/\Omega_{DM})M_{DM}$

4) SFR=$(f_g/\tau_*)\ (\Omega_b/\Omega_{DM})M_{DM}$

5)Observations yield
τ_*=0.1 -1 Gyr   at z=2
fg=0.001 - 0.01 for dwarf galaxies

6) SFR= $\eta\ (\Omega_b/\Omega_{DM})M_{DM}$
with η= 0.001 - 0.1

η → efficiency of SF for
give DM mass (L/M ratios)

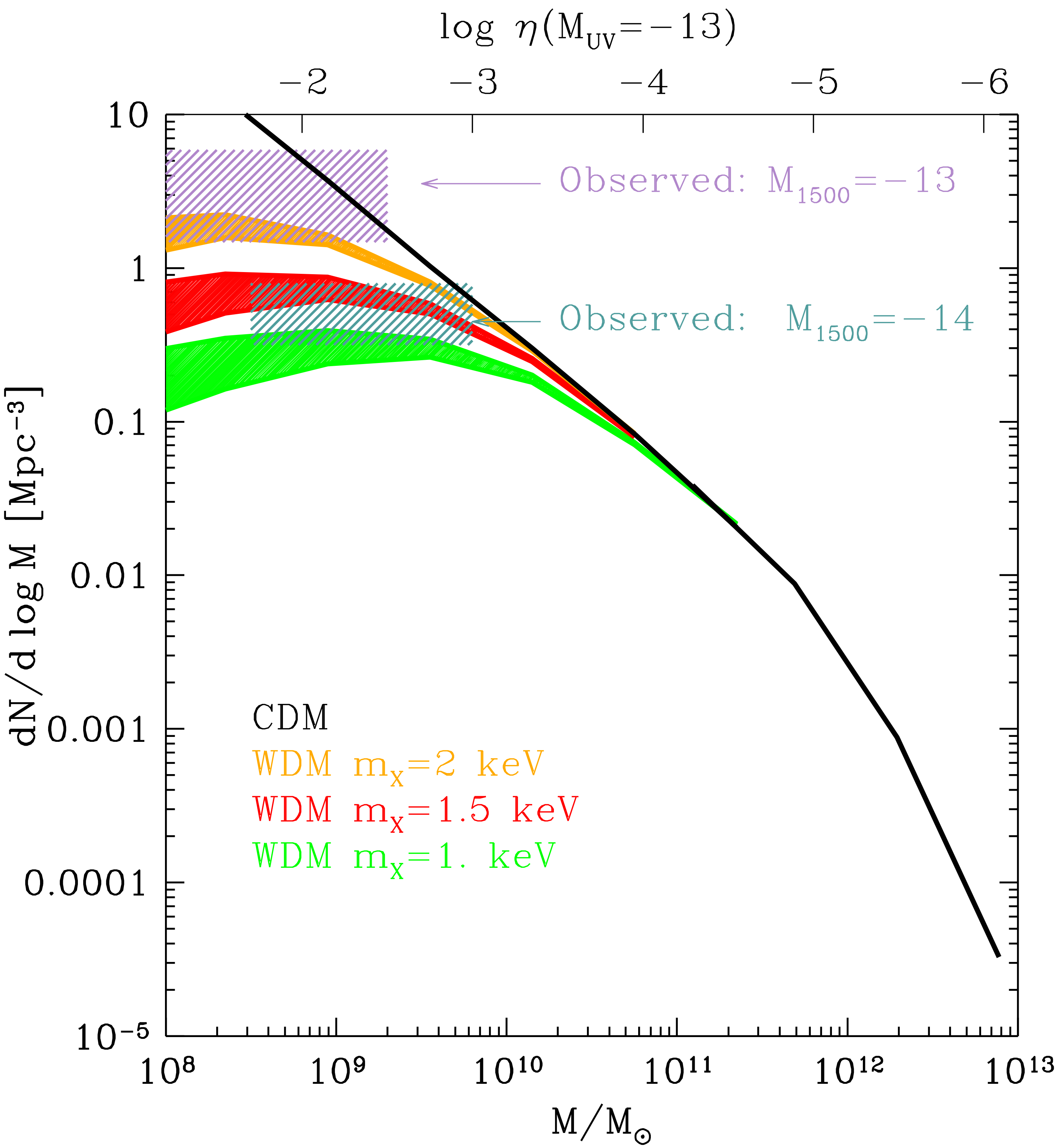

Note:
baryonic processes
can make the LF flatter
but not steeper !

CDM requires low η, i.e., low star formation efficiency. Compares critically with observed M*-Mhalo relations

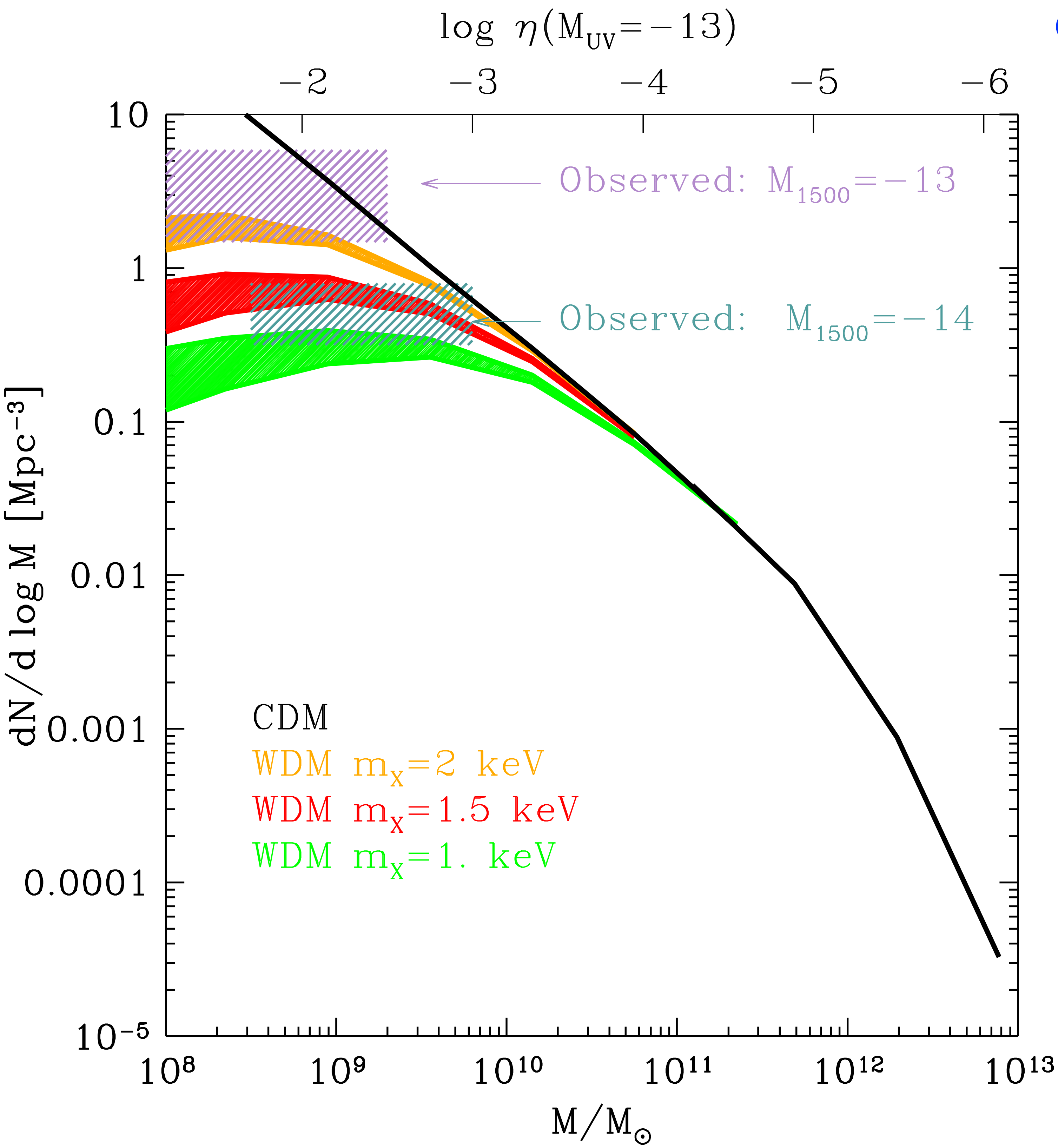

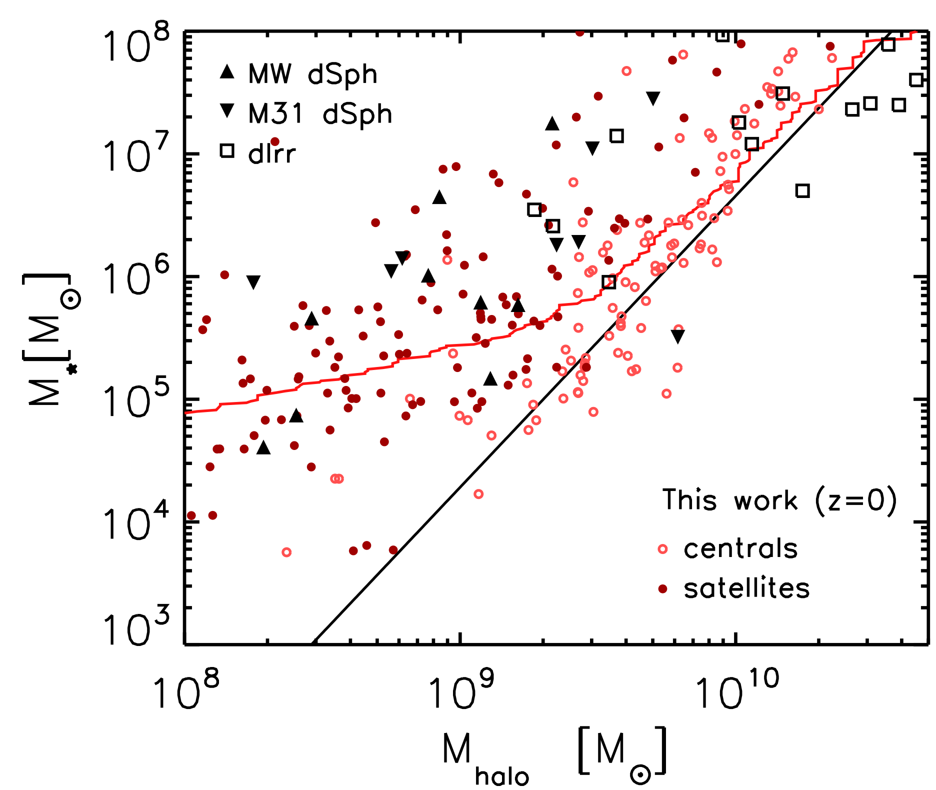

CDM requires
low η, i.e., low star formation
efficiency. Compares critically with
observed M*-Mhalo relations

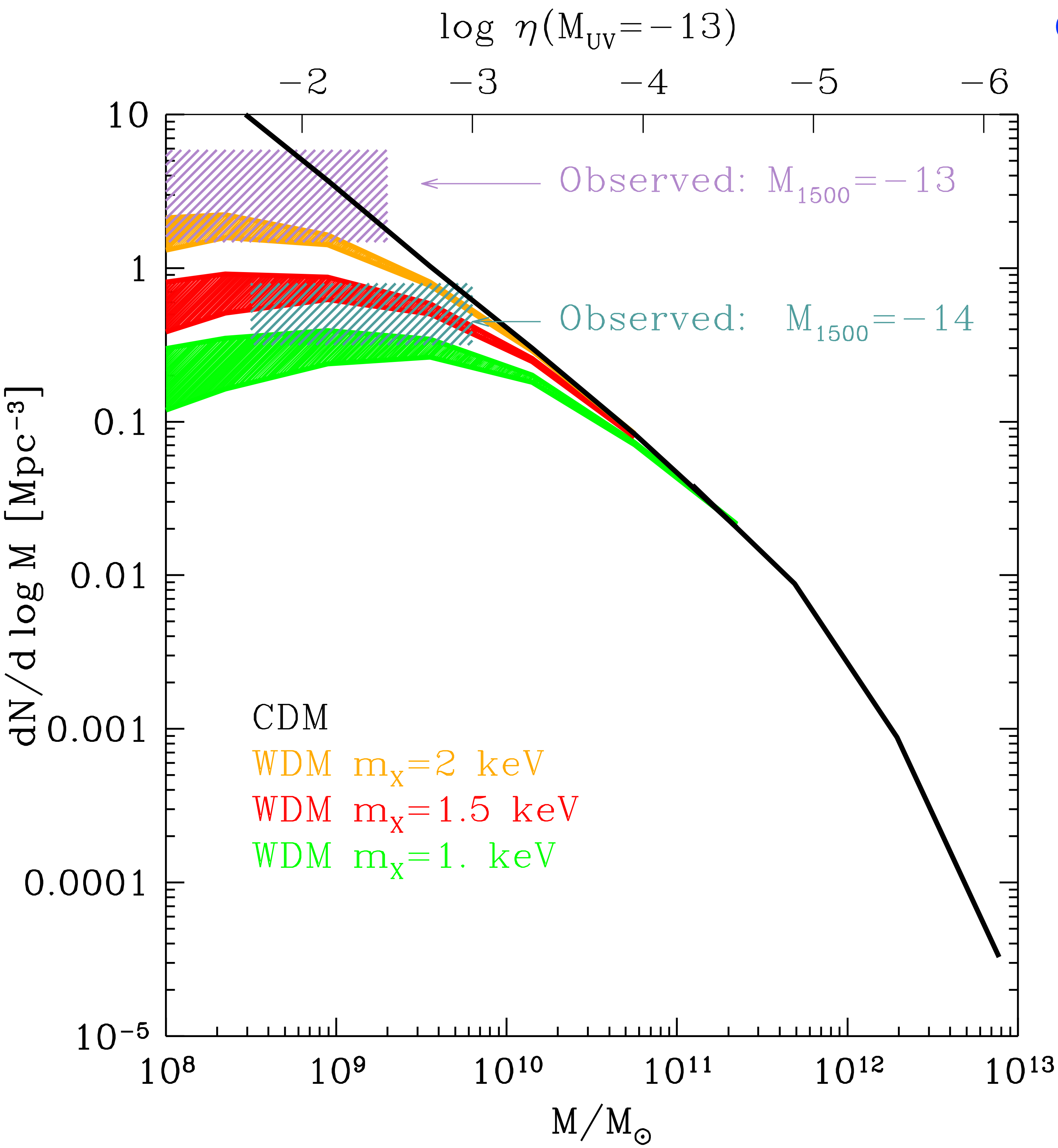

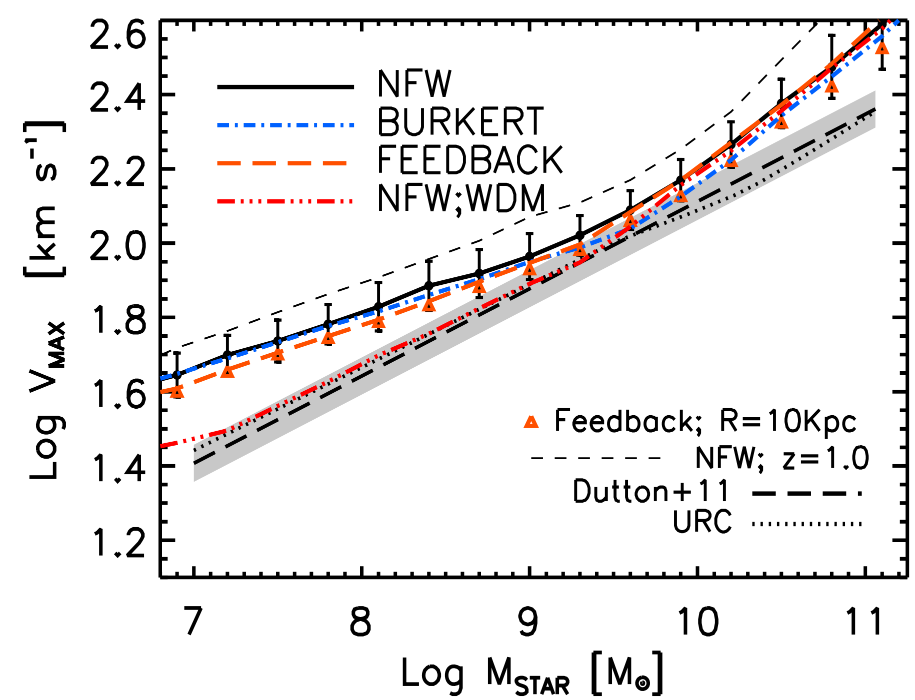

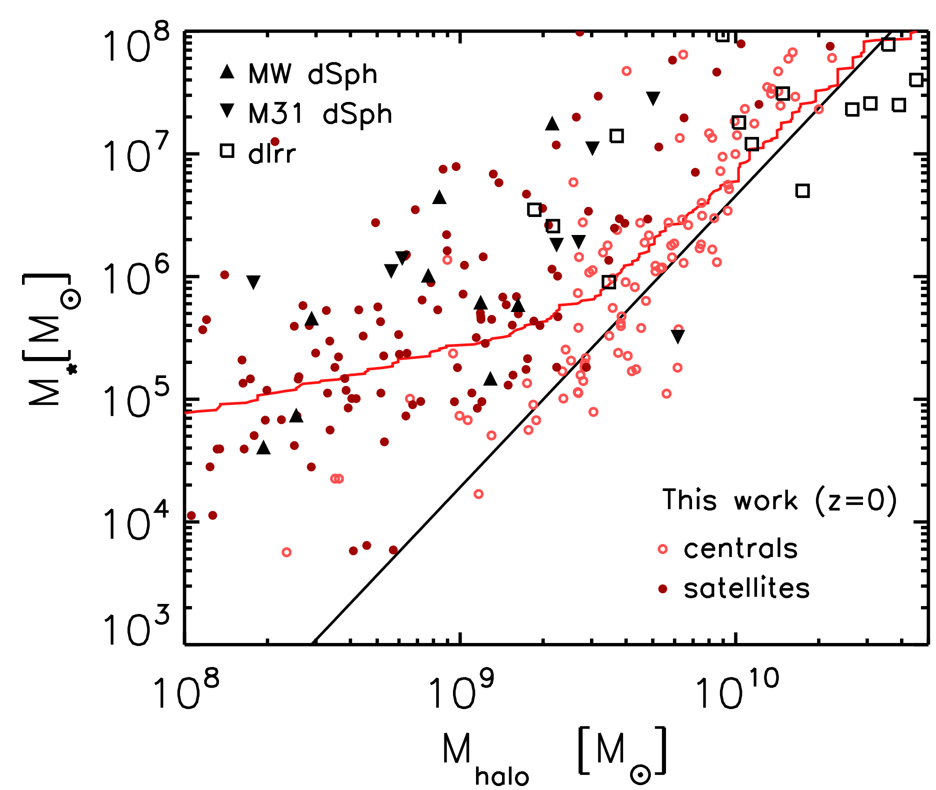

LSB galaxies in Virgo (Giallongo et al. 2015)

TABLE 1
LSB CATALOG IN THE VIRGO-XMMUJ1230 FIELD

ID	LSB Label	RA	DEC	R	μ_0	n^a	M_R^b	r^c (arcsec)	r (pc)^c	b/a	$R-Z$
6490	A	187.3919684	+13.7704609	21.86	24.91	0.92	-9.24	3.07	246	0.7	0.00
6043	B	187.6635951	+13.7391869	20.38	24.54	0.70	-10.79	4.48	359	0.7	0.31
5833	C	187.5879561	+13.7058350	21.59	26.23	0.55	-9.56	4.37	350	0.9	-0.23
5143	D	187.5483601	+13.6914967	18.30	24.01	0.67	-12.87	7.99	639	0.9	0.44
4739	E	187.3814266	+13.6619273	18.75	23.49	0.72	-12.42	5.71	457	0.7	0.35
4367	F	187.3863203	+13.6222745	21.93	24.54	0.88	-9.25	2.73	218	0.6	0.20
3516	G	187.6600347	+13.6196001	18.05	24.25	0.62	-13.12	10.43	835	0.7	0.11
3214	H	187.6224577	+13.5565951	21.14	25.11	0.57	-10.03	3.14	251	0.9	0.39
2245	J	187.4138959	+13.5075398	21.24	25.53	0.69	-9.93	4.19	335	0.8	0.11
2001	K	187.7070994	+13.5053537	19.07	25.79	0.44	-12.11	10.68	855	0.9	-0.30
2003	L	187.7244716	+13.4939191	21.89	26.12	0.30	-9.28	3.05	244	0.9	0.02

[a] Sérsic index
[b] Absloute magnitudes computed adopting an average distance modulus for Virgo $\Delta M = 31.1$ (Mei et al. (2007)), an average galactic absorption of -0.07.
[c] Scale radius from the Sersic profile fitting. An angular scale of 80 pc arcsec^{-1} has been adopted.

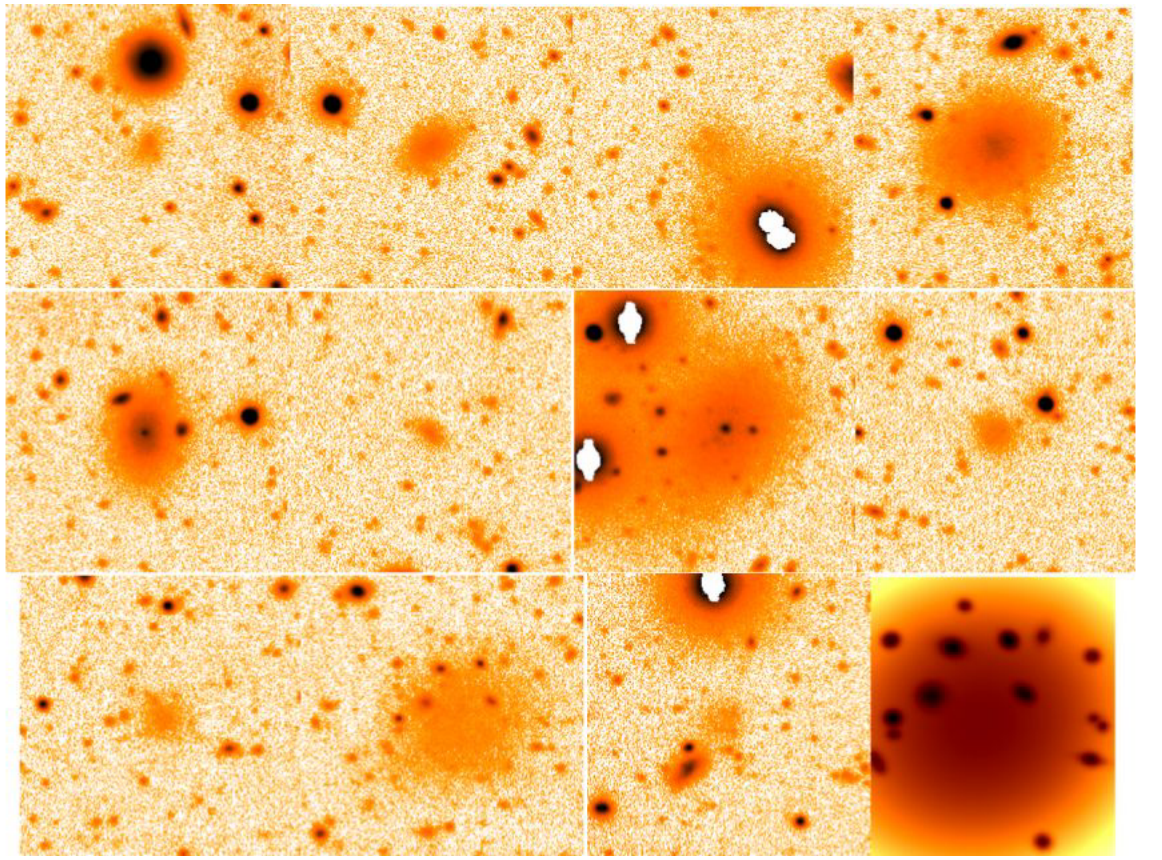

FIG. 2.— Selected LSB dwarfs in the Virgo-xmmuj1230 field; the box size of each image is $\simeq 57$ arcsec. The sequence from the t the bottom follows the list in Table 1. The last box on the bottom right show a zoomed image of the Galfit best fit model of the LS "K". All the small background sources expected within the LSB halo have been fitted separately.

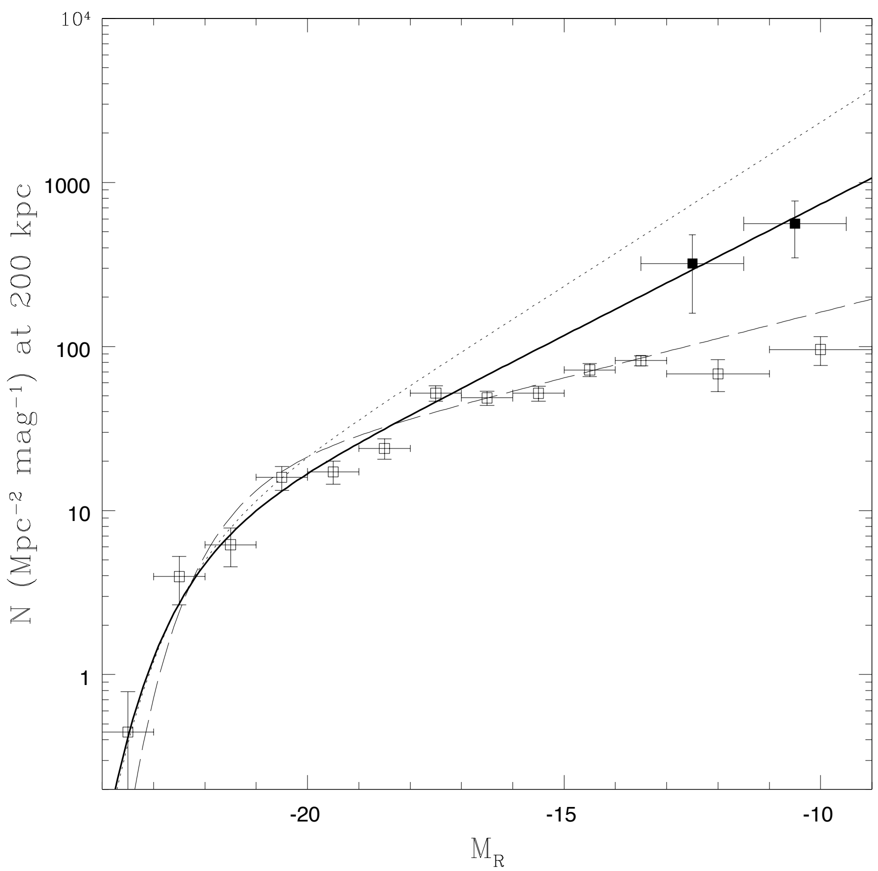

FIG. 3.— Virgo projected luminosity function normalized at 200 kpc. Filled squares are from the present sample after conversion from AB to the Vega magnitude system by $R(Vega) - R(AB) = -0.26$. Empty squares are from Trentham & Tully (2002) in the Vega system. The continuous curve represents a Schechter shape with slope $\alpha \sim -1.4$ and $M^* \sim -22.3$. Two faint slopes $\alpha \sim -1.2, -1.5$ are also shown for comparison (dashed and dotted, respectively).

Steep LF N(L) ~ L$^{-1.4}$

Compute sub-haloes mass function $N(M) \sim M^{-\alpha_{dm}}$
measure α_{DM} for different WDM mass

$\propto$

Compute N(L) for different L/M ratios
i.e., reasonable values of β (assuming $L \sim M^{\beta}$)

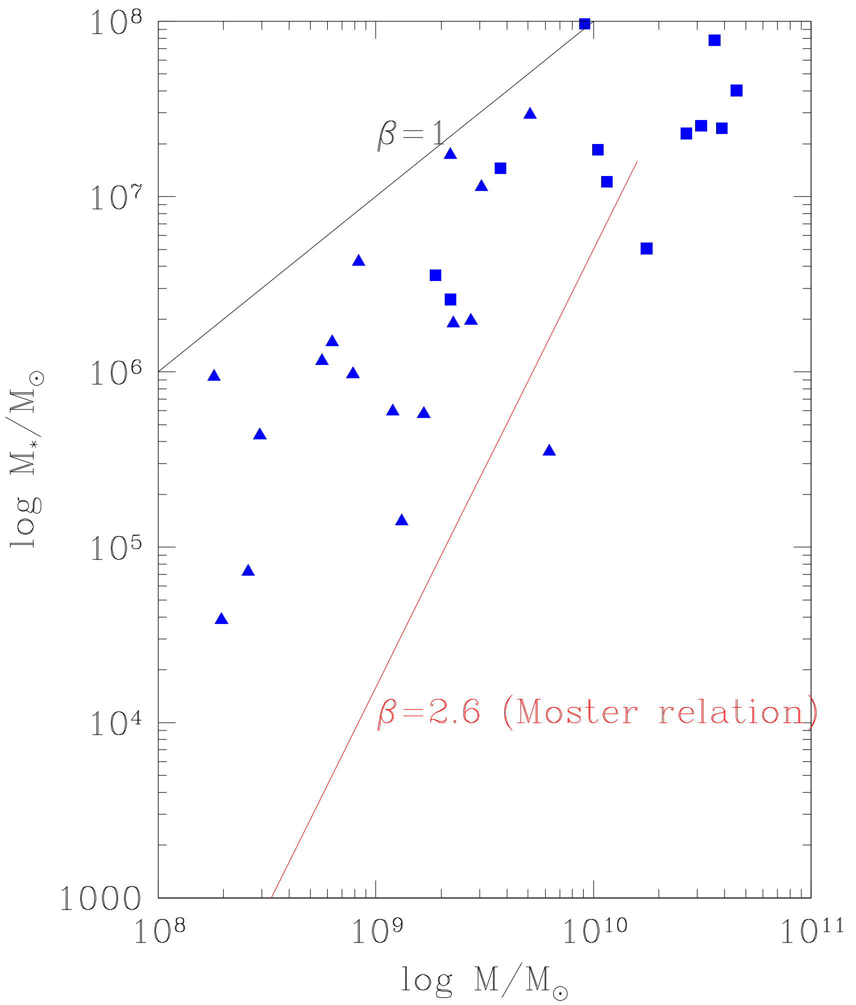

Compare with observed slope

$$L \propto M^{\beta}$$

$$L/M \propto M^{\beta - 1}$$

$$N(M) \propto M^{-\alpha_{dm}} \rightarrow N(L) \propto L^{-\alpha}$$

$$\alpha = \frac{1 - \alpha_{DM} - \beta}{\beta}$$

E.g. α=2 β=1 $\longrightarrow$ $N(L) \propto L^{-3/2}$

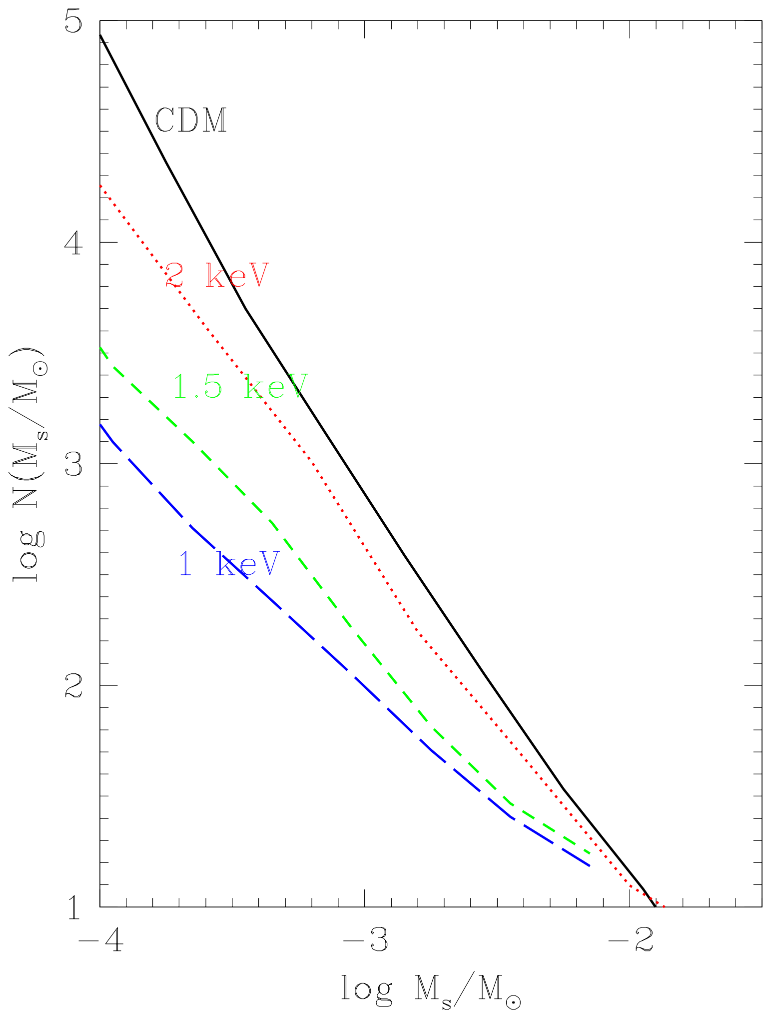

$\alpha(m_{X=}1\text{kev})=1.2$

$\alpha(m_{X=}1.5\text{keV})=1.4$

$\alpha(m_{X=}2\text{kev})=1.6$

$\alpha\text{CDM}=1.8$

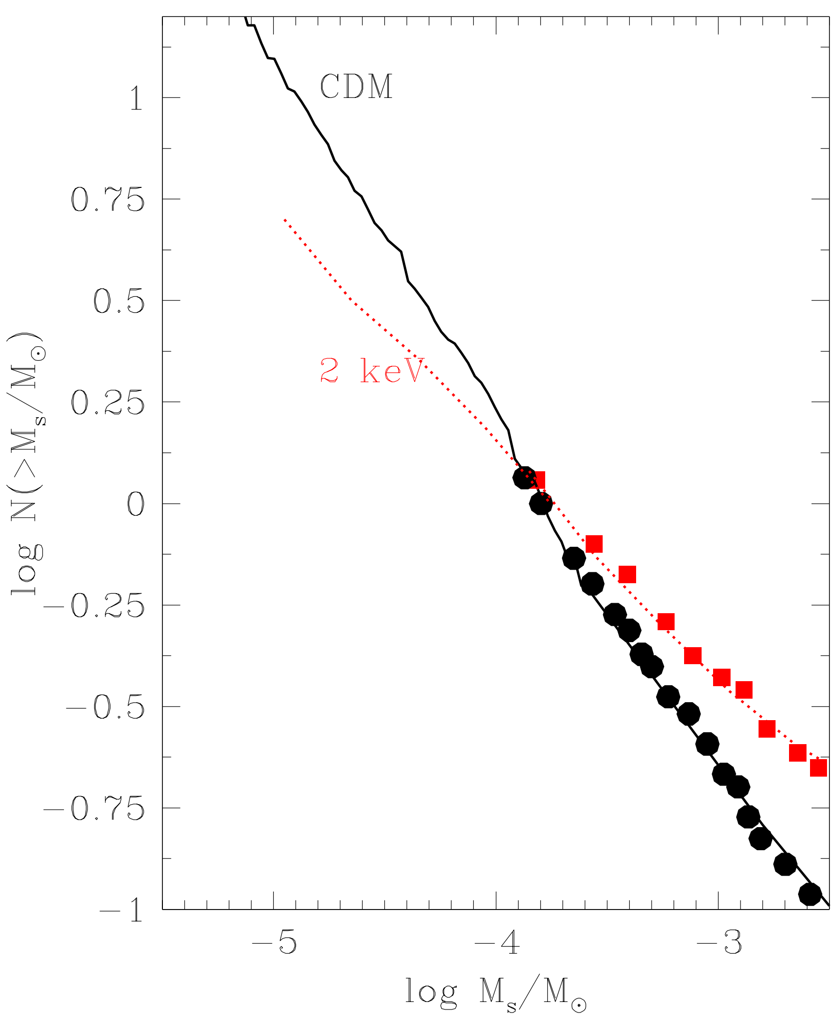

In the CDM and
m_X=2keV case
we can test the results
against N-body results
(but extend to much
smaller satellite masses)

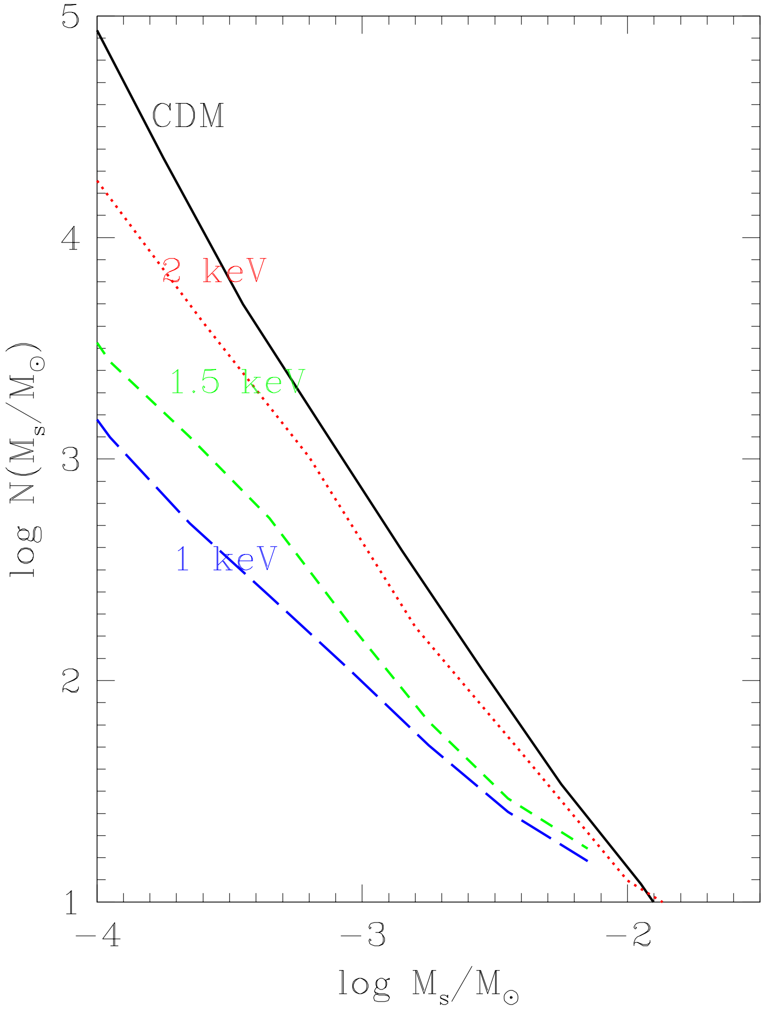

α(m_X=1 keV)=1.2

α(m_X=1.5 keV)=1.4

α(m_X=2 keV)=1.6

αCDM=1.8

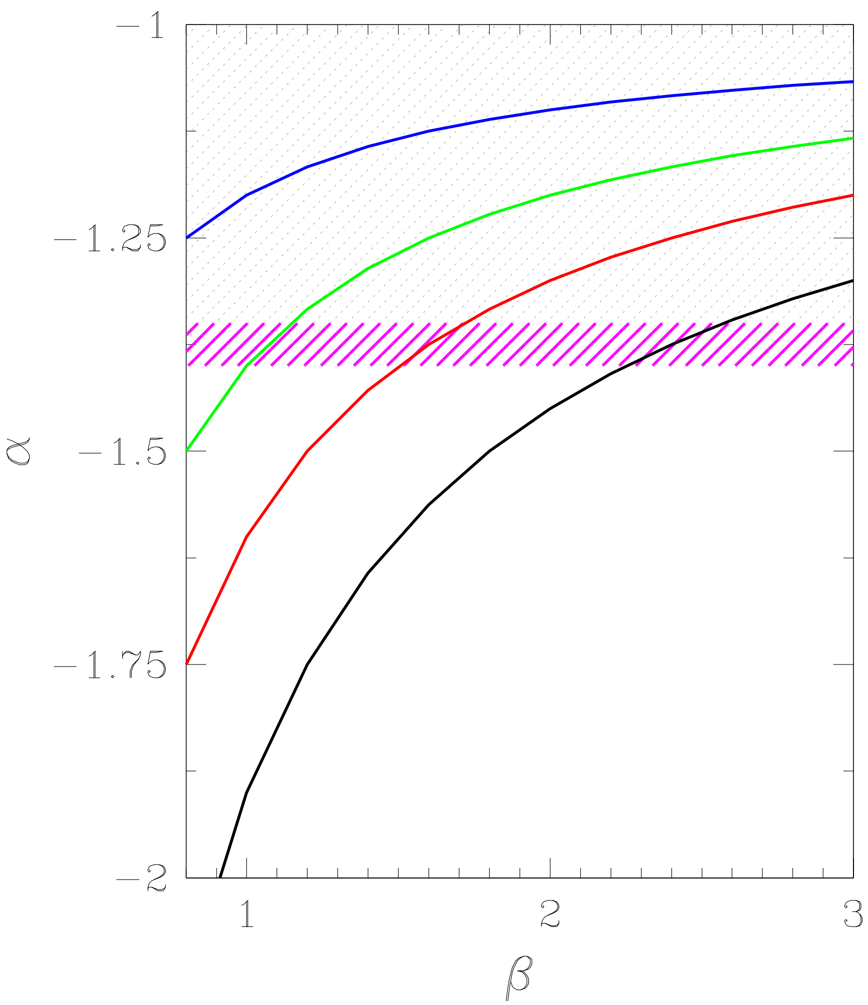

slope of N(L) is too flat in the m_X=1 kev and m_X=1.5 keV cases for any 1<β<3

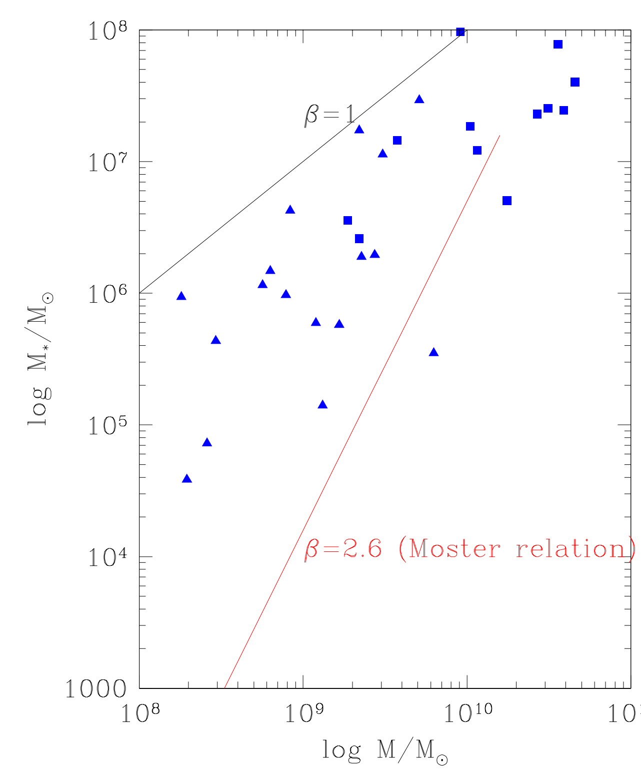

CDM would require β~2.5 unfavoured by data

Conclusions

WDM galaxy formation models provides a solution to several critical issues:

- density profiles (also at high-z)
- abundance of low-mass/low-luminosity galaxies at $z \gtrsim 2$
- luminosity function of AGNs (low-luminosity $L<10^{43}$ erg) at $z \gtrsim 2$
- luminosity function of satellites (large surveys)
- M_*-M_h relation
- Satellite colors (i.e., star formation histories of low-mass galaxies)

Constraints on WDM particle mass

- From MW satellites (but subject to halo-to-halo variance)
- From galaxy luminosity functions/counts
  a) high-redshift (but present observations still not deep enough: constrain $m_X>1$ keV
  b) lower redshift, ultra-deep (down to $M_{UV} \approx -10$) UV luminosity function $m_X>1.5$ keV

Summary

The mass of DM particles has a major impact on galaxy formation
(suppression of small-scale perturbations due to free-streaming)
CDM is the limit of M_{fs}<< masses of cosmological interest

CDM problems on small scales:
- cusps + number of satellite galaxies
- abundance of low-mass (faint) galaxies at low and high redhsifts
- fraction of quiescent satellites
- V_{max}-M_* relation

Baryonic physics can hardly solve all the problems

Galaxy formation in WDM cosmology is a viable solution
if the spectrum is like that corresponding to a thermal relic DM with $m \lessapprox 2$ keV
(analogous to that corresponding to sterile neutrino produced according to Dodelson & Widrow with m_ν<8 keV)

There is a tension with current limits from high-z structure (Lyman-a forest)

Summary

The mass of DM particles has a major impact on galaxy formation (suppression of small-scale perturbations due to free-streaming)
CDM is the limit of M_{fs}<< masses of cosmological interest

CDM problems on small scales:
- cusps + number of satellite galaxies
- abundance of low-mass (faint) galaxies at low and high redhsifts
- fraction of quiescent satellites
- V_{max}-M_* relation

Baryonic physics can hardly solve all the problems

Galaxy formation in WDM cosmology is a viable solution
if the spectrum is like that corresponding to a thermal relic DM with $m \lesssim 2$ keV
(analogous to that corresponding to sterile neutrino produced according to Dodelson & Widrow with m_ν<8 keV)

There is a tension with current limits from high-z structure (Lyman-a forest)

Summary

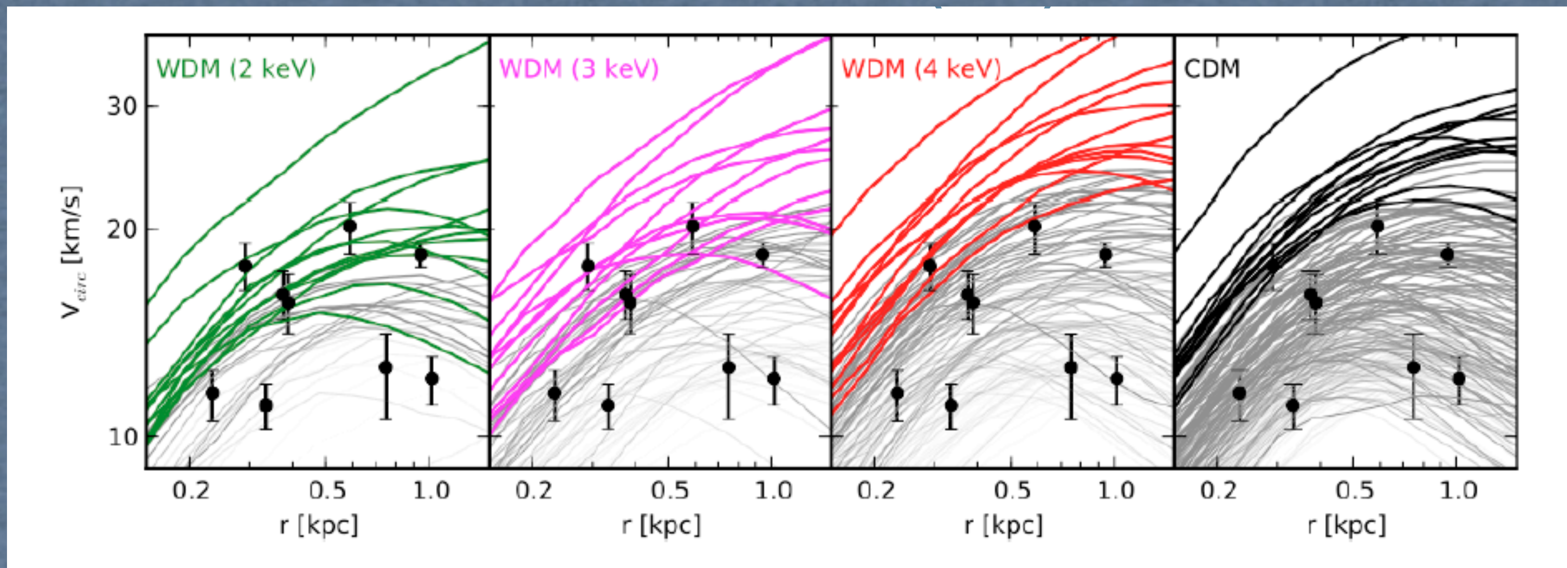

Monthly Notices of the ROYAL ASTRONOMICAL SOCIETY

MNRAS **437**, 293–304 (2014)
doi:10.1093/mnras/stt188
Advance Access publication 2013 October 24

MaGICC-WDM: the effects of warm dark matter in hydrodynamical simulations of disc galaxy formation

Jakob Herpich,[1★] Gregory S. Stinson,[1] Andrea V. Macciò,[1] Chris Brook,[2] James Wadsley,[3] Hugh M. P. Couchman[3] and Tom Quinn[4]

[1] *Max-Planck-Institut für Astronomie, Königstuhl 17, D-69117 Heidelberg, Germany*
[2] *Departamento de Física Teórica, Universidad Autónoma de Madrid, E-28049 Cantoblanco, Madrid, Spain*
[3] *Department of Physics and Astronomy, McMaster University, Hamilton, Ontario L8S 4M1, Canada*
[4] *Astronomy Department, University of Washington, Box 351580, Seattle, WA 98195-1580, USA*

Accepted 2013 October 2. Received 2013 September 20; in original form 2013 August 5

ABSTRACT

We study the effect of warm dark matter (WDM) on hydrodynamic simulations of galax formation as part of the Making Galaxies in a Cosmological Context (MaGICC) project. We simulate three different galaxies using three WDM candidates of 1, 2 and 5 keV and compare results with pure cold dark matter simulations. WDM slightly reduces star formation and produces less centrally concentrated stellar profiles. These effects are most evident for the 1 keV candidate but almost disappear for $m_{WDM} > 2$ keV. All simulations form similar stella

s

ith m≲2 keV

ording to

h-a forest)

Summary

The mass of DM particles has a major impact on galaxy formation (suppression of small-scale perturbations due to free-streaming)
CDM is the limit of M_{fs}<< masses of cosmological interest

CDM problems on small scales:
- cusps + number of satellite galaxies
- abundance of low-mass (faint) galaxies at low and high redhsifts
- fraction of quiescent satellites
- V_{max}-M_* relation

Baryonic physics can hardly solve all the problems

Galaxy formation in WDM cosmology is a viable solution
if the spectrum is like that corresponding to a thermal relic DM with m≲2 keV
(analogous to that corresponding to sterile neutrino produced according to Dodelson & Widrow with m_ν<8 keV)

There is a tension with current limits from high-z structure (Lyman-a forest)

A&A 562, A30 (2014)

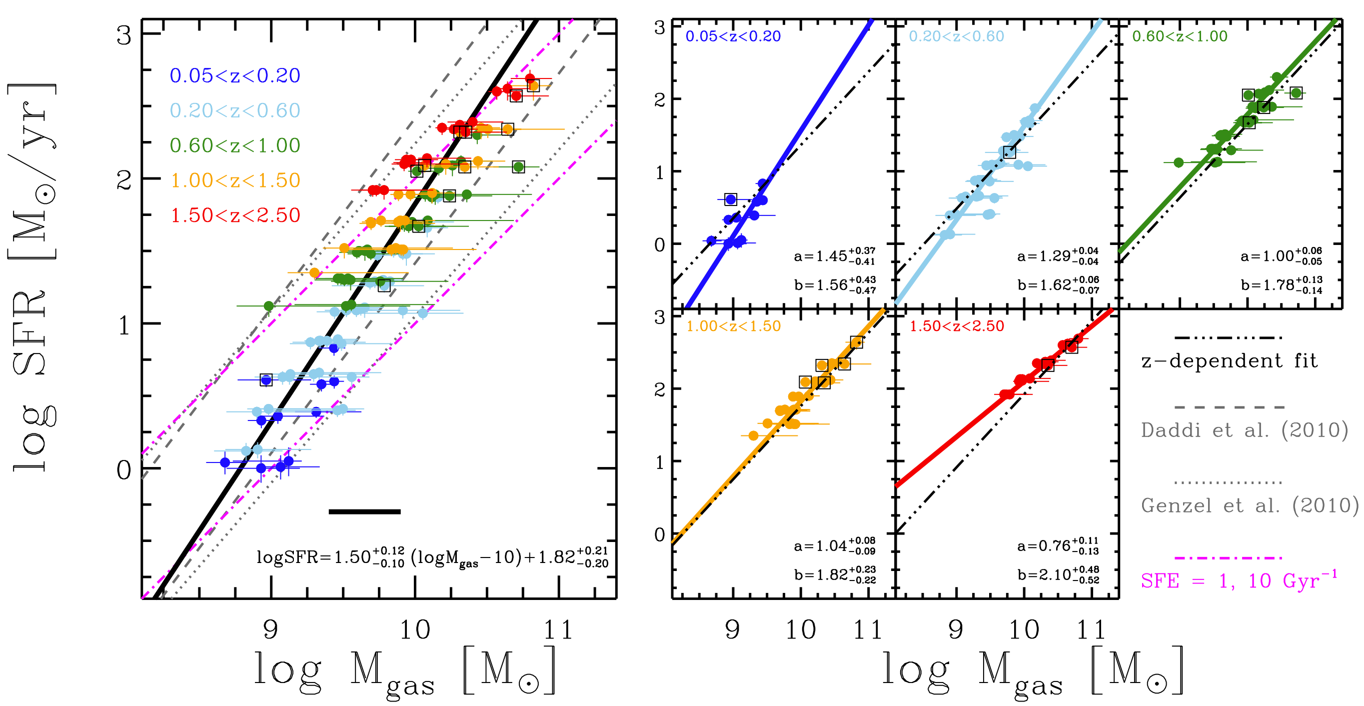

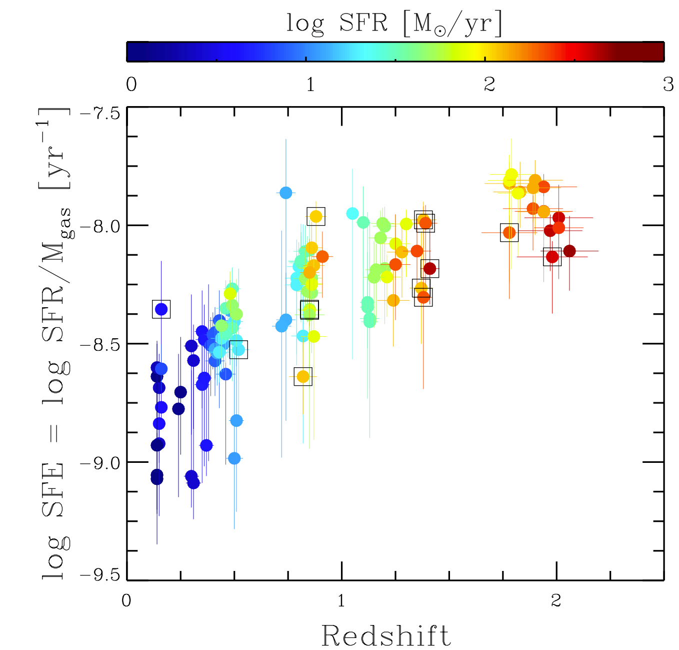

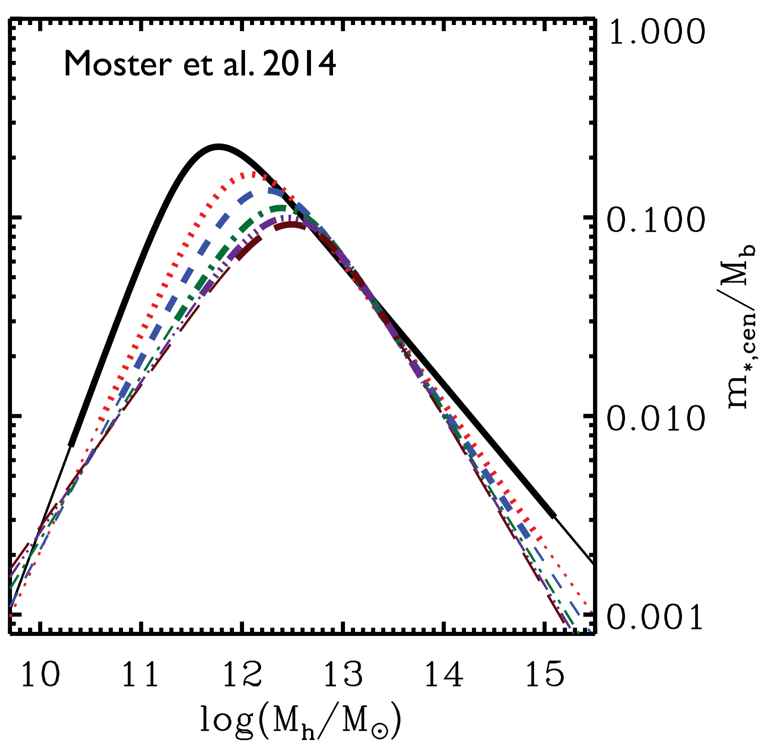

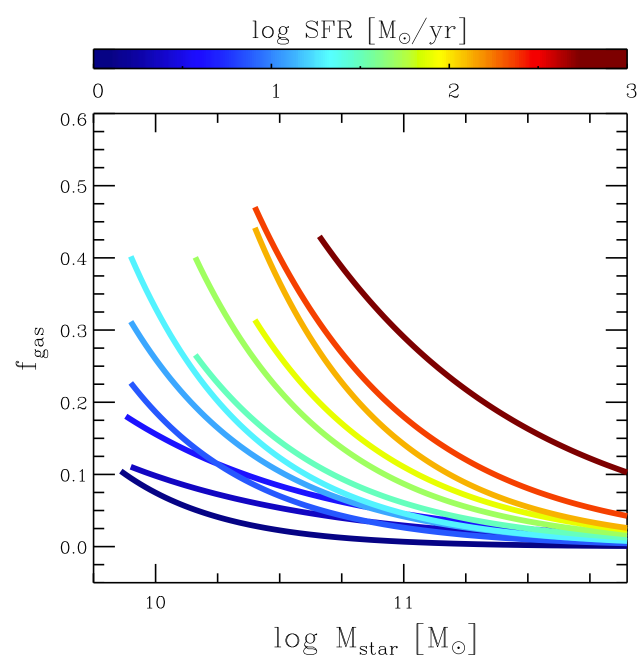

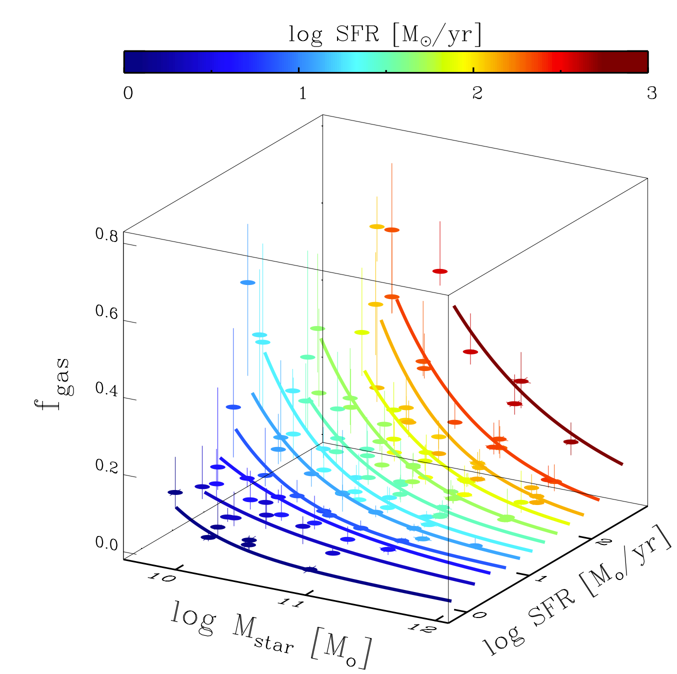

WDM particle mass: limits from the Ly-α forest

Viel et al. 2005-2013

m_{WDM}>3.5 keV	Thermal relics WDM
m_{ν}>12 keV	Sterile ν WDM (DW) **Dodelson-Widrow**

Results subject to further investigations

Still affected by the difficult-to-characterize non-linear growth of baryonic and DM structures (Watson et al. 2012) and uncertainities in the WDM simulations themselves.

WDM particles are 10^{68} times heavier (10^5 $M_{\odot}$) than the real WDM particles. This makes difficult to infer the initial velocity distribution of the effective particles from the known initial velocity distribution of the real WDM particles (Lovell et al. 2012, 2014; Maccio` et al. 2012; Viel et al. 2013).

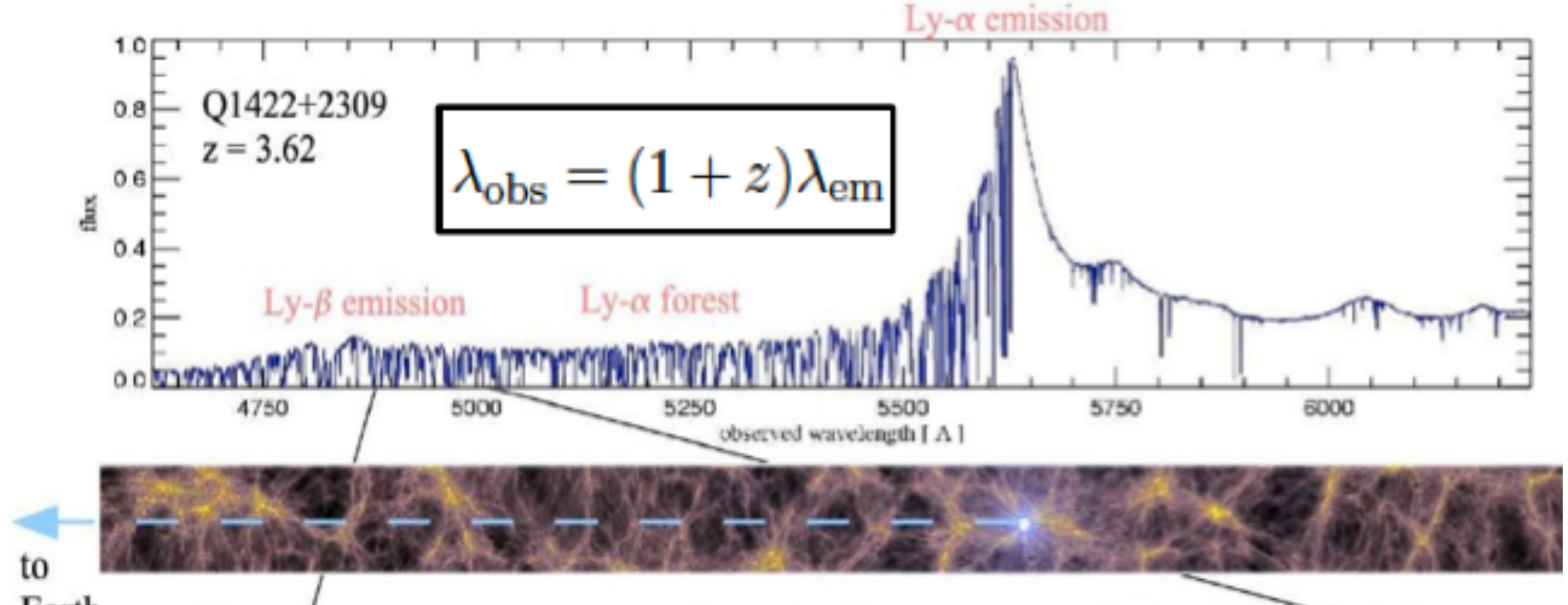

Fig. From Springel et al. 2006

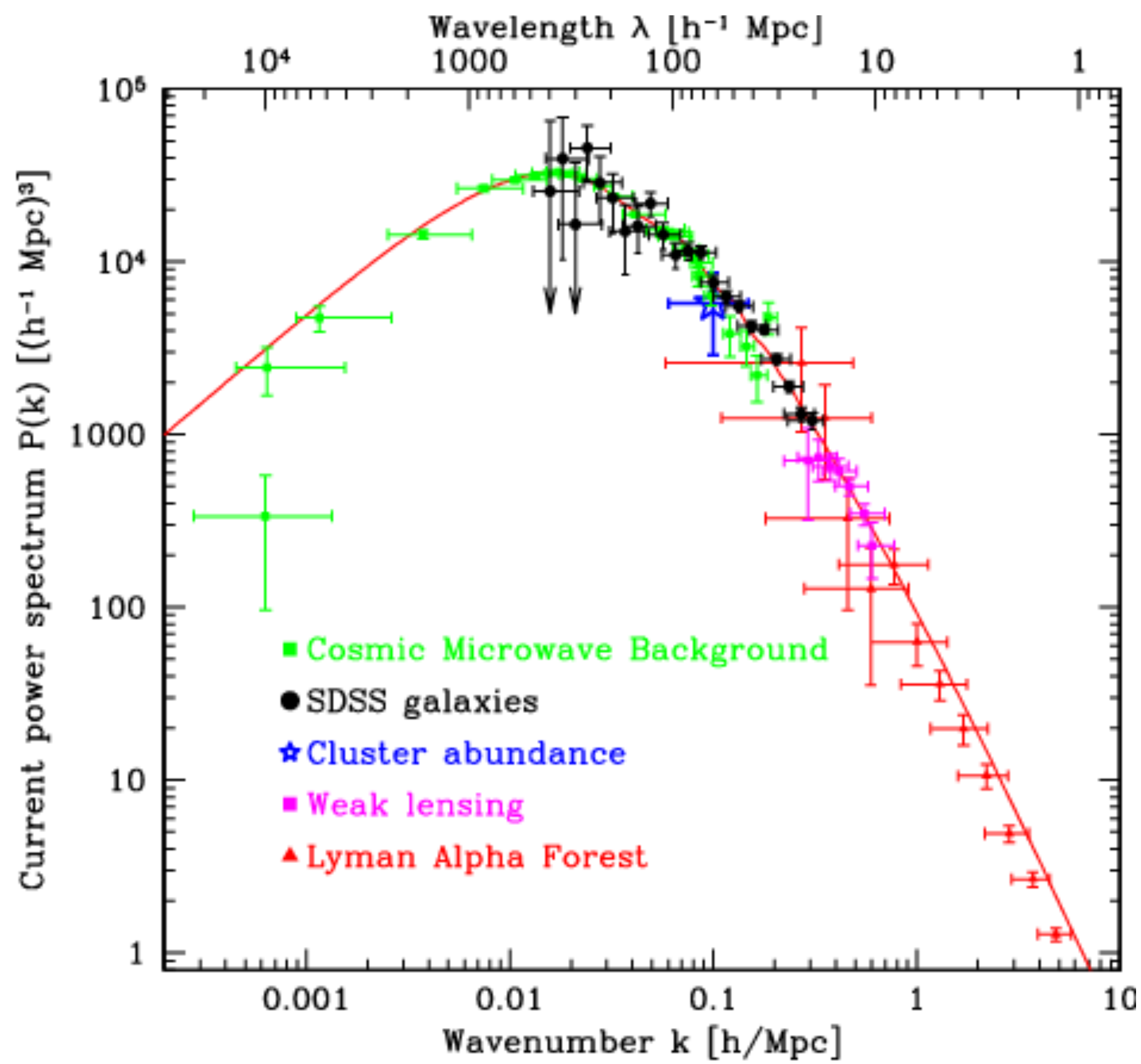

Mass should be m~2 keV (thermal relics)

Schneider et al. 2013

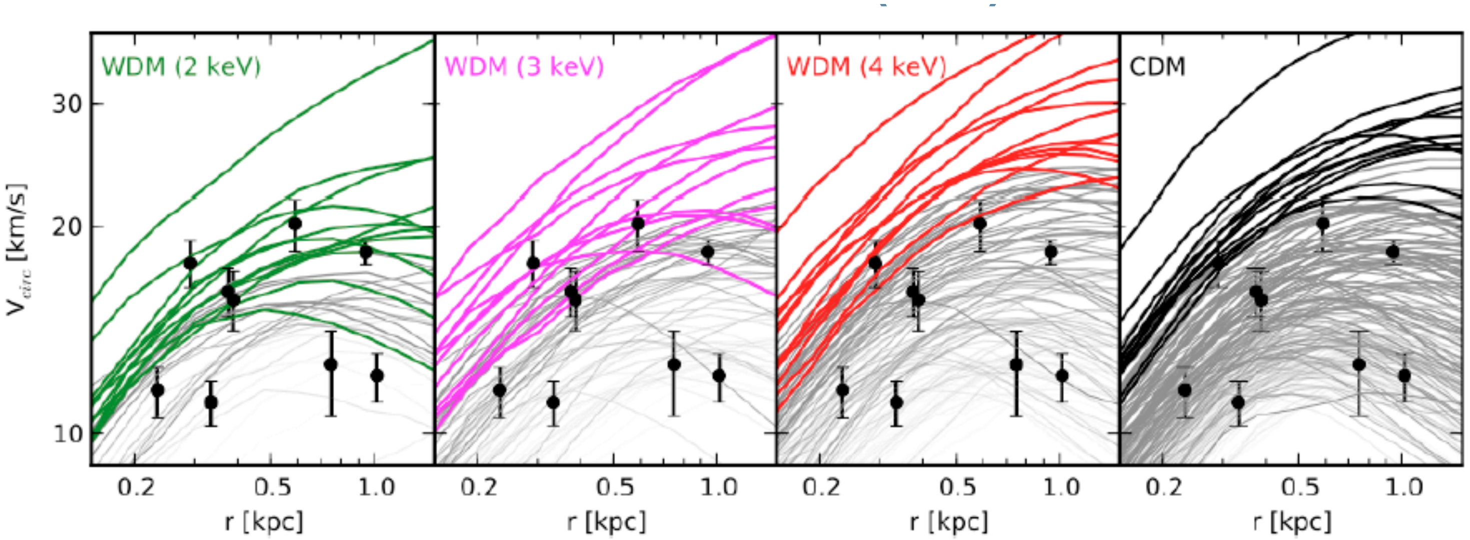

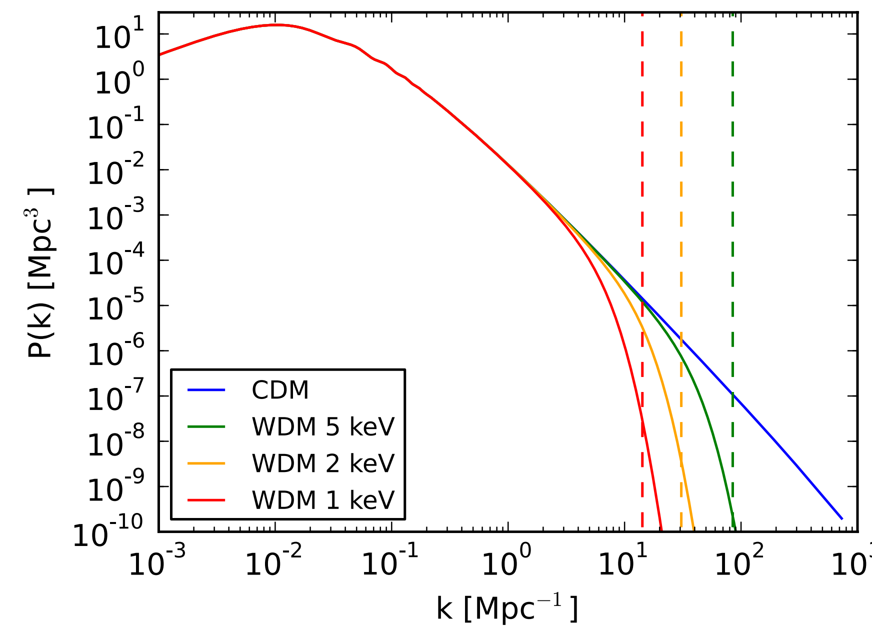

Monthly Notices of the ROYAL ASTRONOMICAL SOCIETY

MNRAS **437**, 293–304 (2014) doi:10.1093/mnras/stt1883

Advance Access publication 2013 October 24

MaGICC-WDM: the effects of warm dark matter in hydrodynamical simulations of disc galaxy formation

Jakob Herpich,[1★] Gregory S. Stinson,[1] Andrea V. Macciò,[1] Chris Brook,[2] James Wadsley,[3] Hugh M. P. Couchman[3] and Tom Quinn[4]

[1]*Max-Planck-Institut für Astronomie, Königstuhl 17, D-69117 Heidelberg, Germany*

[2]*Departamento de Física Teórica, Universidad Autónoma de Madrid, E-28049 Cantoblanco, Madrid, Spain*

[3]*Department of Physics and Astronomy, McMaster University, Hamilton, Ontario L8S 4M1, Canada*

[4]*Astronomy Department, University of Washington, Box 351580, Seattle, WA 98195-1580, USA*

Accepted 2013 October 2. Received 2013 September 20; in original form 2013 August 5

ABSTRACT

We study the effect of warm dark matter (WDM) on hydrodynamic simulations of galaxy formation as part of the Making Galaxies in a Cosmological Context (MaGICC) project. We simulate three different galaxies using three WDM candidates of 1, 2 and 5 keV and compare results with pure cold dark matter simulations. WDM slightly reduces star formation and produces less centrally concentrated stellar profiles. These effects are most evident for the 1 keV candidate but almost disappear for $m_{\mathrm{WDM}} > 2$ keV. All simulations form similar stellar

Constraints from X-ray emission from clusters and galaxies

if $m_s > m_\alpha$ the radiative decay $\nu_s \rightarrow \nu_\alpha + \gamma$ becomes allowed

$$E_\gamma = \frac{1}{2} m_s \left(1 - \frac{m_\alpha^2}{m_s^2}\right) .$$

Emission lines in X-rays from DM concentrations:
- clusters (large signal but also large background)
- galaxies

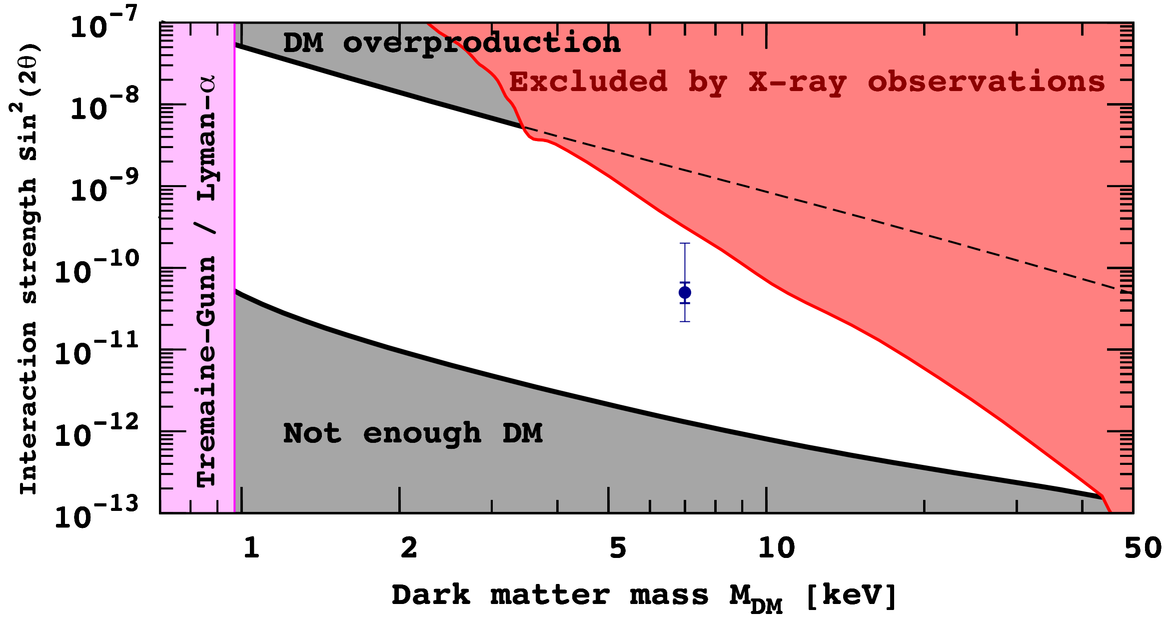

FIG. 4: Constraints on sterile neutrino DM within νMSM [4]. The blue point would corresponds to the best-fit value from M31 if the line comes from DM decay. Thick errorbars are $\pm 1\sigma$ limits on the flux. Thin errorbars correspond to the uncertainty in the DM distribution in the center of M31.

Boyarsky et al. 2014

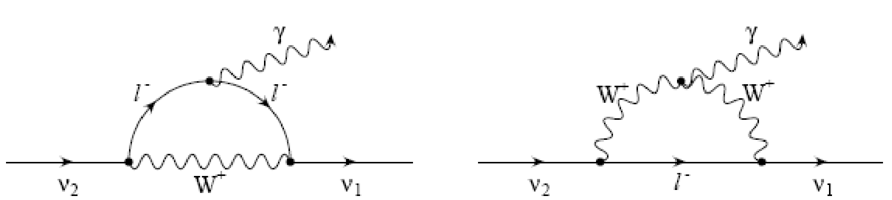

Abazajian et al. 2001-2005

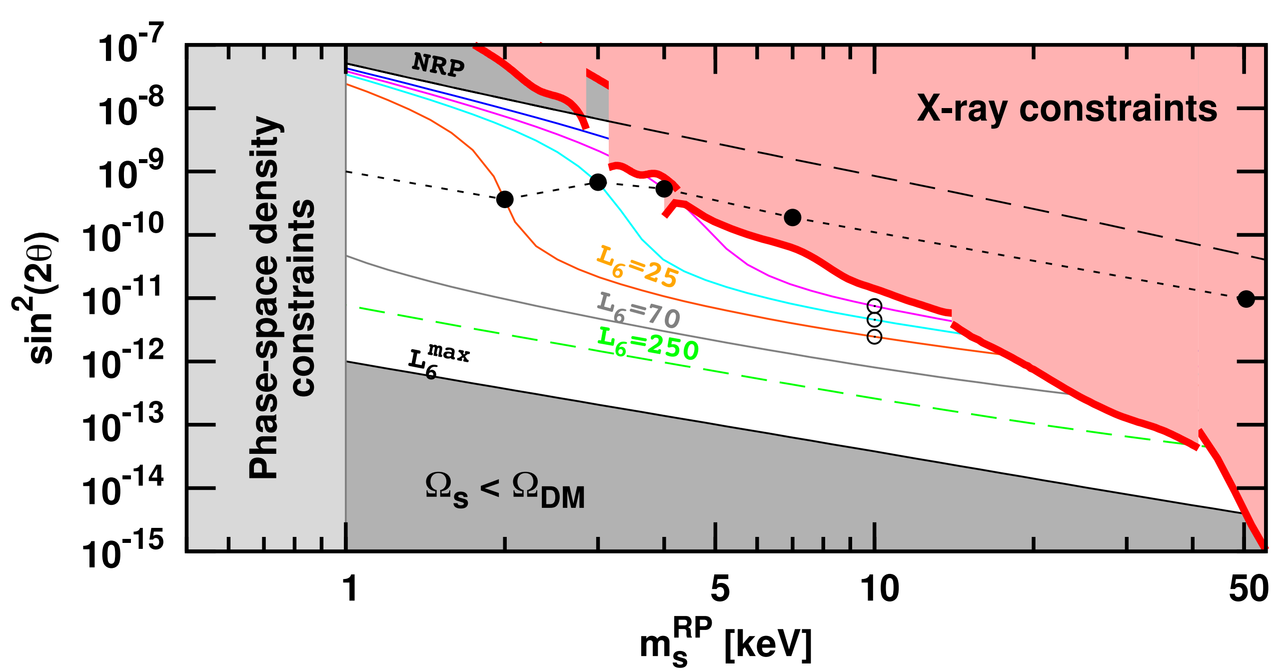

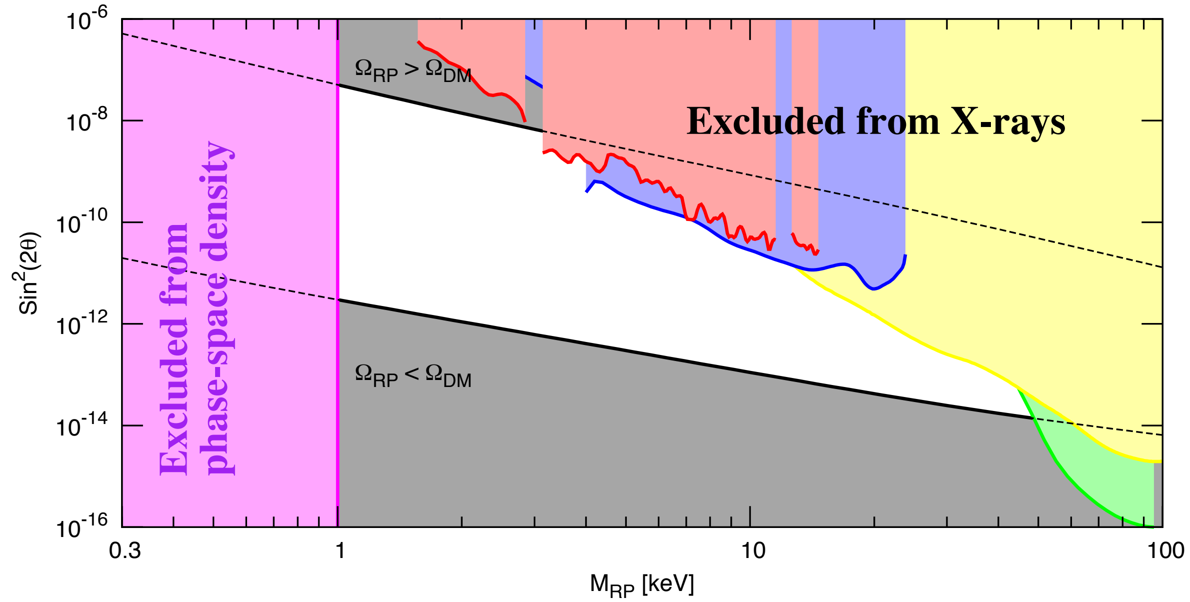

Window corresponds to resonant production

Upper boundary - zero lepton asymmetry

Lower boundary - maximal lepton asymmetry

Boyarsky et al 2009

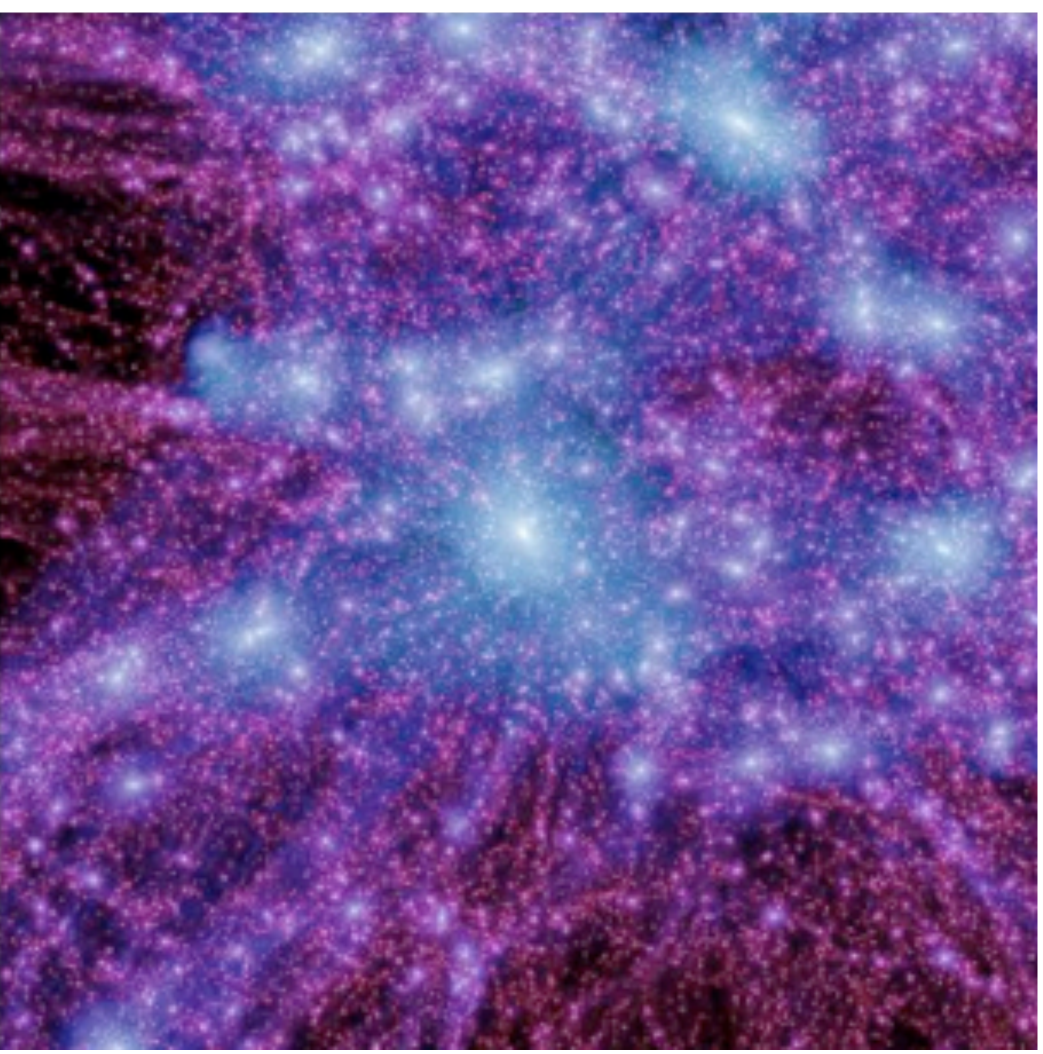

6 – Sterile neutrino resonant production

In presence of a large lepton asymmetry, $\mathcal{L} \equiv (n_\nu - n_{\bar{\nu}})/n_\gamma$, matter effects become important and the mixing angle can be resonantly enhanced. [Shi, Fuller, 1998; Abazajian et al., 2001

$$\boxed{\sin^2 2\theta_m = \frac{\Delta^2(p)\sin^2 2\theta}{\Delta^2(p)\sin^2 2\theta + D^2 + (\Delta(p)\cos 2\theta - \frac{2\sqrt{2}\zeta(3)}{\pi^2} G_F T^3 \mathcal{L} + |V_T|)^2}}$$

The mixing angle is maximal $\sin^2 2\theta_m = 1$ when the resonant condition is satisfied (with $\Delta(p) \equiv m_4^2/(2p)$)

$$\boxed{\Delta(p)\cos 2\theta - \frac{2\sqrt{2}\zeta(3)}{\pi^2} G_F T^3 \mathcal{L} + |V_T| = 0}$$

$$\boxed{\left(\frac{m_4}{1\mathrm{keV}}\right)^2 \simeq 0.08 \frac{p}{T} \frac{\mathcal{L}}{10^{-4}} \left(\frac{T}{100\,\mathrm{MeV}}\right)^4 + 2\left(\frac{p}{T}\right)^2 \frac{B}{\mathrm{keV}} \left(\frac{T}{100\,\mathrm{MeV}}\right)^6}$$

Sterile neutrinos are produced in primordial plasma through

• off-resonance oscillations. [Dodelson, Widrow; Abazajian, Fuller; Dolgov, Hansen;
Asaka, Laine, Shaposhnikov et al.]

• oscillations on resonance, if the lepton asymmetry is non-negligible [Fuller, Shi]

• production mechanisms which do not involve oscillations

– inflaton decays directly into sterile neutrinos [Shaposhnikov, Tkachev] – Higgs physics: both mass and production [AK, Petraki]

Watson et al. 2012

Limits from the
X-ray emission from clusters and galaxies

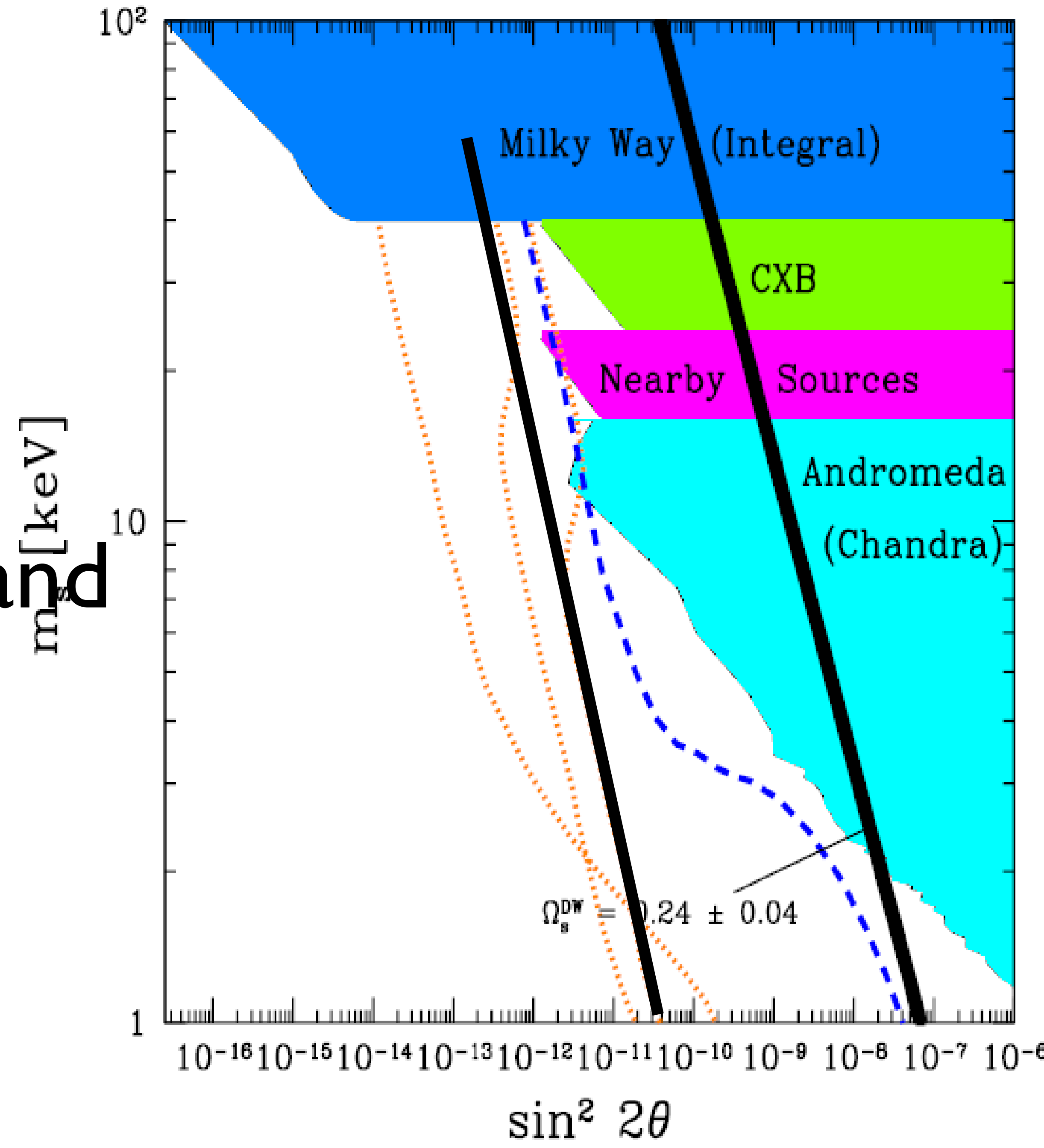

Very small mixing ($\sin^2 2\theta \lesssim 10^{-7}$) between

mass $|\nu_{1,2}>$ &

flavor $|\nu_{\alpha,s}>$ states:

$$|\nu_\alpha\rangle = \cos\theta|\nu_1\rangle + \sin\theta|\nu_2\rangle$$
$$|\nu_s\rangle = -\sin\theta|\nu_1\rangle + \cos\theta|\nu_2\rangle$$

For $m_s < m_e$,

3ν Decay Mode Dominates:

$$\Gamma_{3\nu} \simeq 1.74 \times 10^{-30} s^{-1} \left(\frac{\sin^2 2\theta}{10^{-10}}\right)\left(\frac{m_s}{\text{keV}}\right)^5$$

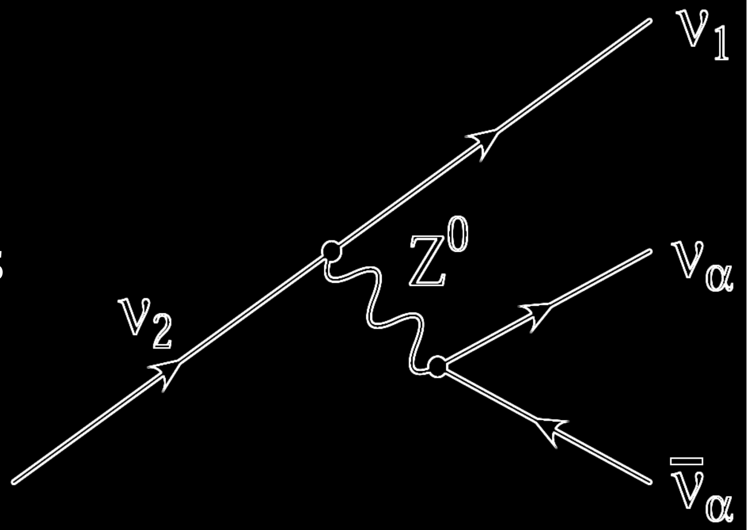

Radiative Decay Rate is:

$$\Gamma_s \simeq 1.36 \times 10^{-32} s^{-1} \left(\frac{\sin^2 2\theta}{10^{-10}}\right)\left(\frac{m_s}{\text{keV}}\right)^5 \quad \nu_s \longrightarrow \nu_\alpha + \gamma$$

WIMP

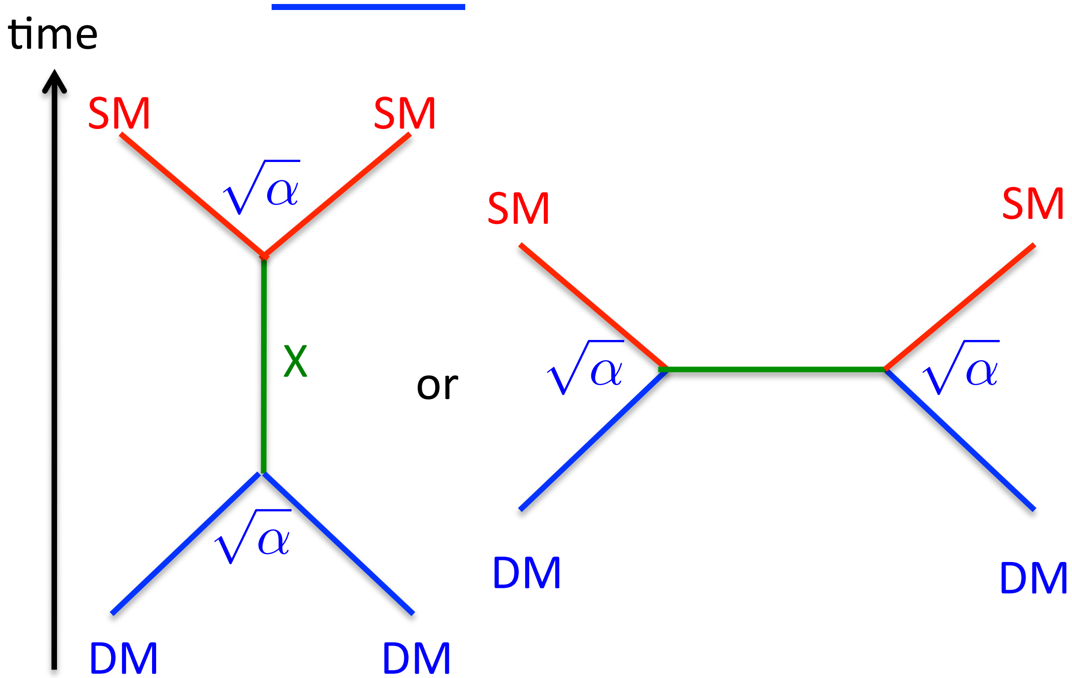

self-annihilation

freeze out

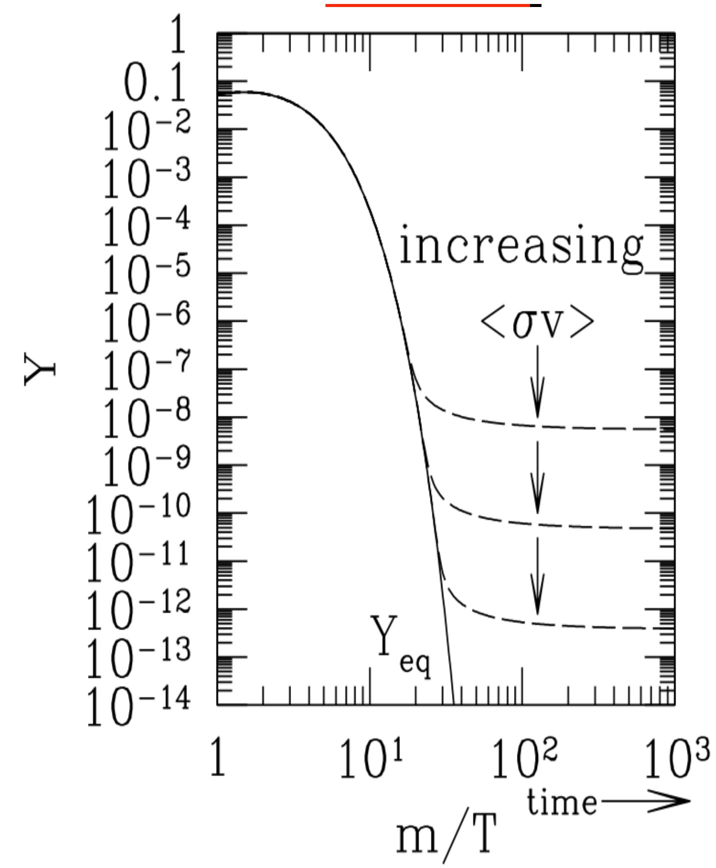

$$\Omega h^2 \approx \frac{3 \times 10^{-27}\ \mathrm{cm^3/s}}{\langle \sigma_{\mathrm{ann}} v \rangle}.$$

$$\langle \sigma_{\mathbf{ann}} \mathbf{v} \rangle \sim \mathbf{10^{-25}} \mathrm{cm^3 s^{-1}} \left(\frac{\alpha}{\mathbf{10^{-2}}} \right)^{\mathbf{2}} \left(\frac{\mathbf{100GeV}}{\mathbf{m_X}} \right)^{\mathbf{2}}$$

➡ Electro Weak Scale(～100GeV) WIMP naturally explains the relic abundance.

TeV scale SUSY & neutralino dark matter

Dispersional relations for active and sterile neutrinos (from real part)

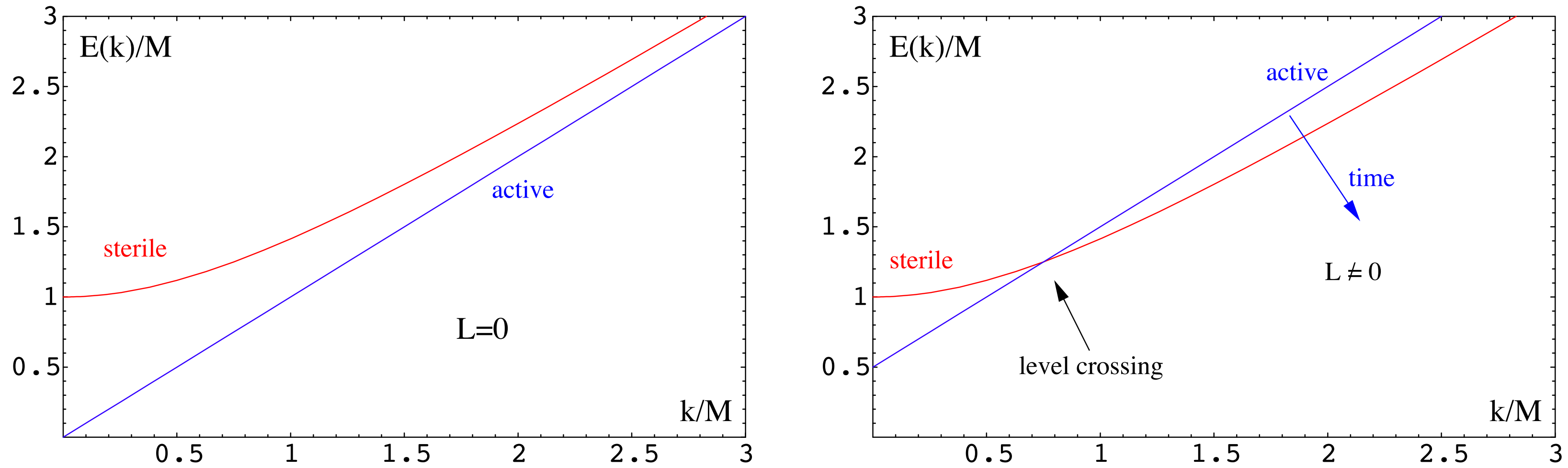

Transitions $\nu \rightarrow N_1$

Dodelson-Widrow

Zero lepton asymmetry

Resonant transitions

Shi-Fuller

Lepton asymmetry

created in $N_{2,3}$ decays

Dark matter and the Lyman-α forest.

The bounds depend on the production mechanism.

$$\lambda_{FS} \approx 1\,\mathrm{Mpc} \left(\frac{\mathrm{keV}}{m_s}\right) \left(\frac{\langle p_s \rangle}{3.15\,T}\right)_{T\approx 1\,\mathrm{keV}}$$

The ratio

$$\left(\frac{\langle p_s \rangle}{3.15\,T}\right)_{T\approx 1\,\mathrm{keV}} = \begin{cases} 0.9 & \text{for production off} - \text{resonance} \\ 0.6 & \text{for MSW resonance (depends on L)} \\ 0.2 & \text{for production at T} > 100\ \text{GeV} \end{cases}$$

- Photon energy:

$$E_\gamma = \frac{M_1}{2}$$

- Radiative decay width

$$\Gamma = \frac{9\alpha_{\mathrm{EM}} G_F^2}{256\pi^4}\,\theta^2\,M_1^5$$

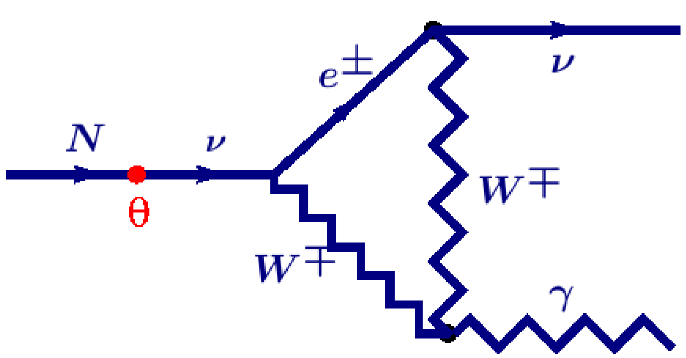

Dark matter made of sterile neutrino is not completely dark

Dolgov & Hansen (2000)

Where to look for DM decay line?

Extragalactic diffuse X-ray background (XRB)	Dolgov & Hansen, 2000; Abazajian et al., 2001 Mapelli & Ferrara, 2005; **Boyarsky et al. 2005**
Clusters of galaxies	Abazajian et al., 2001 **Boyarsky et al. astro-ph/0603368**
DM halo of the Milky Way. Signal increases as we increase FoV!	**Boyarsky et al. astro-ph/0603660** Riemer-Sørense et al. astro-ph/0603661 **Boyarsky, Nevalainen, O.R.** (in preparation)
Local Group galaxies	**Boyarsky et al. astro-ph/0603660** Watson et al. astro-ph/0605424
"Bullet" cluster 1E 0657-56	**Boyarsky, Markevitch, O.R.** (in preparation)
Cold nearby clusters	**Boyarsky, Vikhlinin, O.R.** (in preparation)
Soft XRB	**Boyarsky, Neronov, O.R.** (in preparation)

Need to find the best ratio between the DM decay *signal* and object's X-ray emission

CDM as particle Dark Matter

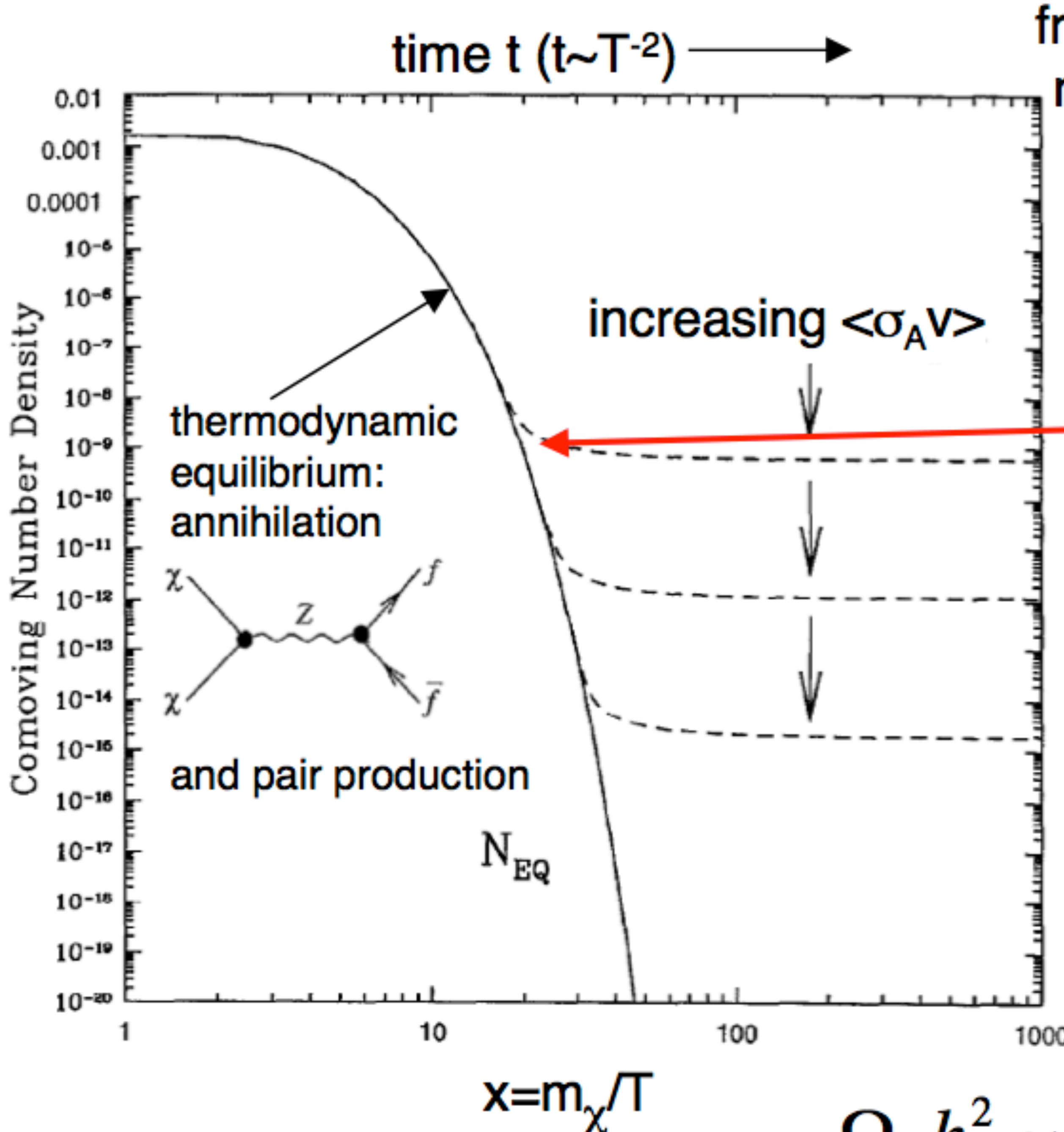

freeze-out of a weakly interacting massive particle (WIMP χ) when reaction rate drops below expansion rate

$T_{\text{freeze-out}}$~ 1/20 x m(WIMP)

Cold Dark Matter:

- non-relativistic

"survival of the weakest"

At or below the weak scale

$$\Omega_\chi h^2 \approx \frac{m_\chi n_\chi}{\rho_c} \approx \frac{3\times10^{-27}\,\mathrm{cm}^3/\mathrm{sec}}{\langle \sigma_A v\rangle}$$